DEVELOPMENT AND PERFORMANCE EVALUATION OF DIATOMACEOUS EARTH-BASED GEOPOLYMER CONCRETE INCORPORATED WITH SISAL FIBRES AND HIGH-DENSITY POLYETHYLENE WASTES

BY

KIPSANAI, JEPCHUMBA JANET

A Thesis Submitted to the Department of Manufacturing, Industrial and Textile Engineering in Partial Fulfillment of the Requirements for the Degree of Doctor of Philosophy in Industrial Engineering

Moi University

2023

DECLARATION

Declaration by the Candidate

This thesis is my original work. It is unauthorized to copy any part of this thesis without the author's and/or Moi University's prior written consent.

Kipsanai, Janet Jepchumba …… Date: 14/11/2023

ENG/DPHIL/IE/01/18

Declaration by Supervisors

With our approval as University Supervisors, this thesis has been submitted for examination.

Prof. (Eng.) Paul Wambua …… Date …16/11/2023

School of Mechanical and Manufacturing Engineering

Technical University of Kenya-Nairobi

Prof. Saul, Sitati Namango … … Date: 15/11/2023

School of Engineering

Moi University-Eldoret, Kenya

Prof. Sofiane AMZIANE …… Date: 16/11/2023

Institut Pascal, UMR 6602

Université Clermont Auvergne (UCA) – CNRS, France

DEDICATION

This research is dedicated to:

My Family

Whose love and support have seen me this far.

ACKNOWLEDGEMENT

I want to express my sincere gratitude to everyone who contributed to the achievement of this thesis.

First and foremost, I owe Almighty God, who is worthy of all praise and honour, the ability and opportunity to carry out this research.

A special thank you to my supervisors, Prof. P. Wambua, Prof. S. S. Namango, and Prof. S. Amziane whose guidance and support steered me through this research. I have become a better researcher, thinker, writer, and presenter as a result of their refusal to settle for anything less than my best. Their commitment to excellence and never-ending advice enabled me to finish this thesis.

I appreciate the financial assistance provided by the African Development Bank (AFDB) via Moi University. I also thank the French government through the French Embassy in Nairobi for financially supporting my experimental work at the Université Clermont Auvergne.

The technical professionals at Moi University, the Eldoret National Polytechnic, Université Clermont Auvergne, and the Ministry of Petroleum and Mining deserve to be thanked for their assistance.

I am thankful for my family's unending love, special attention, and unwavering support, especially throughout my Ph.D. research.

Making you all proud is always what inspires me the most!

ABSTRACT

The building industry is facing challenges in terms of resource management, excessive energy consumption, and CO_2 emissions resulting from the extended usage of concrete made primarily of Portland cement and ceramic bricks. Geopolymer technology has caught the attention of many researchers in an attempt to promote the development of sustainable concrete. This study investigates how to utilize diatomaceous earth as a resource for geopolymers. Little research has been conducted on the use of diatomaceous earth as a stand-alone geopolymer precursor or in combination with natural fibres and/or polymeric additives, although, it has become a significant source of industrial waste that ends up in landfills. The primary goal of the study was to develop and analyse the performance properties of diatomaceous earth-based geopolymer concrete incorporated with sisal fibres and high-density polyethylene wastes. The specific objectives were: to characterize diatomaceous earth in relation to chemical, physical, thermal, and mineralogical features; fabricate geopolymer concrete from alkaline activated diatomaceous earth with the addition of sisal fibres and HDPE waste; analyze the effect of incorporating sisal fibres and HDPE wastes on the performance properties of the geopolymer concrete; and to generate correlational and predictive models for the developed geopolymer performance properties. The methodology involved using standard techniques to characterize diatomaceous earth that had been calcined at 600 °C and in its raw state. After 28 days of curing, the alkaline (lime)-activated specimens were tested for their mechanical, physical, and thermal characteristics. The geopolymer performance correlation and predictive models were developed using linear and polynomial regression approaches. The chemical composition showed that silica was the main constituent, making up 88.12% of the raw sample and 89.92% of the calcined sample. The optimum material mixture for the lime-activated geopolymers was found to contain 83.75 %wt diatomite, 15 %wt lime, and 1.25 %wt sisal fibres yielding 2.72 MPa of compressive strength, 0.72 g/cm^3 bulk density and 0.110 W/mK thermal conductivity. In comparison to the acceptable standards for the concrete masonry units, as stated in ASTM C1634 and ASTM C129, the properties of the lime-activated diatomite-based concrete suggested the necessity for modification. The optimum performance outcomes of the modification, which comprised substituting sodium hydroxide and sodium silicate activation for lime activation, were a compressive strength of 34.10 MPa, a bulk density of 1.32 g/cm^3, water absorption of 13.93 %, and 0.322 W/mK thermal conductivity. Bulk density and water absorption showed a strong correlation with compressive strength. The diatomite under investigation is a class F pozzolan, and it can be used to produce sisal-fibre reinforced geopolymer concrete with acceptable performance for masonry walling materials. There was a strong correlation between certain performance characteristics and the amount of sisal fibre incorporation. Additionally, strong correlations between performance properties were found. The practicality, economic viability, and durability of cellulosic fibre-reinforced geopolymer composites were however deemed to require further study. The development of standards and specifications for the manufacturing of geopolymers as well as their functional properties was also recommended.

TABLE OF CONTENTS

LIST OF TABLES

LIST OF FIGURES

LIST OF SYMBOLS

Symbol	Meaning
Ø	Diameter
GxPy	Specimen of proportional group (G) ‘x’ and compacted at pressure (P) ‘y’

ABBREVIATIONS/ACRONYMS

Abbreviations	Meaning
AAB	Alkaline activated binder
AAS	Atomic absorption spectroscopy
ACI	American Concrete Institute
ASTM	American Society for Testing and Materials
CASH	Calcium aluminosilicate hydrate gel
cN	Centinewton
CO_2	Carbon dioxide
CS	Compressive strength
DE	Diatomaceous earth
DoE	Design of experiment
DSC	Differential scanning calorimetry
D_v	Cumulative volume distribution
EN	European standard
HDPE	High-density polyethylene
FA	Fly ash
GBFS	Granulated blast furnace slag
GHS	Globally Harmonized System
LL	Liquid Limit
L0I	Loss on Ignition
M	Alkali element
MK	Metakaolin
M-OH	Alkali hydroxide
$NaOH/Na_2SiO_3$	Sodium hydroxide and sodium silicate mixture
NASH	Sodium aluminosilicate hydrate gel
NO_x	Oxide of nitrogen
OPC	Ordinary Portland cement
P2	2 MPa compaction pressure
P4	4 MPa compaction pressure
P6	6 MPa compaction pressure
P8	8 MPa compaction pressure
PL	Plastic Limit

POFA	Palm Oil Fuel Ash
SCM	Supplementary cementitious materials
SDE	Spent diatomaceous earth
SEM	Scanning electron microscope
SO_x	Oxide of sulphur
TGA	Thermogravimetric analysis
XRD	X-ray Diffraction
W/g	Heat flow

CHAPTER ONE: INTRODUCTION

1.1 Background to the Study

The construction industry is critical to sustainable growth because it plays a major role to a nation's economy and since its operations are necessary to attaining the socio-economic development objective of delivering housing, infrastructural facilities, and work opportunities (Dianingrum & Rahmadaniyati, 2017; Olga & Antonios, 2019; Rostami et al., 2015). It has been determined that building and construction use over 40% of the global energy while releasing almost as much carbon dioxide (CO_2) (Hung Anh & Pásztory, 2021; Pramanik et al., 2021; Yadav & Agarwal, 2021). Cement-based concrete is so commonly used (Aghdam et al., 2018; Pradena & César, 2022); Resulting in an estimated annual global production of 25 billion tonnes of CO_2 (Joshua et al., 2018; Olofinnade et al., 2019).

According to Manzano et al. (2012), humans utilize cement-based products like concrete in numbers that are second only to water. Cement has been known to be one of the energy-intensive building materials, using between 110 and 120 kWh to create one ton of cement in a conventional cement factory alone, ranking second only to the steel and aluminium industries in terms of energy consumption (Ahmed et al., 2021). On the other hand, around 50% of the carbon dioxide produced in cement factories is immediately released into the atmosphere during the calcination of the limestone. 40% is produced when fuel is burned to heat the rotary kiln, and the remaining 10% is detected during the quarrying and transportation of the limestone (Ahmed et al., 2021). With the enormous population growth forecast by 2050, this eco-footprint is projected to increase. Figure 1.1 depicts how the world's growing population affects the need for cement, based on Favier et al. (2018) report.

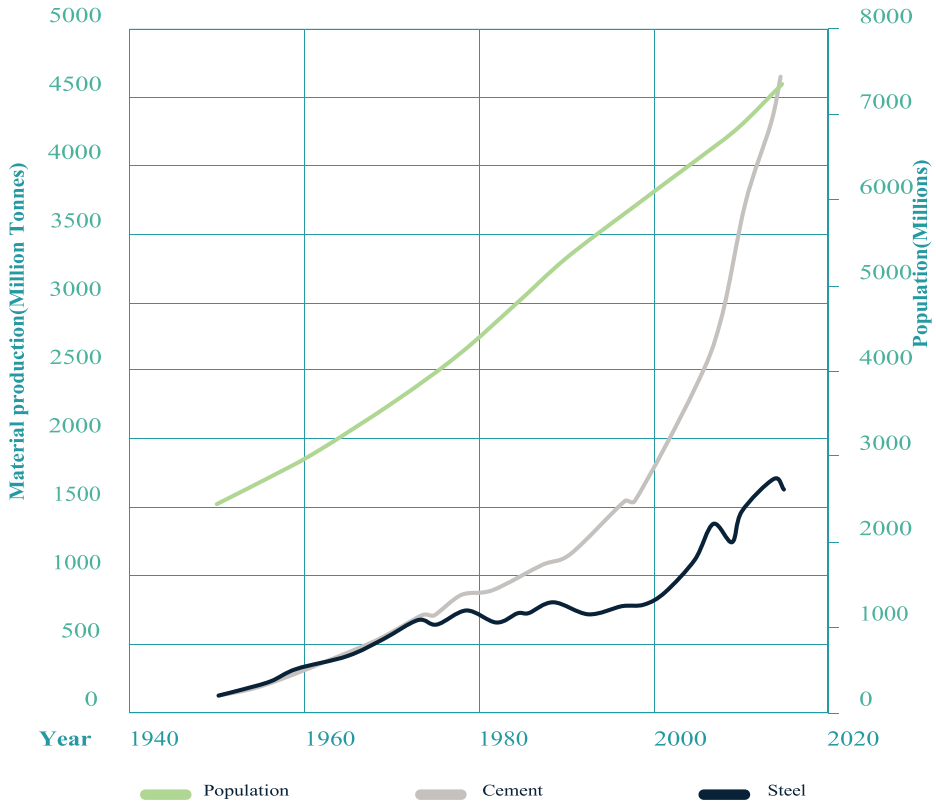

Figure 1.1. Projected global cement demand, in million metric tonnes (Favier et al., 2018)

Cement-based concrete has been the world's most utilized construction resource. However, a substantial quantity of CO_2 is released into the environment during the manufacture of Portland cement, a key ingredient in concrete (Bondar, 2009); which contributes to the greenhouse effect and the global warming of the planet. At the moment, CO_2 emissions are responsible for 65% of greenhouse effect, with the majority of CO_2-related greenhouse gas emissions coming from the manufacturing and use of Portland cement (Ojha & Aggarwal, 2022). Cement manufacturing also produces substantial NO_x and SO_x emissions, which contribute to acid rain, public health problems, and global climate change (Pradena & César, 2022).

Concrete production has emerged as the most significant roadblock to achieving global climate action under the Paris 2050 Agreement (Afrin et al., 2021). This is because of the high embodied energy and significant carbon footprint of regular Portland cement

concrete. Similar environmental damage and excessive energy consumption are associated with bricks created using conventional techniques, such as heating clay at high temperatures in a kiln. The search for alternative sustainable building materials is therefore inevitable (Silva, Kim, Aguilar, et al., 2020).

Figure 1.2 highlights the different approaches that scientists have suggested for producing alternatives to concrete that are more sustainable (Duxson et al., 2007; Hassan et al., 2019; Pradena & César, 2022).

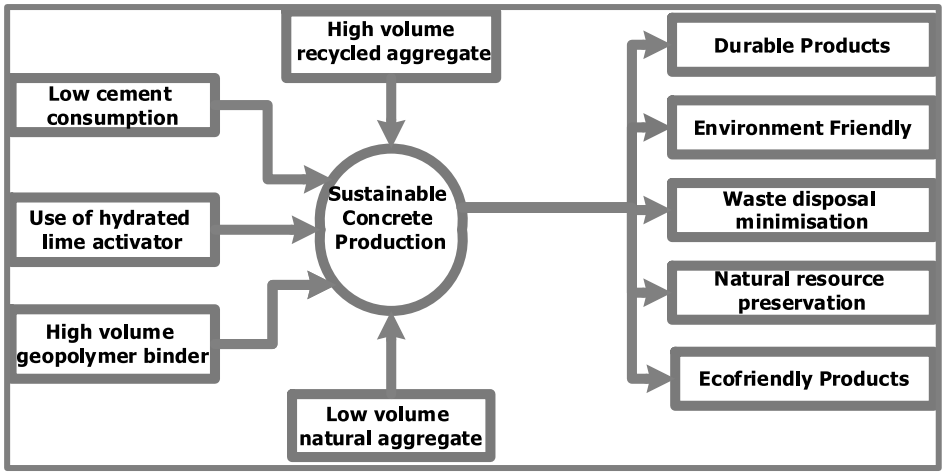

Figure 1.2: Sustainable methods for producing concrete (Hassan et al., 2019)

Designing "green concrete" is among the newest developments in the construction industry. Numerous researchers (Hasanbeigi et al., 2012; Mohajerani et al., 2019; Mohammed et al., 2021; Naqi & Jang, 2019; Nodehi & Taghvaee, 2022; Wan Ibrahim et al., 2015) have grown interest in producing geopolymer composites and utilizing cutting-edge geopolymer technology to achieve sustainability in the concrete production. This is due to the possibility of producing geopolymers at low temperatures, with minimal energy, and by employing various waste as either precursors or supplementary cementitious materials (SCM) (Ojha & Aggarwal, 2022). Geopolymer concrete is the subject of much scientific interest nowadays due to its tendency to be a

more ecologically sound option to conventional Portland cement (El-Dieb, 2016; Lloyd & Rangan, 2009; Nurruddin, 2018). Figure 1.3 illustrates the current trend of attention that is increasingly being given to the research field of geopolymer concrete according to Ma et al. (2018). Pozzolanic materials can be used in place of ordinary Portland cement.

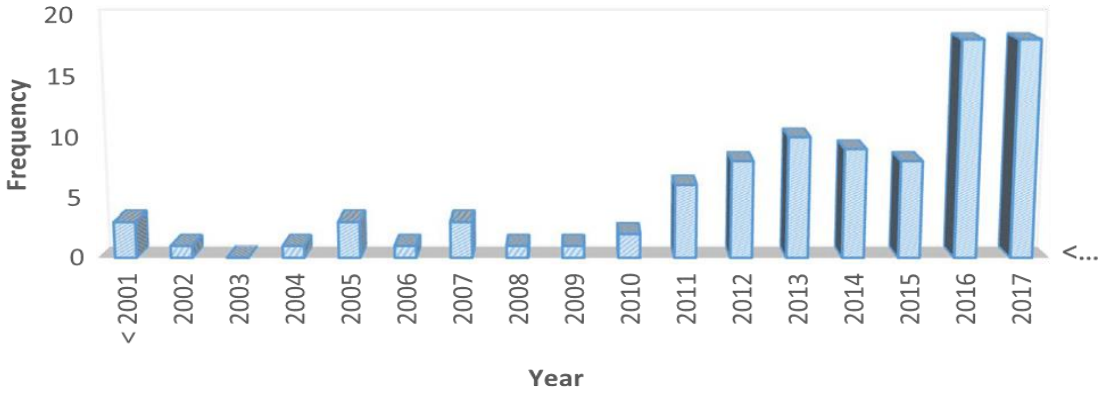

Figure 1.3: Research trend in geopolymer concrete (Ma et al., 2018)

To reduce the consumption and reliance on cement, the use of pozzolanic materials has been a primary area of study in the cement and materials industry in recent years (Danso H & Adu S, 2019). This is because materials bearing phases of alumina and silica have proved to be the best for geopolymer production; the materials being either natural mineral or industrial by-products (Ivanov & Belyakov, 2008; Ma et al., 2018; Mucsi & Ambrus, 2018). According to Korkmaz (2022), utilizing pozzolanic materials is another option to reduce the carbon dioxide (CO_2) footprint in the cement industry. According to Nodehi et al. (2022) and Mohammed et al. (2021) the most common aluminosilicate sources (pozzolan precursors) employed in geopolymer experimental investigations are Metakaolin, fly ash, ground-granulated blast furnace slag, rice husk ash, and fuel ash from palm oil (POFA), waste bottle glass (WBG), sugarcane bagasse ash (SCBA) and ceramic dust waste. Particularly, the production of composites employing by-products such as class F fly ash has been widely explored.

The use of artificial pozzolans like fly ash, has shown good performance, but their production is limited by the high heat treatment of materials with little to no pozzolanicity (Tokyay, 2016). Fly ash, according to Jambhulkar et al. (2018), is regarded as a global environmental risk since it frequently contains organic pollutants and potentially harmful oxides of metals including Se, As, B, V, Al, Pb, Hg, and Cr as well as radio-nuclides like Uranium and Thorium. The negative health impacts of long-term exposure to fly ash include lung cancer, chronic respiratory problems, and bronchitis, among other conditions (Kurda et al., 2018).

The fundamental distinction between natural and artificial pozzolans, according to Tokyay (2016), is that only grinding is necessary for natural pozzolans. Furthermore, natural pozzolans have been discovered to be a tremendous source of reactive silica and alumina needed for the synthesis of geopolymers as an alternative binder for ordinary Portland cement because they are accessible for a low cost and leave a small ecological footprint due to their simplistic extraction (Firdous et al., 2018). This is why the research of siliceous rocks for use as raw materials in geopolymer has attracted attention; because they contain safe, amorphous active silicon dioxide that boosts chemical activity, a fine-porous structure, are light in weight, and have a low thermal conductivity (Elmahdoubi et al., 2021).

The applicability of diatomaceous earth according to Payá et al. (2018) and Milad et al. (2021) shows that it is a naturally occurring pozzolanic material, that is useful in the construction industry. There hasn't really been a lot of emphasis to establish if it works as a geopolymer binder to make cementless (clinker-free) concrete. Besides, diatomaceous earth is among the prevalent industrial by-products nowadays since it is used as a filtration agent by the majority of industries. According to Kipsanai et al.

(2022) review, emphasis has been placed on its integration as a replacement for fine aggregate or as a partial replacement for cement. Its potential for usage as a precursor for geopolymers is enabled by its pozzolanic characteristics, porosity, affordability, availability (Figure 1.4) and ecologically sound nature (Sharma et al., 2021).

Massive accumulations of fossil diatom frustules have reportedly been discovered in numerous lakes located in silica-rich environments, particularly in volcanic and hydrothermally active areas, including Yellowstone Lake in the United States, Lake Myvatn in Iceland, Lake Challa in Tanzania and in Kenya, among others (Zahajská et al., 2020). In Kenya, Gevera et al. (2018) determined that diatomaceous earth sediments are found in the Nakuru-Elmenteita basin near Kariandusi. According to Mumbi et al. (2022), Africa Diatomite Industries Limited (ADIL), which mines diatomite in Gilgil, Kenya, has access to high-quality diatomite reserves estimated to be worth over 6 million tonnes. Westover et al. (2021) reveals that in addition to the diatomite deposits in Gilgil, the mineral has also been found in Baringo county; the quantity hasn't been defined but is believed to be enormous.

The major end-use for processed diatomite nowadays is as a filter aid; uses for filtration include the purification of beer, wine, and other alcoholic beverages, vegetable oil, syrup, pharmaceuticals, motor oil, and swimming pool water (Hoffman, 2006). According to Jaskula (2020), around 55% of diatomite is used for filtration purposes. Consequently, spent diatomaceous earth (SDE) has become a significant source of industrial waste for industries like food processing and brewing (Galán-Arboledas et al., 2017; Mateo et al., 2017). The brewing industry, for instance, produces diatomaceous earth waste estimated at around 378.1 million tonnes each year (Gong et al., 2019; Thiago et al., 2014). This used diatomite ends up in landfills or is applied to

crops as organic fertilizer, both of which squander resources and harm the environment (Galán-Arboledas et al., 2017). Additionally, the usage of diatomaceous earth in agriculture could raise the danger of leaching nitrogenous chemicals found in the discarded material. Moreover, due to the significant energy, labour, and cost requirements, the SDE regeneration may not be a viable option. The use of SDE for more economically viable and environmentally sound applications, such as in geopolymer concrete technology is therefore of great importance.

To determine the diatomaceous earth's suitability as a geopolymer raw material, it is vital to have a thorough understanding of its mechanical, thermal, chemical, and physical properties. In addition, it is crucial to consider the functional qualities of diatomaceous earth-containing concrete and its inclusion in past studies. The current study is primarily concerned with an experimental investigation to assess the mechanical, physical, and thermal performances of geopolymer bricks/concrete made from diatomaceous earth's alkaline activation as an aluminosilicate source material.

Even though geopolymers have been proven to possess greater mechanical properties and greater resistance to fire, sulfates, and acids than OPC-based materials (Singh et al., 2015), they exhibit brittle failure, which may place several restrictions and limitations on their structural functions (Silva et al., 2020). According to the review by Zhang et al. (2020) and other studies, adding fibres to concrete is an effective way to increase its ductility and toughness and prevent cracks from spreading. Jamshaid et al. (2022) pointed out that the most promising method for improving strength without harming the environment and enabling the efficient and sustainable use of renewable resources is to reinforce concrete with fibres. In line with Broeren et al. (2017), sisal fibre has the potential to replace glass fibre in natural fibre composites. Therefore, this

study also assesses the effects of combining diatomaceous earth with sisal fibres and polymeric additives made of shredded high-density polyethylene on the functionality of the geopolymer. Given that solid waste management is currently one of the main environmental challenges in the globe, the incorporation of shredded high-density polyethylene (HDPE) wastes in this research was investigated. The goal was to evaluate the viability of employing HDPE as a filler material in diatomite-based geopolymer while minimizing environmental problems associated with the disposal of waste plastics.

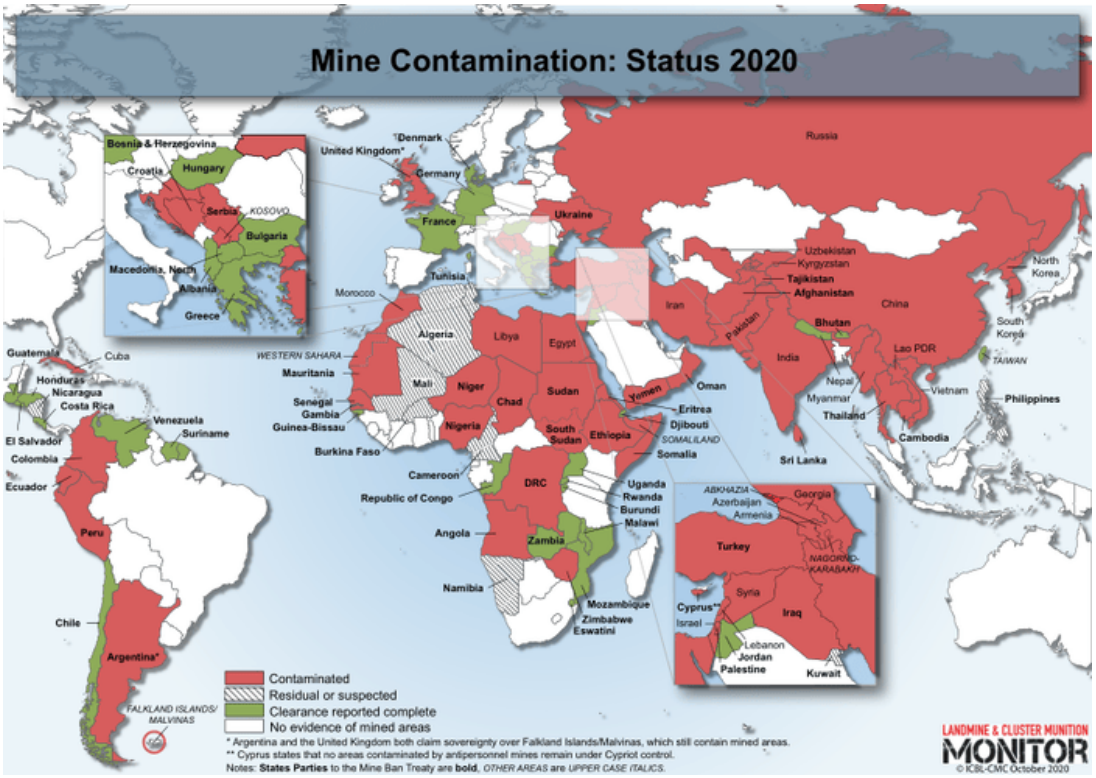

Figure 1.4. Global diatomite deposits and processing plants (Rockwell & Hofstra, 2008)

1.2 Statement of the Problem

Construction, maintenance and building use have a huge environmental impact and are major contributors to irreversible climatic, atmospheric and ecosystem changes around the world. Modern construction technology and material science have greatly reduced

the use of the earth as a building material. A decrease in interest in using soil as a building resource because of the advent of building materials like cement and steel has increased housing expenses as well as environmental effects due to its manufacturing process and high energy consumption globally (Nahar, 2018).

Energy input is needed in large quantities during the Portland cement production process. For instance, the calcination of limestone (calcium carbonate) and silico-aluminous material is performed at extremely high temperatures of approximately 1450–1500°C. Additionally, almost 8% of the world's total CO_2 emissions is attributed to the production of ordinary Portland cement, making it a significant greenhouse gas emitter. Given the daily growth rates of emerging economies and the exponential rise in the demand for infrastructure construction and renovation, it is predicted that the carbon pollution and energy demand associated with the manufacture of cement will surpass 105 Gt (Gigatonne) and 505 TJ (terajoule) in 3 decades, respectively.

Generally, it has been regarded that producing cement is a very energy and emissions-intensive process. As a result, there is an urgent global demand for building materials that offer benefits including eco-friendliness, low energy usage, high strength, and reasonable cost. Alkali-activated pozzolanic materials (geopolymers), a more contemporary green and sustainable substitute for ordinary Portland cement with a substantially smaller environmental imprint, have been developed to solve this (Nodehi & Taghvaee, 2022).

Diatomaceous earth is a naturally occurring pozzolanic substance that can be employed as a geopolymer resource, but little attention has been paid to it. There is therefore a substantial interest in using diatomaceous earth for other economical and environmentally sound usage.

1.3 Objectives of the Study

1.3.1 General Objective

To develop and evaluate the performance properties of diatomaceous earth-based geopolymer concrete incorporated with sisal fibres and high-density polyethylene (HDPE) wastes.

1.3.2 Specific Objectives

The specific objectives of the study are to:

i. Investigate the chemical, physical, thermal, and mineralogical properties of the diatomaceous earth from Gilgil, Kenya, as a raw material for making geopolymer concrete.
ii. Fabricate the alkaline activated diatomaceous earth-based geopolymer concrete mix that includes sisal fibres and HDPE wastes.
iii. Evaluate and optimize the mechanical, physical, and thermal geopolymer concrete's characteristics made of alkaline activated diatomaceous earth that has been reinforced with sisal and HDPE additives.
iv. Develop correlation and predictive models for the performance properties of the geopolymer concrete.

1.4 Justification of the Study

Globally, due to fast urbanization, industrialization, and population growth, there has been a huge demand for building materials during the last few decades, resulting in a chronic scarcity. Concrete made with Portland cement has been a major construction material used worldwide. Regrettably, the manufacture of ordinary Portland cement (OPC) contributes significantly to the greenhouse effect and the planet's warming by releasing massive volumes of CO_2 into the atmosphere. According to Silva et al. (2020),

the use of geopolymers in place of OPC could reduce CO_2 emissions by 89 % for every ton of OPC produced. To arrest the growth of global environmental issues, curbing greenhouse gas emissions and primary energy consumption in concrete production is among the efficacious strategies (Li et al., 2019). Therefore, efforts are needed to develop environmentally friendly construction materials.

Davidovits (2020) found that geopolymer cement had a good environmental reputation than Portland cement because its production needs no high-temperature kilns, significant fuel expenditures, or significant investments in machinery and infrastructure. Geopolymer concrete is fascinating due to the possibility that it can replace conventional Portland cement concrete in an environmentally responsible manner (El-Dieb, 2016; Lloyd & Rangan, 2009; Nurruddin, 2018) and can be created at low temperatures, with minimal energy, using a range of wastes as cementitious materials (SCM) or precursors (Ojha & Aggarwal, 2022; Schincaglia, 2022). Additionally, alumina-silicate materials are naturally abundant around the world and are found in various wastes and by-products.

Snellings et al. (2012) cite three benefits of adding cementitious materials to building and construction projects: financial savings from using less expensive pozzolans or industrial by-products in place of cement; reduced environmental impact from greenhouse gas emissions produced during cement production; and increased end-product sustainability. Due to its sustainability advantages geopolymer concrete has been dubbed the next generation of concrete (Qaidi et al., 2022).

Recycling waste plastic and agricultural waste is currently a common practice in the manufacturing industry because it is a great way to promote global sustainable

development (Jassim, 2017; Yu et al., 2018). The goal of sustainable development puts the built environment and construction industry in sharp focus.

1.5 Significance of the Study

This research will play a vital role in advancing green technology and the creation of sustainable building materials. This is because its focus is on appropriate technology (AT), which is now widely recognized. The choice of sustainable construction materials and design can be helpful in addressing economic social and environmental issues.

This work aims to make a major contribution in the study of the possibility and the interest to employ diatomaceous earth as a resource for geopolymer precursors in the synthesis of sustainable building concrete. The use of sisal fibres and the recycling of high-density polyethylene wastes through their incorporation into construction materials is such an efficient way to deal with the issue of waste disposal and energy-saving materials. Furthermore, for building materials, precise forecasting of attributes like compressive strength, water absorption, bulk density, and thermal conductivity can save money by minimizing laboratory work and reducing the amount of time and energy.

1.6 Scope of the Study

The viability of making geopolymer concrete using diatomaceous earth is the main emphasis of this study. The main focus of the work is an experimental inquiry to evaluate the mechanical, physical, and thermal properties of geopolymer concrete produced by alkaline activation of diatomaceous earth. The study also evaluates the effects of combining diatomaceous earth with sisal fibres and polymeric additives made of shredded high-density polyethylene on the functionality of the geopolymer; because

recycling waste plastic and agricultural residues is becoming a necessary approach in the manufacturing sector to support global sustainable development.

In this study, lime, sodium silicate, and sodium hydroxide are used as the alkaline activators of the precursor material (diatomaceous earth).

All of the raw materials were obtained in Kenya. To assess its potential as a geopolymer resource, the diatomaceous earth is characterized in respect to its chemical, physical, thermal, and mineralogical properties.

The research seeks to fabricate concrete specimens based on diatomaceous earth for examination and evaluation of performance qualities. Compressive strength, flexural strength, bulk density, water absorption, and thermal conductivity are the specific functional characteristics that the study focuses on. Additionally, performance properties are optimized in relation to mixture composition.

The study also develops precise and realistic predictive models linking the compositions of the concrete mixtures with the performance characteristics of geopolymers based on diatomaceous earth. Both linear and polynomial regression analysis techniques are applied, evaluated, and the optimal alternative is selected to achieve the modeling objective.

1.7 Outline of the Thesis

Chapter 1 introduces the concept of sustainable building materials in general and the importance of geopolymers in particular. A brief review of approaches to achieve sustainability in the production of building materials is also included. The need for examining diatomaceous earth as a potential geopolymer precursor and the incorporation of sisal fibres and HDPE wastes is explained.

Chapter 2 reviews the concepts of sustainable construction, geopolymer concrete and the geopolymerization process. The information that is accessible on the use of diatomaceous earth as a geopolymer resource for concrete is comprehensively presented; a thorough review of its physical, chemical, thermal, and mechanical properties is conducted. The performance parameters of the concrete incorporating diatomaceous earth and its inclusion status in the literature are summarized.

Chapter 3 describes the methodology used to attain the objectives set for this research. The experimental programs relating to raw material characterization, creation of geopolymer specimens, and performance property testing are described in detail.

Chapter 4 provides an analysis of the diatomaceous earth characterization results to assess if it is practical to use it as a geopolymer precursor. The findings of the investigation to ascertain how HDPE and sisal fibres influence the performance properties of lime-activated diatomaceous earth are discussed. Considering thermal conductivity, bulk density, water absorption, and compressive strength, the optimum raw material mix proportions and properties obtained are identified. To evaluate the effectiveness of the lime activation on the created geopolymer specimens, the established optimal property values are compared to the predetermined standard specifications for concrete masonry units.

Chapter 5 looks at replacing the lime activator with sodium hydroxide and sodium silicate alkaline activators and eliminating HDPE as proposed by the analysis in Chapter 4 to improve the performance properties of diatomaceous earth-based bricks. The compressive strength, bulk density, water absorption, thermal conductivity, and microstructure of the modified geopolymer specimens were evaluated.

Chapter 6 highlights the main findings of this research. The main conclusions are presented, and potential areas for further investigation are suggested.

Figure 1.5 depicts a summarized structure of this thesis.

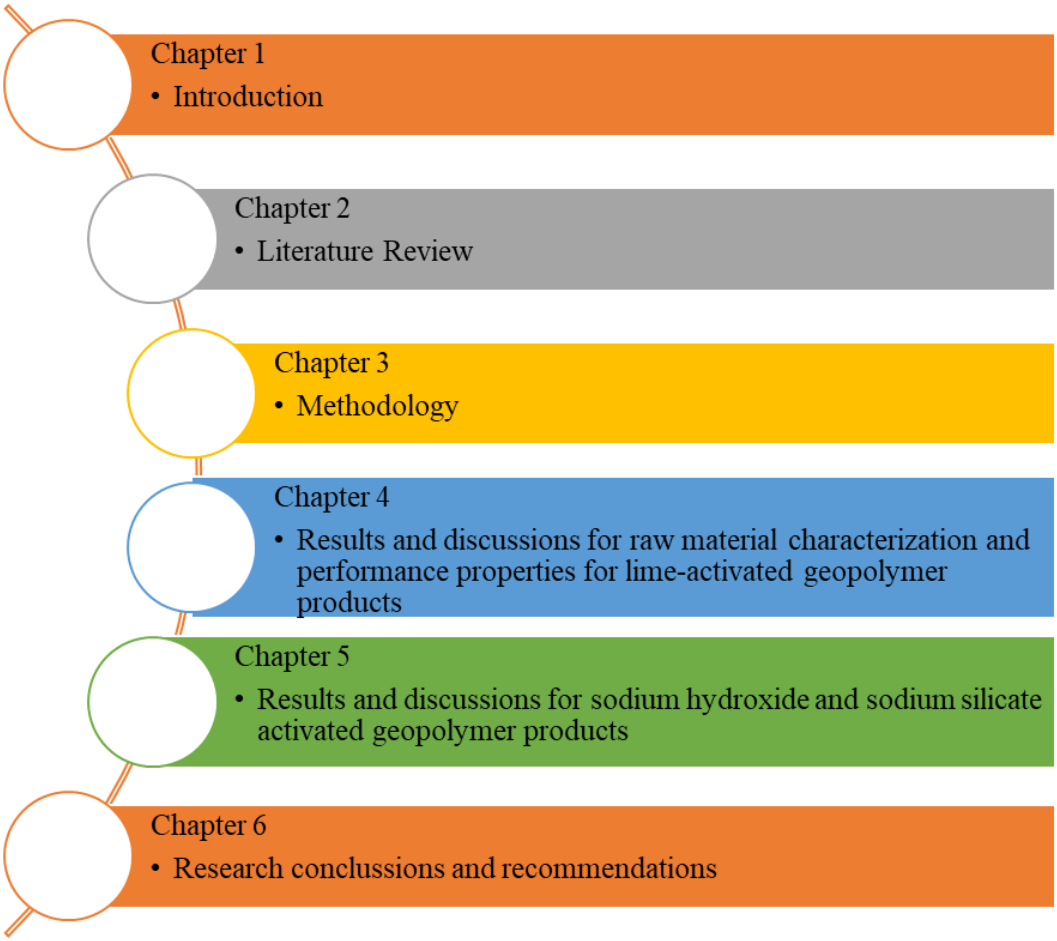

Figure 1.5: Thesis outline

CHAPTER TWO: LITERATURE REVIEW

2.1 Overview of Sustainable Building Materials

One of the most prevalent definitions of sustainable development, which has several variations, is that current generations shouldn't endanger the ability of future ones to meet their demands (Esparham, 2022). By incorporating the major dimensions of sustainable development: environmental, socio-cultural and economic, sustainable building is a more holistic strategy that should be pursued to address important concerns connected to urbanization, climate change, affordable housing, clean energy and poverty reduction.

One method for lowering environmental pollution and fostering sustainable development and economic growth is the utilization of waste material from manufacturing sectors as sustainable resources or recycled materials in rural structures and housing. This is attributable to the fact that construction projects have been estimated to consume over 40% of global energy and produce almost the same quantity of CO_2 as compared to the industrial and transportation sectors (Hung Anh & Pásztory, 2021; Pramanik et al., 2021; Yadav & Agarwal, 2021). Also, according to Rostami et al. (2015) building and maintenance have been considered the largest emitters of harmful gases like CO_2 and the eco-footprint will only grow with the large population growth expected by 2050. As per Maraveas's (2020) research on world population statistics, the human population has been steadily increasing, growing from 6.8 billion in 2009 to 7.7 billion in 2019 and a projected growth to 9.7 billion by 2050. As the population grows, the burden on existing social amenities like housing grows. The construction sector is constantly challenged to reduce its high energy consumption and environmental pollution because one of the fundamental issues of our time is meeting the needs of growing populations while preserving the integrity of vital ecosystems,

combating climate change, and fostering economic productivity and social inclusivity (Klopp & Petretta, 2017).

Construction materials now account for 40 to 50% of all materials used globally on an annual basis, up from 6.7 billion tonnes in 2000 to 17.5 billion tonnes in 2017. For instance, each year in the United Kingdom, 420 million tonnes of materials are used in buildings, equating to 7 tonnes per person (B. Huang et al., 2020). According to Ngui Joan Monthe (2021), the historic demand level of cement in Kenya, has forced cement manufacturers to increase their monthly production to 741,647 metric tonnes, which is also the highest in more than 10 years. As a consequence, construction materials must be used optimally to minimize their negative environmental effects, and energy consumption hence increasing the overall sustainability.

The inefficiency of today's building plans and constructions has created a serious environmental and societal challenge, not only in terms of optimal resource management and recycling but also in terms of high energy consumption and CO_2 emissions (Pramanik et al., 2021). The simplest method for designers to start incorporating sustainable ideas in building projects is to carefully acquire ecological building components (Aghdam et al., 2018).

Figure 2.1 describes the key factors considered in the selection of sustainable (green) building materials. According to Pramanik et al., (2021), the major factors to be considered include; reduction of greenhouse gases, energy efficiency, waste management efficiency, land efficiency, water efficiency and indoor environment improvement.

Figure 2.1: Selection criteria for sustainable (green) building materials (Pramanik et al., 2021)

It is anticipated that, soon, the civil engineering community will need to construct structures in line with the idea of sustainable development, using high-performance materials with minimal environmental impact that are manufactured at affordable prices (Bondar, 2009; Tramontin et al., 2012). Currently, the building industry has attracted criticism for unsustainable natural resource utilization and energy-intensive manufacturing methods (Dove, 2014). This is due to the overreliance on Portland cement-based concrete (Majhi & Nayak, 2020), estimated to have led to an annual global production of over 25 billion tonnes (Joshua et al., 2018; Koteng, 2013; Olofinnade et al., 2019). Limestone, gypsum, or shale deposits are potential sources of calcium carbonate-rich raw materials for cement. According to Favier et al. (2018) and

Ojha et al. (2022), the primary sources of CO_2 emissions during the manufacture of cement are as follows;

i. De-carbonation of limestone in the kiln (approximately 525 kg CO_2 / ton of clinker),
ii. Burning of fuel in the kiln (approximately 335 kg CO_2 / ton of cement),

Figure 2.2 shows a brief synopsis of the cement manufacturing process along with CO_2 emissions.

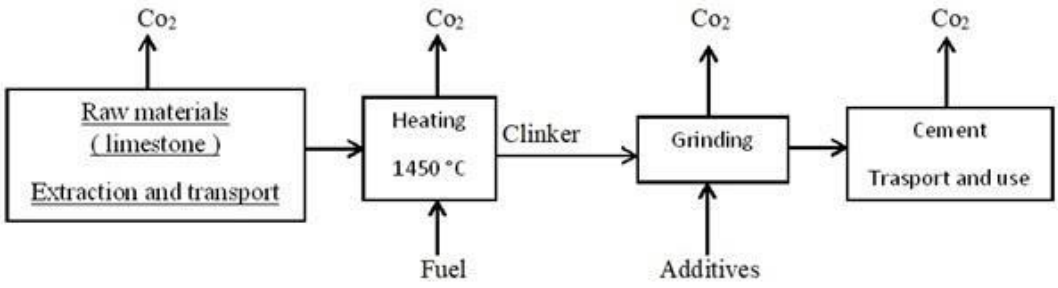

Figure 2.2: CO_2 emissions during cement manufacturing process

As social, economic, and environmental challenges in today's society evolve, there is an increasing demand for low-cost sustainable construction materials (Mostafa & Uddin, 2016). In that regard, sustainable concepts and practices have taken centre stage in several fields of study around the world; because human activities continue to threaten the carrying capacity of earth resources as well as life's basic requirements such as housing (Bediako & Frimpong, 2013).

Scholars have come up with different strategic approaches to developing sustainable concrete substitutes. The proposed sustainable strategies are;

1. Reducing the volume of cement in the concrete mix by partially replacing it with a supplementary cementitious material (H. S. Hassan et al., 2019; Islam et al., 2020).
2. Improving concrete durability to avoid the need for repairs (Busari et al., 2019).
3. Reducing the volume of natural aggregates in the concrete mix by replacing them with various types of waste to preserve natural resources and alleviate waste disposal issues (Pradena & César, 2022).
4. Utilization of concrete based on clinker-free cement (cementless concrete) also known as geopolymer concrete (Duxson et al., 2007).

Figure 2.3 shows a summary diagram representing different approaches to the production of sustainable concrete.

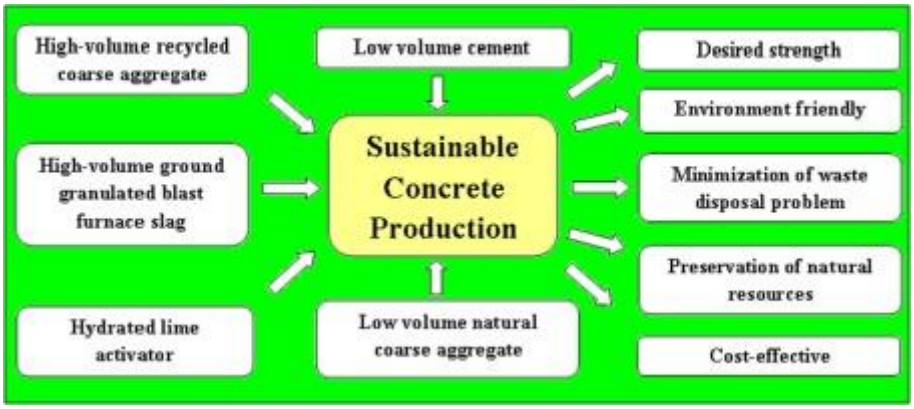

Figure 2.3: Sustainable concrete production approaches (Majhi & Nayak, 2020)

The geopolymer concrete technology seems to be an optimal concrete sustainability strategy because the Portland cement is replaced by alkali-activated aluminosilicate-rich materials.

2.2 Geopolymer Concrete as a Sustainable Building Material

2.2.1 Concept of geopolymer technology

Geopolymer is a term that combines the prefix "geo," which in Greek means "earth," with the word "polymer," which refers to the material's structure, that is made up of different Al and Si monomers (Castillo et al., 2022). Al and Si are both abundant in the earth's crust.

Geopolymer materials are inorganic polymers created by activating pozzolanic minerals, which contain silica and alumina, with alkali or acid solutions. Alzeer & MacKenzie (2013) define geopolymer concrete as ceramic-like materials prepared at low temperatures by reacting natural aluminosilicates (clays) or aluminosilicate wastes (fly ash and blast furnace slag) with alkalis or acids.

Geopolymers occasionally function as zeolitic precursors due to their three-dimensional (3D) tetrahedron structure, which is created by aluminates and silicates (Castillo et al., 2022). Geopolymers have an amorphous structure, but zeolites have a structured crystalline form. In order to achieve the crystalline structure, zeolites are also formed at greater pressures and temperatures (above 100°C and approximately 200 kPa, respectively).

According to Wan Ibrahim et al. (2015), geopolymerization is a type of geosynthesis in which aluminosilicate materials, such as fly ash, blast furnace slag, or thermally activated substances, are exposed to high-alkaline environments (hydroxides, silicates), resulting in the creation of a geopolymer (Wan Ibrahim et al., 2015). When Si-Al minerals are subjected to a significantly quick chemical reaction in a very alkaline environment, a three-dimensional polymeric chain and ring structure made of Si-O-Al-O linkages occurs (Davidovits, 2020); resulting in products such as sodium

aluminosilicate hydrate (N-A-S-H) gel or calcium aluminosilicate hydrate (C-A-S-H) gel, which induce the geopolymers' hardening mechanism and create materials with remarkable durability and structural strength as well as a reduction in greenhouse gas emissions (Abd Razak et al., 2021; Aziz et al., 2019).

Geopolymers have received attention in the building sector due to their high compressive strength, constant volume, low permeability, and robust resistance to high temperature (Castillo et al., 2022) . It is expected that by manufacturing geopolymer construction materials that have less carbon emissions, the escalating fears about global warming caused by carbon dioxide emissions (CO_2) from the typical Portland cement industry can be reduced (Duxson et al., 2007; Ojha & Aggarwal, 2022).

Geopolymer concretes are gaining popularity because they have comparable strength to Ordinary Portland Cement (OPC) based concrete, low shrinkage, acid resistance, low thermal conductivity, and flexible curing rates, while their manufacturing process is more energy efficient and has a lower environmental impact because they are manufactured at room temperature and emit about 80% less CO_2 (Anthony, 2009; Bagci et al., 2017; Cong & Cheng, 2021; Font et al., 2018; Korniejenko et al., 2016). According to Mackenzie & Welter (2014), geopolymer concretes, have superior mechanical strength, good thermal stability >1000°C, and the brittle failure that is characteristic of ceramics. Because of their low processing temperature, they open up new opportunities for the synthesis of ceramic-like composite materials.

The basic steps in the geopolymerization process are the dissolution of solid aluminum-silicate oxide in an M-OH solution, where M is an alkali metal (commonly Na and K); the dissolution of aluminum and silicon interparticle space complexes; the formation of a gel phase through polymerization between silicate solution and aluminum and silicon

complexes; and the final hardening of the gel phase (Abd Razak et al., 2021; Aziz et al., 2019).

From a chemical reaction standpoint, when an alkali hydroxide such as sodium hydroxide (NaOH) or potassium hydroxide (KOH) is exposed to the aluminosilicate compound, it results in the dissolution and hydrolysis of aluminium and silicon as presented in Figure 2.4.

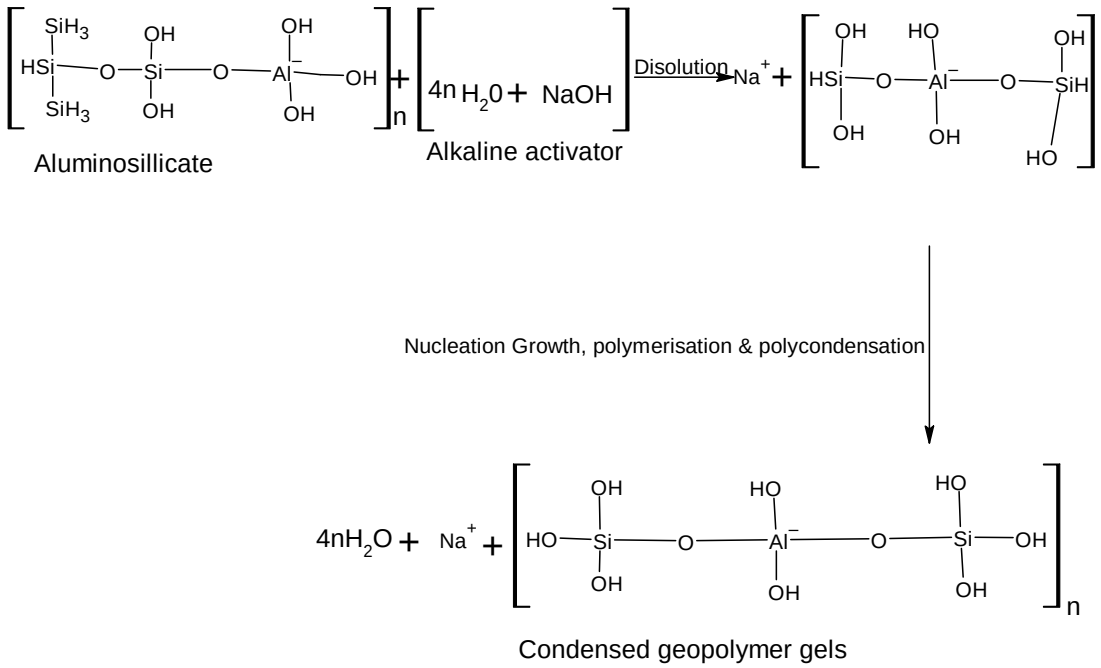

Figure 2.4: Geopolymerization process.

The ion exchange, hydrolysis, network disintegration, and release of Si and Al are the first four processes in the dissolution of an aluminosilicate-based geopolymer cement (Matalkah et al., 2017). With the mere addition of an alkaline activator, these dissolution and breakdown phenomena trigger subsequent speciation, gelation, reorganization, and polymerization processes that result in the solid alkali aluminosilicate hydrate as depicted in Figure 2.5.

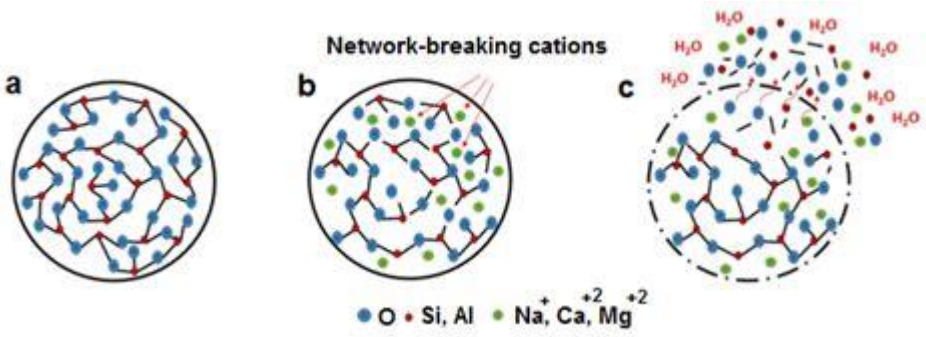

Figure 2.5: Hydration of aluminosilicate geopolymer precursors (Matalkah et al., 2017).

The particles are attacked by the alkaline solution from both the inside out and the outside in, which causes the particles to split open and reveal smaller particles that are either hollow or partially filled (Al-Bakri Abdullah et al., 2012). The procedure will continue until all of the particles have been consumed.

In summary, geopolymerization is a four-step process (Abd Razak et al., 2021; Davidovits, 2020), and is presented in Figure 2.6.

i. Alkaline solution-based dissolution,
ii. Diffusion and reorganization of dissolved ions along with the development of tiny coagulated structures
iii. Soluble species polycondensation to create gel phase (hydrated products).
iv. The gel phase hardens due to the exclusion of excess water to form a geopolymer product

The geopolymer matrix is based on a poly(sialate) Si-O-Al-O framework structure, with alternating SiO_4 and AlO_4 tetrahedra connected in three orientations by sharing all the oxygen atoms (Davidovits, 2020).

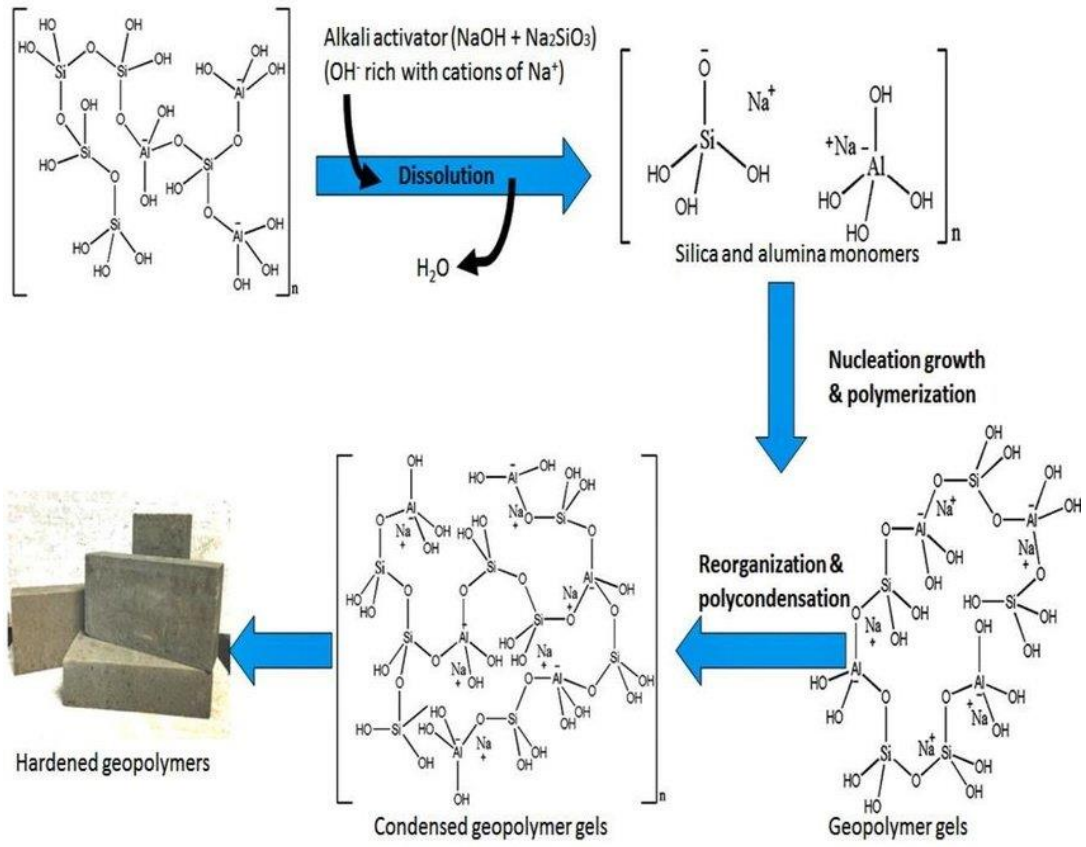

Figure 2.6: Geopolymerization process (Abd Razak et al., 2021)

This reaction results in the release of water, which is typically spent upon dissolution and gives the mixture workability during handling; this contrasts with the chemical reaction that occurs when water is added to Portland cement during the hydration reaction, where heat is released and water is absorbed (Ev et al., 2018).

Figure 2.7 illustrates the chemistry of hardening for both the ordinary Portland cement concrete and the geopolymer concrete.

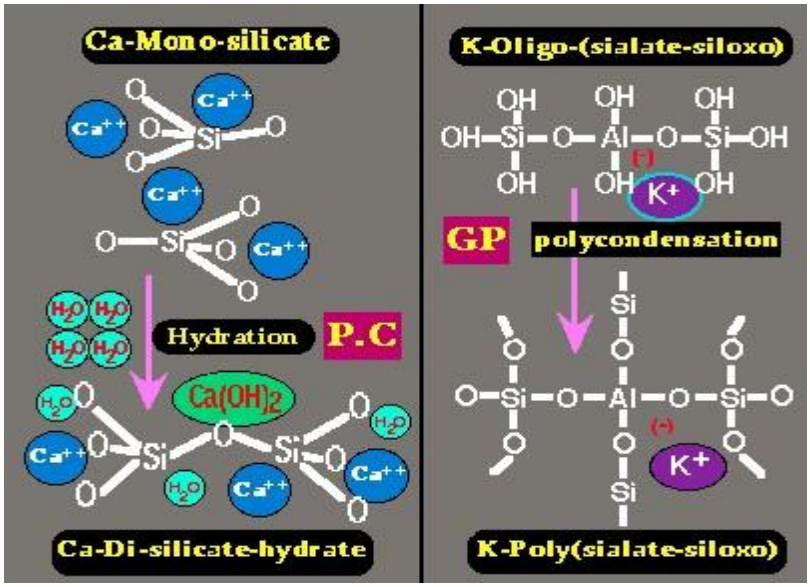

Figure 2.7: Chemistry of Portland cement and geopolymer cement (Barnard, 2014)

Classifications of geopolymers

Geopolymers can be generically categorized as acid-activated and alkali-activated geopolymers, as shown in Figure 2.8.

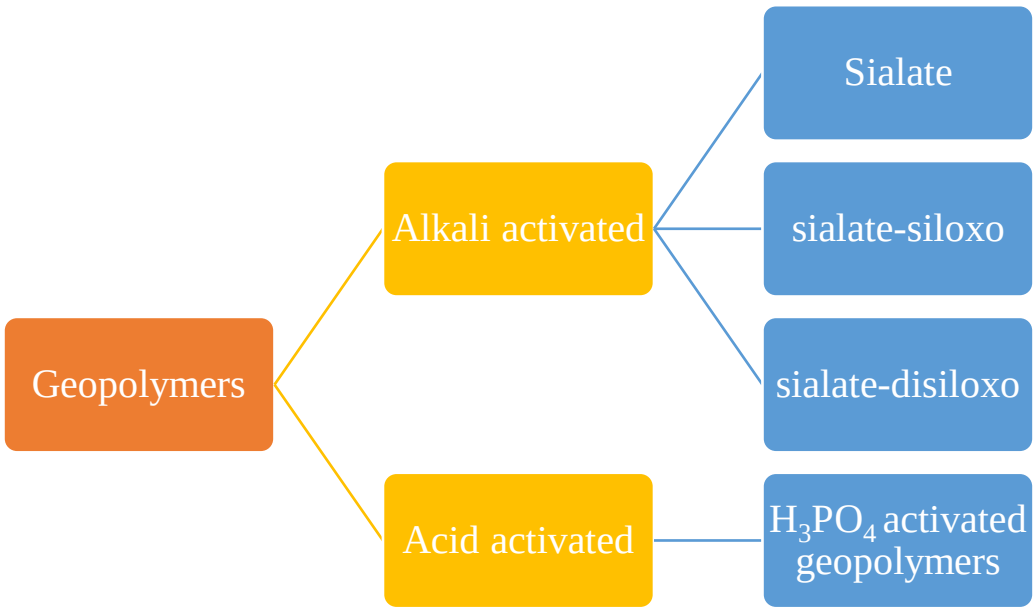

Figure 2.8: Geopolymer classifications

Alkali activated geopolymers, according to Irfan Khan et al. (2014) have drawn a lot of attention in the last forty years due to excellent characteristics over regular Portland cement. An alkali activated geopolymer can take on one of the following three basic forms depending on the alumino silicate matrix:

- Poly(sialate), which has [-Si-O-Al-O-] as the repeating unit.
- Poly(sialate-siloxo), which has [-Si-O-Al-O-Si-O-] as the repeating unit.
- Poly(sialate-disiloxo), which has [-Si-O-Al-O-Si-O-Si-O-] as the repeating unit.

Sialate is an acronym for silicon-oxo-aluminate, a material whose network comprises of SiO_4 and AlO_4 tetrahedra linked alternatively by sharing all of the oxygens. Alkali cations (usually Na^+ and/or K^+) are required to counteract the AlO_4's negative charge (Mucsi & Ambrus, 2018).

Figure 2.9 : Types of poly (sialates) illustrates the different types of poly (sialates).

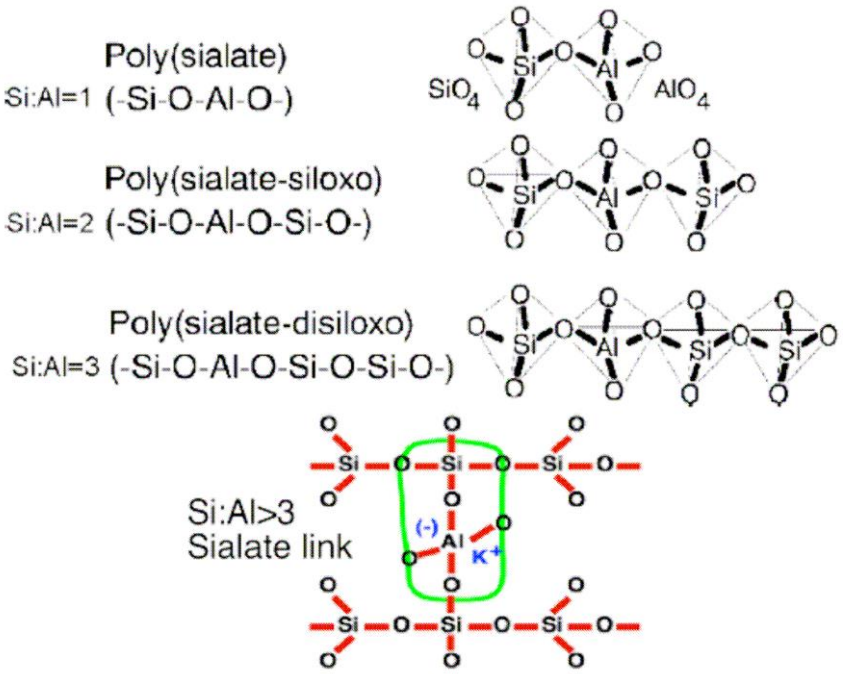

Figure 2.9: Types of poly (sialates) (Davidovits, 2005)

Benefits of geopolymer concrete

Further to being a better option for the environment than conventional Portland cement concrete, geopolymer concretes significantly reduces the carbon footprint of cement production by relying on minimally processed natural materials or industrial waste products. It is also remarkably resilient to many common problems with concrete durability. Generally, the advantages of geopolymer concrete are shown in Figure 2.10 and as summarized by Aziz et al., (2019).

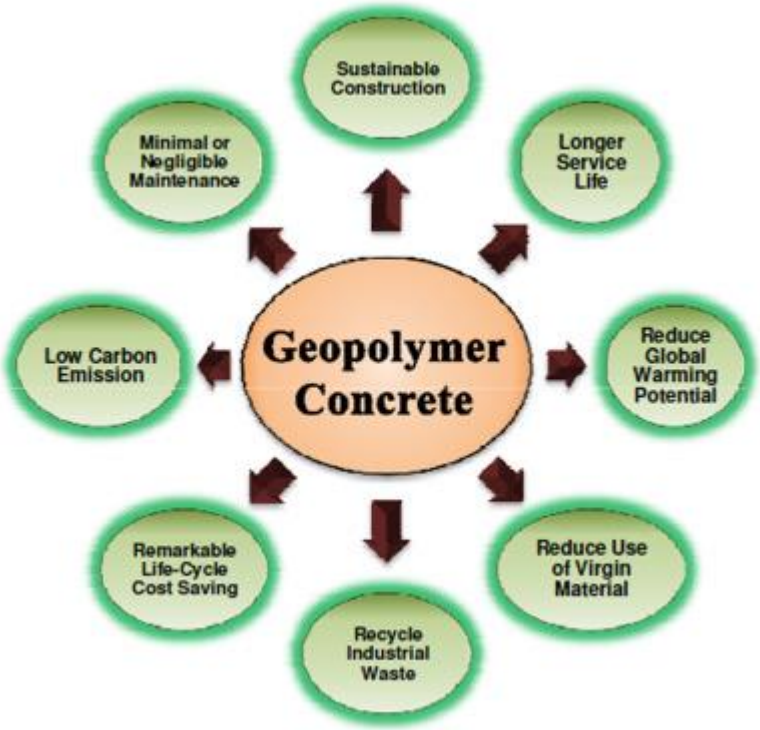

Figure 2.10: Advantages of geopolymer concrete

According to Song et al. (2005), the total CO_2 emission level in geopolymer concrete is theoretically 10 times lower than pure Portland cement concrete in terms of CO_2 emission per unit volume of concrete.

The major geopolymer concrete limitation is that it has poor frost resistance, and the freezing-thawing limit is less than 75 times (Lingyu et al., 2021).

2.2.2 Geopolymer concrete precursor materials

Active silica-rich compounds have been shown to be a suitable substitute for Portland cement when used as supplemental cementitious materials (SCMs) (Pokorný et al., 2016). Particularly, pozzolanic materials have been key research interests in the investigation of cement and geopolymer materials to minimize consumption and dependency on Portland cement (Danso H & Adu S, 2019). Pozzolans are frequently used as a cement substitute in Portland cement concrete due to their beneficial properties, which include cost savings, decreased heat evolution, decreased permeability, control of alkali-aggregate expansion, increased chemical resistance, decreased concrete drying shrinkage, and improved properties of fresh concrete (Chihaoui et al., 2022).

Silicate (Si) and alumina (Al) content is one of the requirements for the raw material to be utilized in the production of geopolymers, and the greater the silicate and aluminum content, the more effective the geopolymers will be (Azimi et al., 2015).

Figure 2.11 highlights the components of the geopolymer system as compiled by Payá et al. (2018).

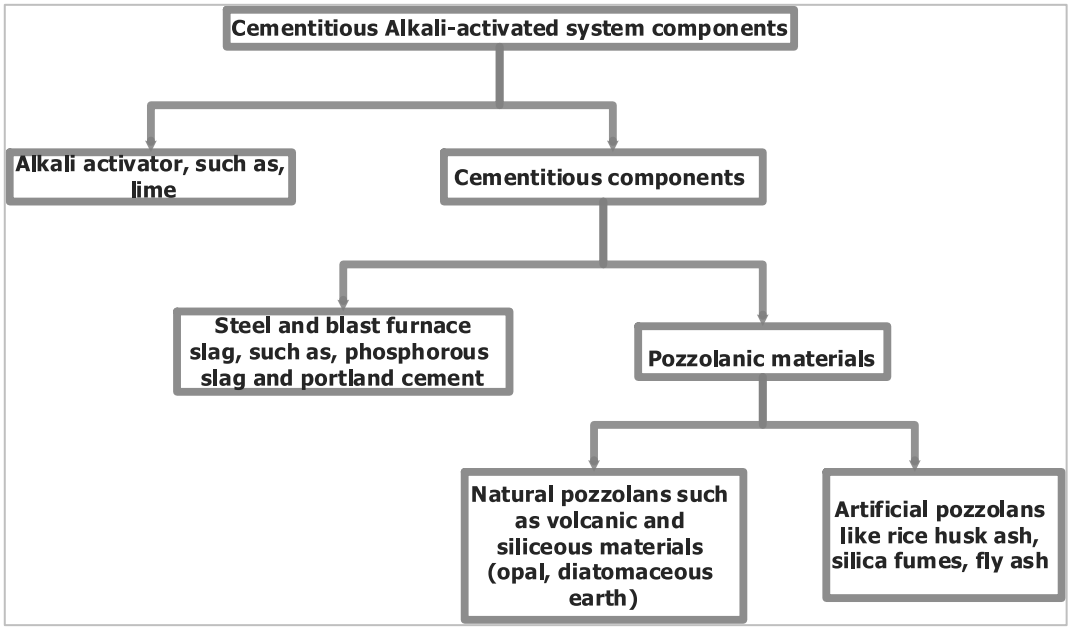

Figure 2.11: Geopolymer system's components.

Categories of raw materials for geopolymerization

i. Primary raw materials

Natural minerals are the primary material sources. Since Al-Si minerals make up more than 65 % of the earth's crust, there are a lot of different and abundant resources that can be used (Mucsi & Ambrus, 2018). Over the past few decades, researchers have studied the geopolymerization of a variety of Al-Si minerals and clays, primarily kaolinite and metakaolin (Balczár et al., 2016).

ii. Secondary raw materials

Industrial wastes and byproducts can also be used as raw materials to produce geopolymers in a way that is eco-friendlier and protects natural resources (Mucsi & Ambrus, 2018). Fly ash and slag are among the most often utilized and researched resources among secondary raw materials.

iii. Wastes and by-products of mineral origin

These materials originate from natural phenomena, but the process of production turns them into wastes. Perlite is one such example. It is utilized as a water absorbent in

agricultural applications, but when its final porosity or particle size are insufficient for future use, it is deemed waste.

Geopolymer precursor materials need to be rich in alumina (Al_2O_3) and silica (SiO_2) because of the significant roles that they play in the hardening of geopolymers and their interactions with other elements to create the N-A-S-H gel, which gives the substance its unique strength (Castillo et al., 2022). In general, various wastes, such as those from mines, power plants, municipalities, and any other sources of aluminosilicate that are currently produced in large quantities worldwide, can be used to create cementitious materials for use in structural concrete, and resistant coatings (Esparham, 2022).

Numerous substances have already been studied as precursors in geopolymer concrete mixtures (Barnard, 2014), including;

- Class F fly-ash (low amount of calcium)
- Class C fly-ash (high calcium content)
- Calcined kaolin or metakaolin
- Natural minerals containing Al and Si
- Silica fume
- Slag
- Red mud
- Albite

Rangan et al. (2005) point out that the chemical properties of geopolymer precursor materials are similar to those of naturally occurring zeolitic materials. Figure 2.12 presents a ternary diagram consisting of some cementitious materials.

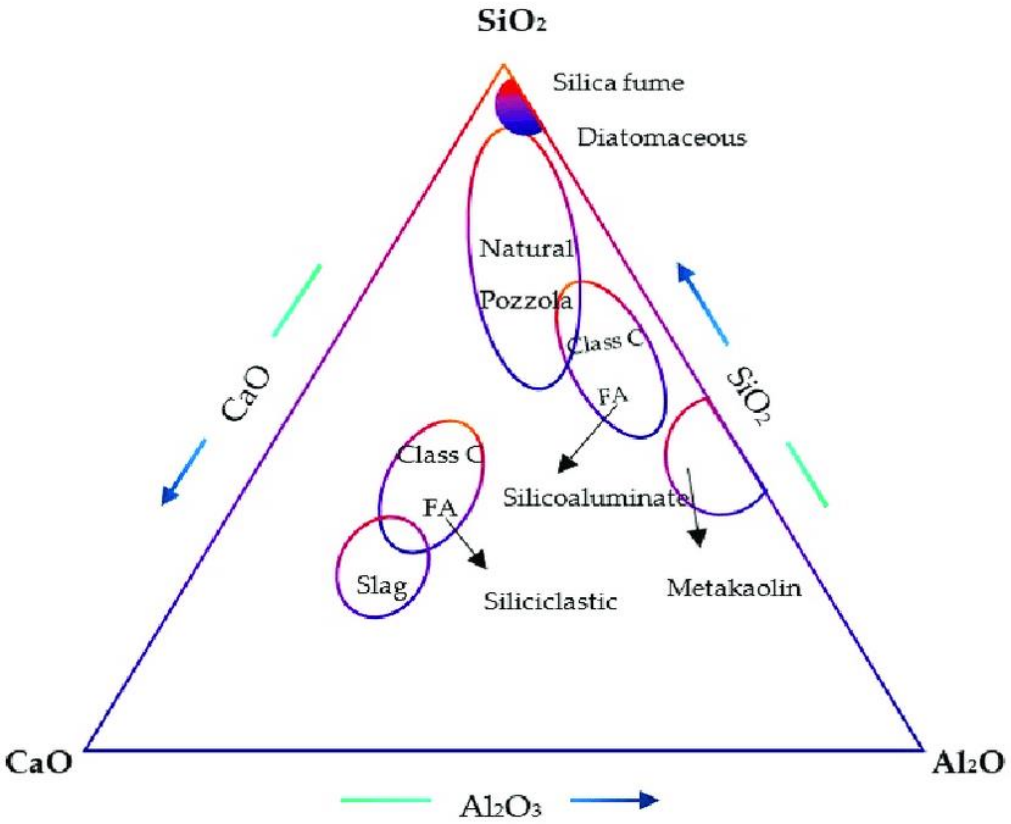

Figure 2.12: $CaO–Al_2O_3–SiO_2$ ternary diagram of cementitious materials (Milad et al., 2021)

In accordance with ASTM C618 (2014) standards, the raw materials for geopolymer are first examined for pozzolanic content. As of Nodehi et al. (2022) and Mohammed et al. (2021), the most common aluminosilicate sources (precursors) that have been used in experimental investigations are fly ash, ground granulated blast furnace slag, metakaolin, and rice husk ash, palm oil fuel ash (POFA), waste bottle glass (WBG), sugarcane bagasse ash (SCBA) and ceramic dust waste. Particularly, the production of environmentally friendly composites employing by-products such as class F fly ash and ground granulated blast-furnace slag (GGBFS) has been widely explored, resulting in the development of Portland cement-free construction materials.

Depending on the type of precursor material utilized during concrete production, there are four different geopolymer categories according to Barnard (2014), including:

i. **Slag-based geopolymer**- Slag is a byproduct of melting iron ore that is partially transparent and typically made of a combination of metal oxides and silicon dioxide.

ii. **Rock-based geopolymer-** Natural rock-forming materials, either calcined or uncalcined, and an appropriate alkali silicate make up rock-based geopolymer cement.

iii. **Fly ash-based geopolymer**- Fly ash is divided into two groups, namely: **type F** fly ash and **type C** Fly ash. Class F and class C fly ashes are commonly used as cement partial replacement material due to its pozzolanic characteristics. The primary difference between class F and class C fly ashes is the Calcium (Ca) content where class F fly ash has Ca less than 10%, while Ca content in class C fly ash is higher than 10% (Wardhono, 2018). Geologically younger coal creates type C fly ash, which is rich in calcium and has 20% or more CaO, whereas older coal produces type F fly ash, which is low in calcium and has a CaO value of less than 10% and is a pozzolan (Hardjito & Rangan, 2006). Because fly ash with a high calcium contentmay interfere with the geopolymerization process, low calcium fly ash is typically preferred to high calcium fly ash (Aziz et al., 2019; Barnard, 2014; Davidovits, 2005).

iv. **Ferro-sialate-based geopolymer**- This form of geopolymer has similar qualities to rock-based geopolymers but contains geological components with a high iron oxide content, giving the geopolymer a red colour (Davidovits, 2005).

An overview of the main raw materials utilized for geopolymer synthesis is provided in Table 2.1.

Table 2.1: Raw materials for geopolymer production

S/N	Raw material	Proportion	Application
1.	FA	100%	Construction concrete
2.	MK	100%	Construction concrete
3.	(POFA+GBFS): FA	POFA+GBFS: FA=1.8	Construction concrete
4.	GBFS+FA	GBFS= 30-55%	Construction concrete
5.	Steel Slag	100%	Photo catalysis
6.	Volcanic Ash	100%	Construction concrete
7.	Rice husk Ash	1-10%	Construction concrete

The study of siliceous rocks for use as geopolymer raw materials have gained interest since it has amorphous active silicon dioxide, which increases chemical activity, has a fine-porous structure, is lightweight, and has a low thermal conductivity (Ivanov & Belyakov, 2008). The applicability of diatomaceous earth according to Payá et al. (2018) and Milad et al. (2021) demonstrated that it is a naturally existing pozzolanic substance that finds use in the building and construction industry. Besides, diatomaceous earth is a prevalent industrial by-product nowadays since it is used as a filtration agent by many industries.

In order to create geopolymer materials, minerals containing amorphous silica (SiO_2), such as diatomaceous earth are useful and appealing resources (Dobrosielska et al., 2021; Mejia, 2015; Reka et al., 2017; Sharma et al., 2021). As a result, they can provide the building industry with a sustainable future. The key to using diatomaceous earth (DE) as a geopolymer, is alkali activation of the amorphous silica, which involves dissolving the DE to release Si^{4+}, resulting in silicon hydroxide ($Si(OH)_4$) or complex silicate ions ($Si(OH)^{5-}$ or $HSiO^{3-}$) at ambient temperatures, generating strong and durable products (Anthony, 2009).

Diatomaceous earth (DE), also called diatomite or Kieselguhr, comes from deposits created by the accumulation of fossilized, siliceous diatom skeletons (Galal Mors, 2010). Diatomaceous earth deposits with both marine and lacustrine origins are mined commercially all over the world, according to Hoffman (2006). Massive accumulations of fossil diatom frustules have reportedly been discovered in volcanic and hydrothermally active areas, including Yellowstone Lake in the United States, Lake Myvatn in Iceland, Lake Challa in Tanzania and Kenya, among others. In Kenya, Washbourn-Kamau (1971) determined that diatomite is found in the Nakuru-Elmenteita basin near Kariandusi, and across much of the basin up to an altitude of around 1930 m, more than 150 m above the existing lakes.

2.2.3 Geopolymer alkaline activators

Lime-based activations as compared to other chemical solutions, have been discovered to be potential sustainable approaches for developing cement-free building materials considering material cost and workability (Jeong et al., 2016; Kang et al., 2019; Wang et al., 2018; K. H. Yang et al., 2012). Lime pozzolan concrete was used by many ancient societies, and it is regaining popularity as an environmentally benign cement alternative for masonry and concrete applications (Bondar, 2009; PAVÍA & WALKER, 2010) due to its greater availability, inexpensive production method, and application simplicity (H. Zhang, 2011). According to Song et al. (2005), the slag study began many years ago with the inclusion of (5 - 8) % caustic soda to the slag slurry, and the resulting concrete was superior to Portland cement concrete. Other studies (Ciancio et al., 2014; Fopossi et al., 2014; Jules et al., 2018; Nahar, 2018; Oti et al., 2009; Riza et al., 2011) have shown that pozzolanic reactions, such as lime activation, occur when pozzolanic minerals are combined with lime in the presence of water to create cementitious compounds. Natural pozzolana minerals comprising silica and alumina have a great

potential to achieve the desired outcome when quicklime (CaO) or hydrated lime (Ca $(OH)_2$) is utilized for lime activation (Makusa, 2012; Vejmelková et al., 2012).

Ideally, any alkali or alkali earth cation such as alkali hydroxide (MOH), non-silicate salts of weak acids (M_2C0_3, M_2S0_3, M_2S, M_3P0_4, and MF), non-silicate strong acid salts (M_2S0_4), and silicate salts ($M_20.nSi0_2$) can be utilized as the alkali element (M) (Abd Razak et al., 2021). Bondar (2009) pointed out that for the silicon and aluminium ions in the source materials to dissolve and create the geopolymer paste, high-alkaline solutions are utilized. Because the reaction between solid aluminosilicates and a very concentrated aqueous alkali hydroxide or silicate solution yields a synthetic alkali aluminosilicate substance (geopolymer), which has special qualities and traits, such as high compressive strength, high-temperature stability, and low thermal conductivity (Abd Razak et al., 2021; Aziz et al., 2019).

The most extensively used chemicals used as geopolymer alkaline activators are NaOH, Na_2C0_3, Na_2Si0_3, and Na_2S0_4 (Bondar, 2009). In earlier investigations, the activators Na_2SiO_3 and NaOH were frequently combined (Aziz et al., 2019; Cong & Cheng, 2021). It has also been demonstrated that when cation size increases, the significance of the cation-anion pair interaction decreases. Smaller silicate oligomers, such as silicate monomers, dimmers, and trimers, respond favorably to the ion-pair reaction when the cation is of a smaller size. As a result, it can be anticipated that smaller-sized Na^+ will be more active in reactions than K^+, which should lead to a greater degree of mineral dissolution in the NaOH solution.

2.3 Diatomaceous Earth as a Pozzolanic Opal Mineral

Opal is a hydrous silica mineral that occurs naturally in a variety of low-temperature surface and near-surface conditions and exhibits various degrees of structural disorder

(Yuan et al., 2019). A group of amorphous and paracrystalline silica species with up to 20% molecular water (H_2O) or silanol (R_3SiOH) or both are collectively referred to as opals (Curtis et al., 2019). Opals differ in terms of crystallinity level and arrangement of crystals. Based on the mineralogical composition, atomic arrangements and the primary component detected by X-ray diffraction (XRD), Fourier infrared spectroscopy (FTIR), Raman spectroscopy, and other techniques, opals can be categorized into three groups (opal-C, opal-CT, and opal-A), where A, C, and T signify amorphous, cristobalite, and tridymite, respectively (Ejigu et al., 2022). Opal-C is a silicate that is well-ordered and mostly composed of α-cristobalite; opal-CT is semi-crystalline and composed of crystalline sections of α-cristobalite and α-tridymite (commonly referred to as "common opals"); and opal-A is the least ordered variety (Smallwood et al., 2008). Opal-A is subdivided into two further categories; opal-AN and opal-AG (Smallwood et al., 2008). Opal-AN, an opaline silica, is created during the quenching of high-temperature silica fluids, and it is subsequently deposited on volcanic rocks as thin botryoidal crusts. Opal-AG is an opal that is created from a solution through the gradual concentration of silica and subsequent precipitation of colloidal particles.

Opal-A is the amorphous silica found in biogenic siliceous sediments (Mustoe, 2005). "Biogenic opal-A" is a term used to describe the natural opal that results from the mineralization of several common Si-bearing organisms, like diatoms and sponges (Yuan et al., 2019). Opal-A, opal-CT (microcrystal cristobalite and tridymite), quartz, and montmorillonite are the principal minerals in natural pozzolana opal shale (Jia & Wang, 2017); High active silicon dioxides have been discovered to exist in both opal-CT and opal-A.

Diatomaceous earth is a type of almost pure sedimentary silica rock that is composed predominantly of opal and is found in tertiary to recent lacustrine and marine

sedimentary depositional environments all over the world (Hanane et al., 2022; Lutyński et al., 2019). The U.S. Geological Survey (2023), reported that an estimated 36 % of the world's total diatomite production was produced in the United States in 2021, followed by Denmark with 17 %, Turkey with 9 %, China with 6%, Argentina, Mexico, and Peru with 4% each. Kenya was one of the countries that mined the remaining 20% of the overall production of diatomite.

The diatomaceous earth sediments are very siliceous, fine-grained, and largely composed of amorphous opaline silica with trace amounts of secondary minerals, non-diatomaceous debris, and organic waste (Hoffman, 2006). Many scientists thought that the formation of diatomite occurred after lake sediments were drawn into crevices on the flanks of volcanoes and later ejected during eruptions; the weathering of volcanic glass was the source of soluble silica (Mustoe, 2005).

The opal-A-rich earth materials can be categorized as clayey and/or marly diatomite if they contain considerable concentrations of clay minerals and micas (Stefanou et al., 2022). According to Conley et al. (2015), diatomaceous opal-A is the product of the aggregation and compaction of fossilized diatom remnants throughout geological time (Conley & Carey, 2015). However, diagenesis can easily modify diatomaceous opal-A rocks, to opal-CT and/or chalcedonic quartz (Stamatakis et al., 2010; Stefanou et al., 2022). Figure 2.13. describes the process and the effects of diatomaceous earth diagenesis.

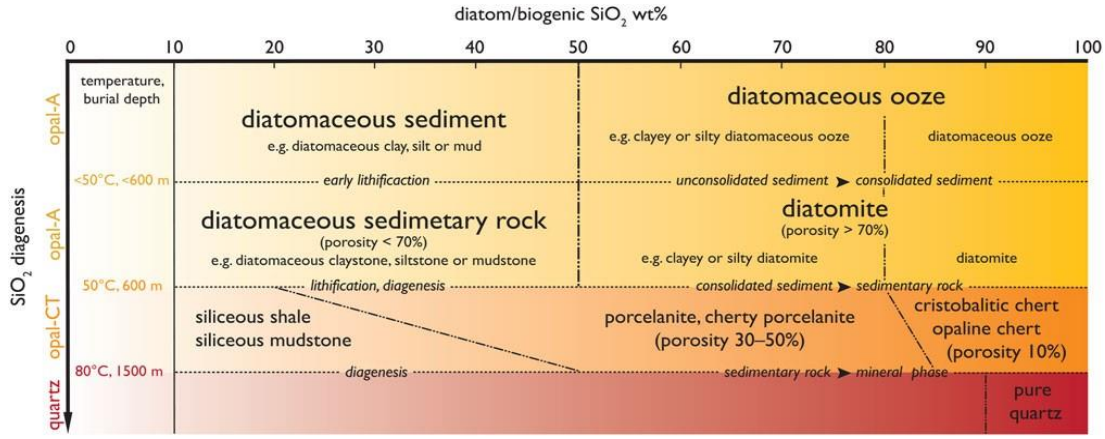

Figure 2.13: Process of diatomaceous earth diagenesis (Zahajská et al., 2020)

Diatomaceous samples with a predominance of opal-CT can be categorized as porcellanitic or porcelaneous diatomite; porcelaneous diatomite is connected to the diagenetic alteration of opal-A-rich diatomite beds (Stefanou et al., 2022). A schematic description of diagenetic changes in the geophysical and mechanical characteristics of siliceous rocks is shown in Figure 2.14.

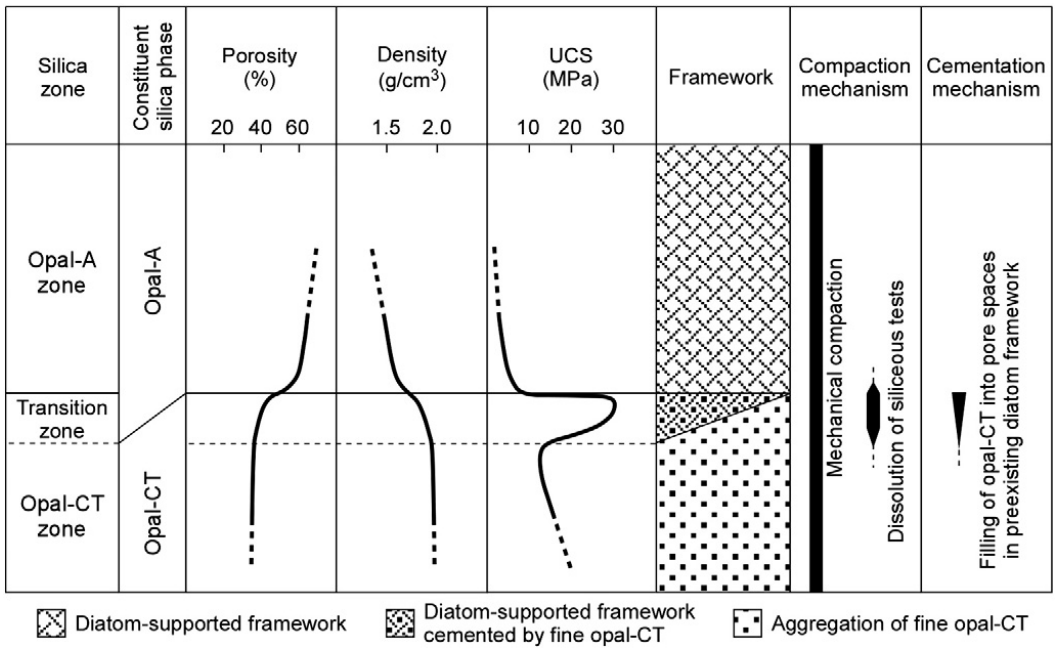

Figure 2.14: Diagenetic changes in the geophysical and mechanical properties of siliceous rocks (Ishii et al., 2011).

According to Yuan et al. (2019), rocks rich in diatomaceous opal are attracting a lot of research interest, as geopolymer precursors due to their high porosities, which are

derived from the original porosity of the diatom frustules. The most researched variety of biogenic opal-A comes from diatoms, a type of single-celled algae (Yuan et al., 2019).

2.4 Diatomaceous Earth Characterization

Diatomaceous earth is a mineral having a low density of 0.25 to 0.50 ton/m^3, a high silica concentration of 60 to 97 %, and an amorphous porous structure (Hoc Thang, 2020). Diatomite was described by Hasan et al. (2020) as microparticles that can be utilized in the replacement of cement in concrete manufacture, despite the fact that its structure and silica content vary widely from one source-point to another. In addition to having a high silica (SiO_2) content, diatomaceous earth also has a high permeability of (0.1–10 mD) and a porosity of (35–65 %), making it permeable, soft, and feeble (Bogoevski & Boskovski, 2014; Reka et al., 2021; Stefanou et al., 2022).

Diatomaceous earth possesses exceptional engineering characteristics, such as a large specific surface area, a low dry density, a high friction angle, a high compressibility, and an unstable reaction to dynamic stresses (Lee, 2014). An important characteristic of diatomaceous earth's use in construction is the material's high concentration of amorphous SiO_2 and associated pozzolana activity (Miller et al., 2010; Reka et al., 2017).

Ojha & Aggarwal (2022) claim that a material with pozzolanic characteristics such as a low calcium content, a high vitreous phase, 80–90% of particle sizes that are less than 45 μm, 5% of unburned material, more than 40% reactive silica, and less than 10% Fe_2O_3 content, results in the best binding properties.

a) Chemical composition

Silica is the most important oxide that should be present in the base material of a geop olymer since it is essential for the alkaline activation of geopolymers (Okeyinka et al., 2019). According to Yuan et al. (2019), amorphous silica makes up the inorganic portion of a diatom frustule (Yuan et al., 2019).

Mehmedi et al. (2012) and other related researches report that 67.80 % to 90.07 % of natural diatomite's chemical components include silica (SiO_2), 0.62 % to 10.30 % alumina (Al_2O_3), 0.20 to 6.85% iron oxide (Fe_2O_3), 0.05 % to 1.21 % titanium oxide (TiO_2), 0.04 % to 0.21% phosphate (P_2O_3). Calcium oxide (CaO), magnesium oxide (MgO), sodium oxide (Na_2O), and potassium oxide (K_2O) are all present in varying amounts, ranging from 0.19 % to 3.0 %, 0.11 % to 1.64 %, 0.13 % to 0.97 %, and 0.13% to 1.47 %, respectively.

A summary of the chemical components of natural diatomite from a few selected nations is shown in Table 2.2. The table demonstrates that diatomite varies by geographic location, as stated by Hasan et al.(2020).

Table 2.2: Chemical components of diatomite from some elected nations (Hoffman, 2006)

Constituent, %	**Nevada***	**Oregon***	**California†**	**Denmark**	**Spain†**	**Mexico†**	**Chile**	**China**
Silica (SiO_2)	89.75	87.92	89.70	67.80	88.60	91.20	89.68	90.07
Alumina (Al_2O_3)	3.08	3.66	3.72	10.30	0.62	3.20	2.18	1.98
Iron oxide (Fe_2O_3)	1.33	1.37	1.09	6.85	0.20	0.70	0.38	0.67
Titanium oxide (TiO_2)	0.14	0.29	0.10	1.21	0.05	0.16	0.05	0.09
Phosphate (P_2O_5)	0.04	0.05	0.10	0.21	na	0.05	0.04	0.06
Lime CaO)	0.41	0.52	0.30	1.35	3.00	0.19	0.41	0.39
Magnesium (MgO)	0.11	0.15	0.55	1.64	0.81	0.42	0.31	0.28
Sodium (Na_2O)	0.19	0.56	0.31	0.46	0.50	0.13	0.97	0.22
Potassium (K_2O)	0.22	0.13	0.41	1.47	0.39	0.24	0.45	0.35
Ignition loss	4.70	5.15	3.70	7.91	5.20	3.60	5.90	6.30
Total	99.97	99.80	99.98	99.20	99.37	99.89	100.37	100.41

na = not available.

The Nitrogen Adsorption Isotherm, X-Ray diffraction, Scanning Electron Microscopy, Transmission Electron Microscopy, Zeta potential, Thermal Gravimetric Analysis (TGA), and atomic absorption spectrophotometry are examples of modern analytical techniques (Kumari & Mohan, 2021). Fourier-Transform Infra-Red (FT-IR) (Benayache et al., 2018); X-Ray fluorescence (XRF) (Hao et al., 2019; Hasan et al., 2020; S. Xu et al., 2016); wet chemical analysis (WCA) (Šaponjić et al., 2015); and using sector field mass spectrometry with inductive coupling to plasma (ICP-MS) (Escalera et al., 2015), have also been employed to identify and characterize diatomaceous earth minerals.

The sampled studies shown in Table 2.3, silica (SiO_2), which ranges in concentration from 56 % to 93.5 % by weight, is the primary chemical constituent of diatomaceous earth. Alumina (Al_2O_3), which ranges in concentration from 0.05 % to 12.28 % by weight, iron oxide (Fe_2O_3), which ranges in concentration from 0.2 % to 26.4 % by

weight, calcium oxide (CaO), which ranges in concentration from 0.22 % to 16 %, MgO (0.05 % -2.25 % wt), MnO (0.005 % -0.22 % wt), TiO_2, K_2O (0.09 % -2.28 % wt), P_20_5 (0.03 % -1.53 % wt), and Na_2O (0.1 % -5.69 % wt) are its other minor ingredients.

When creating geopolymers, low-calcium binders are preferred because a change in the microstructure brought on by a high calcium content might slow down the rate at which the polymerization occurs (Chindaprasirt & Ridtirud, 2020). According to Okeyinka et al. (2019), calcium oxide (CaO) is required in minor proportions in the composition of geopolymer base material since its presence in significant amounts frequently interferes with the geo-polymerisation procedure (Okeyinka et al., 2019). In general, a geopolymer binder is deemed to be siliceous when the combined amounts of its three main components, SiO_2, Al_2O_3, and Fe_2O_3, reaching a maximum of 70% or when the amount of reactive calcium oxide falls below 10% (Aziz et al., 2019; Nyale et al., 2014).

A pozzolanic substance classified as a Class F normal kind of pozzolan or a silicate glass substance by ASTM C618 (2014) has a total SiO_2, Fe_2O_3, and Al_2O_3 content greater than 70% by weight and less than 10% by weight of CaO.

The total alkaline versus silica (TAS) classification system presented in Figure 2.15 is used to identify some common types of rocks based on their bulk chemical composition and the correlations between the combined alkali content and the silica content. For the rocks that have undergone chemical analysis, the classification seems straightforward to utilize.

Table 2.3: Chemical components for various reported diatomite analyses

S/N	Major oxides (% wt.)											Reference
	SiO_2	Al_2O_3	Fe_2O_3	CaO	MgO	MnO	TiO_2	K2O	P_20_5	Na_2O	LOI	
1	56	6.5	26.4	-	-	-	-	-	-	-	-	(Hasan et al., 2020)
2	73.68	12.28	3.29	0.7	0.44	-	-	1.01	-	0.12	8.26	(Šaponjić et al., 2015)
3	60.71	7.9	1.17	16.25	0.4	0.04	0.25	1.06	-	-	14.65	(Benayache et al., 2018)
4	92	0.05	0.82	-	-	0.08	0.11	0.34	0.04	0.55	6.01	(Ahmadi et al., 2018)
5	82.02	3.76	5.14	2.61	0.6	-	0.35	0.2	0.73	0.33	2.35	(Sarıdemir et al., 2020)
6	71.35	4.87	7.98	11.71	-	-	-	3.1	-	-	-	(S. Xu et al., 2016)
7	70.65	4.26	1.07	0.83	2.25	0.01	0.52	1.67	1.53	5.69	11.1	(Escalera et al., 2015)
8	86.3	2.9	1.7	0.8	0.2	-	0.5	0.5	0.5	0.3	6	(Galán-Arboledas et al., 2017)
9	93.5	1.6	1.1	0.4	0.05	-	-	0.09	-	2.51	0.35	(Hasanzadeh & Sun, 2019)
10	67.2	10.09	2.74	1.36	0.63	-	-	0.67	-	0.36	10.3	(Ünal et al., 2007)
11	71.16	12.25	2.16	0.39	0.5	-	-	0.76	-	0.34	10.3	(Hao et al., 2019)
12	83.48	11.51	1.82	0.163	0.554	0.01	0.353	1.81	0.04	-	-	(Luan et al., 2019)
13	70.77	6.61	9.02	1.14	-	0.22	-	0.51	-	-	-	(MacEdo et al., 2020)
14	80.13	5.43	1.23	0.53	-	-	-	-	-	-	12.66	(Xiao & Liu, 2019)
15	68.67	10	3.54	10.71	0.68	-	-	0.71	-	-	5.69	(Ergün, 2011)
16	79.86	9.01	6.29	0.51	0.47	-	0.56	2.28	0.1	0.16	0.6	(Posi et al., 2013)
17	89	0.64	0.23	0.2	0.07	0.005	0.031	0.11	0.03	0.1	9.1	(Reka et al., 2000)

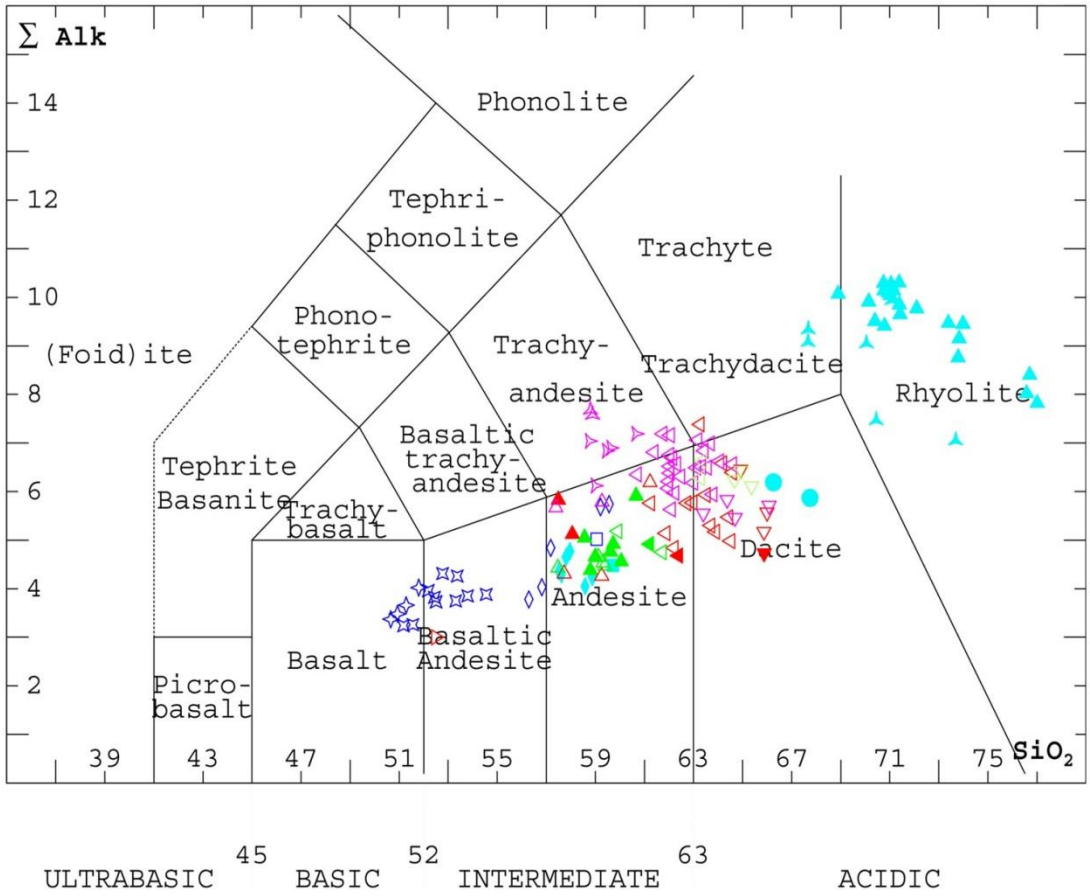

Figure 2.15: Total Alkaline versus Silica (TAS) classification diagram (Santos & Hartmann, 2021)

The chemical composition analysis is significant because silica and alkali ratios are key factors in determining both real and normative mineralogy. Table 2.4 displays the chemical and physical properties of some of the geopolymer precursor materials that have been investigated by other scientists.

Table 2.4: Properties of alternative geopolymer precursors (Amran et al., 2020)

Property	Fly ash (FA)	Rice husk ash (RHA)	Ground granulated blast furnace slag (GGBS)	Silica fume (SF)	Palm oil fuel ash (POFA)
Bulk Density (g/cm^3)	1.3	0.96-1.6	1.2	1.35-1.51	2.4-2.5
Specific gravity	2.2	2.11	2.9	2.2	2.14
Silica (SO2) (%)	38-55	>90	30-40	>85	>80
Alumina (Al2O3) (%)	20-40	>9	5-20	<2	16-18
Iron oxide (Fe2O3) (%)	6-16	>2.8	<2	<1	8-10
Calcium oxide (CaO) (%)	1.8-10	1-2.2	35-40	-	5-18
Magnesium oxide (MgO) (%)	1-5	>1	5-18	-	>1.2

With a comparable chemical composition to rice husk ash (RHA), silica fume (SF), and palm oil fuel ash (POFA), diatomaceous earth appears to be very light in weight.

b) Specific gravity

Specific gravity is a crucial index attribute of soils that is strongly related to mineralogy or chemical composition. It is the ratio of the mass of soil solids to the mass of an equivalent volume of water (Roy & Kumar Bhalla, 2017). Typical values of specific gravity with their corresponding type of soils are given in Table 2.5.

Table 2.5: Specific gravity values for different soils (Roy & Kumar Bhalla, 2017)

Type of soil	**Specific gravity**
Sand	2.65-2.67
Silty sand	2.67-2.70
Inorganic clay	2.70-2.80
Soil with mica or iron	2.75-3.00
Organic soil	1.00-2.60

The diatomaceous earth's specific gravity according to Reka et al. (2021) is approximately 2.25 g/cm^3. Table 2.5 shows that, the specific gravity of diatomaceous earth and organic soils fall in a similar range.

Loss on ignition (LOI)

The loss on ignition (LOI) is the amount of chemically combined water (H_20) and occasionally organic matter content found in inorganic materials (Reka et al., 2021). Opal has a high level of silanol groups, which increases its adsorption capacity (N. Li et al., 2022). This indicates that opal's degree of adsorption is based on the quantity of silanol and the portion of free silanol. Studies have proved that silanol groups and molecular water (H_2O_{mol}) are both present in opal (H_2O_{SiOH}) (N. Li et al., 2022). The loss on ignition (LOI) for diatomaceous earth vari es from 0.35 % to 14.65 % wt. A schematic illustration of the water forms in opal is depicted in Figure 2.16. The loss on ignition is determined following ASTM D 7348-13, (2013).

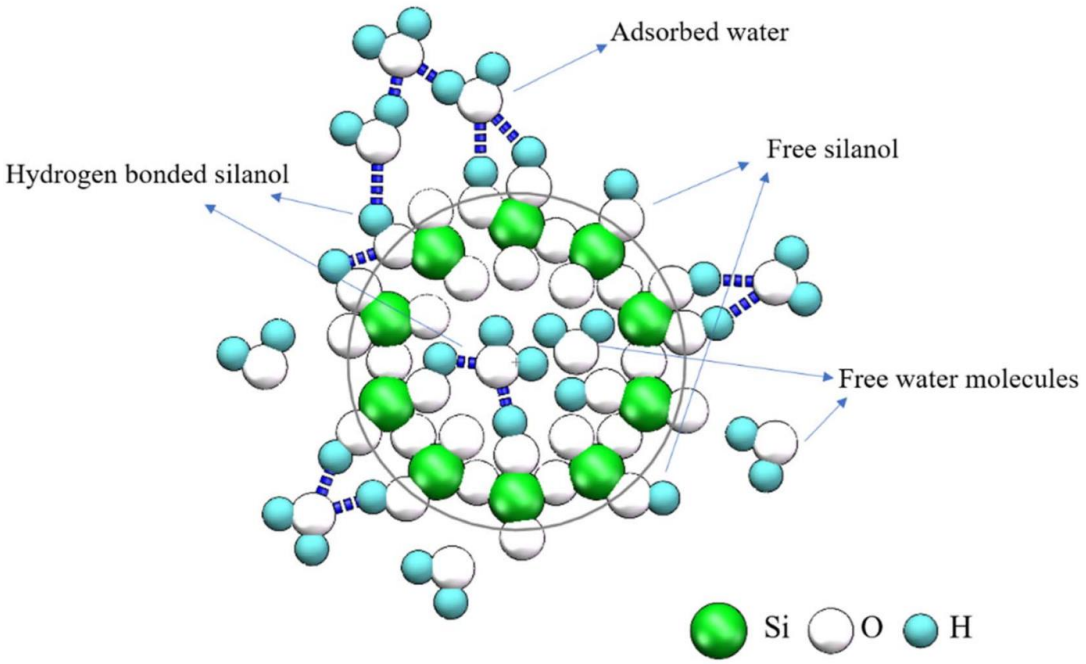

Figure 2.16: Different forms of water in opal (N. Li et al., 2022)

The combined water contained within the opaline structure of frustules ranges between 1.9 wt% and 9.6 wt%, according to Hoffman (2006).

c) Atterberg Limits

The Atterberg limits test offers a way to gauge the soil's plasticity and provides details on the amount of clay present (Mostafa & Uddin, 2016). This is because the clay particles in soil have a significant impact on the soil's capacity to swell.

ASTM D4318-17 (2017) governs the Atterberg Limit tests, which measure the soil's plastic limit (PL), liquid limit (LL), and plasticity index (PI). The difference between the plastic and liquid limits is that the plastic limit determines where the soil transitions from a semi-solid to a plastic (flexible) state, while the liquid limit determines where the soil transitions from a plastic to a viscous fluid state (Hall et al., 2012; Krishna Reddy, 2016). The plasticity index (PI) describes the variation between LL and PL and it represents the range of moisture contents within which the soil behaves as a plastic solid.

The predefined and acceptable ranges for PI and LL for earth construction materials according to Hall et al. (2012) are;

- Favorable: PI < 16% and LL < 36%
- Satisfactory: PI = 15–30% and LL = 36–45%
- Unfavorable: PI > 30% and LL > 45%.

The relationships between the plasticity index, soil type, degree of plasticity, and degree of cohesiveness of soils according to Atterberg's classification are shown in Table 2.6.

Table 2.6: Soil types as per the plasticity index (Roy & Kumar Bhalla, 2017)

Plasticity index	Soil type	Degree of plasticity	Degree of cohesiveness
0	Sand	Non-plastic	Non-cohesive
<7	Silt	Low plastic	Partly cohesive
7-17	Silt clay	Medium plastic	Cohesive
>17	Clay	High plastic	Cohesive

High liquid limit values have been observed in diatomaceous soils from Mexico and Japan, with undisturbed lacustrine deposits exhibiting liquid limits of 20–100%, according to Zuluaga et al. (2021).

d) Mineralogy of diatomaceous earth

In the diatomaceous earth deposits, chert and volcanic ash are frequently abundant elements, although secondary materials such as clays, quartz, gypsum, mica, calcite, and feldspars are also occasionally encountered (Hoffman, 2006). The best primary approach for defining and categorizing opal-A, opal-CT, and opal-C is through X-ray diffraction (XRD) (Curtis et al., 2019). According to Ghisoli et al. (2010), the XRD patterns of opals display a broad and diffuse reflection at about 21.5°2Θ. The diffraction peak at around 21.6°2Θ is the highest peak of opal, and it is thought to be caused by the convergence of the tridymite (404) plane and the cristobalite (101) plane (N. Li et al., 2022). Some authors referred to this broad peak as a "glass peak" because it resembles the diffuse peak created by the glass. In addition to serving as the diagnostic peak for Opal-CT, the diffraction peak at 4.3 Å is connected to the tridymite (040) plane and the cristobalite (101) plane (Curtis et al., 2019; N. Li et al., 2022). The presence of the diffraction peak at 4.3 Å has been proved to indicate that the cristobalite in the opal is in a low-temperature state. Figure 2.17 illustrates the appearance of the X-Ray diffraction peaks for silica polymorphs and opals. Curve A represents synthetic α-

cristobalite. Curve B represents Opal-C. Curves C to F shows the presence of Opal-CT. Curves G and H identify Opal-A. Quartz-related peaks are denoted with a Q, while tridymite-related peaks are denoted with a T.

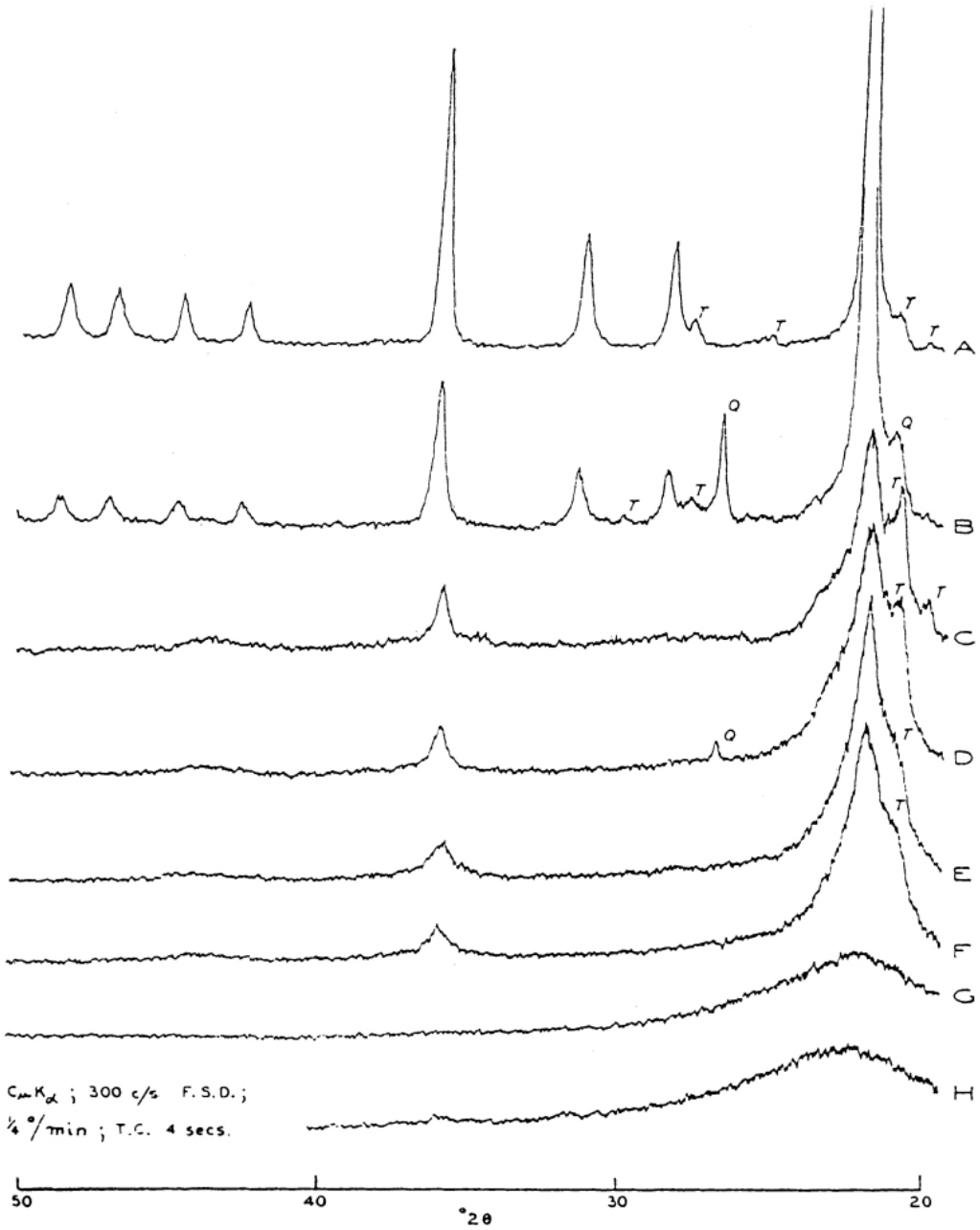

Figure 2.17: X-Ray diffraction patterns for opals and silica polymorphs (N. Li et al., 2022).

e) Diatomaceous earth's mechanical and physical features

The mechanical and physical characteristics of diatomaceous earth from a few sampled studies are displayed in Table 2.7. The experimental tests on physical properties such as bulk density, porosity, specific gravity and water absorption seem to be more relevant than the mechanical properties. From the table, the diatomaceous earth bulk density (g/cm^3) ranges between 0.32–0.767, the porosity (%) is between 73–77, and the specific gravity is about 1.9.

Table 2.7: Mechanical and Physical properties of diatomaceous earth

S/N	Bulk Density (g/cm^3)	Porosity (%)	Specific gravity	Water absorption (%)	Dry compressive strength (MPa)	Reference
1	0.55 - 0.60	73–75	-	-	3.4–4.6	(Reka et al., 2000)
2	0.767	-	1.9	6.5	-	(Hasan et al., 2020)
3	0.6	-	1.85	-	-	(Posi et al., 2013)
4	0.32-0.64	-	-	-	-	(Mejia, 2015)
5	0.559	77	-	-	-	(Taoukil et al., 2021)

2.5 History of Diatomaceous Earth Use in Concrete Production

Diatomaceous earth's industrial value is due to its porous and permeable structure, chemical resistance and large surface area (Hoc Thang, 2020; Lutyński et al., 2019). Mejia (2015) reported that diatomaceous earth is suitable for a variety of applications, including the production of lightweight aggregates incorporated into concrete for heat insulation purposes.

Diatomaceous earth has become a substitute for environmental management that can assist in lowering the number of pollutants in the soil, water, and air after the carbon footprint resulting from its application as an input for bio-agriculture was examined (Escobar et al., 2014; Ren et al., 2021). Dosages of chemical fertilizer were decreased as a result. Additionally, Abrão et al. (2019) found that using Portland pozzolan cement combined with diatomaceous earth reduced the amount of CO_2 that was released during the production of concrete.

The various applications of diatomaceous earth in concrete manufacturing to increase the material's overall sustainability are examined in this section.

2.5.1 Use of diatomaceous earth as a cement substitute

Because the amount of greenhouse gas emitted from the global production of ordinary Portland cement (OPC) is estimated to account for about 7% of total greenhouse emissions into the Earth's atmosphere, a significant portion of the concrete industry is becoming increasingly interested in reducing the use of ordinary Portland cement (OPC) (K.-H. Yang et al., 2011). Portland cement can be replaced with active silica-rich materials, typically industrial byproducts, as supplemental cementitious materials (SCMs) (Pokorný et al., 2016).

Li et al. (2019) investigated replacing a maximum of 40% Portland cement (PC) with pozzolanic diatomaceous earth (DE), which is highly reactive, in mortar and concrete formulations. They found that the best option was to replace PC with DE at a rate of 30% by weight, hence increasing concrete strength while decreasing energy use and greenhouse effect by over 30%. Degirmenci and Yilmaz (2009) showed that using up to 15% by weight of diatomite boosted the mortar's sulfate resistance and compressive strength while significantly reducing mortar density and water absorption.

Ahmadi et al. (2018) report that diatomite powder can substitute up to 40% of the cement in mortars without lowering compressive strength while in the same manner improving tensile strength and other functional properties. However, the mortars with a 15 % addition of calcined diatomaceous earth displayed the excellent mechanical qualities at both low and high temperatures (Sarıdemir et al., 2020). Macedo et al. (2020) found that the ideal amount of diatomaceous earth substitution for cement is 10% since good outcomes were achieved showing that diatomite has excellent potential as a substitute material for cement in concrete mix formulations.

Xu et al.(2016) found that adding 20% diatomite/fly ash improved mechanical properties. This improvement was due to the pozzolanic interaction that happens during the curing phase, between the calcium hydroxide ($Ca(OH)_2$) and the mineral admixtures. On the other hand, Ergün (2011) replaced cement with diatomite and waste marble powder, and it was determined that the optimum mechanical properties were found in the concrete that contained 5% spent marble and 10% raw diatomite.

Further to being used to replace cement, diatomite has been added to asphalt mixtures to serve as a pore-forming agent (Mohd Shukry et al., 2018), magnesium phosphate cement (Luan et al., 2019), and straw fibre cement-based composites (Xiao & Liu, 2019). This improves the materials' resistance to stripping, resistance to moisture damage, setting time, porosity, and thermal insulation while also promoting the hydrogenation reaction.

While most research found that utilizing diatomite as cement substitute material improved the mechanical qualities, Pokorný et al. (2016) investigation showed an increase in flexural strength and a decrease in compressive strength. Hasanzadeh and Sun (2019), in contrast to an analysis of mechanical properties, examined how the

transport properties will be affected by replacement levels of cement up to 10%. They found that by adding DE to cement paste, viscosity was raised while flow diameters, bleeding rate, setting times, and heat of hydration were decreased.

2.5.2 Diatomaceous earth as a resource for lightweight aggregate (LWA)

Lightweight aggregates are porous and have a granular structure with a loose bulk density of less than 1.20 g/cm^3 (Martínez-García et al., 2021). In eliminating the use of heavy building materials and maintaining thermal regulation requirements, the use of lightweight aggregates with excellent thermal insulation properties resulting from their porous structure can improve the insulation capacity of concrete elements (Taoukil et al., 2021). Diatomaceous earth can be utilized as lightweight aggregates in mortar and concrete for insulating reasons because of its unique properties, such as its low density and porous structure, which are preferable for thermal performance, fire resistance, and sound absorption (Gencel et al., 2016; Mejia, 2015; Stefanou et al., 2022).

After pelletizing a combination of diatomite and 2–5 % sawdust at 1100 °C, Fragoulis et al. (2004) produced laboratory aggregates with strength and weight that were comparable to those of commercial lightweight aggregates (LWAs). On the basis of their mechanical, physical, and thermal study findings, Posi et al. (2013) determined that diatomite is a good lightweight aggregate for the production of compressed lightweight concrete blocks. Furthermore, Taoukil et al. (2021) and Hasan et al. (2021) examined the viability of substituting up to 100 percent of diatomite for sand in mortars; the results showed that the compressive and flexural strengths decreased but the thermal insulation capacity rose.

Mehmedi Vehbi GÖKÇE (2012) evaluated the use of cement as a binder up to 40% of the volume when making diatomite-based lightweight building materials. He

considered it inconvenient and recommended more research to better sustainably bond diatomite. However, Ünal et al. (2007) claimed that lightweight concretes containing diatomite can be used in buildings to obtain great insulation while lowering the structure's self-weight.

Studies by Xu and Li (2014), Benayache et al. (2018) and Costa et al. (2020) showed that stable phase transition materials (PCMs) made of diatomite, other aggregates, and paraffin are present potential choices for thermal energy storage in structures with maximum service temperatures of about 40 °C because of their superior thermal resistance and energy storage capability.

Investigations into diatomite's capacity as a pore-forming agent for building components like waterproofing barriers (Tavares et al., 2016), pyrophyllite support layers (Ha et al., 2015), and humidity control materials (Vu et al., 2013) have produced evidence of the material's excellent performance for construction applications at reasonable costs. Galán-Arboledas et al. (2017) also tried to substitute clay, a material typically used to make bricks, with up to 10% by weight of diatomaceous earth (DE) residues and found that doing so enhanced open porosity, decreased bulk density by up to 10%, and significantly decreased the flexural modulus to about 10 MPa.

A mixture of diatomite and oyster shells (OS) (Hao et al., 2019); diatomite, rice husk ash, and sawdust (Hoc Thang, 2020); diatomaceous earth and Brazil nut shells (Escalera et al., 2015); clay with kieselguhr (Farías et al., 2017; Ferraz et al., 2011; Mateo et al., 2017); and diatomite, sugar-filtered mud, and dolomite (Man et al., 2017) were mixed together to create porous refractory composites. Despite losses in bending and compressive strength and the adoption of an unsustainable sintering method, the

refractory products displayed technical features that met the expectations of porous and insulating materials.

2.5.3 Diatomaceous earth as a raw material in the manufacture of cementless (clinker-free) concrete

Any substance that can be made plastic and then hardens to resemble artificial stone is referred to as a "cementitious material" (Kett, 1999). Lime and hydraulic cement, particularly Portland and natural cement, have been the main cementing agents employed in construction. Clinker, the primary component of cement, is made by calcining clay and limestone. Clinker manufacturing is an energy-intensive process that results in emissions of 875 kg of CO_2 per tonne of clinker, of which 30–40% come from the energy needed to heat clay and limestone to 1500°C and 60%–70% from the chemical reaction of limestone decarbonization (Favier et al., 2018).

Pozzolan cement, the first known type of cement, was created by combining lime with a type of volcanic ash called pozzolana (Kett, 1999). Research into the production of concrete using gypsum, lime, and diatomaceous earth (Loganina et al., 2014; Pimraksa & Chindaprasirt, 2009; Reka et al., 2017), identified the presence of a pozzolanic feature in diatomaceous earth, defining it as a promising sustainable building material.

The treatment of diatomaceous earth with sodium hydroxide solutions (NaOH) (Font et al., 2018), potassium hydroxide (KOH) (Nakashima et al., 2021), and potassium silicate (K_2SO_3) (Bagci et al., 2017) showed that diatomaceous earth may be used well as a clinker-free concrete resource in geopolymeric systems when it was employed to create porous diatomite-based concrete at room temperatures.

Some researchers have tried activating diatomaceous earth with things like gelatin solution in order to create porous silica ceramics (Matsunaga et al., 2017), boric acid

(Šaponjić et al., 2015), and polyethylene glycol (PEG) (Akhtar et al., 2010). Despite the products' excellent ceramic characteristics, the production processes are deemed unsustainable because they call for high sintering temperatures and compaction pressures.

Phoo-ngernkhama et al. (2013) looked at the effects of adding up to 40% calcined diatomite to a high calcium fly ash geopolymer paste together using sodium hydroxide (NaOH) and sodium hydroxide (Na_2SiO_3) solutions as alkaline activators. Despite the fact that it was obvious that adding diatomite accelerated the setting process, increased strain capacity, and decreased the density of the hardened paste, a 15% substitution of diatomite was found to be the most effective, producing a compressive strength of 64.0 MPa.

2.5.4 Incorporating recycled materials into diatomaceous earth for concrete production

Studies have shown that various industrial and household wastes can be recycled and employed as concrete components to create "green concrete" (Olofinnade et al., 2019).

a) Polymeric additives

Plastics are ubiquitous materials and find applications in all parts of our life and economy (Sofi et al., 2019). Unfortunately, the rate of demand has dramatically increased from 200 million tonnes a year in 2002 to 322 million tonnes in 2015 and the number is expected to reach 485 million tonnes in 2030 (Poonyakan et al., 2018). Gardete and Luzia (2020) expressed concern that plastics' reuse and recycling rates are still below ideal levels, due to poor waste management, collection, and segregation of plastic wastes.

The use of polymeric additives in the construction industry may help to reduce the use of raw materials, energy, and unfavorable environmental effects while simultaneously promoting the production of inexpensive bricks with enhanced thermophysical properties (González-Montijo et al., 2019; Limami et al., 2020).

Polyethylene, possibly the most common kind of plastic in the world, is the synthetic substance frequently used in the production of compressed earth blocks and other building materials, such as concrete (Mohammed et al., 2019; Mostafa & Uddin, 2016; Poonyakan et al., 2018).

Numerous studies, (Ahmed and Raju, 2015; Akinwumi et al., 2019; Alani et al., 2019; Ali et al., 2017; Hassan et al., 2021; Janfeshan Araghi et al., 2015; Journal & Sambhaji, 2016; Limami et al., 2020; Mahesh et al., 2016; Mahmood & Kockal, 2020; Mohammed et al., 2019; Mondal et al., 2019; Muntohar et al., 2013; Pereira et al., 2017; Poonyakan et al., 2018; Vanitha et al., 2015; Záleská et al., 2018) have been undertaken to investigate the sustainability of using plastic wastes as stabilising agents in ordinary soils or concrete for building materials.

The particles of waste Polyethylene Terephthalate (PET) can be utilized as lightweight aggregates in concrete production because of their low unit weight, even though they reduce the compressive, tensile, and flexural strengths (Sadrmomtazi et al., 2016). According to Alani et al. (2019), the addition of PET shreds and ultra-fine palm oil fuel ash (UPOFA) to concrete significantly improved the material's porosity, initial surface absorption, gas permeability, water permeability, and rapid chloride permeability.

Harni et al. (2018) investigated the effects of high-density polyethylene (HDPE) plastics and fly ash on the mechanical properties of concrete. Although it was noted that strength decreased as HDPE percentage increased, the compressive strength of all

the mixes was still within the acceptable threshold for the majority of structural applications at 28 days. The reinforcement of geopolymers formed with fly ash, blast furnace slag, or lime with polyethylene (PE) and polyvinyl alcohol (PVA) fibres was studied by Nematollahi et al. (2017), who demonstrated that geopolymer composite matrices may be successfully made with polymeric additions of about 2%. Fly ash-based geopolymer with a 2 % PVA dosage was found to have the greatest flexural strength (P. Zhang, Wang, et al., 2020).

The usage of polyethylene terephthalate has received the majority of attention in the research that has been done so far on the combined influence of plastic aggregates and pozzolanic materials on concrete properties (PET). However, the feasibility of stabilizing geopolymer binders (pozzolanic material), especially those based on diatomaceous earth, with plastic wastes for the manufacture of sustainable construction materials has not been fully investigated, if at all.

b) Natural fibres

Natural fibres have been used in adobe and other traditional types of earthen architecture as a more environmentally acceptable alternative to reduce plastic shrinkage cracking and boost ductility, durability, tensile and shearing strengths (R. Ahmad et al., 2019; Danso et al., 2015; Mostafa & Uddin, 2016). Natural fibres have the potential to be superior replacements for conventional fibres as reinforcement of different composites due to their benefits of low cost, lightweight, and excellent mechanical qualities. Natural fibres can replace conventional fibres like glass, since they are environmentally friendly and biodegradable. In general, adding natural fibres improves the qualities of structural building materials. According to Ajmal et al. (2023), unreinforced masonry structures function well when subjected to gravity loads because of the reasonable compressive strength of masonry units. However, it

becomes challenging for engineers to raise the tension and shear capacity of structural components to obtain improved efficiency under seismic loading.

Jamshaid et al. (2022) pointed out that the inclusion of natural fibres up to 1% of the cement mass increased the concrete's compressional properties, and the occurrence of unexpected brittle failures is reduced as the number of fibres increases. Similarly, Yan et al. (2016) indicate that the percentage of cellulosic fibre used in cementitious materials should be kept within the range of 0.2% to 2.0%. Namango (2006) and Danso et al. (2015) in their studies employed sisal fibres in the range of 0.25%-1.25%. Low percentage fibre inclusion is encouraged because a high fibre concentration in concrete can make it difficult to mix and distribute the fibre evenly, and it can even make the fresh concrete harder to work with, which could lead to a considerable increase in porosity.

Animal fibres are less desired than plant fibres because large-scale gathering of animal fibres is more difficult and, as a result, impractical for large-scale processing (Mohanty et al., 2005; Silva et al., 2020). Most of mineral fibres go through multiple processing steps before being used, and the only mineral fibre that can be obtained without going through these steps is asbestos, which is a substance that is known to cause cancer (Silva et al., 2020) and is not suitable for the creation of eco-friendly composites.

Plant fibres have been recognized as ideal reinforcing components for geopolymer matrices because geopolymerization takes place in very alkaline environments and lignocellulose fibres have a high resistance to these conditions (Batista dos Santos et al., 2021; Silva et al., 2020); the composition of the geopolymer matrix contains pozzolanic elements and alkaline activators, which serve as fibre treatments (Batista dos Santos et al., 2021). Silva et al. (2020) and Li et al. (2022) reviewed recent

developments in the manufacturing of natural fibre-reinforced geopolymers as potential sustainable building materials; an overview of effective natural fibre reinforcements was published, with most of the studies concentrating on industrial by-products like fly ash, ground-granulated blast furnace slag, building and demolition wastes, and mine tailings. Fibres serve as the concrete's microcracking control units, acting as bridges in the fractured area to carry loads from the crack to the concrete when the first fracture emerges (Li et al., 2022; Mahmood et al., 2021). This increases the effectiveness of fibre-reinforced concrete.

There have been numerous studies on geopolymeric composites reinforced with vegetable fibres, including cotton (Alomayri & Low, 2013; Korniejenko et al., 2016; Zhou et al., 2020), bamboo (Sá Ribeiro et al., 2016), flax (Alzeer & MacKenzie, 2013; Lazorenko et al., 2020), sisal (Batista dos Santos et al., 2021; da Silva Alves et al., 2019; Korniejenko et al., 2016; Panwar et al., 2018; Silva, Kim, Bertolotti, et al., 2020; Wongsa et al., 2020), coconut (Wongsa et al., 2020), and jute (Silva, Kim, Aguilar, et al., 2020).

When diatomite was employed in place of quartz sand in a study on the long-term mechanical properties of cellulose fibre-reinforced cement mortars, Ince et al. (2019) found that pozzolans can improve the durability properties of cellulose-cement composites. Regarding the cellulosic fibre-reinforced cement-based composites, Ardanuy et al. (2015) noticed that softwood, sisal pulps and sisal strands were the most studied fibre form for preparing cellulose cement composites.

In general, the existence of voids within the concretes, produced by fibre inclusion, advantages a better strength-to-weight ratio, increased heat and sound insulation

properties, a lower thermal expansion coefficient, and a higher tensile strain capacity.(Saman et al., 2017).

The results of the literature review on the background of the use of diatomaceous earth are summarized in Figure 2.18.

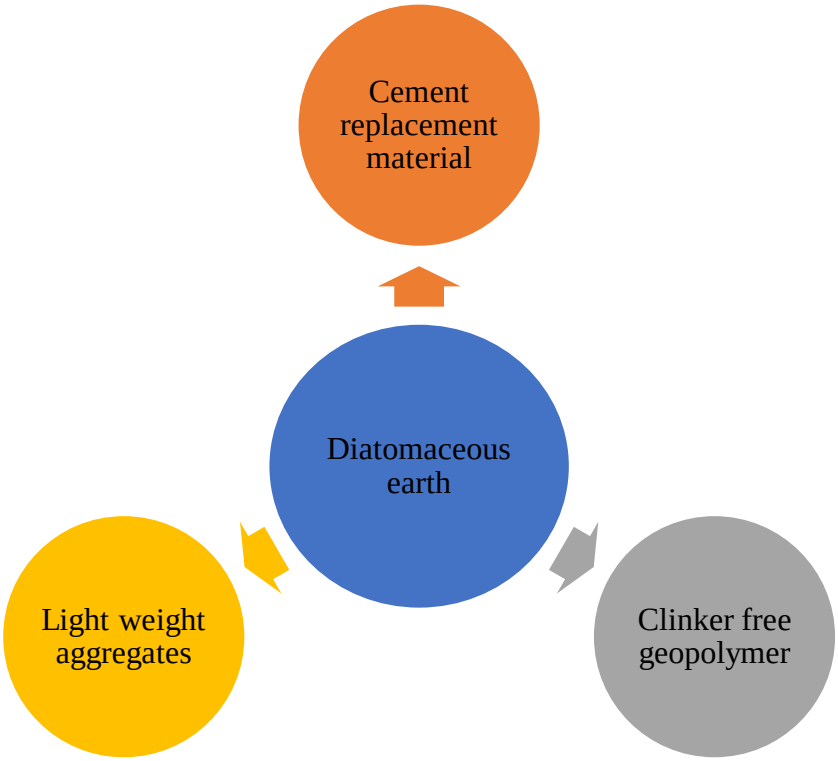

Figure 2.18: Summary of the diatomaceous applicability

2.6 Production Process for geopolymer concrete

Pozzolanic materials (precursors) and activator additives, which hasten the hydration process, are the main components utilized in the production of geopolymer elements (Abd Razak et al., 2021). Two methods of geopolymer preparation exist, according to Ghazy et al. (2022).

a) One-part geopolymer preparation

b) Two-part geopolymer preparation

Figure 2.19 depicts the general geopolymer production system adopted by most of the researchers.

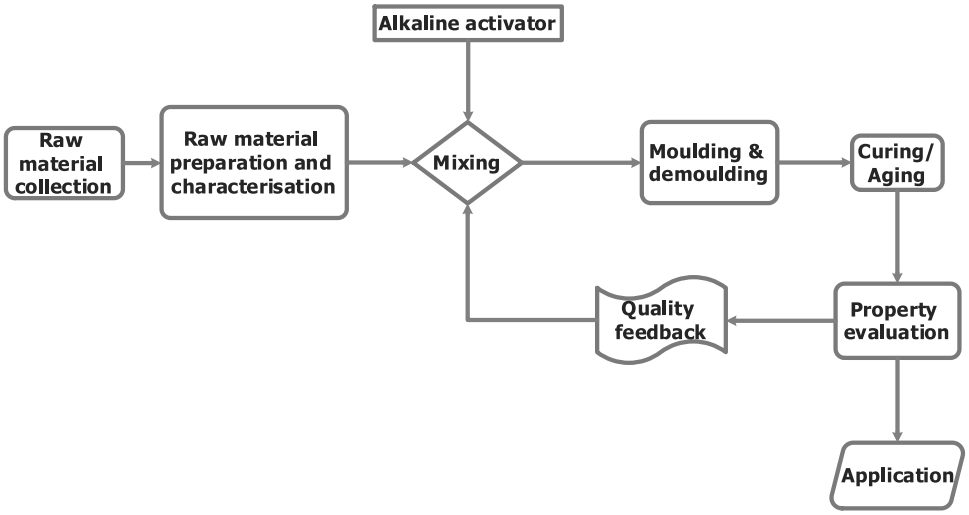

Figure 2.19. General geopolymer production process adopted by most of the researchers.

a) One-part geopolymer synthesis

For the one-part technique, the precursor material and solid activator are both well dried and mixed before water is slowly added while the mixture is stirred (Alrefaei et al., 2019; Dong et al., 2020; Ghazy et al., 2022; Luukkonen et al., 2018). Subsequently, moulding and curing follow (Han et al., 2018; Mandal, 2021; Wongsa et al., 2020; Zhou et al., 2020). Table 2.8 shows the production conditions for lightweight concrete adopting diatomite as a source for light aggregate and the one-part geopolymer preparation method.

Table 2.8: The specifications for making lightweight concrete using diatomite as a resource

S/N	Water: binder ratio	Specimen size (mm)	Compaction Pressure (MPa)	Curing /sintering	Reference
1.	0.56	30 x 30 x 30	-	Room temperature	(Loganina et al., 2014)
2.	0.5-0.7	250 × 250 × 20 160 × 40 × 40	-	Room temperature	(Taoukil et al., 2021)
3.	-	Ø35 x 35	15	750-950°C	(Escalera et al., 2015)
4.	-	120 x 28 x18 Ø85 x 10	Extrusion	850-1050 °C	(Galán-Arboledas et al., 2017)
5.	0.15	100 x 100 x 100		Room temperature	(Ünal et al., 2007)
6.	2	60 x 8 x 6	15	700-900°C	(Hao et al., 2019)
7.	2	50 x 50 x 50	0.85	Room temperature	(Posi et al., 2013)
8.	0.55-1	Ø150 x 300 150 x 150 x 600	-	Room temperature	(Hasan et al., 2021)
9.	-	60 x 8 x 6	15	800 °C	(Man et al., 2017)
10.	0.5	Ø5–10 Ø10–15 Ø 15 – 20	-	1100 °C 12– 15min	(Fragoulis et al., 2004)
11.	0.1	35 x 75 x 150	3.5	Autoclaved-0.14MPa 130°C-4h	(Pimraksa & Chindaprasirt, 2009)
12.	2.18-7	100 x 100 x 100	-	Room temperature	(Mehmedi Vehbi GÖKÇE, 2012)
13.	0.4	220 x 110 x 65	10	1200 °C	(Hoc Thang, 2020)
14.	0.4	Ø16–10	10	Autoclaved-130°C-3h	(Reka et al., 2017)

The research by (Fragoulis et al., 2004; Galán-Arboledas et al., 2017; Hoc Thang, 2020; Mejia, 2015) seems untenable in light of the high sintering temperatures and high compaction pressures required by their concrete production practices. Due to the requirement for extrusion and autoclaving equipment, Reka et al. (2017), Galán-Arboledas et al. (2017), and Pimraksa et al.(2009) may have difficulties with cost sustainability.

The experiment by Loganina et al. (2014) was carried out without the use of compaction pressure at room temperature, but the resulting specimens were feeble, only reaching a maximum strength of 3.92 MPa after a 28-day curing period. Cement was used as a binder to hold the lightweight diatomaceous earth aggregates together (Mehmedi Vehbi GÖKÇE, 2012; Taoukil et al., 2021; Ünal et al., 2007). Hasan et al. (2021) had to pelletize diatomaceous earth at a temperature of 650 °C in addition to employing cement as a binder.

b) Two-part geopolymer preparation

In a two-part geopolymer preparation process, the activator solution is added to the dry precursor material, and mixed until homogeneity is reached. Moulding and curing then take place.

Table 2.9 displays the manufacturing parameters for the two-part geopolymer mixes that use diatomaceous earth as a precursor source.

Table 2.9: Specifications for making geopolymer mixtures with diatomite as a precursor

S/N	Alkaline activator	Specimen size (mm)	Compaction pressure (MPa)	Curing	Reference
1.	3M KOH	40 x 40 x 13 Ø5 x 13	6.25	70°C for 24h	(Nakashima et al., 2021)
2.	KOH	10 × 10 × 100 Ø3 × 6	-	50°C for 24h	(Bagci et al., 2017)
3.	Gelatine	Ø40 x 18	40	1150-1350°C -2h	(Matsunaga et al., 2017)
4.	Boric acid	Pellets	40	1150 °C	(Šaponjić et al., 2015)
5.	Na_2SiO_3 / 10M.NaOH=2	50 x 50 x 50 Ø50 x 100	-	60°C for 24 h	(Phoo-Ngernkham et al., 2013)
6.	NaOH	Mortar pastes	-	20°C for 28days	(Font et al., 2018)
7.	polyethylene glycol (PEG)	Ø10 x 10	50 MPa	900-1400 °C	(Akhtar et al., 2010)

Sodium and potassium-based alkali activators are the most prevalent. Previous studies have shown that sodium-based alkali activators are more effective at activating compounds than potassium-based activators (Cong & Cheng, 2021). A further drawback of geopolymer with potassium hydroxide as the alkaline activator was that it was less resistant to sulphuric acid (Song, X.J., Marosszeky, M., Brungs, M. and Munn et al., 2005).

Potassium hydroxide (KOH) was used as an alkaline activator and diatomite served as a precursor in the successful geopolymer specimens produced by Nakashima et al. (2021) and Bagci et al. (2017), with maximum strengths of 5.78 MPa and 71 MPa, respectively. High-pressure compaction and high-temperature sintering techniques

utilized by Matsunaga et al. (2017), Akhtar et al. (2010) and Šaponjić et al. (2015) reduced the sustainability potential of the resulting geopolymers.

Elahi et al. (2020) showed that the samples activated with NaOH alone had a lower compressive strength than those activated with sodium silicate (Na_2SiO_3), also known as water glass, solution plus sodium hydroxide (NaOH). When fly ash-based concrete was activated by NaOH and water glass together rather than by NaOH alone, Fernandez and Palomo (2006) reported that the strength was more than doubled.

Geopolymers' strength can be increased by adding sodium silicate as an activator since it speeds up the polymerization process and produces a silica-rich reaction product.

A mixed alkaline activator comprising sodium hydroxide and sodium silicate has been proposed to synthesize geopolymers with better compressive strength because the inclusion of additional silicate can supply adequate silicon in the alkaline solution to start the geopolymerization. A mixed alkaline activator comprising sodium hydroxide and sodium silicate has been proposed to synthesize geopolymers with better compressive strength because the inclusion of additional silicate can supply adequate silicon in the alkaline solution to start the geopolymerization (Song, X.J., Marosszeky, M., Brungs, M. and Munn et al., 2005). Zhang et al. (2020) discovered that a higher early compressive strength with less porosity and water absorption may be attained with a higher sodium hydroxide (NaOH) concentration and that a mixture of sodium silicate (Na_2SiO_3) and sodium hydroxide (NaOH) at a ratio of Na_2SiO_3: NaOH =2.5 is a more effective activator than either Na_2SiO_3 or NaOH is on its own.

Lithium hydroxide solution has been shown to be an efficient alkali initiator by researchers; lithium can be coated with geopolymer particles to lessen the dissolving of active silica and the likelihood that dissolved active silica will form an Alkali-silica

reaction (ASR) gel. Fly ash and silica fume-based geopolymers were activated with solid Na_2CO_3 and hydrated lime, yielding strengths of approximately 50 and 85 MPa in 28 days at curing temperatures of 25 °C and 85 °C, respectively (Cong & Cheng, 2021).

Phoo-ngernkhama et al. (2013) developed high-performance geopolymers, however, because they only employed up to 40% of high calcium fly ash, it is difficult to assess the potential of diatomite in the mixture. This also applies to Font et al. (2018), who used diatomite in place of rice husk ash.

In designing a geopolymer concrete mix, it has also been noted that the mass ratio of water to geopolymer solid is crucial (Vora & Dave, 2013).

Generally, three types of activation can be used to increase the reactivity of natural pozzolan: thermal, mechanical, and chemical activation. According to Bondar (2009), a comparison based on the strength-cost relationship shows that the chemical activation method is the most efficient and least expensive.

Ugwuishiwu et al.(2013), advised that it is typical practice to compact stabilized earth bricks at compaction pressures between 2 MPa and 8 MPa. In that regard, Danso (2016) presented a characterisation of moulding pressure for earth/soil blocks;

i. Very low: 1-2 MPa
ii. Low: 2–4 MPa
iii. Average: 4–6 MPa
iv. High: 6–10 MPa
v. Hyper: 10–20 MPa
vi. Mega: 20–40+ MPa

The fundamental standard practices used in creating concrete mixtures are shown in Table 2.10.

Table 2.10: Standardized practices for preparing concrete and its raw materials

S/N	Characterisation Type	Standard
i.	Distribution of particle sizes	(ASTM D6913 / D6913M-17, 2017) (ASTM C136/C136M - 14, 2014) (ASTM B822-17, 2017)
ii.	Chemical analysis	(ASTM C114-10 2010)
iii.	Pozzolanic nature of earth material	(ASTM C311/C311M, 2013)
iv.	Specific gravity	(ASTM-D854, 2010)
v.	Loss on ignition	(ASTM D 7348-13, 2013)
vi.	Standard Specification for Natural Pozzolan, Raw or Calcined, for Use in Concrete	(ASTM C618 2014)
vii.	The ratio of water to the binder for a regular consistency	(ASTM C187, 2016)
viii.	Making mortar and concrete mixtures	(ASTM C305-14, 2009)
ix.	Determination of the initial and final setting time	(ASTM C191-08, 2008)
x.	Making and Curing Concrete Test Specimens	(ASTM C31-19, 2019)

2.6.1 Raw material preparation and characterization

a. Earth-based material

The earth-based material is reduced in size either manually or mechanically in a ball mill until an appropriate ratio of coarse particles to fine particles is attained, sieved, and then dried for 24 hours at 105 °C before being classified (Hao et al., 2019; Saeed et al., 2020). Before stabilization, Saeed et al. (2020) and other researchers suggest that

characterizing the raw materials is an essential step since it entails figuring out the Atterberg limits, moisture content, specific gravity, chemical and mineral contents.

The internationally accepted standard soil particle size ranges for gravel, sand, silt, and clay are between 60 mm and 2 mm, 2 mm and 0.06 mm, 0.06 mm and 0.002 and less than 0.002 mm respectively (Danso, 2016a).

b. Plant-based fibres

Plant fibres are typically composed of lignocellulose materials, which include cellulose, hemicelluloses, lignin, pectin, and waxy substances (R. Ahmad et al., 2019). When it comes to concrete reinforcement, fibres' capacity to withstand tensile stress improves with an increase in their specific strength or tenacity, which also raises the flexural strength of reinforced concrete (Halvaei et al., 2016)

For physical and mechanical characteristics, fibre tensile tests are performed following ASTM D3039, (2010). The characteristic features of a few selected plant fibres are presented in Table 2.11.

Table 2.11: Characteristic properties of selected plant fibres (R. Ahmad et al., 2019; Ansell & Mwaikambo, 2009; Banerjee et al., 2015)

Plant fibre	**Cellulose (%)**	**Hemi-cellulose (%)**	**Lignin (%)**	**Pectin (%)**	**Density (g/cm^3)**	**Tensile/Tenacity strength (cN/Tex)**
Cotton	82-96	2-6.4	0-5	<1-7	1.51	20-45
Flax	60-81	14-20.6	2.2-5	1-4	1.5	45-55
Hemp	70-92	18-22	3-5	1	1.48	12-35
Jute	51-84	12-20	5-13	0.2	1.3	30-45
Kenaf	44-87	22	15-19	2	1.45	30-45
Ramie	68-76	13-15	0.6-1	2	1.5	40-65
Banana	60-65	6-19	5-12	3-5	0.75-0.95	10-30
Sisal	43-78	10-24	4-12	0.8-2	1.5	40-45
Oil palm	43-63	28-33	17-19	1	0.7-1.55	30-60

c. Polymeric materials

Although aggregates made of polymeric materials are not frequently employed in structural concrete, it is reasonable to explore possible constraints on their application as structural components based on physical and mechanical specifications (González-Montijo et al., 2019). The plastic's non-biodegradability (durability), adaptability, low density, hardness, low linear dilation coefficient, superior chemical resistance and high heat resistance are the key attributes that make it desirable for use in concrete. According to the analysis performed by Belmokaddem et al. (2020), it was found that adding plastic particles to concrete affects the final product's physical, mechanical, and thermal qualities. The characteristic features of a few selected polymer materials are presented in Table 2.12.

Table 2.12: Properties of some selected polymeric materials (S & P, 2022)

Plastic-type	**Density (g/m^3)**	**Specific gravity**	**Thermal Conductivity (W/mK)**	**Tensile strength (MPa)**
PET	1300-1400	1.34	0.15	55-80
PE	910-925	1.34	0.33-0.52	18-30
PVC	1380	1.4	0.17-0.21	50-60
PP	900-990	0.9	0.12	25-40
PS	1050	1.05	0.105	30-55

2.6.2 Mixing and shaping

The formulation of industrial products frequently involves mixture experiments whereby, products are created by combining two or more substances (Brown Mathematics, 2014; Khashab, 2018). Mixture trials are conducted to determine the preferred mixed blends. The total of a mixture's component or ingredient proportions is always 1% or 100% (Galvan et al., 2021).To explore how each component affects certain quality characteristics that are of interest, mixture experiments are frequently

developed and analysed, and the ideal amount of each component is normally sought to optimize these quality features (Altarazi & Allaf, 2017).

The mixture designs (MDs) stand out among other numerous experimental designs (EDs), which are statistical tools used in the design of experiments to integrate and optimize trials and are regarded as a high-quality technology to achieve product perfection (Galvan et al., 2021).

For proper model fitting and testing, the experimental design must be chosen carefully. Following Altarazi et al. (2017), standard mixture designs, such as simplex lattice designs and simplex-centroid designs, are used when the proportions of the ingredients are only constrained to add up to one. However, when the components are also constrained to have a maximum and/or minimum value, constrained mixture designs or extreme vertices designs are more suitable.

During concrete production, dry components are mixed thoroughly for about five minutes before gradually adding the determined amount of water and then mixing further for another five minutes (Saeed et al., 2020). In cases where fibres are involved, the fibres are then added slowly by hand and mixing is continued to ensure a uniform distribution of the fibres throughout the soil matrix: care is taken to avoid aggregation of the fibres within the matrix (Mesbah et al., 2004).

Koteng (2013) pointed out that care must be taken while determining the water-to-binder (w/b) ratio value during the mixing of concrete components. Because, at a very low w/b ratio, concrete is difficult to compact and becomes very porous, resulting in a loss of strength and durability. On the other hand, a high w/b ratio results in workable concrete, but excess water eventually evaporates, resulting in high drying shrinkage

with the potential for cracking, and porosity. Figure 2.20 illustrates the effect of the mixture water to binder ratio on the concrete's final strength.

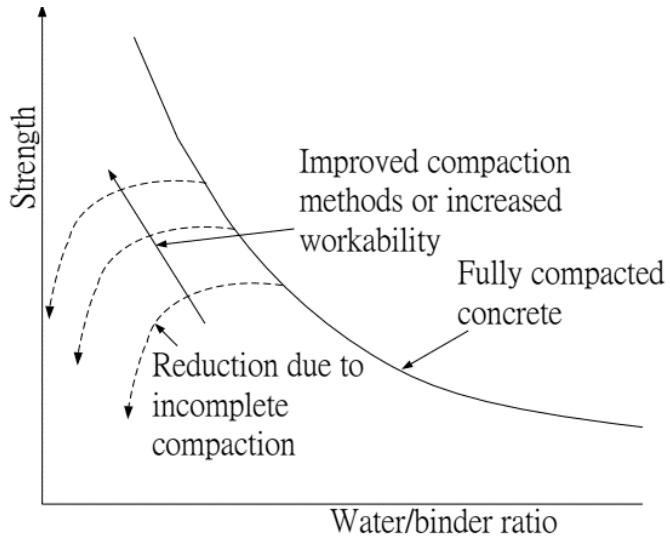

Figure 2.20. Water binder ratio (Koteng, 2013)

Other important parameters governing the performance of geopolymer binder according to Mohammed et al. (2021) are;

a) activator solution-to-source material (fly ash, slag, etc.) ratio,
b) the concentration of NaOH solution (molarity),
c) sodium silicate solution-to-sodium hydroxide solution ratio (Na_2SiO_3/NaOH),
d) curing temperature,
e) curing period and
f) water content

Size and shape specifications for testing specimens vary greatly between nations (Nithurshan & Elakneswaran, 2023). For instance, the Bureau of Indian Standards (IS 1725: 2013, 2013) suggests a standard brick size of 190 mm x 90 mm x 90 mm, while the United States and Canada use cylindrical specimens with a length-to-diameter ratio of 2 (i.e., 300 mm to 150 mm). Similarly, the typical brick size in Kenya is 225 x 110

x 75 mm. The standard measurements for concrete bricks should be 40 mm by 40 mm by 160 mm, according to the European standard (Bs En 196, 2016).

During the shaping of concrete mixes, compaction is essential because it is the process of mechanically densifying by pressing the particles together to come to a close state of contact so that the occupied air can be expelled from the soil mass (Nahar, 2018). The purpose of compacting mixes, according to Taallah et al. (2014), is to enhance the quality and functionality of products made from moulded mixtures.

2.6.3 Curing

One of the most crucial steps in the creation of concretes is the curing process since it significantly affects the characteristics of the finished product. The primary factors for the growth of oligomeric chains are temperature, humidity, and the duration of the curing process (Sotelo-Piña et al., 2019). To acquire the best qualities for an alkali-activated material system, common processes include heating (thermal curing), sealing (wrapping), steaming, and immersion in water (Nodehi & Taghvaee, 2022). For geopolymer concrete, researchers have experimented with a variety of curing methods, including oven curing, membrane curing, steam curing, hot gunny curing, hydrothermal curing, room temperature curing, and water curing; of these, oven curing has proven to be the most successful (A. A. Mohammed et al., 2021). To promote chemical reactivity during the initial phases of hardening, thermal curing within the first three days has been generally recommended (P. Zhang, Wang, et al., 2020). Previous reports state that the curing period lasts between 6 and 72 hours at temperatures between 40 and 100 °C. Preferably, a temperature range of 60°C–80°C (Sturm et al., 2015), 60°C to 90°C (Duxson et al., 2007), 80°C to 90°C (Fernández-Jiménez et al., 2006), 40°C to 85°C (Singh et al., 2015), 40°C to 100°C (Heah et al., 2011) 40°C to 90°C (Wattanachai & Suwan, 2017) during the initial 24 hours have been proposed. Recent studies have

demonstrated that thermal curing can significantly increase strength while reducing porosity (Ke et al., 2015; Provis, 2014). Optimal curing temperatures, such as 50°C (Bagci et al., 2017), 60°C (Lloyd & Rangan, 2009; Phoo-Ngernkham et al., 2013; Vijai et al., 2010), 70°C (Abdullah et al., 2015; Nakashima et al., 2021) and 80°C (Yewale et al., 2016) have been determined.

It is advised that geopolymer products be cured under controlled humidity at room temperature after a 24-hour thermal curing period to prevent unfavourably high levels of water evaporation during the setting of the geopolymer binder, which reduces strength and causes sample breakage (Bhutta et al., 2019; Hadi et al., 2018; G. Huang et al., 2018; Mackenzie & Welter, 2014). According to Abdullah et al. (2015), practical applications do not call for heat curing to last longer than 24 h since the rate of strength growth is quick up to a certain point, but after 24 h, the rate of strength gain is only moderate.

2.7 Design of Experiment (DoE) for Mixtures

The design of experiments includes carefully planning, carrying out, evaluating, and interpreting tests to get accurate and unbiased results regarding the process or product of interest (Lamberti et al., 2022).

A useful strategy for carrying out experimental designs is to construct a factorial experiment where multiple factors are changed simultaneously rather than one at a time (Lamberti et al., 2022). This is because the factorial design enables the exploration of both the existence of interactions between/among factors as well as the determination of whether each component affects the response. Fractional factorial designs have been chosen over full factorial designs to reduce the amount of time and resources needed

for data analysis. Figure 2.21 illustrates the difference between the full factorial and the fractional design of experiments that apply to mixtures.

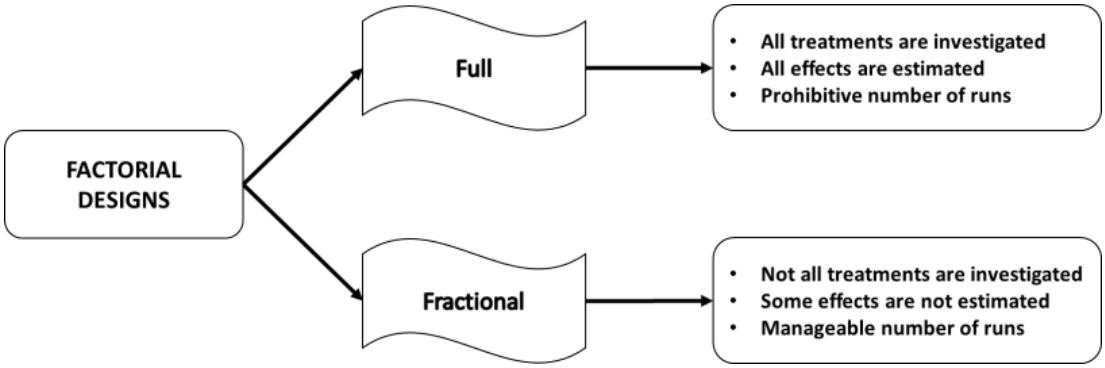

Figure 2.21. Distinction between the full factorial and the fractional mixture designs (Lamberti et al., 2022)

Figure 2.22 presents mixture systems that guide the design of experiments for mixtures consisting of up to four components.

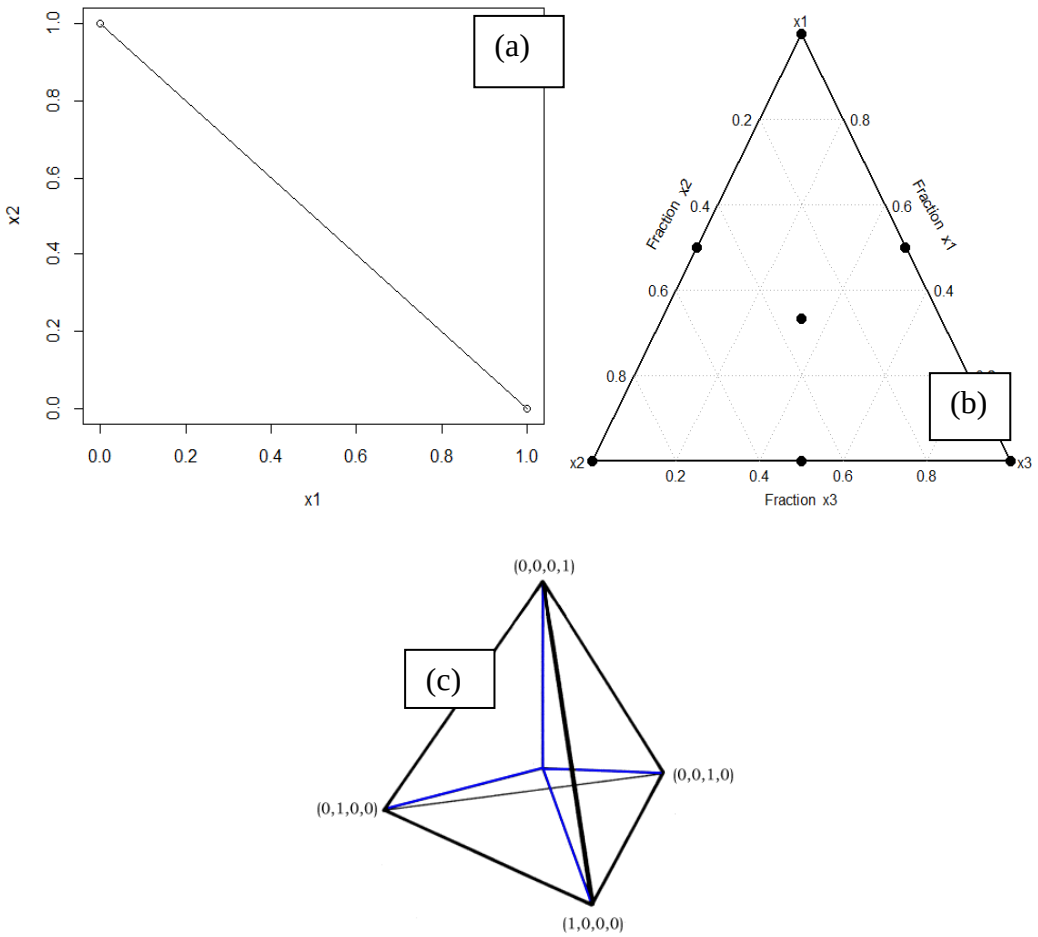

Figure 2.22: Mixture systems for (a) 2 components, (b) 3 components and (c) 4 components (Lamberti et al., 2022)

2.8 Performance Properties of Geopolymer Mixtures

Mechanical characterization is needed for structural work and safety assessments; this comprises compression strength, flexural strength, shear strength, and hardness tests. Compressive strength and durability tests, in particular, are viewed as crucial markers of masonry's viability (Adam & Agib, 2001; Fopossi et al., 2014; Islam et al., 2020; Saeed et al., 2020; Teixeira et al., 2020). The physical characteristics are also more significant since they can be utilized to forecast shrinkage, apparent bulk density, size or texture, moisture content, porosity, permeability, adhesion, and thermal properties (Yalley & Manu, 2021).

Geopolymer concretes' fundamental properties, such as compressive strength, elastic modulus, tensile strength, flexural strength, and other performances, are normally examined in the same way as cement-based (OPC) concretes due to the absence of testing standards for them (P. Zhang, Wang, et al., 2020).

The flexural strength of geopolymer concretes has frequently been found to be higher than that of OPC concretes, which normally changes in the same trend as compressive strength but is substantially lower. The results of earlier investigations, according to Zhang et al. (2020), have established that geopolymer concrete is more brittle than OPC concrete and that the fracture energy of geopolymer concrete may be empirically connected to its compressive strength.

Lightweight materials are being used as an option to reduce building structural weight and increase the thermal insulation effectiveness of buildings (Schincaglia, 2022). According to Day et al. (2013), structural lightweight concrete has a density between 1200 and 2000 kg/m^3 and a strength of at least 10 MPa. The compressive strength, bulk density and water absorption specifications for concrete-facing bricks mandated by ASTM C1634 (2020) are displayed in Table 2.13. According to the ASTM C129 (2017) standard specification, the compressive strength should range between 3 and 4 MPa for non-load-bearing concrete masonry units.

Table 2.13. Strength and water absorption specifications for concrete-facing bricks (ASTM C1634, 2020)

Density classifications	The oven-dry density (Kg/m^3)	Max. water absorption (%)		Min. compressive strength (MPa)	
		Average of 3 units	Individual units	Average of 3 units	Individual units
Lightweight	Less than 1,680	15	17	24.1	20.7
Medium weight	1,680-2,000	13	15	24.1	20.7
Normal weight	2,000 or more	10	12	24.1	20.7

According to the European Standard TS EN 206 (2016), the required 28-day compressive strength values for regular and heavyweight concrete are 8-100 and 10-115 MPa for cylindrical samples with a diameter of 150 mm and a height of 300 mm and a cubic sample with a side length of 150 mm, respectively. For lightweight concrete, the requirements of 8-80 and 9-88 MPa are relevant (Luukkonen et al., 2018). In accordance with Mackenzie and Welter (2014), the compressive strengths of geopolymer matrix materials range widely, from 1 MPa for the extremely weak products of solid-state synthesis through 26 MPa for geopolymers made using the sol-gel method to 110 MPa for a product made from fly ash activated with sodium silicate and NaOH solution.

Regarding the compressed and stabilised earth blocks, Deboucha and Hashim (2011)suggest that where building loads are small (in the case of single-storey constructions), a compressive strength of 1 - 4 MPa may be sufficient while, Teixeira et al. (2020) suggest that the minimum compressive strength requirements vary between 1.0 MPa and 2.8 MPa.

Bricks are frequently employed in circumstances where bending loads are feasible; as a result, they should have adequate strength against transverse loads (flexural modulus of rupture), which can be assessed using a three-point bending test. Common building bricks must have a minimum flexural strength of 10 kg/cm^2 (Dove, 2014).

Energy efficiency and thermal comfort in buildings are crucial since most people spend around 90% of their time inside, and both factors heavily depend on the thermo-physical qualities of the building materials (Asadi et al., 2018). Low thermal conductivity concrete reduces heat transfer and energy usage in structures. Due to their inorganic structure, geopolymers have great thermal stability, making them suitable for use in high-temperature applications such as heating system linings, heat insulation, and wall panels (Sotelo-Piña et al., 2019).

ASTM C332-17 (2009), provides the standard specification for thermal insulating properties of concrete made from lightweight aggregate as shown in Table 2.14.

Table 2.14. Thermal conductivity for lightweight concrete

Maximum average 28^{th}-day properties	
Oven -dry bulk density (Kg/m^3)	Thermal conductivity (W/m.K)
800	0.22
1400	0.43

Additionally, Zhang et al. (2020) determined that lightweight concretes should have a thermal conductivity in the range of 0.15 to 0.48 W/mK.

According to Asadi et al. (2018), conventional-weight concrete has a thermal conductivity of 0.6 to 3.3 W/m.°K while lightweight concrete has a range of 0.2 to 1.9 W/m.°K.

Table 2.15 a,b shows conclusively that porosity, bulk density, thermal conductivity, and compressive strength are the characteristic parameters that are most frequently taken into account in the majority of investigations. The diatomaceous earth-containing concrete mixtures seem to be porous, with porosity ranging from 25 to 92.5 %; lightweight, with densities falling between 0.37 and 1.81 g/cm^3; low thermal conductivity ranging from 0.09 to 0.45 W/mK; and the majority of them exhibit notably high compressive strengths. Since density affects the thermal insulating properties, low-density materials are necessary for optimum thermal conductivity (Fan, 2015). Furthermore, diatomite can be used as an alkaline-activated precursor (binder) rather than a light aggregate to produce stronger concretes.

Zhang et al. (2020) found that geopolymer concrete had a greater crack resistance coefficient than OPC cement-based concrete. Cong et al. (2021) argue that the durability of geopolymers depends on their resistance to hostile environments, including their abrasion performance, porosity, chemical erosion resistance, dry shrinkage, and carbonization resistance.

Verma et al. (2022) claim that geopolymer concrete outperforms Portland cement concrete in terms of its physical, mechanical, and durability properties, as well as its resistance to corrosion caused by salt, sulfate, and acid. The performance characteristics of concrete reported by several studies in Table 2.15 a,b lend support to Ojha & Aggarwal's (2022) conclusions that geopolymer qualities may vary not only by the origin, shape, and particle size of the binder, but also by the metal, alkali, and amorphous components.

Table 2.15. (a): Concrete's performance characteristics when diatomaceous earth is used as a lightweight aggregate (b): The performance properties of concrete when diatomaceous earth is utilized as a clinker-free geopolymer material.

S/N	Porosity (%)	Density (g/cm3)	Thermal conductivity W/Mk	Sound Transmission km/s	compressive strength MPa	water absorption %	flexural strength MPa	Reference
	(a) When diatomite is used as a lightweight aggregate resource							
1	-	-	-	-	3.92	-	-	(Loganina et al., 2014)
2	47.08	1.14	0.16	-	7.66	37.19	2.4-0.74	(Taoukil et al., 2021)
3	49	1.06	0.2	-	8.5	9	-	(Escalera et al., 2015)
4	30	1.64	0.45	-	16.3	-	6	(Galán-Arboledas et al., 2017)
5	-	0.9-1.19	-	-	2.5-8	-	-	(Ünal et al., 2007)
6	50.2	1.26	-	-	18.8	-	-	(Hao et al., 2019)
7	58-61	1-1.2	0.15–0.19	-	7.8–12.9	61–72	-	(Posi et al., 2013)
8	-	1.81	-	-	28	21.1	-	(Hasan et al., 2021)
9	50.39	1.25	-	-	-	-	10.05	(Man et al., 2017)
10	-	0.55-0.79	-	-	-	-	-	(Fragoulis et al., 2004)
11	-	0.73	0.13	-	17.5	46	-	(Pimraksa & Chindaprasirt, 2009)
12	74.28-92.45	0.37-0.6	0.0878-0.1035	15.78-17.35	-	-	-	(Hoc Thang, 2020)
13	45	-	-	61.3	4.29	-	-	(Mehmedi Vehbi GÖKÇE, 2012)
14	58.53	0.71-0.91	-	-	14.7–19.4	52.63	-	(Reka et al., 2017)
	(b) When diatomite is used as a clinker-free geopolymer resource							
1	-	-	0.171	-	5.78	-	-	(Nakashima et al., 2021)
2	-	-	-	-	71	-	9.2	(Bagci et al., 2017)
3	-	-	0.09 - 0.16	-	-	-	-	(Matsunaga et al., 2017)
4	68	-	-	-	-	-	-	(Šaponjić et al., 2015)
5	-	1.76	-	-	17.24	-	-	(Phoo-Ngernkham et al., 2013)
6	-	-	-	-	30	-	-	(Font et al., 2018)
7	25	1	-	-	106	-	-	(Akhtar et al., 2010)

It has been found that the properties of geopolymers also rely on a number of other factors, including the concentration of the alkaline activator, the ratio of the alkaline solution to the binder, the ratio of sodium silicate to sodium hydroxide, the alkaline liquid to the binder ratio, the duration and temperature of the curing process, the amount of superplasticizer, and the proportion of water to the binder.

The permeable pore volume is a crucial aspect in determining the durability of cement-based materials, therefore any decrease in the permeable pore volume suggests some gain in its durability performance, and vice versa (Fopossi et al., 2014; S. Abo Dhaheer et al., 2018; Teixeira et al., 2020; Thong et al., 2016; Ugwuishiwu et al., 2013). Water absorption for high-quality bricks according to Ahmad et al. (2017) shouldn't be more than 20% of the dry brick's weight, although the Malaysian standard limit is 15% (Islam et al., 2020).

In addition to mechanical strength, a building material's thermal characteristics can be a crucial factor in achieving desired functionality (Samuel et al., 2023). Dondi et. al, (2004) stated that thermal conductivity is influenced in a complex way by many variables. They explained that not only porosity and bulk density but also the size and shape of pores, as well as the presence of certain mineralogical components, can play a very important role in influencing the thermal conductivity of a material. Utilizing networks of strategically oriented particles or fibres, particularly those with high aspect ratios, may allow for further advancements in thermal conductivity (Samuel et al., 2023). There are both organic and inorganic thermal insulation panels available on the market; however, the organic panels have the drawback of being flammable, the fibrous inorganic panels are unhealthy, and the particulate inorganic panels densify when sintered at high temperatures, necessitating the development of new processing techniques that incorporate controlled porosity (Alvarado et al., 2023). It has been

found that geopolymer concrete has superior thermal insulation qualities to OPC concrete of the same density.

The typical test methods used to assess the various concrete performance qualities are shown in Table 2.16.

Table 2.16: Testing procedure reported in the literature.

S/N	Property tested		Standard test method
1.	Physical	Density	(ASTM-C642, 2013)
		Porosity	(ASTM C20-00, 2015)
		Water absorption	(ASTM C373-14, 1999)
2.	Mechanical	Compressive strength	(ASTM C109/C109M, 2007)
			(ASTM C773-88, 2007)
		Flexural strength	(ASTM C78/C78M – 02, 2002)
3.	Insulation	Thermal conductivity	(ASTM C1113, 1999)
		Pulse velocity	(ASTM C597, 2016)

Generally, and according to Elahi et al. (2020), concrete made with alkaline activated binders (AAB) has been shown to have excellent or equivalent physical properties to those made with OPC, including compressive strength, setting time and hardening, reduced shrinkage, better thermal properties, freeze-thaw resistance, alkali-silica reactivity and improved durability.

According to Duxson et al. (2007), geopolymer concrete can have the following properties depending on the components' composition, curing environments, and other factors:

- High compressive strength
- Low shrinkage
- Good abrasion resistance
- Fast and controllable hardening

- Fire resistance (up to 1000ºC)
- High resistance against acids and salt solutions
- High resistance to alkali-aggregate reactions
- Low thermal conductivity
- Good adhesion to concrete surfaces, steel, glass and ceramics

2.9 Factors Influencing the Geopolymer Concrete Properties

Extensive collection of research has shown that a variety of factors, including the physical and chemical characteristics of the source materials, the type and concentration of the alkaline solution, the mixing proportions, and the curing routine, affect the properties of concrete made from alkaline-activated materials. Most studies have focused on the mechanical and microstructural aspects of hardened concrete as well as its durability characteristics (Elahi et al., 2020; Mansour et al., 2016).

The physical, chemical, mechanical, hydraulic, and thermal properties of the geopoly mers are significantly influenced by the raw material from which they were produced (Nawaz et al., 2020). Therefore, different aluminosilicate precursor-derived geopolymers with variable activator concentrations have been known to create different compressive strengths.

It has been determined that geopolymer concrete mixtures' strength is influenced by the water-to-binder ratio. According to Bondar (2009), it may be considered that the concrete in a structure that is resisting failure generates both cohesion and internal friction, which are largely correlated with the water-to-binder ratio and curing temperature.

Based on data from prior investigations, it is clear that the concentration of alkaline activator significantly affects the reactivity, pore structure, formation of the

aluminosilicate gel, and consequently, a variety of mechanical and chemical properties of the resulting geopolymers (Nawaz et al., 2020). Due to a greater degree of dissolution and an increase in the amount of reactant available to complete the geopolymerization process, the activation energy of the reaction likewise increased as the alkaline solution concentration rose (Nath & Kumar, 2019). There is much less natural pozzolan dissolution at lower activator concentrations (less than 5M), which results in the creation of a gel phase with a weaker binding strength (Bondar, 2009). However, because the alkaline hydroxide solution has a higher viscosity at concentrations greater than 7.5M, the resulting geopolymer pastes require more time and/or heat to evaporate the excess water from the system before forming a monolithic geopolymer, which reaches its full strength as a result of the formation of the 3-D network of aluminosilicate. Zhang et al. (2020) discovered that although molarities of 10M, 12M, and 14M have been adopted by most studies, there hasn't been a reliable reference standard for choosing sodium hydroxide concentration due to the variety of raw materials and the complicated reaction mechanism. While some research indicated that 14 was the perfect molarity, others found that 12 was the most effective NaOH solution molarity value for the alkali solution (Mohammed et al., 2021). The effect of sodium hydroxide concentration on the compressive strength of geopolymer concrete is illustrated in Figure 2.23.

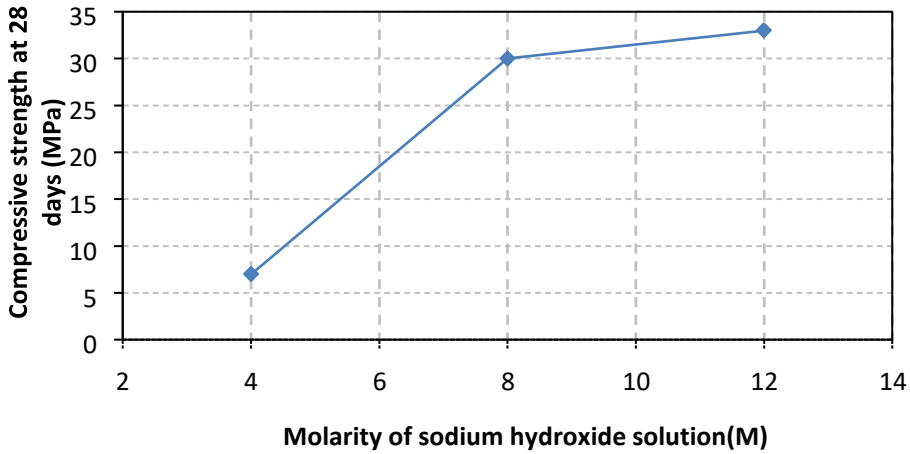

Figure 2.23: Influence of the sodium hydroxide concentration on the compressive strength (Barnard, 2014)

The ratio of Na_2SiO_3 to NaOH is another element that has been identified as influencing the compressive strength (CS) of geopolymer concretes (GPC). To make GPC with a suitable CS, the effective ratio of Na_2SiO_3 to NaOH ranges from 1.0 to 3.0, with 2.5 being the most popularly and successfully utilized value (Hassan et al., 2019; P. Zhang, Wang, et al., 2020). The impact of the Na_2SiO_3: NaOH ratio on the compressive strength of geopolymer concretes is demonstrated in Figure 2.24.

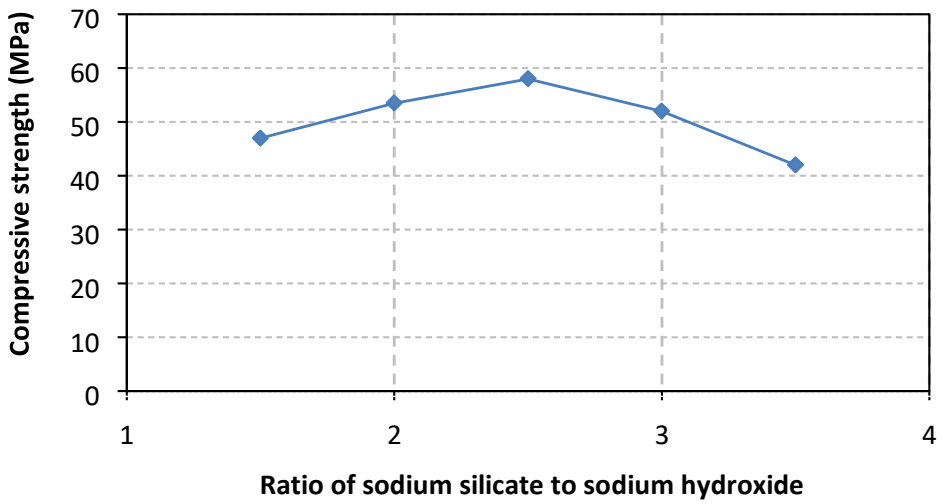

Figure 2.24: Influence of the SS/SH ratio on the compressive strength (Barnard, 2014)

The temperature has a significant impact on the curing process because it accelerates the geopolymerization, which results in a more effective dissolution process (Hardjito

& Rangan, 2006). Higher compressive strengths can be achieved with longer curing times at elevated temperatures because the geopolymerization process is more effective (Barnard, 2014). However, Hardjito & Rangan (2006) observed that compressive strength remained stable after 24 hours of thermal curing. Studies have shown that geopolymer concrete can reach strengths of up to 70% of its ultimate strength within the first three to four days of the curing process.

Studies have also revealed that aggregates have a significant impact on the development of the compressive strength of geopolymers, with those containing higher levels of fine aggregate showing higher compressive strengths (Zhang et al., 2020).

The engineering qualities of construction materials have also been reported to be adversely affected by the presence of pores and microcracks. Danso (2019) asserts that composite building materials frequently experience bonding issues that reduce their strength.

Despite having good thermal and durability qualities, geopolymers are brittle by nature and have a limited tolerance to tensile and flexural loadings, rendering them unsuitable for a number of structural applications (Mahmood et al., 2021). However, concentrating on enhancing geopolymers' ductility and tolerance to tensile stresses using synthetic and natural fibres will aid to alleviate this issue and make it possible to achieve sustainability goals.

2.10 Performance Correlation and Prediction Modelling

Testing for concrete quality control is typically done 7 to 28 days after the fabrication process. However, the subsequent construction process may be delayed by the time needed to conduct tests. This is because, while determining compressive strength is rather simple, assessing the durability properties of concrete is sometimes tedious and

time-consuming. Disregarding testing will harm quality control on a large scale. For this reason, quick and accurate prediction of concrete properties is crucial for quality control. Consequently, time and construction expenses will be saved if the mixture's proportion is changed. According to Muliauwan et al. (2020), it is essential to predict concrete strength early on to plan projects, monitor quality, and determine how long it would take to open the concrete formwork. Therefore, a modelling system that does not rely on experiments but can accurately predict concrete qualities is required.

A significant indicator that is widely used in design codes to predict the performance properties of concretes is compressive strength (Xie et al., 2020). Due to its inherent significance in the structural design of concrete structures, experts have always chosen it as the benchmark parameter. Baghabra Al-Amoudi et al. (2009) claim that the construction sector frequently views the 28-day compressive strength as the only criterion for approving a concrete mix. The other properties of concrete, such as durability, physical, and thermal resistance, are infrequently examined due to the cost, difficulty, and time required to determine them. Relationships between concrete properties must therefore be established for quality control purposes, nevertheless, to make it easier to evaluate them.

In contrast to traditional experimental techniques, empirical regression approaches are preferred to assess the performance capacity of concrete (Farooq et al., 2021). Regression techniques can be used to match the relationship between dependent and independent variables (Imran et al., 2022; Wei et al., 2016).

The linear regression (LR) model is one of the most popular techniques for predicting the performance properties of concrete (Ahmed et al., 2021).

Equation 2.1 illustrates a linear equation.

$$\boldsymbol{y = a + bx} \qquad \text{Equation 2. 1}$$

Where $\boldsymbol{x}$ is the explanatory variable and $\boldsymbol{y}$ is the dependent variable. The slope of the line is $\boldsymbol{b}$, and $\boldsymbol{a}$ is the intercept (the value of $\boldsymbol{y}$ when $\boldsymbol{x}$ = 0).

Due to its widespread acceptance and ease of use, linear regression is frequently the first method used in prediction modelling (Fahrmeir et al., 2013).

Equation 2.2 represents an sth order polynomial regression for s > 1.

$$\boldsymbol{y = w_0 + w_1 x + w_2 x^2 + w_3 x^3 + \cdots + w_s x^s} \qquad \text{Equation 2. 2}$$

where x is the input variable, y is the output variable, w_0 is the intercept, and w_1, w_2, . . . w_s are the polynomial regression coefficients.

A regression with many variables is known as multivariate polynomial regression (MPR) (Imran et al., 2022). Multiple Regression Analysis (MRA), which combines linear and non-linear methods using least-squares fit, is one of the most used methods for predicting the compressive strength of concrete (Chithra et al., 2016). Equation 2. 3 depicts an sth order (s > 1) MPR for a system with 'n' input variables:

$$\boldsymbol{y = w_o + \sum_{l_1=1}^{n} w_{l_1} x_{l_1} + \sum_{l_1=1}^{n} w_{l_1 l_2} x_{l_1} x_{l_2} + \cdots +}$$

$$\boldsymbol{\sum_{l_1=1}^{n} \sum_{l_2=l_1}^{n} \cdots \sum_{l_k=l_{k-1}}^{n} w_{l_1 l_2 \ldots l_k} x_{l_1} x_{l_2} \ldots x_{l_k}} \qquad \text{Equation 2. 3}$$

Even though the MPR adapts a non-linear model to the data, the multivariate function (Equation 2. 4) is a linear function to its coefficients, therefore when the least-squares method is used, the MPR model has the same solution as the multivariate linear regression (MLR) scenario (Imran et al., 2022).

According to Mooi et al. (2011), the key benefits of using regression analysis are that it can:

i. Indicate if independent variables have a significant relationship with a dependent variable.
ii. Indicate the relative strength of different independent variables' effects on a dependent variable.
iii. Make predictions

An excellent correlation between the fitted parameters is indicated by a regression coe fficient, R^2, of more than 0.80, according to Baghabra Al-Amoudi et al. (2009).

Examples of correlation and prediction equations between the compressive strength and flexural strength (modulus of rupture) of concrete are shown in equations 2.4 to 2.7.

Equation 2.4 and Equation 2.5 shows the flexural strength models based on ACI committee 318 (2011) and Australian Standard AS 3600 (2009) for compressive strength ranges of 10-55 and 55-80 MPa respectively.

$$\boldsymbol{f_r = 0.62\sqrt{f_c}} \qquad \text{Equation 2. 4}$$

$$\boldsymbol{f_r = 0.6\sqrt{f_c}} \qquad \text{Equation 2. 5}$$

Where f_r (MPa) and f_c (MPa) represent the modulus of rapture (flexural) and compressive strengths of concrete respectively.

Equation 2.6 was suggested by ACI Committee 363 (2005) for the prediction of the rapture modulus of high-strength concrete, which ranges from 21 to 83 MPa.

$$\boldsymbol{f_r = 0.94\sqrt{f_c}} \qquad \text{Equation 2. 6}$$

The approximate corresponding compressive strength for a given flexural strength can be derived from Equation 2.7 according to Kett (1999) :

$$f_r = k\sqrt{f_c} \quad \text{for} \quad k = 0.7 \text{ to } 0.8 \qquad \text{Equation 2. 7}$$

It appears that the suggested models are only appropriate for a limited range of compressive strengths, and as Prachasaree et al. (2020) pointed out, there are still no generic prediction models available. The difficulty in developing generalized performance prediction models for concretes may be caused by a wide range of several factors, including hydration rate, curing method, nature of primary binder materials, mixing patterns, and microstructural composition.

According to Asadi et al. (2018) and ACI Committee 213 (2013), equations 2.8 and 2.9 demonstrate a considerable correlation between the bulk density (ρ) of concrete and the thermal conductivity (λ) value.

$$\lambda = 0.193e^{0.146\rho} \qquad (R^2=0.92) \qquad \text{Equation 2.8}$$

$$\lambda = 0.303e^{0.965\rho} \qquad (R^2=0.98) \qquad \text{Equation 2.9}$$

According to the existing literature, much research has been performed regarding the correlation and prediction of concrete's mechanical properties as compared to the physical, thermal and durability properties. However, according to Baghabra Al-Amoudi et al. (2009), the recorded compressive strength values can be used to predict concrete's durability characteristics since concrete's compressive strength has been shown to increase with durability. As a result, correlations between compressive strength and durability indices need to be established for quality control so that the latter values can be calculated using the former.

2.11 Potential Applications of Geopolymer Concrete

Porous ceramics are employed in a variety of applications in our everyday life, including fluid filtering, sound absorbance, vibrational reduction, energy absorption, and walls (Alvarado et al., 2023). Because of benefits like low density, low thermal conductivity, high specific surface area, stable chemical properties, heat and corrosion resistance, and other qualities, porous ceramics are more often used as filter media, adsorbent, thermal insulators, catalyst support, and other functionalities, according to (Wu et al., 2023).

Although geopolymer concrete has demonstrated its suitability for use in civil engineering projects like road construction, walkways, and pipework, additional testing is necessary before being widely employed in structural applications and the creation of national codes of practice (Ajmal et al., 2023).

In building applications, geopolymers can meet and even exceed the majority of the current performance standards, especially when acid resistance and heat resistance are needed (P. Zhang, Gao, et al., 2020). Materials with geopolymeric features are useful in the automotive, mechanical, and primarily civil construction industries (Schincaglia, 2022). Hermann et al. (1999) and Davidovits (2020) suggested potential uses for geopolymers based on the molar ratio of Si and Al, which are depicted in Table 2.17 and Figure 2.25.

Table 2.17: Geopolymer applications

Si/Al	Application
1	Fire protection, bricks and ceramics
2	Low CO_2 cements, concrete, radioactive & toxic waste encapsulation
3	Heat resistance composites, foundry equipment, fibreglass composites
> 3	Sealants for Industry
20 < Si/Al < 35	Fire resistance and heat resistance fibre composites

Even in applications requiring the use of steel reinforcements, geopolymer concrete is an efficient alternative to Portland cement concrete (Almutairi et al., 2021).

Geopolymer concrete can be utilized for concrete constructions like sewer pipe fabrication, coastal bridges, and underwater concrete supports that will be constantly attacked by saltwater due to its excellent resistance to chloride corrosion (Almutairi et al., 2021). Additionally, geopolymer can be used as a material for repairing roadway infrastructures, according to Yun et al. (2014).

Zhang et al. (2020) postulates that the use of geopolymer might be expanded to a variety of industries, including aeronautical engineering, the nuclear industry, and even archaeological research, in addition to its use as an OPC replacement.

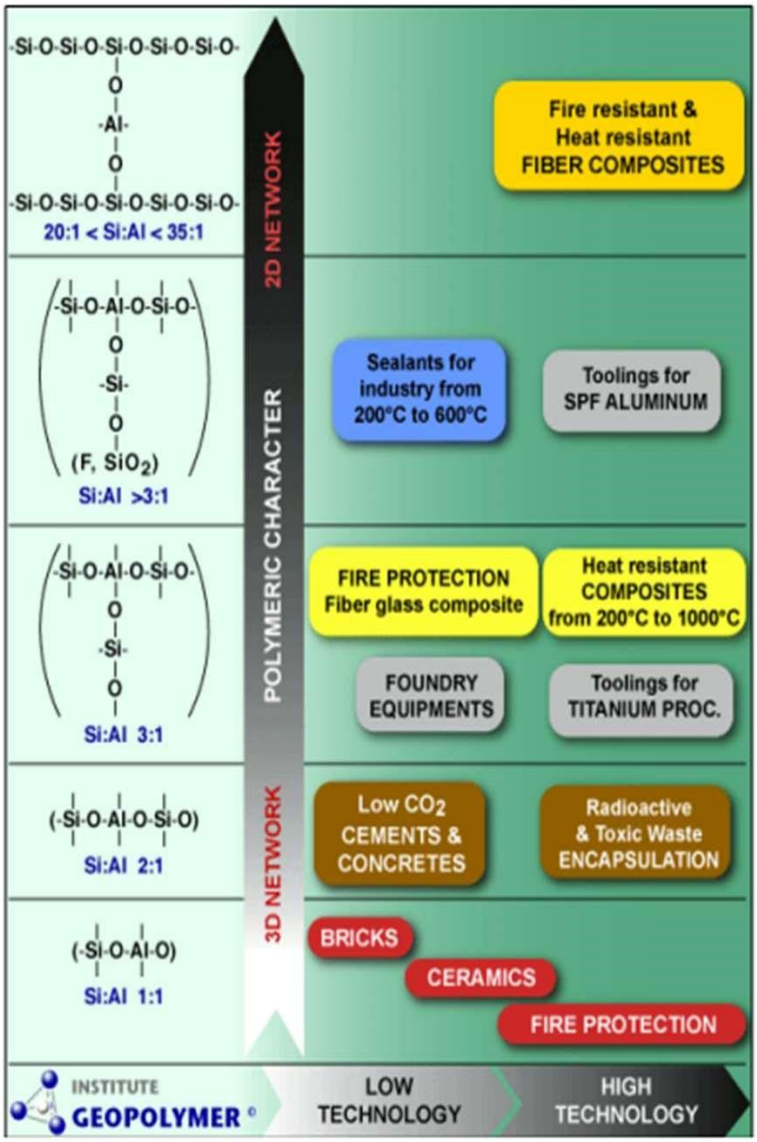

Figure 2.25: Geopolymer application

Toxic metals, organic contaminants, and newly emerging micropollutants are just a few of the many toxins that geopolymers can efficiently remove from water. The use of geopolymers as adsorbents in water treatment applications has grown in popularity in recent years because of their high specific surface area, porous structure, and ion exchange capacities (Elgarahy et al., 2023). Geopolymer-based adsorbents are gaining popularity due to their excellent potential, sustainability, and ability to solve the urgent problems caused by water pollution.

2.12 Gaps in Knowledge to be Filled

Geopolymer concrete offers a lot of potential as an alternative to cement-based concrete, due to the growing demand for building materials with a low carbon footprint and minimal energy use. In comparison to OPC concrete, it demonstrates to have promising performance characteristics. However, it was noted that low calcium fly ash geopolymer concrete served as the foundation for most of the study.

The applicability of diatomaceous earth thus far shows that it is a pozzolanic material that occurs naturally and has applications in the building and construction sector. The literature review shows that using diatomaceous earth is one of the effective ways to create sustainable, insulating, and lightweight construction materials while minimizing the harmful effects of industrial solid wastes on the ecosphere. The potential of this material as a geopolymer for making cementless (clinker-free) concrete, however, has not received a lot of research. Most research has focused on its incorporation as a replacement for fine aggregate or as a partial replacement for cement.

The comprehensive survey of the literature on the subject of utilising diatomaceous earth in the production of geopolymer concrete reached the following conclusions:

- The outstanding compressive strength of geopolymer concrete has been demonstrated, however, its tensile strength is low, and brittle fracture happens frequently. Because of this, it is necessary to add a toughening effect by utilizing a fibre-reinforcing material to acquire the required mechanical and thermal qualities for any application.
- Despite the fact that silica-based raw materials have been the subject of extensive research as potential sources for geopolymeric concrete, the reinforcement of these

materials, particularly those based on diatomaceous earth, with either synthetic fibres or a combination of the two has not been addressed.

- This analysis revealed that, despite the authors' significant interest in the mechanical, physical, and thermal properties of building materials, astonishingly little work has been put into theoretical property correlation modelling for performance prediction. For geopolymer concrete to be a suitable replacement for OPC concrete, technology must improve to the point where the composition of a geopolymer matrix with a given strength can be determined before mixing. Similarly, the review conducted by Mohammed et al. (2021) revealed the same limitation.

CHAPTER THREE: METHODOLOGY

3.1 Introduction

The collection, processing and characterization of the key raw materials are covered in this chapter. The geopolymer specimens are prepared and subsequently cured with the guidance of the design of experiment. Finally, a description of the techniques used to evaluate the products' mechanical, physical and thermal performance is provided. The research plan employed in this study is depicted in Figure 3.1.

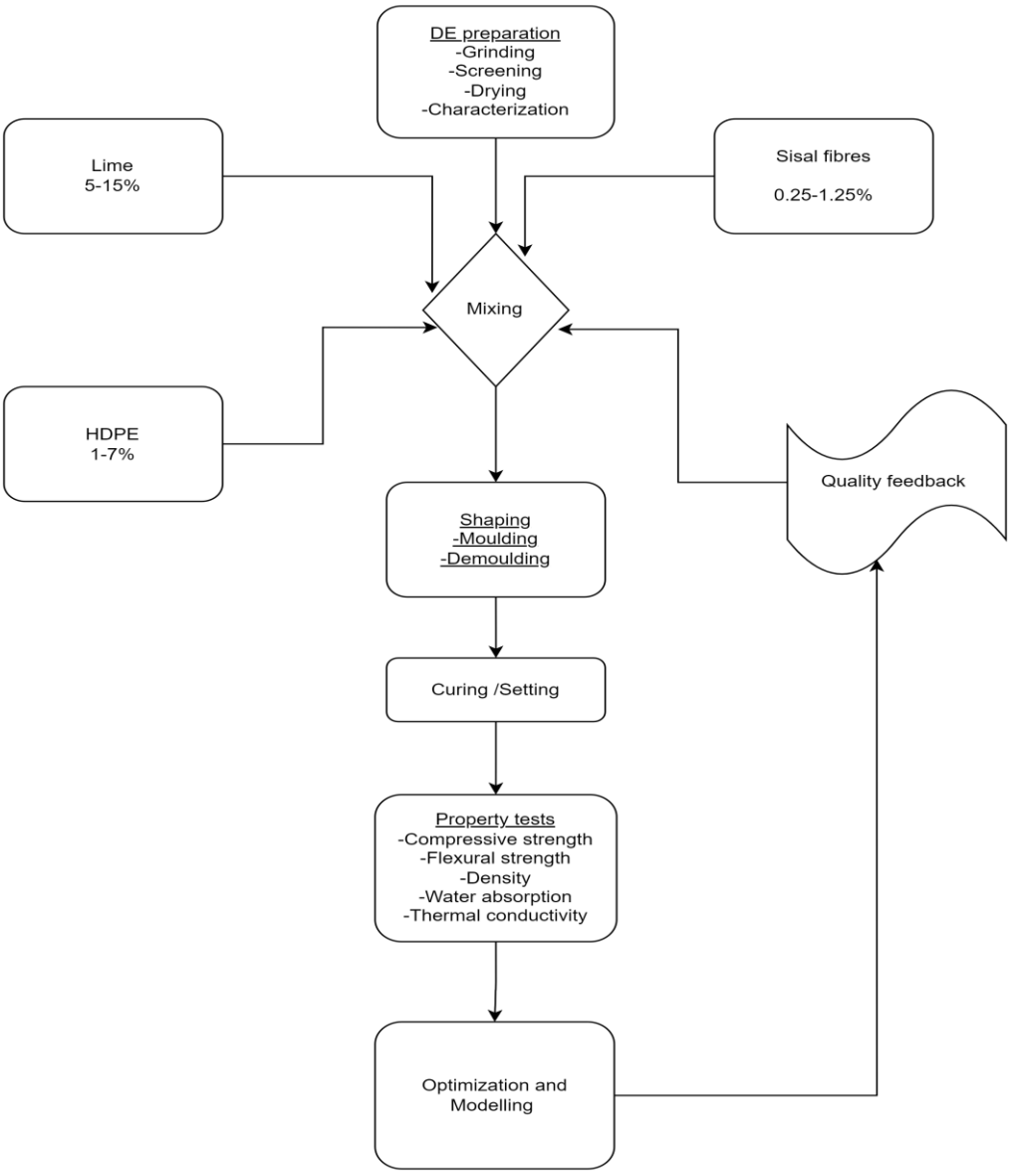

Figure 3.1: Research plan

3.2 Collection, Processing and Characterization of the Raw Materials

3.2.1 Material collection

The materials used in this research are diatomaceous earth, sisal fibres, shredded high-density polyethylene (HDPE) wastes, alkaline activators and water. The raw materials were collected from sources within Kenya; specifically, diatomaceous earth was acquired from Elementaita (indicated in Figure 3.2), sisal fibres from Mogotio, and HDPE wastes from Eldoret and its environs.

Quicklime, which is an earth-alkaline source, was used in this study as an elementary alkaline activator with the idea that, if necessary, it might be replaced with more advanced chemical activators like sodium hydroxide and/or sodium silicate to improve the specimens' properties. Lime according to experts, is greener than cement because of its low energy requirements, minimal CO_2 emissions during manufacture and CO_2 absorption during setting (Scrivener et al., 2018). It has been found that the calcium content has a significant impact on the setting time and ultimate strength of concrete. Therefore, the strength of an alkali-activated natural pozzolan could be increased by adding quicklime (CaO) content to a natural aluminosilicate (Bondar, 2009). Quicklime, was procured from commercial suppliers in Eldoret town.

Figure 3.2 presents a geological map of Nakuru County in Kenya which hosts the diatomaceous earth reserves (Gevera & Mouri, 2018).

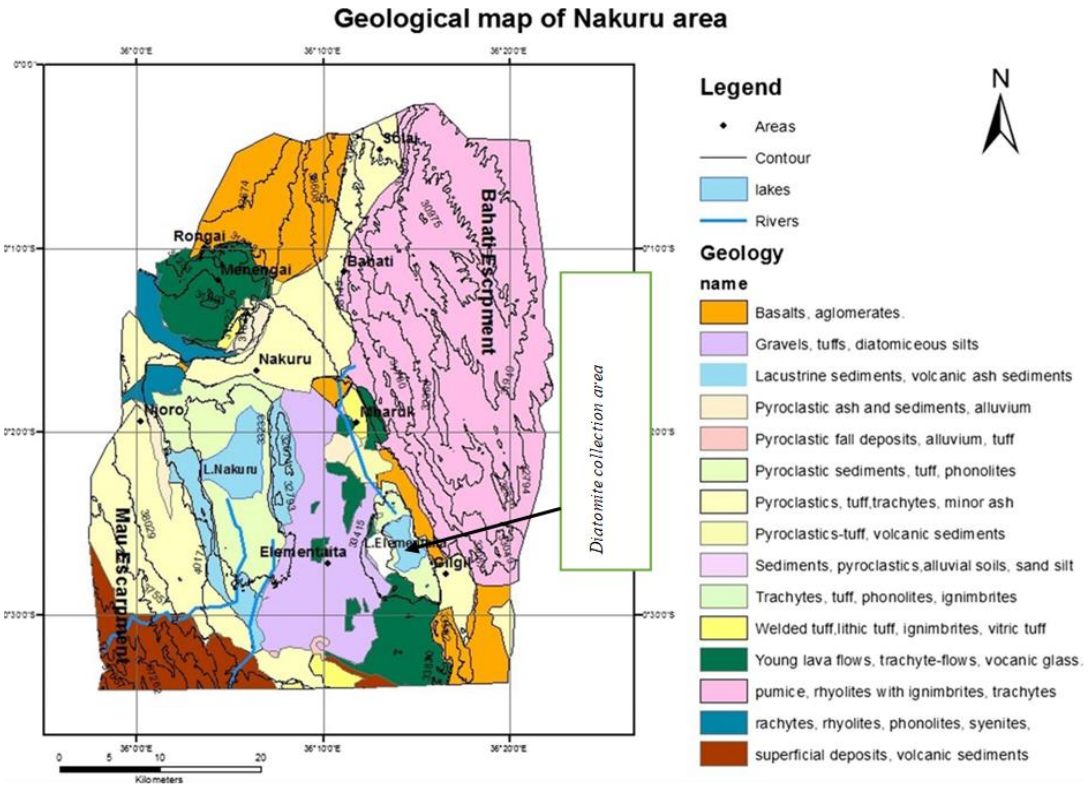

Figure 3.2: Geological map of Nakuru county-Kenya

3.2.2 Material processing and characterization

a) Diatomaceous earth and lime

It was necessary to ascertain the mineralogy, chemical composition, and physical properties of the diatomaceous earth used in the current study because the nature of the starting materials has been known to influence the formation of the geopolymer gel phase.

The diatomaceous earth had already been finely pulverized when it was received. For comparison, tests on the diatomite in its raw and calcined (at 600 °C) states were performed.

The Bruker S1 portable X-Ray fluorescence (XRF) analyser was used to determine the chemical composition of the diatomite samples as per ASTM C114-10 (2010).

Following ASTM C 1365 (2006), the X-ray powder diffraction (XRD) patterns were taken using a Bruker D8 Advance diffractometer at a scan rate of 1° /min.

The Atterberg limits test, conducted following ASTM D4318-17 (2017), was used to determine the clayey nature of diatomaceous earth. Utilizing an LS 13 320 Laser Diffraction Particle Size Analyzer and following ASTM B822–17 (2017) guidelines, a particle size distribution analysis was performed. Following ASTM-D854, (2010) and ASTM D 7348-13, (2013), respectively, the specific gravity and loss on ignition were also carried out.

The thermal characterization of diatomaceous earth was performed by Thermogravimetric (TGA) and Differential Scanning Calorimetry (DSC) analysis techniques according to ASTM E1131, (2015). The simultaneous TGA-DSC analysis was performed for both the calcined diatomite and the raw diatomite. The diatomite specimens were heated at a rate of 10 °C/min, from room temperature to 950 °C in a static air environment. The heating rate for the DSC was also 10 °C/min, from -50 °C to 450 °C in a static air environment. The Pozzolanic reaction behaviour of the diatomite and lime mixture was also observed through the TGA-DSC analysis. The characterization methods employed are illustrated in Figure 3.3.

To be assured of the composition of the calcium-based alkaline activator, the chemical composition of lime was examined using an XRF device.

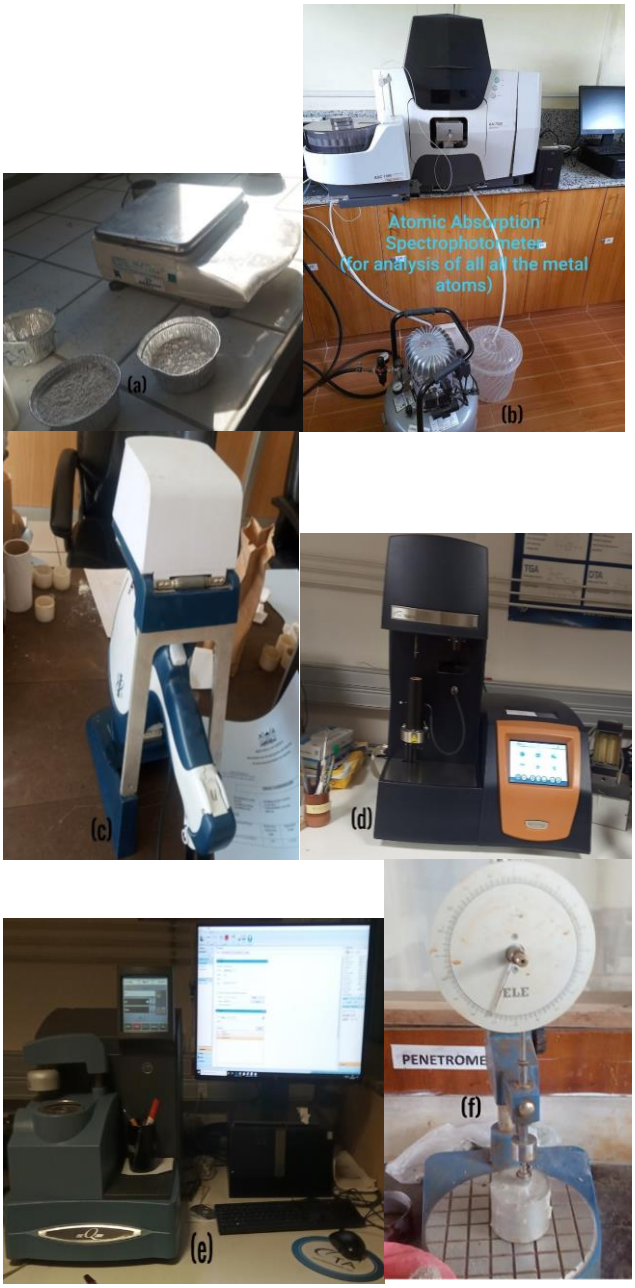

Figure 3.3: Diatomaceous earth and lime characterization (a) Test Samples (b) AAS (c) XRF (d) TGA (e) DSC (f) Atterberg testing

b) Sisal fibres

The decorticated long fibre bundles were extracted from the leaves of the sisal plant, washed, dried in the air, and then cut into average lengths of 3 to 10 mm as shown in Figure 3.4. The fibre tensile strength (tenacity) was performed on the Universal Instron Tester (Model 3345) following ASTM D3039, (2010). The bulk density of sisal fibres

was measured using a pycnometer. By using high-performance liquid chromatography (HPLC) at 85 °C for 30 min per sample with a flow rate of 0.6 mL/min of the mobile phase (deionized and degassed water) and a refractive index detector, the cellulose, lignin, and hemicellulose contents of the sisal fibre were determined.

The incorporation of random short fibres was inspired by earlier researchers (A. Mahmood et al., 2021; Namango, 2006; Yan et al., 2016), who postulated that random short fibres in a cementitious media enhance toughness, ductility, and strength by bridging and minimizing the cracks; and do not require complex processing procedures. Additionally, because they do not require sophisticated processing methods and can be mixed using conventional mixing machines, short random fibre reinforcing of geopolymer matrices is of particular relevance for large-scale applications such as building materials (Silva, Kim, Aguilar, et al., 2020). According to Jamshaid et al. (2022), the addition of small-size natural fibres to concrete that is evenly dispersed and randomly orientated might lessen drying shrinkage by stopping the spread of microcracks while also boosting strength. The percentage proportion range utilized for sisal fibres was 0%-1.25% as per Namango (2006) and Danso et al. (2015) work.

Figure 3.4: Sisal fibres (a) Long fibres (b) Short fibres

c) The high-density polyethylene (HDPE) wastes

The excellent qualities of HDPE wastes, as highlighted by (Harni et al., 2018), among other researchers, were the basis for their use in this study. The high-density polyethylene wastes were gathered from municipal waste collection stations and landfills, shred into little pieces, and then cleaned, dried, and sieved to produce tiny fragments up to 3 mm in size as done by Belmokaddem et al. (2020). In this study, high-density polyethylene (HDPE) served as the aggregate filler material instead of sand and could enhance the strength characteristics of the concrete. Figure 3.5 presents the preparation process for the HDPE wastes. The percentage proportion range utilized for plastics was 0-7% as per the work of Akinwumi et al. (2019).

Figure 3.5: HDPE Preparation (a) Shredding (b) Drying (c) Sieving

3.3 Fabrication of Lime Activated Diatomaceous Earth Geopolymer Concrete Specimens

3.3.1 Mixing of Materials at different proportions

The experimental mixture design (custom of extreme vertices design) facilitated by the design expert software was employed in this study. The design of experiment (DoE) was applied in the determination of the proportions of the raw materials in each brick specimen throughout the mixing process as illustrated in Figure 3.6. G stands for proportional group and P for compaction pressure in the design of experiment (DoE) table. For instance, G1P2 defines a specimen that belongs to the proportional group 1 and that was compacted at a pressure of 2MPa.

Lime was added between 5 and 15 %, sisal fibres between 0 and 1.25 %, and HDPE between 0 and 7 %; all based on the weight of diatomaceous earth. Based on the literature survey, the quantity of water used was fixed at 70 % of the diatomaceous earth weight.

The two-stage mixing sequence was used since, according to the literature analysis, it has been found to be the most common for handling dry raw materials. The fabrication of the specimens was performed at room temperature, and the water used for mixing was regular lab tap water.

Figure 3.6. (a) Rationing (b) & (c) Mixing

The design constraints for the design of the experiment (DoE) are displayed in Table 3.1. Table 3.2 provides a summary of the design of the experiment shown in Table 3.3. The DoE table was derived from the fraction of extreme vertices design using design expert software.

Table 3.1: Design constraints concrete mixture composition

Low Limit (%)		**Constraint**		**High Limit (%)**
76.750	≤	A: DIATOMITE	≤	100.000
0.000	≤	B: LIME	≤	15.000
0.000	≤	C: SISAL	≤	1.250
0.000	≤	D: HDPE	≤	7.000
		A+B+C+D	**=**	**100.000**

Table 3.2: Brick Development Summary

Input variables	**Unit**	**Quantity**	**Variation**	
			Fixed	**Variable**
Diatomite	%	76.75-100		✓
Lime	%	0-15		✓
Sisal fibres	%	0-1.25		✓
HDPE	%	0-7		✓
Water	%	70	✓	
Moulding Pressure	MPa	2-8		✓
Curing	Days	28	✓	

Table 3.3: Design of experiment table

Group	Run	Factor 1	Factor 2	Factor 3	Factor 4	Factor 5	Specimen Name
		A: DIATOMITE	B: LIME	C: SISAL	D: HDPE	E: PRESSURE	
		% Weight	% Weight	% Weight	% Weight	Mpa	
1	1	100	0	0	0	2	G1P2
	2					4	G1P4
	3					6	G1P6
	4					8	G1P8
2	5	93.75	5	0.25	1	2	G2P2
	6					4	G2P4
	7					6	G2P6
	8					8	G2P8
3	9	89.5	7.5	0.5	2.5	2	G3P2
	10					4	G3P4
	11					6	G3P6
	12					8	G3P8
4	13	85.25	10	0.75	4	2	G4P2
	14					4	G4P4
	15					6	G4P6
	16					8	G4P8
5	17	81	12.5	1	5.5	2	G5P2
	18					4	G5P4
	19					6	G5P6
	20					8	G5P8
6	21	76.75	15	1.25	7	2	G6P2
	22					4	G6P4
	23					6	G6P6
	24					8	G6P8
7	25	83.75	15	1.25	0	2	G7P2
	26					4	G7P4
	27					6	G7P6
	28					8	G7P8
8	29	78	15	0	7	2	G8P2
	30					4	G8P4
	31					6	G8P6
	32					8	G8P8

3.3.2 Moulding and compacting at different Moulding loads.

Figure 3.7 depicts the mould that was employed during the shaping of the concrete mixtures.

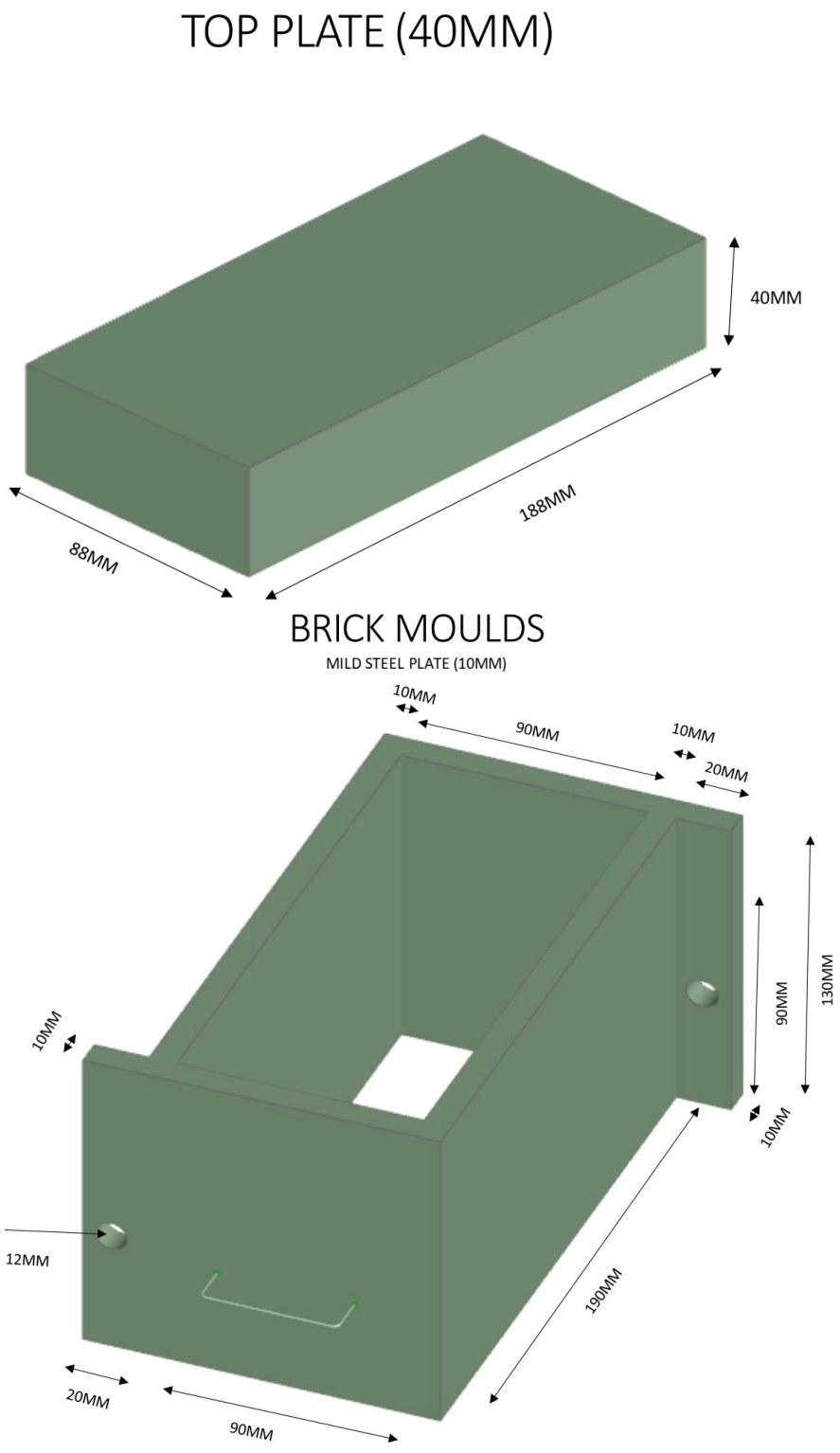

Figure 3.7: Brick Mould

The brick samples were moulded into the desired shape and size according to the Bureau of Indian Standards guideline (IS 1725: 2013, 2013).

The forced compaction technique, according to Gupta et. al. (2020), was used under various stresses ranging from 2 to 8 MPa.

Figure 3.8 illustrates the processes of moulding and compaction that were carried out.

Figure 3.8: Moulding and compaction process

After demoulding, the bricks were oven dried for 24 hours at 70° C and thereafter air-dried at room temperature at about 20°C for 28 days. To fully hydrate the lime, the products were wet daily during the first 14 days of curing under polythene wrapping. After that, they were allowed to dry in the open air, as shown in Figure 3.9, for an additional 14 days before being put through performance testing.

Figure 3.9: Curing of the brick specimens

3.4 Fabrication of $NaOH/Na_2SiO_3$ Activated Diatomaceous Earth Geopolymer Specimens

Materials

1. Diatomaceous earth
2. Sisal fibres
3. Sodium hydroxide and sodium silicate gel ($NaOH/Na_2SiO_3$) alkaline activators
4. Distilled water

Methodology

- Lime as an alkaline activator was replaced with a solution of Sodium hydroxide and sodium silicate gel ($NaOH/Na_2SiO_3$). This is due to the possibility that the chemical reactivity between lime and diatomaceous earth for the lime-activated geopolymers was minimal, leading to the creation of relatively porous and weak specimens. The choice to employ the $NaOH/Na_2SiO_3$ solution was made in light of earlier geopolymer concrete research, specifically by Cong et al. (2021), among other specialists. Sodium hydroxide (99% NaOH) was bought from Kenworks Ventures Company Limited outlet shop in Eldoret; while sodium silicate was bought from one of the outlet shops of Shreeji Chemicals ltd.
- The HDPE wastes were not incorporated into the concrete mix of $NaOH/Na_2SiO_3$ activated diatomaceous earth. This is so because the performance study and evaluation of the lime-activated concrete (chapter four)

demonstrated that eliminating HDPE would allow for the optimization of the concrete's overall performance. Given that polymeric materials are inert by nature and that geopolymerization entails chemical reactions, the HDPE may be impeding the interaction of the geopolymer precursor particles and the alkaline activator.

- The percentage levels of sisal (between 0% and 1.25%) that were employed for the lime-activated concrete were retained. This is because the sisal fibres had a positive impact on the mechanical and physical properties of the fabricated concrete.
- The 100 %wt quantity of diatomite that was utilized for the lime-activated geopolymers was also retained.
- A solution with the desired concentration of sodium hydroxide pellets was created by dissolving them in distilled water at least 24 hours before usage. In reference to the research by (Cong & Cheng 2021; Ganesan et al., 2019; Lavanya et al., 2020), 12M NaOH solution was used for preparing the geopolymer specimens and the ratio of sodium silicate to sodium hydroxide (Na_2SiO_3: NaOH) was kept at 2.5 as in the works of (Al Bakri Abdullah et al., 2013; Al-Bakri Abdullah et al., 2012; Ganesan et al., 2019; Lavanya et al., 2020; P. Zhang, Wang, et al., 2020). In the preparation of 12M NaOH solution, 480 gm of NaOH was dissolved in 1000 ml of distilled water.
- A constant water-cement ratio of 0.7 was applied. The process of preparing NaOH/Na_2SiO_3 activated geopolymer preparation is shown in Figure 3.10.

Figure 3.10: NaOH/Na_2SiO_3 activated geopolymer preparation

The experimental plan that was used to create the NaOH/Na_2SiO_3-activated geopolymer concrete mixtures is shown in Table 3.4.

Table 3.4: Design of experiment for diatomite NaOH/Na_2SiO_3 activation

Group	**Run**	**A: DIATOMITE**	**B: SISAL**	**C: Alkaline activator**		**Specimen Name**
		% wt	**% wt**	**Na_2SiO_3 %wt**	**NaOH %wt**	
1	1	100	0	50	20	D100
2	2	99.5	0.5	50	20	DS0.5
	3	99.125	0.875	50	20	DS0.875
	4	98.75	1.25	50	20	DS1.25

With reference to Ghafoor et al. (2021), Figure 3.11 presents the flow diagram that was followed in the process of diatomite's chemical activation for geopolymer development.

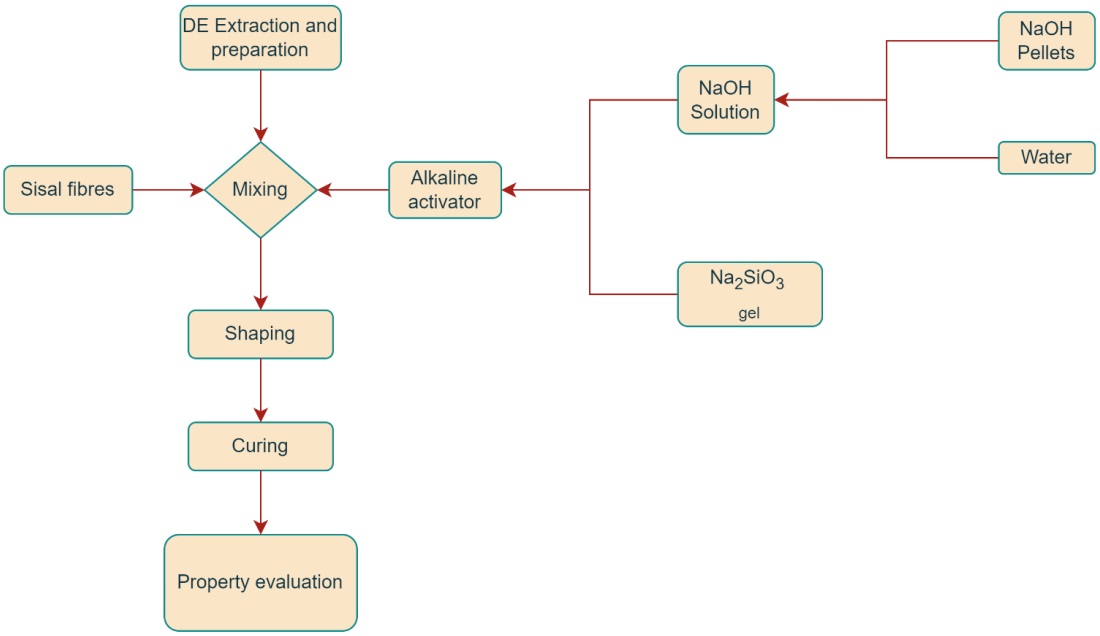

Figure 3.11: Flow chart for diatomite activation.

- After mixing, the geopolymer bricks were shaped in a mould of 160 mm by 40 mm by 40 mm at a constant compaction pressure of 8MPa as suggested by Danso (2016). The dimensions of NaOH/Na_2SiO_3 activated geopolymer specimens were readjusted to reduce on the quantity of the raw materials to be used.

- The geopolymer moulding procedure is shown in Figure 3.12.

Figure 3.12: Geopolymer moulding process

Upon demoulding, the brick specimens were heat treated at 70°C in an oven for 24 hours and thereafter stored at room temperature. The curing procedure is depicted in Figure 3.13.

Figure 3.13: Geopolymer curing

3.5 Lime Activated Diatomaceous Earth Geopolymer Performance Evaluation

a) Compressive Strength

Concrete's compressive strength is one of the key factors used to assess its suitability for various purposes, and structural designs for concrete are frequently based on its value. The Mitutoyo ABSOLUTE Digimatic Vernier Caliper (500 series), which has a 0.01 mm precision, was used to measure the dimensions of the concrete brick samples. The compressive strength of the bricks was determined using a 50kN-WP 310 Universal Materials Testing Machine (as indicated in Figure 3.14), following the ASTM C109/C109M (2007) standard. Although some researchers contend that the wet compressive strength would be a superior criterion to assess the durability of blocks, this work is instead based on the dry strength values. This is because, according to Namango et al. (2015), earth blocks will always remain dry, thus computing the dry

strength would be the more sensible option. During testing, the loading was distributed uniformly using two sheets of 10 mm thick metal, one on each loading face. The load was constantly applied at a constant rate of 1mm/min until failure. Four experimental trials were considered. Compressive strength is determined by the application of Equation 3. 1.

Figure 3.14: Compression strength testing process

$$\boldsymbol{Compressive\ strength\ (CS) = \frac{Maximum\ load\ (N)}{Cross\text{-}sectional\ area\ (mm^2)\ of\ specimen} = \frac{P}{A}\ MPa}$$

Equation 3. 1

CS = Compressive Strength P = Maximum load at failure A= Specimen's cross-sectional area

b) Flexural strength

To assess the flexural features of the brick specimens, the flexural strength, also known as the Modulus of Rupture (MOR), was determined using the three-point bend method following ASTM C78/C78M–02, (2002) while using the 50kN-WP 310 Universal Materials Testing Machine, as shown in Figure 3.15. The specimen was supported by

two rollers that were spaced equally apart from the specimen's length edges during the bending test. In the middle of the specimen, a third roller was positioned on top; a load was then gradually applied to the upper roller until failure occurred. The flexural strength was determined for each specimen using the maximum failure load (F), the specimens' width (b), depth (d) and length (l) and as expressed in Equation 3. 2

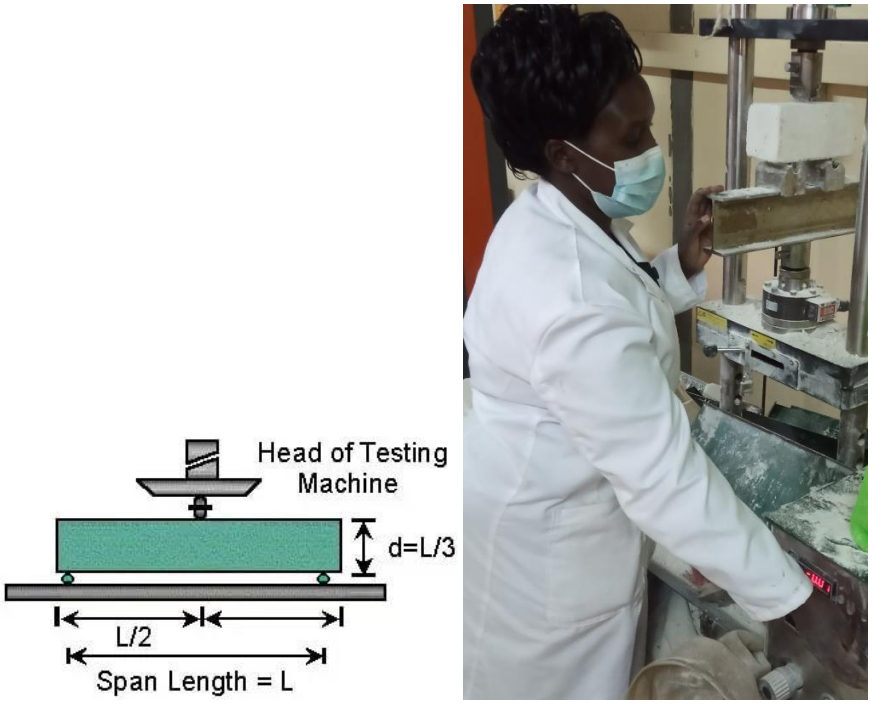

Figure 3.15: Flexural Strength experimental setup

The flexural strength was calculated by using the following relation.

$$f_s = \frac{3FL}{2bd^2}\ MPa \qquad \text{Equation 3. 2}$$

f_s= flexural strength, F = maximum load, L = Span length, b = Width, and d = thickness.

c) Bulk Density

The bulk densities for the brick specimens were determined in compliance with ASTM-C642, (2013). The Alpha TS200 Digital Weighing Scale was used to weigh the dried specimens with an accuracy of 0.05g, and the Mitutoyo ABSOLUTE Digimatic Vernier Caliper was used to measure the specimens' dimensions. Figure 3.16 describes the bulk density experimental test. The specimen volume (V) was computed using the measured dimensions.

Figure 3.16: Bulk density determination

The density was calculated using the equation;

$$\boldsymbol{Density}\ (\boldsymbol{D}) = \frac{DW}{V} \qquad \text{Equation 3. 3}$$

Where, DW = Dried Weight; V = Volume

Volume=length x width x height

d) Water absorption

It was possible to conduct the water absorption experiment following ASTM E514/E514M**,** (2015) or ASTM C373-14, (1999). Following the former standard, the water absorption test was performed using the Karsten Tube, which is a simple Penetration Test for measuring the degree of water penetration into building materials such as concrete bricks, stone, and plaster. The method is one of the in-situ (in-service) and non-destructive performance evaluation techniques whereby, the water resistance of a material can be determined, either in the laboratory or while in service. The test consists of a glass tube which is filled with water and bonded to the test material with a plasteline. Water pressure is then exerted on the surface. A graduated scale indicates the amount of water penetrating the surface over a certain time frame. According to Hendrickx (2013) and Liu et al. (2020), the hydrostatic head produced by the water column in the tube can be connected to rain that is falling at a specific pace. Figure 3.17, shows the Karsten Tube Penetration Test tool kit and water-holding glass tubes.

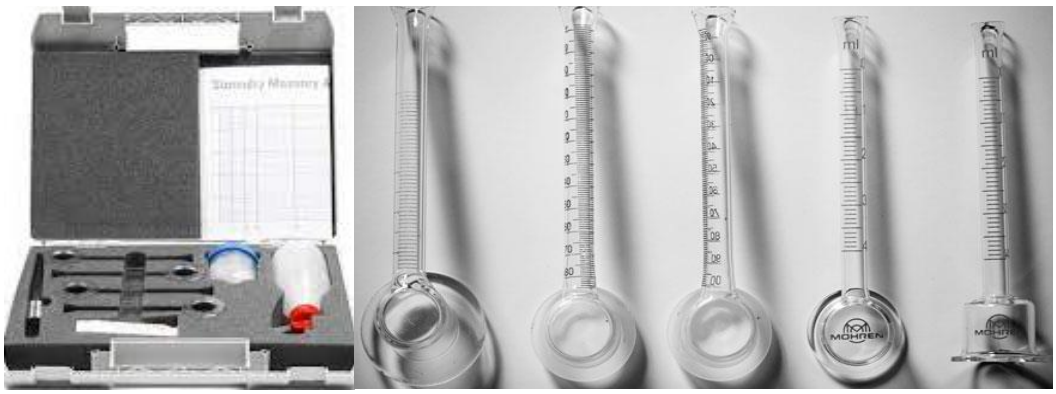

Figure 3.17: Karsten Tube Penetration Test tool kit and water-holding glass tubes

A glass tube was temporarily fixed to the surface of the brick specimen using a plasteline as shown in Figure 3.18. The tube, graduated between 0 - 5 mL in 1/10th mL graduations, was filled with water up to a maximum height at time t = 0. The amount of absorbed water was recorded as a function of time.

Figure 3.18: Karsten penetration test set up

According to ASTM C373-14, (1999), the water absorption test process entails drying the specimens to a constant weight, submerging in water for a predetermined period, for instance 24 hours and reweighing. Equation 3. 4 calculates the increase in weight as a percentage of the initial weight, which is given as its absorption.

$$W_a\% = \frac{W_s - W_d}{W_s} \; X \; 100 \qquad \text{Equation 3. 4}$$

$\mathbf{W_a\%}$ = percentage water absorption, $\mathbf{W_s}$ = the saturated weight, while $\mathbf{W_d}$ = the dry weight

The Karsten tube test was solely used to determine the water absorption rate for the lime-activated brick specimens. The rate of water absorption was so high hence it was not possible to make any recording within the first 5 minutes. The specimens' high porosity made it difficult to execute the water immersion test.

e) Thermal analysis of concrete brick samples

The thermal characterisation was carried out using the transient Hot Plate method in line with ASTM C1113 (1999) to ascertain the thermal capacity of the brick specimens in terms of thermal conductivity, thermal effusivity, and thermal diffusivity.

The basic principle of measurement consists of inserting a probe, which acts both as a source of heat and a sensor of the rise in temperature between two specimens as shown in Figure 3.19. The measurement consists of imposing power on the sample from an instant (t = 0) and then following the rise of the probe temperature over time. The application of the Neotim software helped analyse and illustrate the rise in temperature as a function of time, illuminating the material's thermal properties.

(a) Thermal Probes

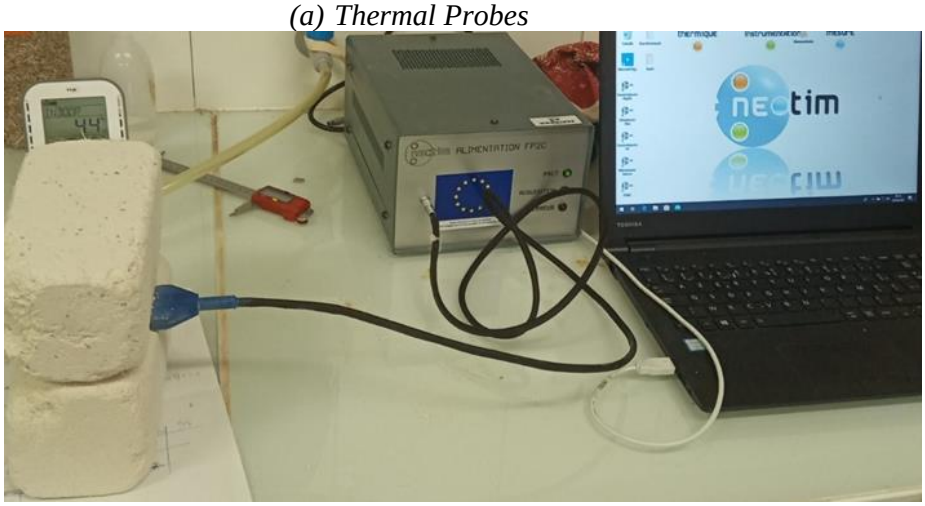

(b) Experimental set up

Figure 3.19: Thermal characterization experimental setup and the thermal testing probes

f) Scanning Electron Microscopic (SEM) Analysis

In order to evaluate the failure characteristics, surface morphology, and elemental distribution at the surface of the concrete samples, a scanning electron microscope (SEM) with an energy-dispersive X-ray spectrometer (EDS) was used. This was done because the microstructure of any composite material has a significant impact on its performance characteristics.

3.6 NaOH/Na2SiO3 Activated Diatomaceous Earth Geopolymer Performance Evaluation (Property Tests)

The property characterization of the NaOH/Na_2SiO_3 activated diatomaceous earth-based geopolymer was carried out following the same methodology that was applied for the lime activated geopolymers. Figure 3.20 provides the pictorial descriptions of the compression strength, bulk density and water absorption experimental tests.

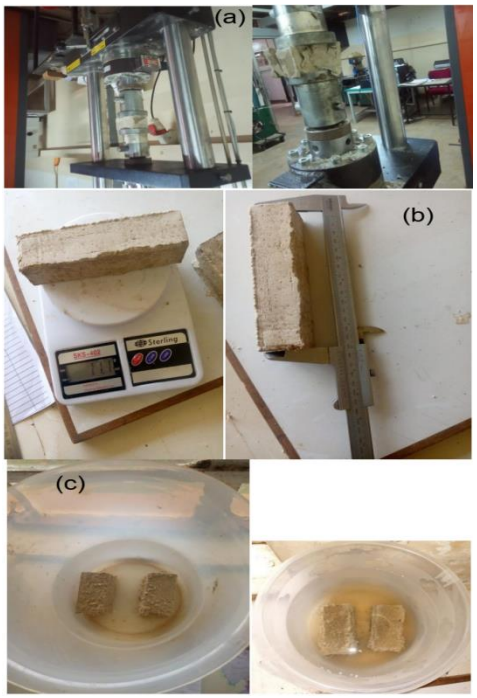

Figure 3.20. (a) Compressive strength test (b) Bulk density test (c) Water absorption test

Additionally, assessed were the thermal conductivity of the NaOH/Na_2SiO_3 activated geopolymer specimens and the water absorption by the Karsten test.

3.7 Correlation and Predictive Modelling for the Performance Properties of the Developed Concrete

Since a regression coefficient, R^2, of greater than 0.80 indicates a strong correlation between parameters, in this study, it is theoretically reasonable to create correlational model equations to link the geopolymer-related variables so that, if one is known, the

other may be calculated using the correlation equation. The correlation matrix was crucial since it enables the identification of the parameters with strong correlations, allowing for the creation of model equations.

The performance properties of the diatomaceous earth-based geopolymer investigated include compressive strength, water absorption capacity, bulk density and thermal insulation capacity. A correlation matrix between the experimental results on various engineering parameters related to the investigated diatomaceous earth-based geopolymer was generated. It is worth noting that the results selected for correlation and prediction purposes are the ones attained utilizing comparable specimens and testing procedures.

Regression analysis was carried out employing the Minitab software to develop various linear and non-linear models to predict the performance aspects. The accuracy of the prediction was estimated using the regression coefficient (R^2).

CHAPTER FOUR: RESULTS AND DISCUSSION

4.1 Introduction

This chapter presents the results and discussions of the test experiments performed on the raw materials and the developed diatomaceous earth-based concrete specimens. To create a sustainable, environmentally friendly concrete material that can be used for building construction, the effectiveness of diatomaceous earth as an alkaline activated raw material (binder) incorporated with sisal fibres and shredded HDPE wastes at various proportions is examined. In addition, the use of sisal fibres as pore-forming agents and the associated impact on the resulting geopolymer concrete's performance properties including compressive strength, bulk density, water absorption, and thermal performance are evaluated. Furthermore, the effect of incorporating HDPE waste as a part of geopolymer concrete and as a means of conserving natural resources and mitigating the negative environmental impact of non-biodegradable wastes is examined in this study.

The findings of the raw material characterization are described here, and the resulting mechanical, physical and thermal characteristics of the fabricated geopolymer bricks are also shown and analysed.

4.2 Raw Material Characterization: Chemical, Physical, Thermal and Mineralogical Properties

4.2.1 Diatomaceous earth characterization

a) Chemical and physical analysis

The diatomaceous earth and lime chemical analysis results determined according to ASTM C114-10 (2010) are shown in Table 4.1. For each sample, the sum of the principal component oxides should roughly equal 100%.

Table 4.1: Chemical analysis for diatomaceous earth and lime

Specimen type	**Chemical content (%)**								
	SiO_2	**Al_2O_3**	**CaO**	**MgO**	**K_2O**	**TiO_2**	**MnO**	**Fe_2O_3**	**P_20_5**
Diatomite (Raw)	88.120	4.254	4.257	0.861	0.673	0.130	0.02	1.528	0.073
Diatomite (Calcined)	89.918	4.292	1.823	1.404	0.689	0.141	0.015	1.534	0.068
Lime	0	2.29	95.935	0	0	0.035	0.023	0.580	0.825

The total sum of oxide concentrations in diatomaceous earth was found to be within the XRF's 99 percent confidence limit, as specified in Declercq et al. (2019).

The diatomaceous earth is highly siliceous and could be considered a relatively good natural pozzolan. Silica (SiO_2) was the predominant component in both the raw and calcined diatomite, with percentages of 88.120% and 89.918%, respectively (a tiny difference between the two). This indicates that the diatomite under study is an acidic rock belonging to the opal A + CT category, as described by Stefanou et al. (2022). Additionally, the silica content fits within the 56-93.5%wt range established in the literature review (section 2.4).

Diatomaceous earth is an acidic stuff that belongs to the rhyolite family in terms of its chemical constituents (Columbu, 2018). This is because the sum of key oxide composition contents (SiO_2+Al_2O_3+Fe_2O_3) was greater than 70% for both raw and calcined diatomite. In this study, the diatomite used was a Class F pozzolanic material according to ASTM C618 (2014).

The diatomaceous earth samples had low CaO + MgO contents, which gave a true picture of opaline rocks which lack carbonate minerals in their mineralogy. However, the CaO content of both the raw and calcined diatomite reveals that the diatomite is

pozzolanic following the work of Aziz et al. (2019) who claimed that a mineral is classified as pozzolanic if it contains less than 10% lime (CaO). The fact that diatomite has a low CaO content in its oxide composition, indicates that it may work more effectively when combined with an alkaline activator for geopolymerization reaction. According to Okeyinka et al. (2019), low-calcium binders are best for creating geopolymers because excessive calcium concentrations can slow down the polymerization-setting rate.

Following the calcination procedure, it was found that the CaO concentration had decreased from 4.257 % to 1.823 %. According to Tang et al. (2022), this reduction suggests that the matrix $CaO\text{-}Al_2O_3\text{-}SiO_2$ ternary may have developed during the heat treatment process.

Figure 4.1 is a pie chart that illustrates the chemical composition of diatomaceous earth.

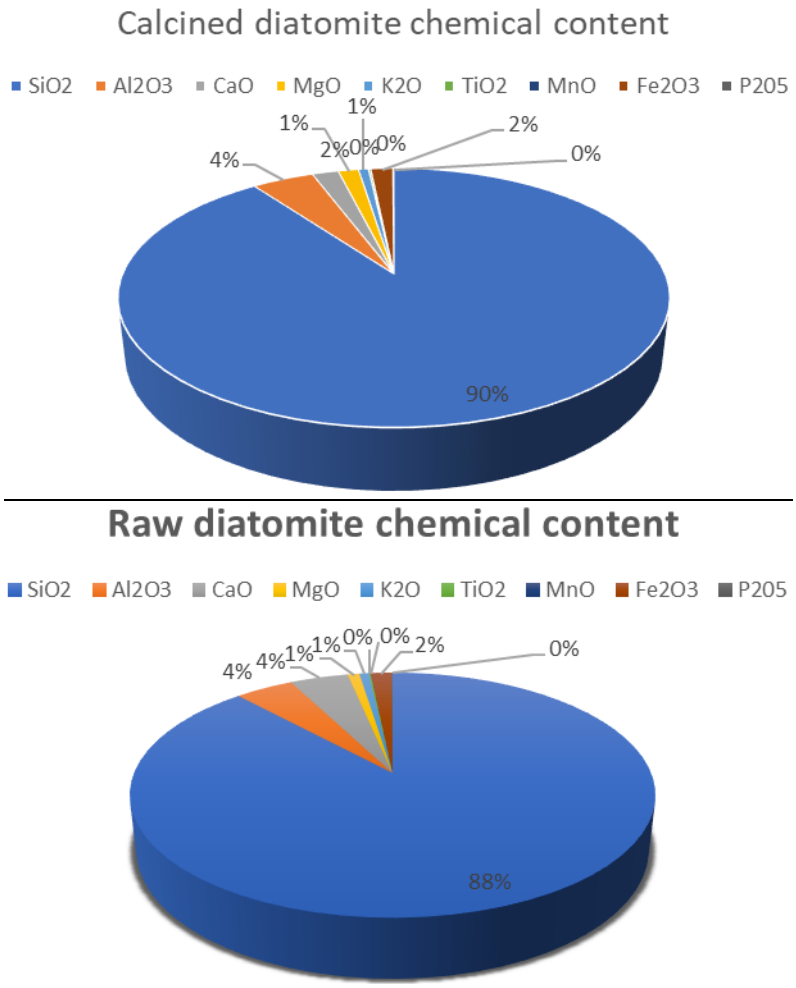

Figure 4.1: Pie Chart illustrating the chemical content of diatomite

The diatomite's alumina (Al_2O_3) content revealed that the diatomite under study wasn't clayey because it was lower than the 14–16% range suggested by the literature (Chen et al., 2020; Fragoulis et al., 2004; Stefanou et al., 2022; Yilmaz & Ediz, 2008). There were also trace levels of other oxides such as MgO, K_2O, TiO_2, MnO, Fe_2O_3, and P_20_5.

Generally, due to the high silica content, alkaline aluminosilicate gel and, ultimately, geopolymer concrete, may emerge from the utilization of diatomaceous earth as a geopolymer base raw material.

b) X-Ray diffraction (XRD) patterns of diatomaceous earth

The XRD analysis (Figure 4.2) drawn from the data in Appendix I shows that cristobalite was the predominant mineral in the Kenyan sampled diatomaceous earth.

According to the classification by Ejigu et al. (2022), Smallwood et al. (2008) and other literature, the observed diffraction peaks are typical peaks for paracrystalline silica polymorph opal-CT derived from the volcanic environment. According to Stefanou et al. (2022), diatomaceous samples with a predominance of opal-CT can be categorized as porcelanites or porcelaneous diatomites; which are connected to the diagenetic alteration of opal-A-rich diatomite beds.

The strongest reflection peak is at about 21.8°, with weaker peaks at around 29°, 32°, 36°, 45°, 57°, and 65°. The resulting diffraction peaks show the presence of α-cristobalite together with variable degrees of stacking disorder, which causes maxima that are linked to tridymite.

The X-ray diffractometry (XRD) mineralogical finding strongly supported Hoffman (2006) and Washbourn-Kamau (1971) hypothesis that the Kenyan Rift Valley hosts diatomaceous earth deposits which appear to be of lacustrine origin (from lacustrine diatomite diagenesis) pre-dating one or more episodes of faulting and vulcanicity. The diatomaceous earth mineralogical result from this study also appears to diverge from the findings of earlier researchers who claimed that it is made up of the fossilized skeletal fragments of diatom, a unicellular aquatic plant related to the diatom algae skeleton fragments. The mineralogical result finding of this study therefore, supports Pavlková et al. (2022) claim that diatomaceous earth needs to be researched on a case-by-case basis due to variations in its mineralogical and chemical composition, morphology, fineness, and pre-processing characteristics.

The Kenyan diatomaceous earth samples tested may have originated as biogenic silica opal-A before dissolving or re-forming as opal-CT as a result of the thermal alteration

of the rock caused by the high heat flow rates created in the rift zones by the penetration of dacite sills as a mechanism of the volcano-sedimentary succession.

The XRD results agreed with the XRF chemical analysis output which showed that silica (SiO_2) was the predominant chemical compound. It is evident from the analysis that materials with high SiO_2 concentrations also contain high concentrations of silica minerals (opal A + CT).

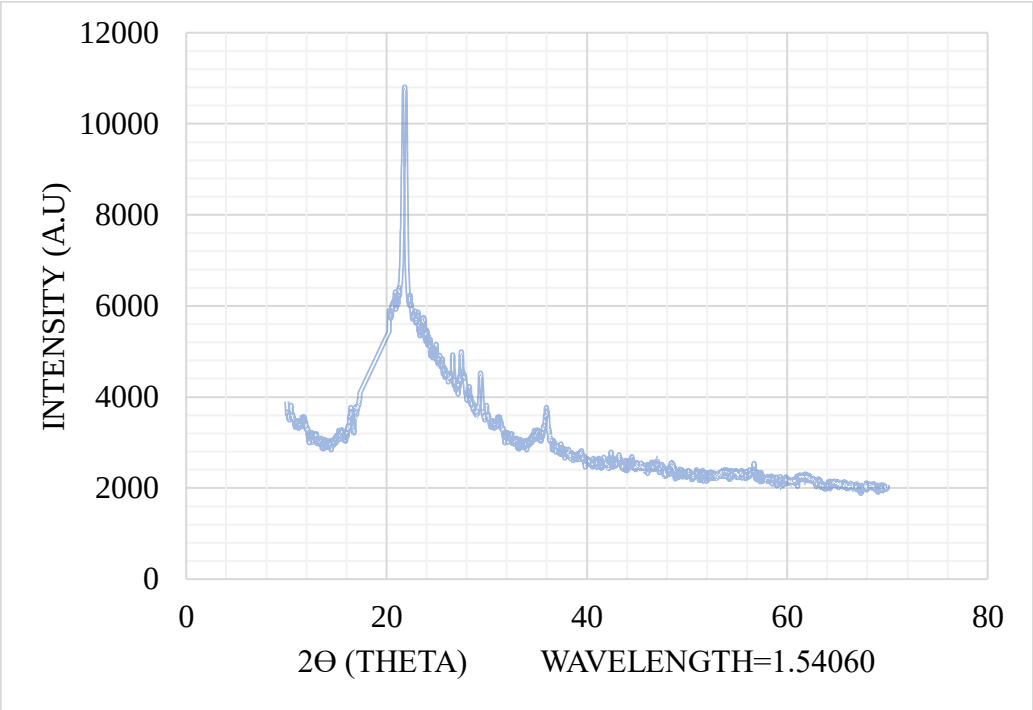

Figure 4.2: XRD analysis results for the diatomaceous earth.

Lime activator

The chemical investigation data shown in Table 4.1 demonstrated that quicklime was the alkaline activator used since it had a CaO content of above 95%.

Table 4.2 presents the physical features of the diatomaceous earth that was employed in this research.

Table 4.2: Physical Analysis

Specimen type	**Physical property**			
	Permeability (mD)	**Porosity (%)**	**Specific gravity**	**Bulk density (g/cm^3)**
Diatomite (Raw)	2.3	40	2.1	1.4
Diatomite (Calcined)	2.7	32	1.9	1.33

The permeability of raw diatomite was determined to be 2.3 mD while that of calcined diatomite was 2.7 mD; also, the porosity of raw diatomite was 40% while that of calcined diatomite was 32%; The raw diatomite had lower permeability and porosity than thermally treated diatomite, which suggests that thermal treatment reduces the overall volume of the raw diatomaceous earth's pores. Despite differences between the findings for raw and calcined diatomite, all the values were still within the ranges suggested by researchers (Bogoevski & Boskovski, 2014; Reka et al., 2021; Stefanou et al., 2022) in the literature. The observed porosity of ≤40 for both raw and calcined diatomaceous earth, as described by Ishii et al. (2011), could mean that the tested samples belong to the opal CT family of siliceous rocks.

It was found that the specific gravity of raw diatomite was higher than that of calcined diatomite, but both specific gravity values fall within the range of 1-2.6 as stated in the literature by Roy & Kumar Bhalla (2017), demonstrating that diatomite is an organic soil earth material.

c) TGA-DSC thermal characterization of diatomaceous earth

Figure 4.3 to Figure 4.8 show the outcomes from the thermogravimetric analysis (TGA) and differential scanning calorimetry (DSC) apparatus.

Thermogravimetric analysis (TGA) analysis

It can be seen from Figure 4.3 that the total weight loss for the calcined diatomite at 950 °C was only 0.736%. This is because a considerable amount, approximately 8.2% of mass was lost during the calcination process.

A small weight loss between 600°C and 700 °C can be attributed to the dehydroxylation of OH-groups and the release of structural water from its impurities and amorphous silica structure to form the amorphous metakaolin, as shown by Equation 4.1 and further explained by Ibrahim & Selim (2012). It is also evident that diatomite had been subjected to calcination at 600 °C causing water loss.

$$Al_2O_3.2SiO_2.2H_2O \xrightarrow{Heat} Al_2O_3.2SiO_2 + 2H_2O \qquad \text{Equation 4.1}$$

The weight loss starts to stabilize as soon as the temperature hits 800 °C, signifying the complete dehydration of the diatomite structure and the emergence of a new silicate substance.

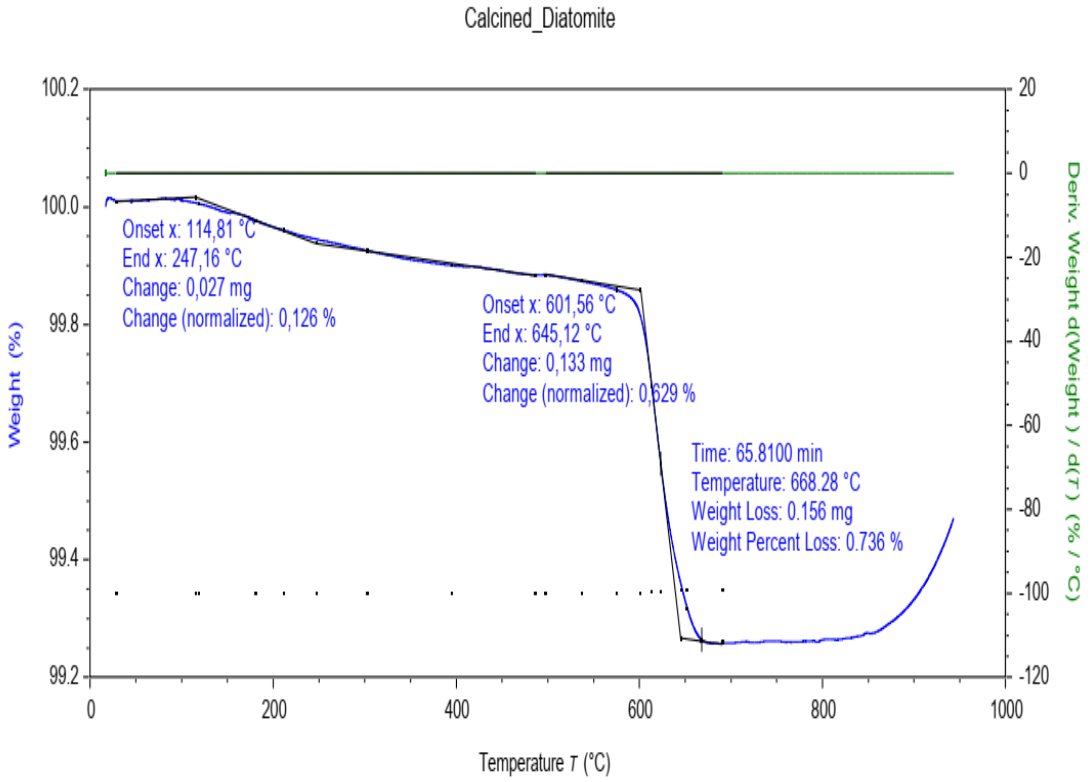

Figure 4.3: Weight loss analysis of calcined diatomite

Regarding the raw diatomite (uncalcined) depicted in Figure 4.4, there was a total mass loss of 9.94%. This may have been caused by the release of both free and bound diatomite as well as any organic stuff that may have been present.

It is evident from the TGA results that diatomite is a thermally stable raw material and that its melting temperature is greater than 950 °C.

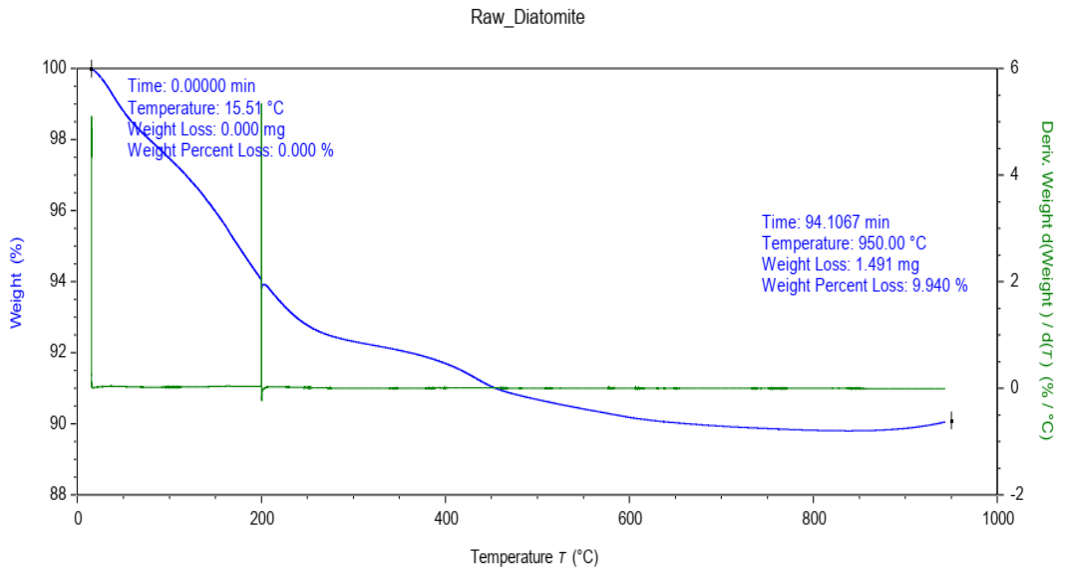

Figure 4.4: Weight loss analysis of raw diatomite

Figure 4.5 shows that the dried raw diatomite lost a total of 5.68% of its weight after being oven dried at 105 °C for six hours to allow the free water to evaporate.

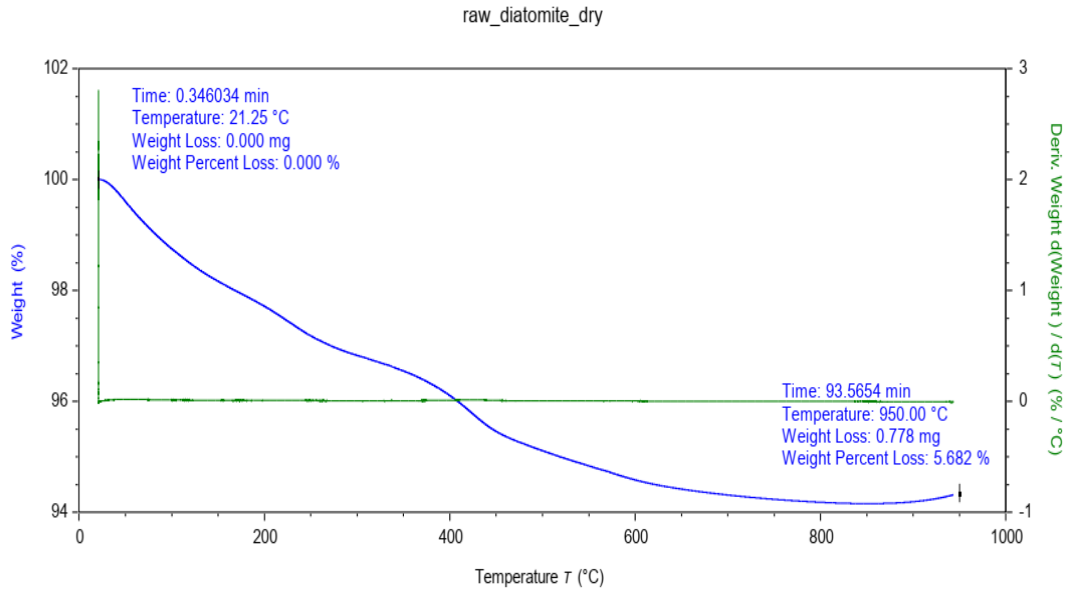

Figure 4.5: Weight loss analysis of oven-dried raw diatomite

This resulting loss on ignition (LOI) value was still below the maximum value of 6% allowed by ASTM.C618 (2014).

Differential scanning calorimetry (DSC) analysis

The DSC thermograms for raw and oven-dried diatomite shown in Figure 4.6, revealed endothermic peaks between 120 °C and 280 °C, which are caused by the dehydration process (water evaporation), that is a result of diatomite's high-water absorption capacity. Since the calcination process was done at 600 °C, there was no enthalpy change for the calcined diatomite as at 450 °C.

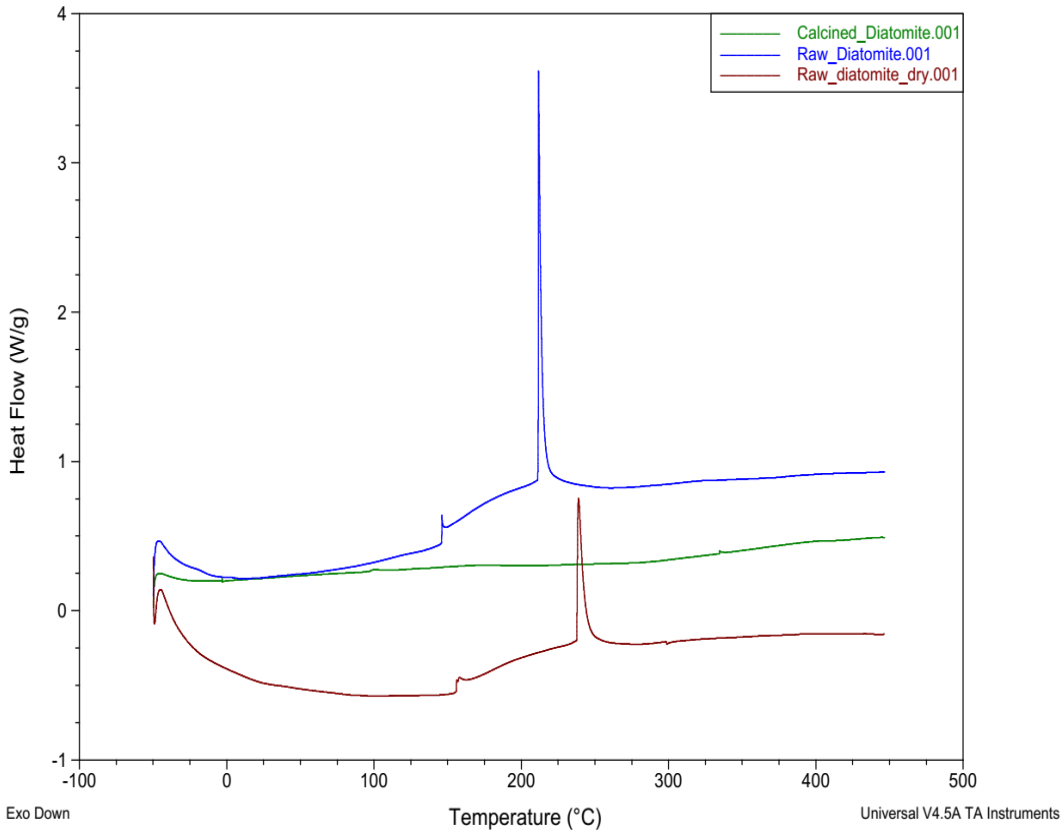

Figure 4.6. DSC analysis for raw, oven-dried and calcined diatomite

d) Loss on ignition (LOI)

The loss on ignition was determined through the thermogravimetric analysis (TGA) of the diatomaceous earth under study. Figure 4.3 shows that the loss on ignition for already calcined diatomite was 0.736 %; Figure 4.4 presents the loss on ignition for raw diatomite as 9.94 %. The oven-dried raw diatomite in Figure 4.5 presented a loss on ignition of 5.68%. This resulting LOI value was still below the maximum value allowed

by ASTM C618 (2014). It is evident from the LOI results that the diatomite's impurity content was significantly reduced during the calcination process. However, based on Table 4.1, it appears that the chemical content was not significantly affected by the impurities since there was a very small difference between the chemical composition of the raw and the calcined diatomite.

e) Pozzolanic reaction analysis of diatomite and lime mixture

Thermogravimetric analysis (TGA) of the Diatomite-Lime mixture in Figure 4.7 shows that there was a rapid weight loss which started at a temperature of 18.71 °C up to 62.58 °C resulting in a loss of about 26.22 %. This indicates the presence of a chemical reaction. It, therefore, means that the pozzolanic reaction between lime and diatomite takes place immediately after mixing and at room temperature. The lime reacts with reactive silica ingredient of pozzolana, and forms a cementitious compound which is responsible for setting and hardening. That is, the pozzolanic reaction causes calcium hydroxide to combine with pozzolanic material, forming a tobermorite (C-S-H) gel as is illustrated by Equation 4.2.

$$Lime + Pozzolan = CSH \qquad \text{Equation 4.2}$$

According to Borges et al. (2021), lime reacts with the active silica ingredient (shown in equation 4.3), which is the main reactant constituent present in the diatomaceous earth.

$$3Ca(OH)_2\ (lime) + 2SiO_2\ (reactive\ silica\ of\ diatomite) = 3CaO.2SiO_2.3H_2O\ (tobermorite\ gel)$$

Equation 4.3

The rapid weight loss is due to the loss of water that results from the reaction of the two materials.

At about 395 °C another weight loss starts which progresses gradually up to around 650 °C when it stabilizes. This may be due to the dehydration of the hydrated Calcium Sulfoaluminate and the consumption of any organic matter that could be present. As at 950 °C the total weight loss was 34.44 %.

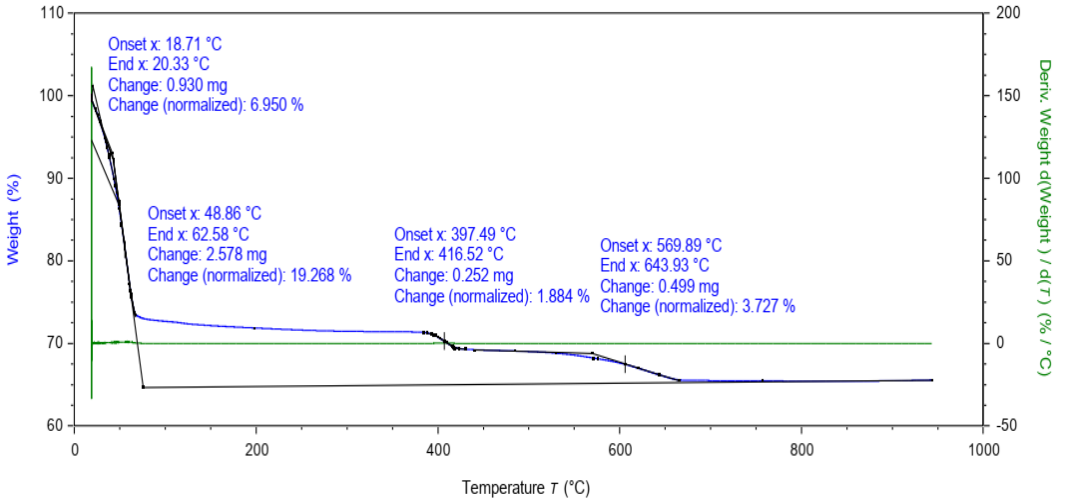

Figure 4.7: TGA Analysis for Lime_Diatomite mixture

Figure 4.8 presents the DSC analysis for the Diatomite-Lime mixture. Two endothermic peaks are portrayed. The first peak occurred at 2 °C with a heat flow of 2.189W/g and could be a result of the reaction between lime and diatomite. The second peak is at 138.93 °C with a heat flow of 5.064W/g and indicates the process of water evaporation from the mixture.

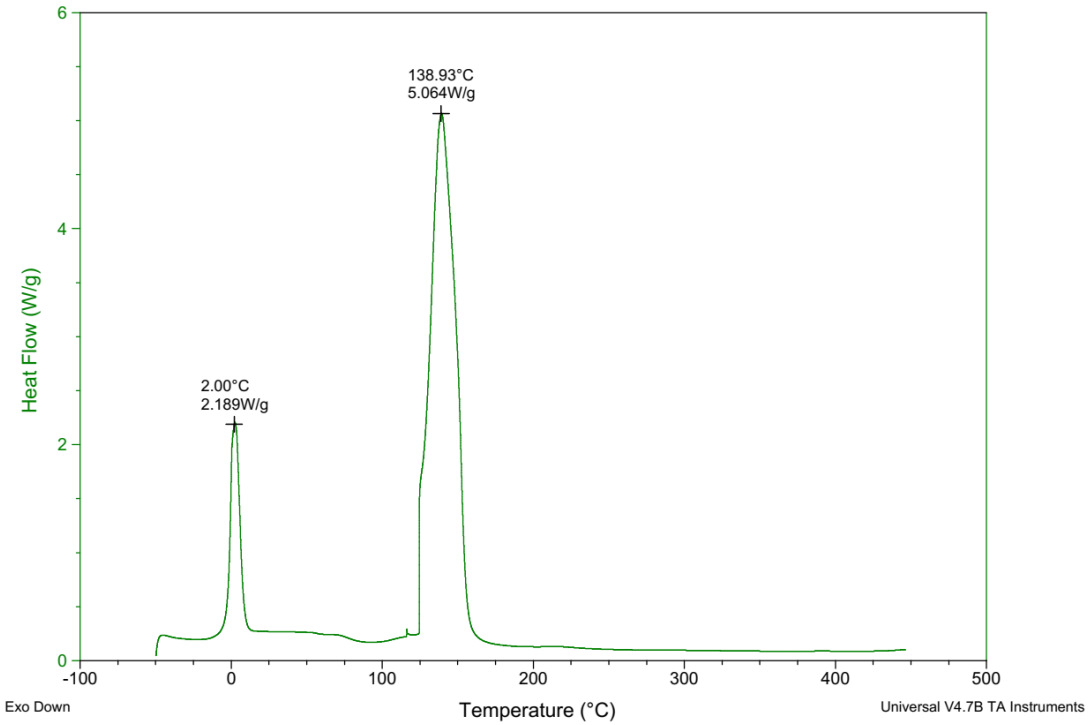

Figure 4.8: DSC Analysis for Lime_Diatomite mixture

Figure 4.9 shows that when lime and diatomite are mixed in the presence of water, then distinct endothermic reactions are observed as compared to those of the individual materials.

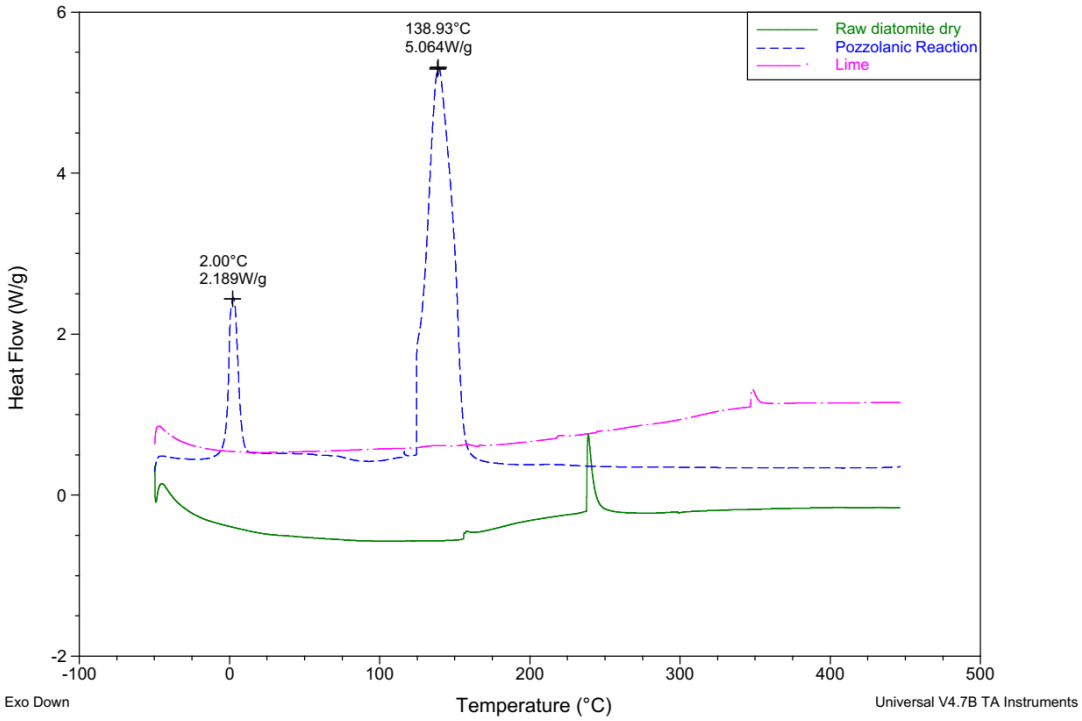

Figure 4.9: Comparative DSC curves for Lime, Diatomite and the mixture

The lime-diatomite mixture loses the maximum mass between 0 ° c and 200°C, which is primarily a result of the loss of both free water and some of the chemically bonded water from the cement paste. According to He et al. (2020), another mass loss that results from the dissolution of carbonate species typically manifests at temperatures over 750°C.

Both the TGA and DSC analysis of the diatomite and lime mixture shows that the chemical reaction between the two occurs immediately and at ambient temperatures.

f) Diatomaceous earth particle size analysis

The raw diatomite particle size distribution as obtained from the laser particle analyzer was Dv (10): 7.58 µm, Dv (50): 23 µm and Dv (90): 50.4 µm. It is clear that the raw diatomite is more similar to cement as stipulated by Osborne (2013), in terms of particle size, since about 90% of its particles were smaller than 50.4 µm. Most of the particle

sizes were, therefore, closer to 45 µm permissible size for geopolymer precursors (Fernández-Jiménez et al., 2006).

Figure 4.10 shows the raw diatomite particle size distribution. The corresponding data is presented in Appendix 2.

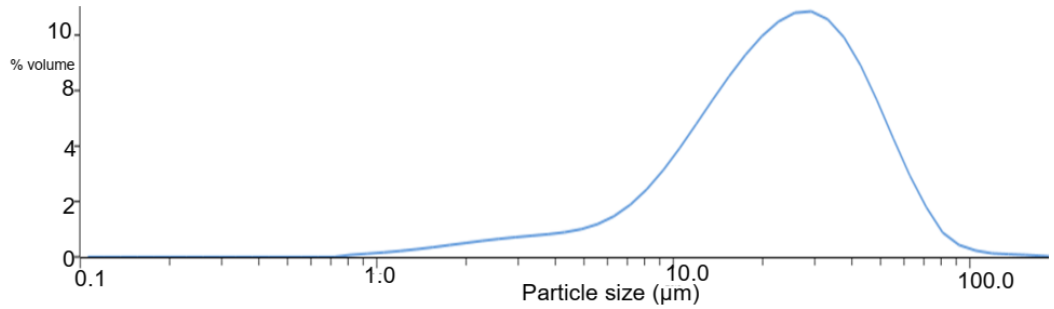

Figure 4.10: Raw diatomite particle size analysis

The results for the calcined diatomite demonstrated that the properties of its particles fell between the fine and medium sand as described by Daryati et al. (2019). This is because the values for Dv (10), Dv (50), and Dv (90) were 21 µm, 168 µm, and 728 µm, respectively. This indicates that more than 50% of the sample included particles larger than 75 µm. The calcined sample still contained very little amount of very fine, silt-like particles. The distribution of calcined diatomite particle sizes is illustrated in Figure 4.11. The corresponding data is presented in Appendix 3.

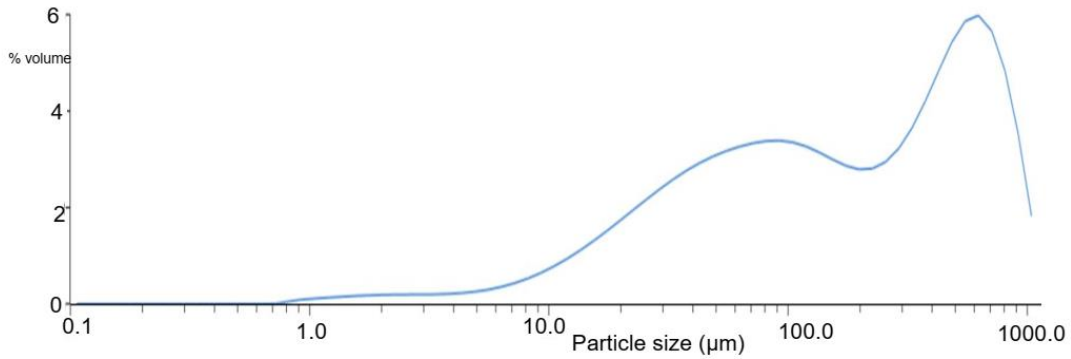

Figure 4.11: Calcined diatomite particle distribution

The analysis of the diatomaceous earth particle size revealed that the calcination process causes the agglomeration of the individual diatoms and fragments hence increasing the average particle size. This finding agrees with the findings of Yilmaz et al. (2008).

The particle size analysis also showed that both the raw and calcined diatomite are fine-grained earth materials making them suitable for use as geopolymer precursor raw materials following the argument by Makusa (2012) that fine-grained granular materials are the easiest to stabilize.

The fineness of the raw diatomaceous earth and its chemical composition in this study formed the basis for its use in the development of geopolymer concrete specimens. This is because according to Okeyinka et al. (2019), the strong reactivity of the activation process is influenced by the fineness of the particles in the geopolymer's base material.

g) The Atterberg limits test

The plastic limit (PL), liquid limit (LL), and plasticity index (PI) were obtained using the Atterberg limit test as described by ASTM D4318-17 (2017). Average values resulting from three (3) trials are presented in Table 4.3.

Table 4.3: Atterberg Limits Data

	Raw Diatomite		**Calcined Diatomite**	
	Average	**Std**	**Average**	**Std**
Mass of empty, clean can + lid (grams)	20	1.16	20	1.45
Mass of can, lid, and wet soil (grams)	35.14	1.32	35.37	1.97
Mass of can, lid, and dry soil (grams)	30.79	2.01	31.52	1.93
Mass of soil solids (grams)	10.79	1.5	11.52	1.46
Mass of pore water (grams)	4.35	0.43	3.84	0.63
Water content, w%	40.34	2.89	33.33	2.31
No. of drops (N)	233	4.51	66	0.86
Plastic Limit (PL)	**40.34**	**1.56**	**33.33**	**1.72**
Liquid Limit (LL)	**53**	**2.31**	**37**	**1.89**
Plasticity Index (PI)	**12.66**	**1.96**	**3.67**	**1.57**

According to the data from the Atterberg limits experiment, the plasticity index for raw diatomite was around 13, whereas that for calcined diatomite was about 4. As suggested by Hall et al. (2012), diatomaceous earth employed in this study generally appears to be favourably good for usage as an earth construction material as its PI, both in the raw and calcined states, is less than 16%.

Comparing the Atterbergs categorization described by Roy and Kumar Bhalla (2017) with the findings of this study reveals that raw diatomite is a cohesive and medium plastic silt clay, whereas calcined diatomite is a partly cohesive and low plastic silt soil

4.2.2 Sisal fibre characterization

The main properties of the sisal fibres that were utilized in this research are presented in Table 4.4.

Table 4.4: Main characteristics of sisal fibres

S/No.	Characteristic property	Average Value attained	Std
1	Cellulose (% mass)	76.6	1.32
2	Lignin (% mass)	8.9	0.86
3	Hemicellulose (% mass)	13.6	1.03
4	Pectin (% mass)	0.9	0.09
5	Density (g/cm^3)	1.42	0.12
6	Tensile strength (cN/Tex)	40.22	1.63

The sisal fibre properties that were obtained were comparable to those of ordinary sisal which has been documented in the literature. The fibres contained cellulose as their primary component. Cellulose, a natural polymer, serves as the main reinforcement material in plant fibres. According to Stevulova et al. (2016), the use of natural cellulosic fibres as reinforcing elements in building materials is constantly expanding

and can play a significant part in the shift to renewable resources, which also supports a healthy and comfortable type of habitation.

4.3 Performance Evaluation of the Lime-Activated Diatomite-Based Geopolymer Concrete Brick

4.3.1 Compressive strength

Dhaheer et al. (2018) among other researchers stressed the necessity to take into account concerns about concrete's durability. This is because while lowering the concrete industry's significant annual CO_2 emissions is important, developing durable concretes is another step in the direction of sustainability. Sousa et al. (2012) suggest that the durability of bricks can be improved by enhancing the compressive strength and reducing water absorption through the application of good stabilization methods. Also, according to Zhang et al. (2020) and other experts, compressive strength and durability tests are considered very important indicators of the viability of masonry.

The mean compressive strength of five test specimens representing each particular mix composition was determined. The results are presented in Table 4.5 with the accompanying summary in Table 4.6.

P2, P4, P6 and P8 represent the compaction pressures of 2MPa, 4MPa, 6MPa and 8MPa respectively which were applied during brick moulding.

Table 4.5: Compressive strength results

Proportional group	**Mixture Components**				**Compressive Strength (CS)**			
	A: Diatomite	B: Lime	C: Sisal	D: HDPE	CS for P2	CS for P4	CS for P6	CS for P8
	% Weight	% Weight	% Weight	% Weight	MPa	MPa	MPa	MPa
1	100	0	0	0	0.25	0.28	0.30	0.36
2	93.75	5	0.25	1	0.27	0.29	0.34	0.73
3	89.5	7.5	0.5	2.5	1.32	1.16	2.01	2.5
4	85.25	10	0.75	4	0.43	0.53	0.95	0.97
5	81	12.5	1	5.5	0.77	1.45	1.73	2.14
6	76.75	15	1.25	7	0.61	0.77	1.05	1.93
7	83.75	15	1.25	0	1.61	1.82	2.02	2.66
8	78	15	0	7	0.78	0.91	1.15	1.41

Table 4.6: Compressive strength Results Summary

Name	**Lower Limit (MPa)**	**Upper Limit (MPa)**
CS for P2	0.25	1.61
CS for P4	0.28	1.82
CS for P6	0.30	2.02
CS for P8	0.36	2.66

A graphical presentation of compressive strength results is shown below in Figure 4.12.

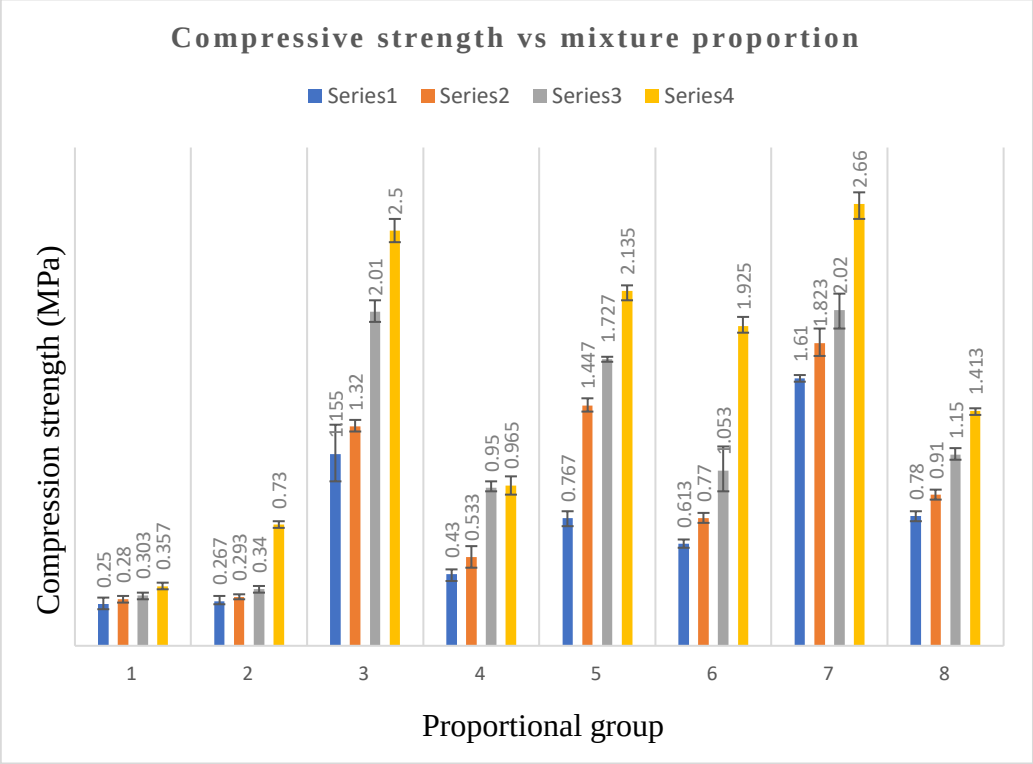

Figure 4.12: Compressive strength versus brick proportion

Figure 4.12, shows that the inactivated diatomaceous earth produces very weak concrete bricks. Activation with lime improves the compressive strength of the bricks; the more lime, the stronger the bricks. Sisal fibres also increase the compressive strength of concrete, which is in line with Nawaz's (2020) findings. The compressive strength values also bring out the fact that the compaction pressure applied during moulding has an impact on the strength of the bricks. As would be expected, the compressive strength appears to increase with an increase in the compaction (moulding) pressure.

Figure 4.13 illustrates the effect of individual mixture components on the compressive strength of the developed lime-activated geopolymer. It can be interpreted that the addition of sisal fibres and lime to the geopolymer concrete causes a positive deviation in the compressive strength. The statistical analysis of the influence of lime and sisal fibres on the compressive strength suggests that their maximum incorporation, that is,

15% lime and 1.25% sisal fibres, yields an optimum compressive strength. Regarding the sisal fibres, the increased strength might have resulted from the development of an isotropic matrix with omnidirectional fibres that resist particle movement, boosting both the tensile and compressive strengths. This result is consistent with earlier research showing that as stress increases, fibres in concrete work against the development of cracks.

Figure 4.13: Effect of mixture components on the compressive strength

The presence of significant amounts of HDPE in the concrete mixes appears to lower the compressive strength of the geopolymer bricks. The statistical analysis regarding the influence of the HDPE on the compressive strength suggests a complete elimination of HDPE (0%) in the concrete mixture. The HDPE's coarse texture may have also contributed to the low compressive strength. Hence, more research needs to be conducted to ascertain the adhesive characteristics between the HDPE particles and the mix.

The decline of compressive strength with an increase in the diatomaceous earth (beyond 83.75%) justifies the fact that pure diatomaceous earth cannot produce strong concretes. Therefore, there is a need for its activation and/or reinforcement.

Material mix and compressive strength optimization

The material constituents are one of the many factors that influence the compressive strength of concrete, so optimizing them is a requirement that is getting a lot of attention. To identify the combination of mixture components that jointly optimize the compressive strength of the developed lime-activated geopolymer brick, response optimization was carried out using the Minitab software. The compressive strength optimization was performed for the compressive strength attained after a compaction pressure of 8MPa (P8); because the developed geopolymers had better compressive strength.

The compressive strength optimization input parameters are presented in Table 4.7.

Table 4.7: Compressive strength optimization input parameters

Mixture component	**Lower limit (%wt)**	**Upper limit (%wt)**	**Compressive strength for P8 (MPa**		
			Goal	lower	Target
Diatomite	76.75	100	Maximum	0.36	2.66
Lime	0	15			
Sisal fibres	0	1.25			
HDPE	0	7			

The optimization process was run, and the solution obtained was presented in Table 4.8.

Table 4.8: Compressive strength Optimization solution

Optimal Solution			**Predicted Response**					
Diatomite % Weight	=	83.75	CS for P8	=	2.72 MPa	Desirability	=	1.000000
Lime % Weight	=	15						
Sisal % Weight	=	1.25						
HDPE% Weight	=	0						

The optimal solution suggests that lime and sisal fibres should be incorporated at their maximum values. Because their incorporation was found to positively affect the compressive strength of the bricks. With the HDPE's negative impact on the compressive strength of the developed geopolymers, the optimal solution suggests its elimination from the geopolymer mixture composition. The negative impact of the HDPE on the compressive strength of geopolymer concrete could be due to its inert nature hence, hindering the chemical reaction between the diatomite (pozzolan) and the alkaline activator (lime) for effective geopolymerization to take place.

For an optimum compressive strength of 2.72 MPa to be attained, the statistical analysis suggests that the concrete mixture should consist of 83.75% diatomite, 15% lime and 1.25% sisal fibres.

4.3.2 Flexural strength (FS)

The flexural strength values for the concrete specimens made with lime-activated diatomaceous earth are shown in Table 4.9.

Table 4.9: Flexural strength results

Proportional group	**Mixture Components**				**Flexural strength (FS)**			
	A: Diatomite	B: Lime	C: Sisal	D: HDPE	FS for P2	FS for P4	FS for P6	FS for P8
	% Weight	% Weight	% Weight	% Weight	MPa	MPa	MPa	MPa
1	100	0	0	0	0.03	0.03	0.03	0.04
2	93.75	5	0.25	1	0.03	0.03	0.03	0.05
3	89.5	7.5	0.5	2.5	0.07	0.06	0.08	0.09
4	85.25	10	0.75	4	0.04	0.04	0.06	0.06
5	81	12.5	1	5.5	0.05	0.07	0.08	0.09
6	76.75	15	1.25	7	0.05	0.05	0.06	0.08
7	83.75	15	1.25	0	0.07	0.08	0.08	0.1
8	78	15	0	7	0.05	0.06	0.06	0.07

Figure 4.14 shows a graphic depiction of the experimental data on flexural strength. Flexural strength appears to rise as the amount of compaction pressure applied

increases, mirroring the results of compressive strength tests. The proportions of the mixtures that had yielded better compressive strengths also had higher flexural strengths.

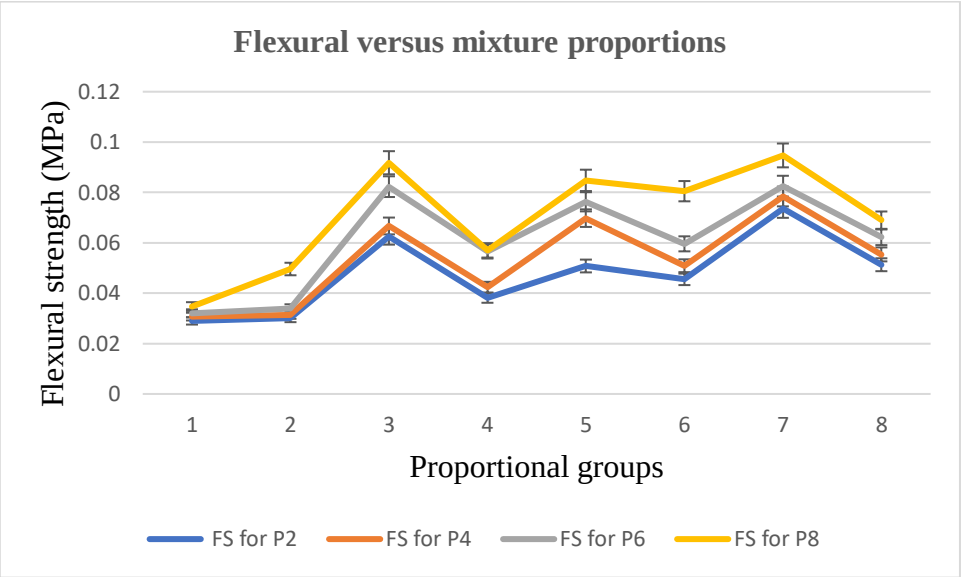

Figure 4.14. Flexural strength versus mixture proportions

The information in Figure 4.15 shows that there is a strong correlation between compression strength and flexural strength for specimens that had been compacted at 8 MPa with a correlation factor of 99%.

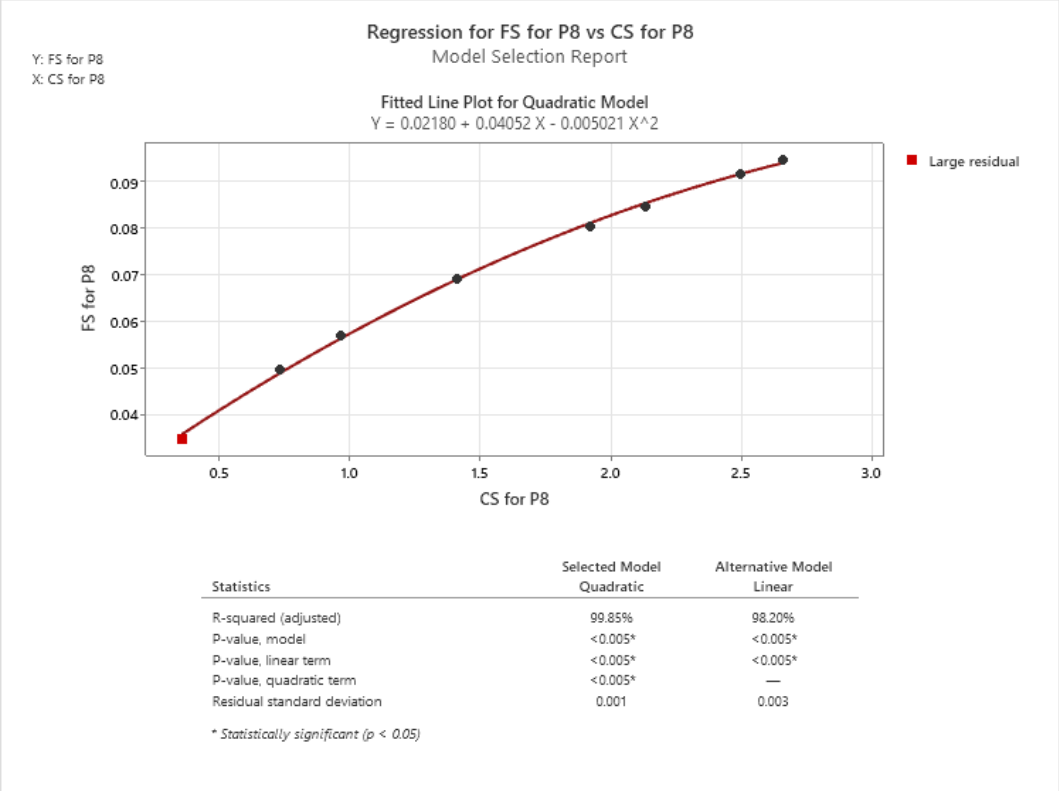

Statistics	Selected Model Quadratic	Alternative Model Linear
R-squared (adjusted)	99.85%	98.20%
P-value, model	<0.005*	<0.005*
P-value, linear term	<0.005*	<0.005*
P-value, quadratic term	<0.005*	—
Residual standard deviation	0.001	0.003

** Statistically significant ($p < 0.05$)*

Figure 4.15: Correlation analysis between Flexural Strength and Compressive strength

The statistical analysis showed that the optimum equation relating flexural strength and compressive strength is:

$$y = 0.0218 + 0.0405x - 0.005x^2$$

Where, y= Flexural strength and x= Compressive strength

4.3.3 Bulk density

The bulk density of the prepared diatomaceous earth-based geopolymer specimens after 28 days is presented in Table 4.10.

Table 4.10: Specimen density results

Proportional group	**Mixture Components**				**Density**			
	A: Diatomite	B: Lime	C: Sisal	D: HDPE	Density for P2	Density for P4	Density for P6	Density for P8
	% Weight	% Weight	% Weight	% Weight	g/cm^3	g/cm^3	g/cm^3	g/cm^3
1	100	0	0	0	0.650	0.772	0.778	0.953
2	93.75	5	0.25	1	0.788	0.809	0.822	0.961
3	89.5	7.5	0.5	2.5	0.879	0.889	0.935	0.979
4	85.25	10	0.75	4	0.795	0.809	0.866	0.896
5	81	12.5	1	5.5	0.660	0.694	0.725	0.767
6	76.75	15	1.25	7	0.685	0.736	0.896	0.902
7	83.75	15	1.25	0	0.588	0.600	0.623	0.704
8	78	15	0	7	0.753	0.764	0.788	0.902

The bulk density of the bricks was determined and the results showed that the bricks were lightweight with their densities ranging between 0.588 to 0.979 g/cm^3.

Figure 4.16 illustrates the characteristic of the lime-activated geopolymers in terms of bulk density. The highest compaction pressure applied (8MPa) presents higher densities. This study agrees with the findings of (Bruno et al., 2016; Indra et al., 2018) that a higher compaction effort increases the dry density and, consequently, the stiffness and strength of the concrete/brick materials.

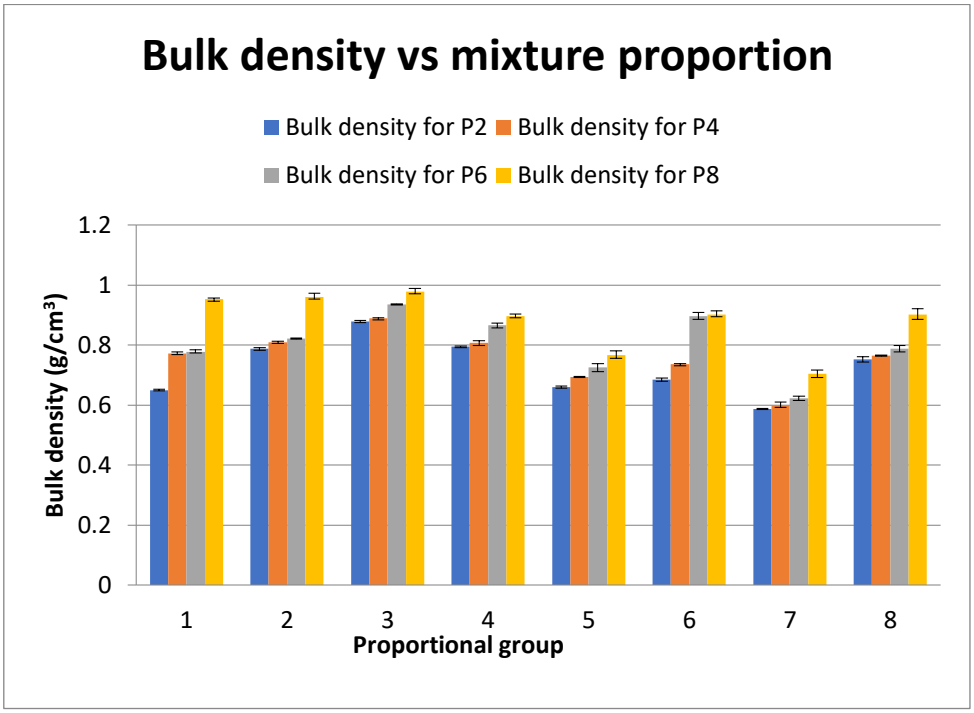

Figure 4.16: Bulk density distribution

Material mix and bulk density optimization

To benefit from the advantages of lightweight concrete mixes, such as a reduction in the dead weight of buildings, an improvement in thermal conductivity, and a reduction in transport and handling costs, the objective function of bulk density optimization was set at minimization. The bulk density optimization input parameters are presented in Table 4.11

Table 4.11: Bulk density optimization input parameters

Mixture component	Lower limit (%wt)	Upper limit (%wt)	Bulk density for P8 (g/cm³)		
			Goal	Upper	Target
Diatomite	76.75	100	Minimization	0.979	0.704
Lime	0	15			
Sisal fibres	0	1.25			
HDPE	0	7			

The bulk density optimization findings are presented in Table 4.12.

Table 4.12: Bulk density optimization solution

Optimal Solution			**Predicted Response**					
Diatomite % Weight	=	83.75	Bulk density for P8	=	0.716 g/cm^3	Desirability	=	1.000000
Lime % Weight	=	15						
Sisal % Weight	=	1.25						
HDPE% Weight	=	0						

The optimization solution suggests that the incorporation of HDPE in the concrete mix is translated by an increase in the bulk density, and therefore for the achievement of the bulk density minimization function, the HDPE should be eliminated. Figure 4.17 illustrates the effect of the mixture components on the density. For an optimum bulk density of 0.716 g/cm^3 to be attained, the statistical analysis suggests that the concrete mixture should consist of 83.75% diatomite, 15% lime and 1.25% sisal fibres.

The incorporation of the sisal fibres seems to contribute positively to the achievement of the concrete bulk density minimization objective function, therefore the statistical analysis suggests that sisal should be incorporated at its maximum (1.25%). According to Mahmood et al. (2021), the sisal fibres have a low density in the range of 1.03–1.45 g/cm^3.

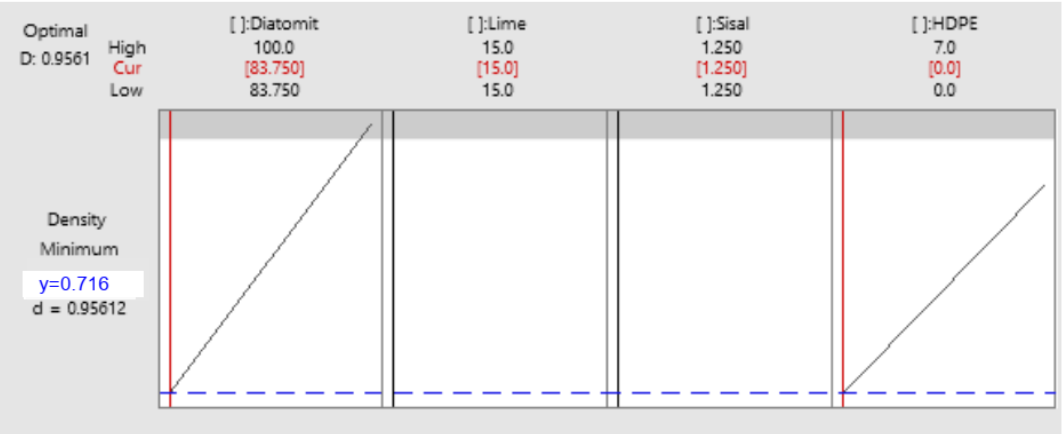

Figure 4.17: Effects of the mixture components on density

4.3.4 Water absorption

Water is the main in-service degradation agent affecting the durability and hygrothermal behaviour of facades (Duarte et al., 2011). Therefore, water resistance is one of the important properties that need to be determined for all building materials that are susceptible to water while in service.

The Karsten tube test technique registers the volume of water absorbed during specific periods, usually 30, 60 or 180 min, and then determines the permeability of the analysed surface to liquid/water under low pressure, which enables the evaluation of its waterproof capacity (Duarte et al., 2020).

The results were supposed to be recorded in a graph as shown in Figure 4.18 but for the lime-activated specimens that were tested, the data could not be recorded because the rate of water absorption was very fast. This means that the specimens were very porous hence very weak. Hendrickx (2013) noted that sufficient performance is reached if the level of water decreases no more than 20% of its initial height over the 20-minute test period. This contradicted the water absorption behaviour that was seen for the lime-activated specimens.

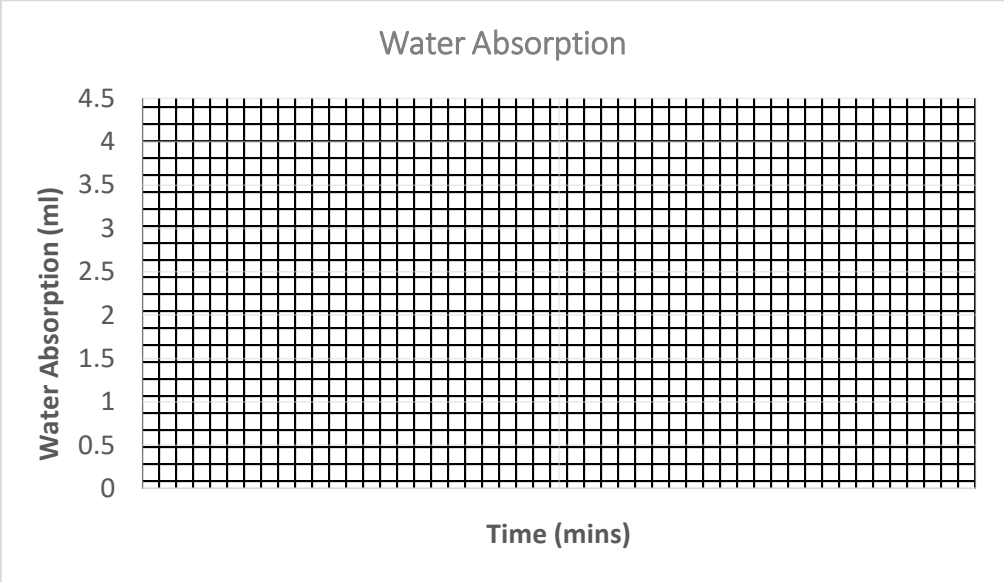

Figure 4.18: Water Absorption results

The possibility of incomplete geopolymerization between the diatomite and the alkaline activator could be the cause of the high-water absorption of the geopolymer specimens. The inclusion of HDPE in the composition of the geopolymer may have made the porosity and water absorption worse, supporting the claim made by Zhang et al. (2020) that recycled aggregate is not a suitable replacement for natural aggregate for structures in humid environments.

4.3.5 Thermal analysis of brick samples

The specimens that presented reasonably higher compressive strength were taken through thermal property evaluation to assess their insulation characteristics. The thermal conductivity was measured using the transient Hot Plate method since according to Mansour et al. (2016), the method is suitable for measuring a thermal conductivity of between 0.02 and 5Wm^{-1} K^{-1}. The principle of this method involves placing the heating wire (hot wire probe) between the surfaces of two samples of the material to be characterized while applying a constant heat flux level (ϕ) to the heating

wire and raising the evolution of the temperature T(t) of the thread. The results are presented in Table 4.13.

Table 4.13: Thermal properties

Proportional group	**Mixture Components**				**Property**			
	A: Diatomite	B: Lime	C: Sisal	D: HDPE	Density	Thermal Conductivity (λ)	Thermal effusivity (β)	Thermal diffusivity (α)
	% Weight	% Weight	% Weight	% Weight	g/cm^3	(W/mK)	$(Ws^{1/2}/m^2/K)$	$(m^2 s^{-1})$ X10E-7
1.	89.5	7.5	0.5	2.5	979.82	0.122	285	4.07
2.	78	15	0	7	902.74	0.117	257.25	3.59
3.	81	12.5	1	5.5	767.57	0.116	250	3.87
4.	76.75	15	1.25	7	902.34	0.117	252.75	3.91
5.	83.75	15	1.25	0	704.72	0.109	218.25	4.04

The thermal analysis results are more focused on thermal conductivity because thermal diffusivity and effusivity are directly proportional to it. Generally, the thermal conductivity for all the bricks was low as compared to the provisions of ASTM C332-17 (2009) and therefore it can be said that the materials can be good for insulation applications. The thermal conductivity ranged between the values 0.109 to 0.122 (W/mK).

Figure 4.19, shows the relationship between thermal characteristics and the different percentage weight proportions of the raw materials in the bricks studied.

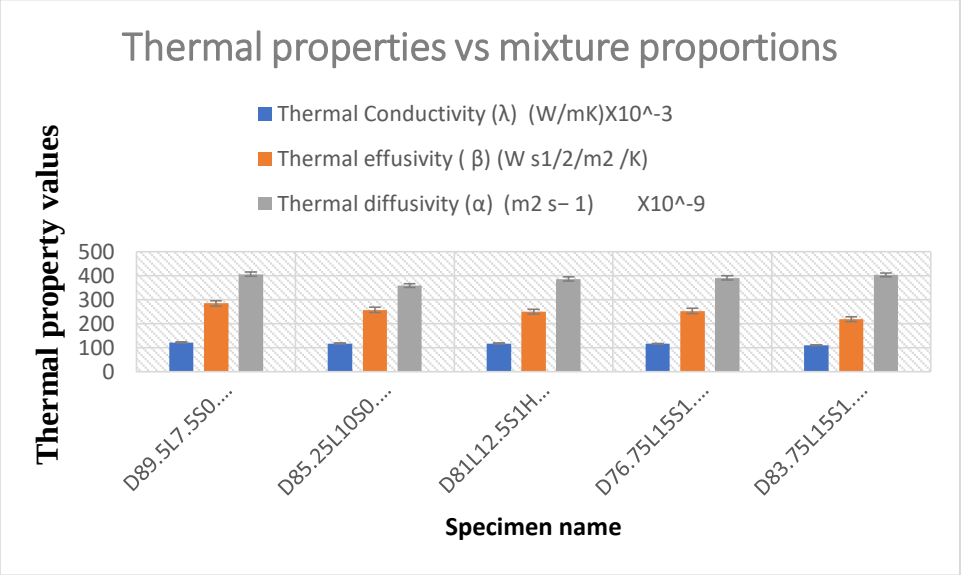

Figure 4.19: A chart of thermal characteristics versus the material proportions

Sisal fibre incorporation leads to the presence of pores which reduces the density on one hand while hindering heat conductivity on the other hand. The bricks which presented the highest thermal conductivity, had higher density which could also mean that they were less porous. The lowest thermal conductivity was attained on the concrete bricks that had 83.75% diatomite, 15% lime and 1.25% sisal fibres. The thermal conductivity test outcome can also be interpreted that the HDPE component in the concrete mixes filled out the air pores hence enhancing the thermal conductivity. Figure 4.20 shows the relationship between the thermal properties and the bulk density of the tested concrete mixes. The bricks with the minimum density presented the least heat conductivity translating to the fact that the concrete mixes bulk density is directly proportional to its thermal conductivity.

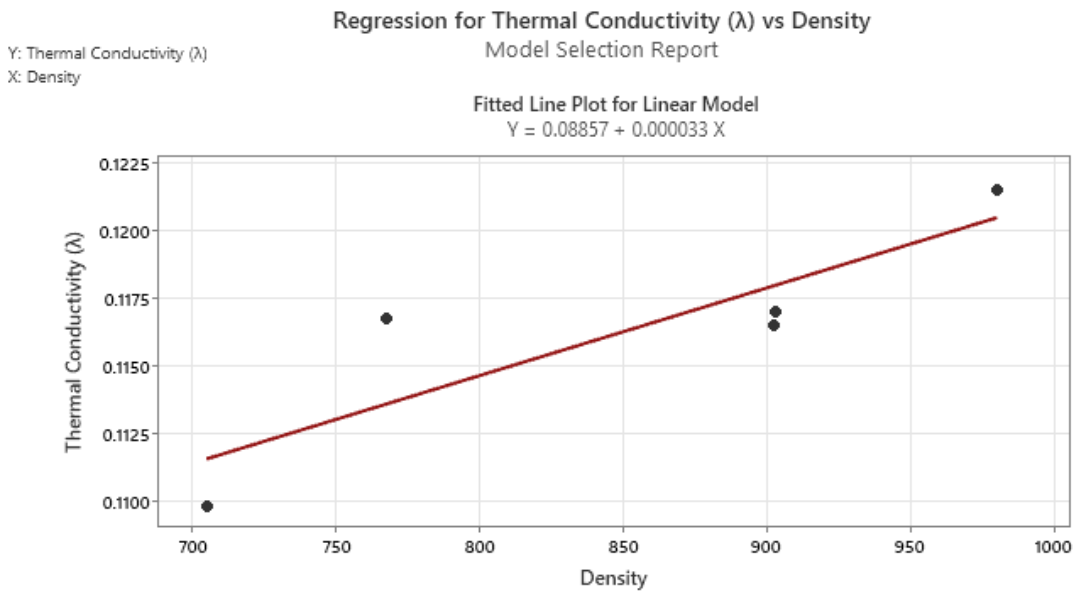

Statistics	Selected Model Linear	Alternative Model Quadratic
R-squared (adjusted)	67.24%	51.17%
P-value, model	0.056	0.244
P-value, linear term	0.056	0.847
P-value, quadratic term	—	0.920
Residual standard deviation	0.002	0.003

Figure 4.20: A chart of the relationship between thermal conductivity and density

The thermal conductivity result shows that the bulk density and heat transmission are both decreased by increasing porosity. The finding concurs with He et al. (2020), who found that thermal conductivity decreases with decreasing geopolymer density.

Material mix and thermal conductivity optimization

The thermal conductivity optimization objective function was set at minimization to ensure a reduction in heat transfer. The thermal conductivity optimization parameters are portrayed in Table 4.14.

Table 4.14: Thermal conductivity optimization input parameters

Mixture component	**Lower limit (%wt)**	**Upper limit (%wt)**	**Thermal Conductivity for P8 (W/mK)**		
			Goal	Upper	Target
Diatomite	76.75	100	Minimization	0.122	0.109
Lime	0	15			
Sisal fibres	0	1.25			
HDPE	0	7			

The statistical optimization presented in Table 4.15 and Figure 4.21 suggest a complete elimination of HDPE from the concrete. Accordingly, the mixture should consist of diatomite (83.75%), lime (15%) and sisal fibres (1.25%) for optimal thermal conductivity to be attained.

Table 4.15: Thermal conductivity optimization solution

Optimal Solution			**Predicted Response**					
Diatomite % Weight	=	83.75	Thermal conductivity for P8	=	0.109	desirability	=	1.000000
Lime % Weight	=	15						
Sisal % Weight	=	1.25						
HDPE% Weight	=	0						

Figure 4.21: Effect of mixture components on the thermal conductivity

The statistical analysis also showed that sisal fibres have a beneficial impact on thermal conductivity, hence the optimization solution recommends adding the fibres at their highest level (1.25%).

4.4 Summary and Recommendation of the Performance Properties Optimization

The right mixing and curing of the ingredients are the foundation of mix optimization to create workable concrete that hardens to the correct strength and durability. By the analysis of the optimization of individual performance properties discussed in section 4.3, it is observed that all the responses identified optimal mixture components as 83.75% diatomite, 15% lime, 1.25% sisal fibres and 0% HDPE. The summary optimization solution for all three optimal predicted responses is presented in Table 4.16.

Table 4.16: Response optimization for lime-activated specimens

Optimal Solution			**Optimal Predicted Responses**		
			Compression Strength (MPa)	Density (g/cm^3)	Thermal Conductivity (W/mK)
Diatomite % Weight	=	83.75	2.715	0.716	0.109
Lime % Weight	=	15			
Sisal % Weight	=	1.25			
HDPE% Weight	=	0			

According to the overall optimization, HDPE ought to be removed from the concrete mixture's constituent materials. Since from the analysis, it appears that it has no beneficial effect on achieving the best possible performance characteristics.

It is important to note that during performance optimization, flexural strength was not considered because, according to prior research, it often varies along the same trend as compressive strength despite being significantly lower.

Although the lime-activated geopolymers created for this study exhibit excellent thermal insulation capability, their low compressive strength and high porosity suggest that the overall performance parameters could be improved with significant modifications.

4.5 Conclusions on the Performance of Lime-Activated Diatomaceous Earth-Based Geopolymer

The mechanical, physical, and thermal properties of the lime-activated diatomaceous earth-based geopolymer specimens were tested, presented and analysed at different proportions of sisal fibres, HDPE shredded wastes and lime content. The effects of sisal fibres, HDPE waste, and various lime contents on the properties of geopolymer specimens have been examined and presented. Importantly, it was noted that it is feasible to use diatomaceous earth as a source of silica in geopolymer concrete formulations, fostering the production of sustainable concrete.

The statistical analysis showed that a geopolymer may be produced with performance characteristics like 2.715 MPa compressive strength, 0.716 g/cm^3 bulk density, and 0.109 W/mK thermal conductivity using a concrete mixture consisting of 83.75 % diatomite, 15 % lime, and 1.25 % sisal fibres.

The developed concrete brick's optimal bulk density revealed that it was light, fitting within the ASTM C1634 (2020) provided acceptable bulk density limitations for lightweight concretes.

The thermal conductivity of the examined brick samples was low, even below the minimum requirements set forth by ASTM C332-17 (2009) for the thermal insulating attributes of concrete made of lightweight aggregate.C332-17 (2009). This suggests that geopolymers based on diatomaceous earth may be appropriate for use in thermal insulation applications.

The optimal compressive strength of 2.715MPa fall within the ASTM C129 (2017) standard specifications for non-load-bearing concrete masonry units. However, the compressive strength was substantially lower than the requirements specified by ASTM C1634 (2020) and TS EN 206 (2016) for concrete face bricks. In addition, the porosity of the lime-activated geopolymers was so high that neither the Karsten test tube nor the water immersion test could be used to evaluate the water absorption rate.

Diatomaceous earth's silicic nature might have negatively impacted its dissolution kinetics, favouring the carbonation process up until complete consumption of the available calcium ions occurred. It is also possible that the diatomite composition and lime activator had low polymerization reactivity (very low diffuse pozzolanic reaction with the lime), which prevented the activator from completely dissolving the silicon and aluminium phases, and so preventing the final hardened materials from developing appropriate cohesive characteristics. The insufficient polymerization reactivity could have resulted in poor bonding since the structural performance of geopolymer concrete is highly dependent on the bond behaviour. This investigation thus confirms Song et al. (2005) assertion that extremely concentrated alkaline solutions are required to activate class F fly ash.

The possibility of insufficient mixing cannot be completely ruled out because the geopolymerization reaction path is influenced by the efficiency of mixing the components of the concrete.

This study looked at sodium hydroxide and sodium silicate alkaline activators (discussed in chapter five) as possible lime substitutes after it became clear that diatomaceous earth-based geopolymer needed to be improved in terms of strength and water absorption capacity. The investigation of sodium hydroxide and sodium silicate as alkaline activators were prompted by the fact that their use in geopolymer technology has been found to successfully activate geopolymer binders, particularly fly ash, to produce very strong and durable geopolymer concretes that meet the standard specifications for both load bearing and non-load bearing applications. Moreover, the usage of sodium-based alkaline activators may be advantageous given that low-calcium geopolymers have been found to have strong acid resistance.

CHAPTER FIVE: PERFORMANCE ANALYSIS OF SISAL REINFORCED DIATOMACEOUS EARTH GEOPOLYMER ACTIVATED WITH SODIUM-BASED ALKALINE ACTIVATORS

5.1 Introduction

The mechanical, physical and thermal performance properties of the geopolymer specimens activated with sodium-based alkaline activators were evaluated and analysed.

5.2 Property Characteristics for Naoh/Na_2SiO_3 Activated Diatomaceous Earth-Based Geopolymer

The results for the performance evaluation of NaOH/Na_2SiO_3 activated diatomaceous earth-based geopolymer are presented in Table 5.1.

Table 5.1: NaOH/Na_2SiO_3 activated diatomite performance properties

S/No	Specimen Name (Mix ID)	28th-day performance properties				
		Compressive strength (MPa)	Density (g/cm^3)	Water Absorption (%)	Thermal conductivity (W/mK)	Flexural strength (MPa)
1	D100	22.98	1.38	9.32	0.491	1.40
2	DS0.5	34.05	1.36	12.14	0.379	5.42
3	DS0.875	33.62	1.31	12.49	0.313	5.71
4	DS1.25	27.68	1.29	20.42	0.309	1.56

5.2.1 Compressive strength

Regarding the use of NaOH/Na_2SiO_3 as alkaline activators instead of lime, there was a great improvement in terms of compressive strength. For instance, in the lime-activated specimens, the maximum compressive strength (CS) that could be achieved was 2.66 MPa, whereas the NaOH/Na_2SiO_3-activated specimens yielded a maximum compressive strength CS of 34.05 MPa and a minimum CS of 22.98 MPa. Figure 5.1 shows the trend of compressive strength with the addition of sisal fibres into the geopolymer mixture composition. The trendline of sisal incorporation versus

compressive strength indicates that there is a positive relationship so that the increase in the quantity of sisal fibres leads to an increase in compression strength up to some point (approximately 0.8% sisal fibre loading) beyond which the compressive strength is reduced. These observations, which are supported by the law of mixtures, have been made by several other studies, and they suggest that a further increase in fibre loading may lead to the formation of voids, which may then cause the material to fracture under compression stress.

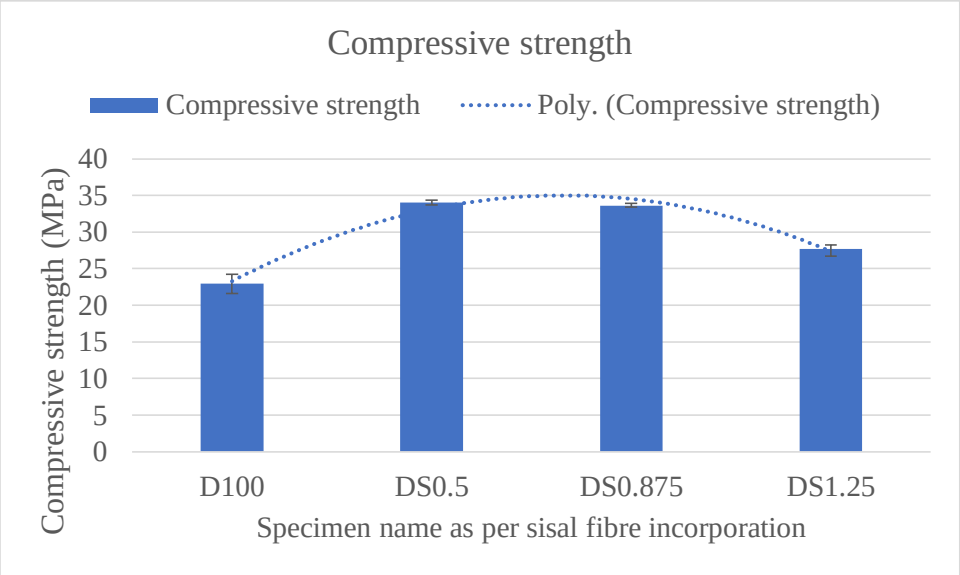

Figure 5.1: Compressive strength versus sisal fibre incorporation

All of the tested specimens met the prerequisite requirements for the concrete masonry units as per ASTM C1634 (2020). The improvement in strength with $NaOH/Na_2SiO_3$ alkaline activation occurs mainly due to the formation of hydration product Na-S-H (sodium silicate hydrate) gel which is formed due to hydration reactions (Islam et al., 2020).

Figure 5.2 shows the impact of sisal fibre incorporation on the microstructure of the diatomaceous earth-based geopolymer. Increased sisal fibre content may have caused microfractures to form at the interfaces, lowering compressive strength. The fundamental reason for this flaw is that natural fibres are hydrophilic by nature due to

the presence of hydroxyl groups and other polar groups, which makes them incompatible with the hydrophobic composite matrix. The hydrophilicity of natural fibres denotes high fibre absorbability, which is the primary factor in the hydrophobic matrix's poor adhesion to them. This affects the surface's friction and abrasion as well as the swelling or delamination of the fibres (Kurpińska et al., 2022), and agrees with the work of Ugwuishiwu et al. (2013). Sisal fibres displayed a propensity to clump during mixing, which could affect the composites' strength since the fibre clumps may settle inside the microstructure of the concrete, impeding the geopolymerization process. Higher sisal fibre loadings may result in voids and uneven fibre orientation, which may also explain the decreasing strength.

The absence of sisal fibres in the D100 specimens may have led to insufficient diatomaceous earth material dispersion during the alkaline activation process. The presence of unreacted diatomaceous earth from insufficient geopolymerization may have made the concrete brittle, which explains the poor compressive strength result.

The sisal fibre reinforcement in the diatomaceous-based geopolymer concrete's microstructure analysis demonstrates the necessity of fibre reinforcement to reduce the concrete's brittleness, increase compressive strength, and produce sufficient porosity to support thermal insulation capability. It is crucial, therefore, to note that to maximize the performance of the concrete and minimize the negative effects of over-reinforcement, an optimal fibre quantity should be determined.

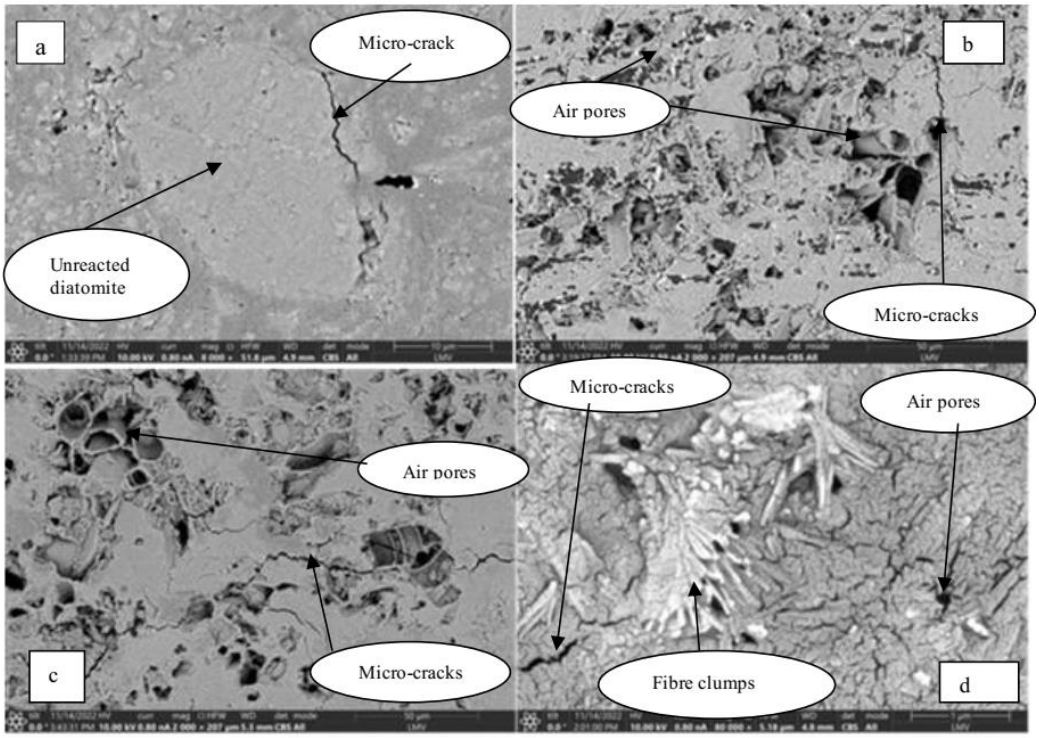

Figure 5.2: Scanning electron microscopy (SEM) images. MAG: 2000x: a) D100 b) DS0.5 c) DS0.875 d) DS1.25

The relationship between the sisal fibre content and compressive strength of the geopolymer specimens is illustrated in Figure 5.3. The correlation behaviour shows that the incorporation of sisal fibres has a direct influence on the concrete. Additionally, the statistical analysis demonstrates a non-linear relationship between the inclusion of sisal fibre and compressive strength, with a correlation factor (R^2) of 99 %.

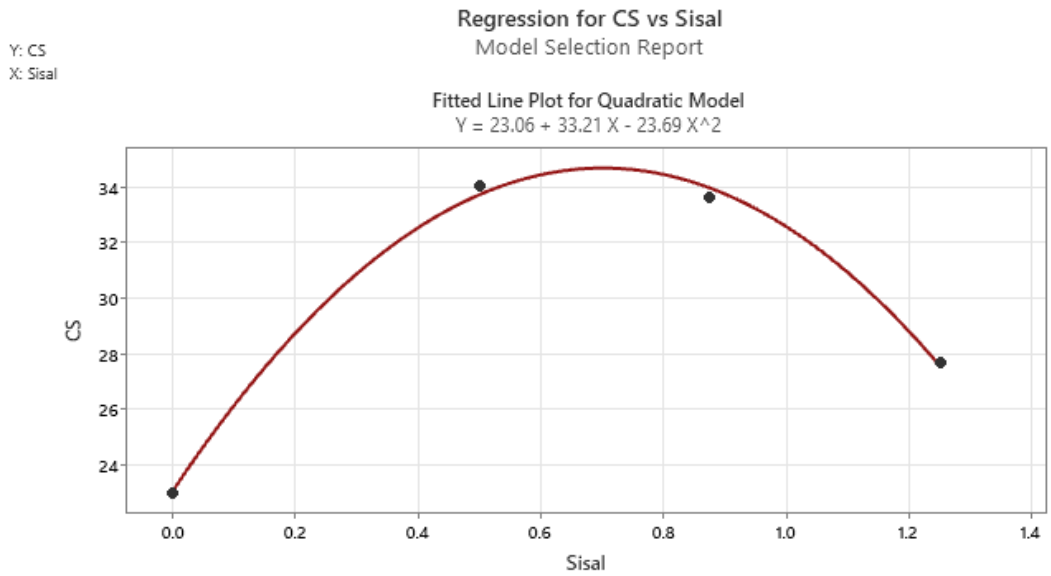

Statistics	Selected Model Quadratic	Alternative Model Linear
R-squared (adjusted)	99.10%	0.00%
P-value, model	0.055	0.599
P-value, linear term	0.035*	0.599
P-value, quadratic term	0.038*	—
Residual standard deviation	0.501	5.921

** Statistically significant ($p < 0.05$)*

Figure 5.3: Correlation between the sisal fibre content and the compressive strength

5.2.2 Flexural strength

The flexural test experiment on the developed diatomaceous earth-based geopolymer was performed to determine the maximum bending stress that it could sustain before fracture. As shown in Table 5.1, the diatomaceous earth-based geopolymers attained a flexural strength that varied from 1.4 MPa to 5.71 MPa after being activated with sodium-based alkaline activators. This suggests a significant improvement in the investigated geopolymers' bending resistance. The flexural strength of the diatomaceous earth-based geopolymers appeared to rise with the amount of sisal fibre incorporation up to 0.875 % of sisal inclusion, but after that point, the flexural strength declined. Figure 5.4 illustrates the relationship between the amount of sisal fibre incorporated and the flexural strength attained.

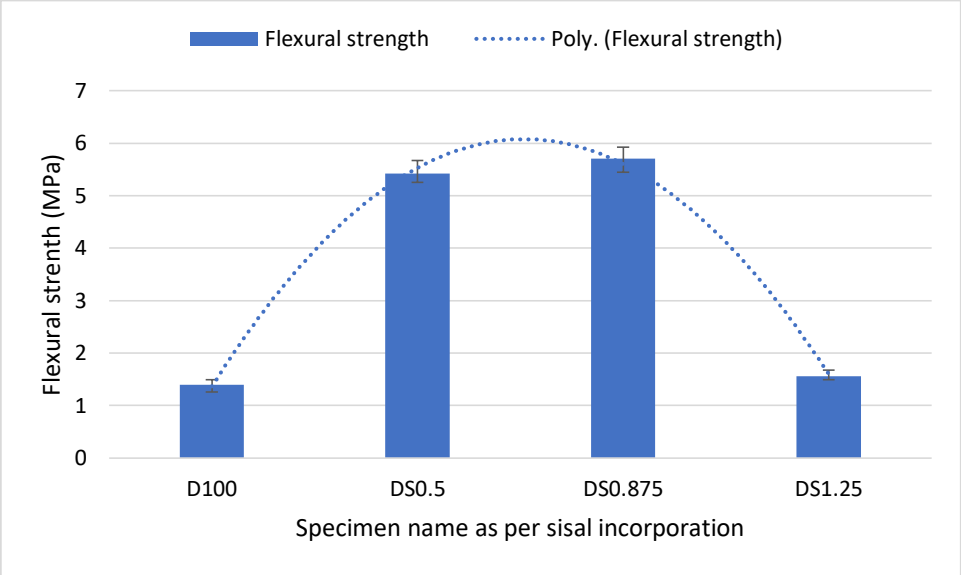

Figure 5.4: Flexural strength versus sisal fibre incorporation

The effect of sisal fibre incorporation on the compressive strength of the geopolymers being studied is comparable to the effect on flexural strength. The flexural strength result confirms that the diatomaceous earth particles were better bonded when sodium-based alkaline activators were used instead of lime activation.

Table 5.2 shows the maximum bending displacements that the diatomaceous earth-based specimens experienced during the flexural test experiment before fracture occurred.

Table 5.2: Maximum flexural deflection

Specimen Name	D100	DS0.5	DS0.875	DS1.25
Max. displacements (mm)	0.32	1.40	1.64	1.76

Figure 5.5 shows the trend of flexural deflection with increasing sisal fibre incorporation. This demonstrates how the sisal fibres in the geopolymer concrete improved its ductility and decreased its brittleness.

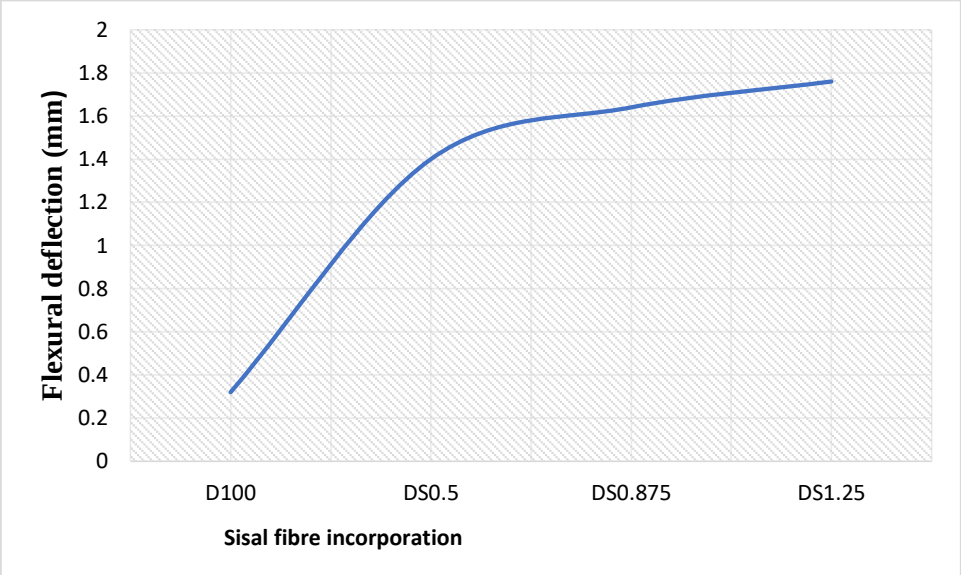

Figure 5.5: Flexural deflection versus fibre incorporation

5.2.3 Bulk density

The density of the modified geopolymers was higher than the lime-activated products. The $NaOH/Na_2SiO_3$ activated geopolymers were denser since they yielded a maximum density of 1.38 g/cm^3 and a minimum density of 1.29 g/cm^3, while the lime-activated specimens had a maximum density of 0.996 g/cm^3. The density values of the $NaOH/Na_2SiO_3$ activated geopolymer were found to be within the permitted density of less than 1.68 g/cm^3 for lightweight concrete masonry units as recommended in ASTM C1634 (2020). The produced geopolymers also complied with TS EN 206 (2016) and ACI Committee 213R-03 (2013) criteria for permissible lightweight concrete density, which is less than 2 g/cm^3. Since there is currently no standard for geopolymer concretes (or mortars), these criteria can be used to categorize geopolymer concretes (or mortars) based on unit weight. In this respect, it may be said that the geopolymer concretes that were developed can be categorically referred to as lightweight.

Although there was only a slight impact of the sisal incorporation on the density of the geopolymer specimens, it was observed that the density reduced as the sisal fibre content increased, as illustrated in Figure 5.6. This is because including additional

fibres would result in the introduction of more voids or air spaces, which would increase volume and cause a drop in mass, leading to low density.

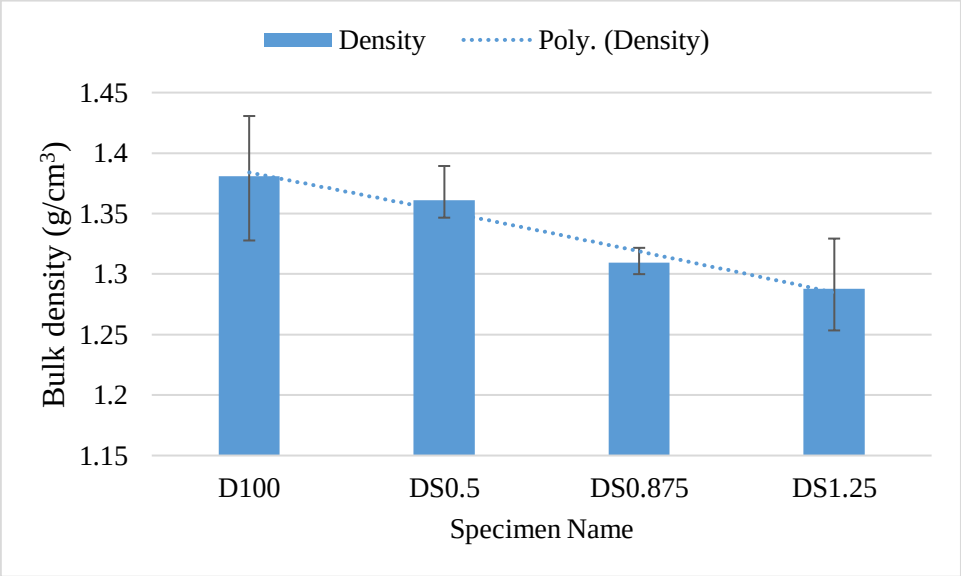

Figure 5.6: Bulk density versus sisal fibre incorporation

Figure 5.7 shows a significant association between the sisal fibre content and the bulk density of the developed geopolymer concretes, with a correlation factor (R2) of 92 %. This explains that the sisal fibre incorporation has a direct impact on the bulk density of the concretes.

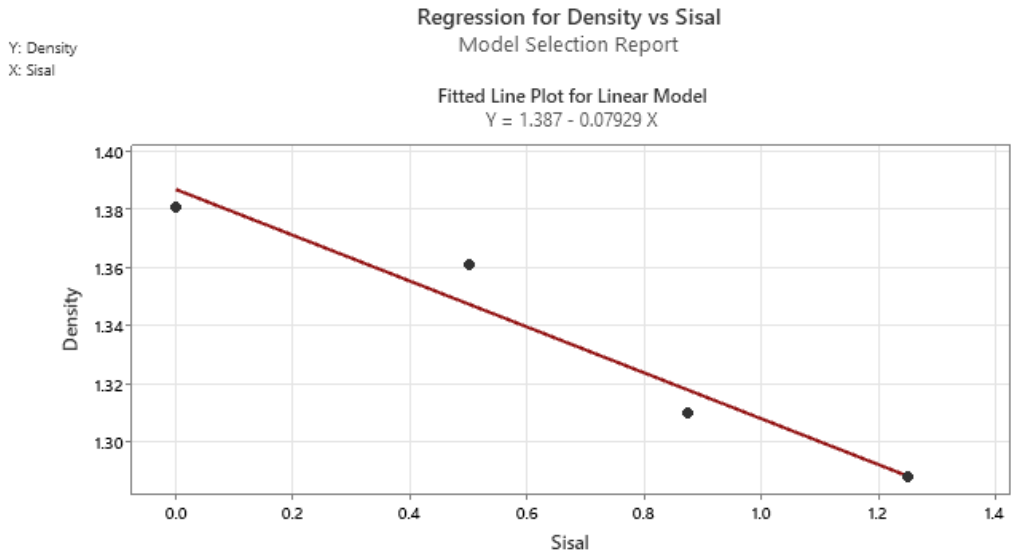

Statistics	Selected Model Linear	Alternative Model Quadratic
R-squared (adjusted)	92.28%	87.45%
P-value, model	0.026*	0.205
P-value, linear term	0.026*	0.517
P-value, quadratic term	—	0.715
Residual standard deviation	0.012	0.015

** Statistically significant ($p < 0.05$)*

Figure 5.7: Correlation between the sisal fibre content and the density

5.2.4 Water absorption

1. Water immersion method

In terms of water absorption, an improvement in durability was observed, with a bit of weathering being noted in some bricks. With the sodium-based alkaline activation, porosity seems to have reduced significantly due to better bonding. The results showed that the diffusion coefficient and maximum water content values increase as the fibre content increases, although all the values fall within the acceptable range of ≤20% according to Ahmad et al. (2017). Higher fibre loading percentages resulted in greater water absorption ability as shown in Figure 5.8. As a result, the brick specimens with the highest sisal fibre inclusion absorbed more water, even more than the permitted maximum limit of 15% as per ASTM C1634 (2020). This phenomenon can be

explained by the hydrophilic nature of vegetable fibres which is causing a rise in concrete water absorption from about 9% to 20%.

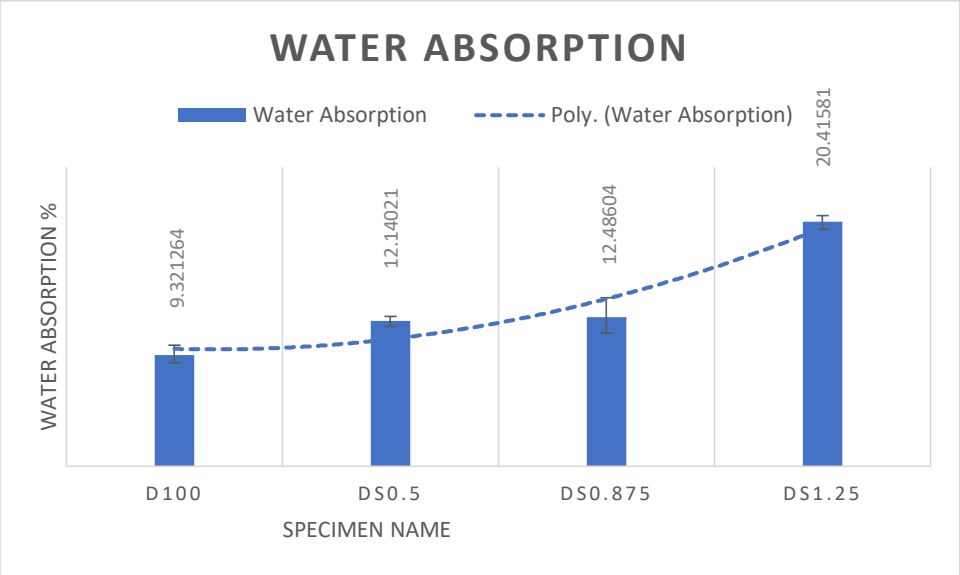

Figure 5.8: Water absorption versus sisal fibre incorporation

The higher the cellulose content, the higher the water absorption rate, and consequently, the higher the diffusion coefficient of the specimens. The correlation between the sisal fibre content and the water absorption of the geopolymer specimens is illustrated in Figure 5.9.

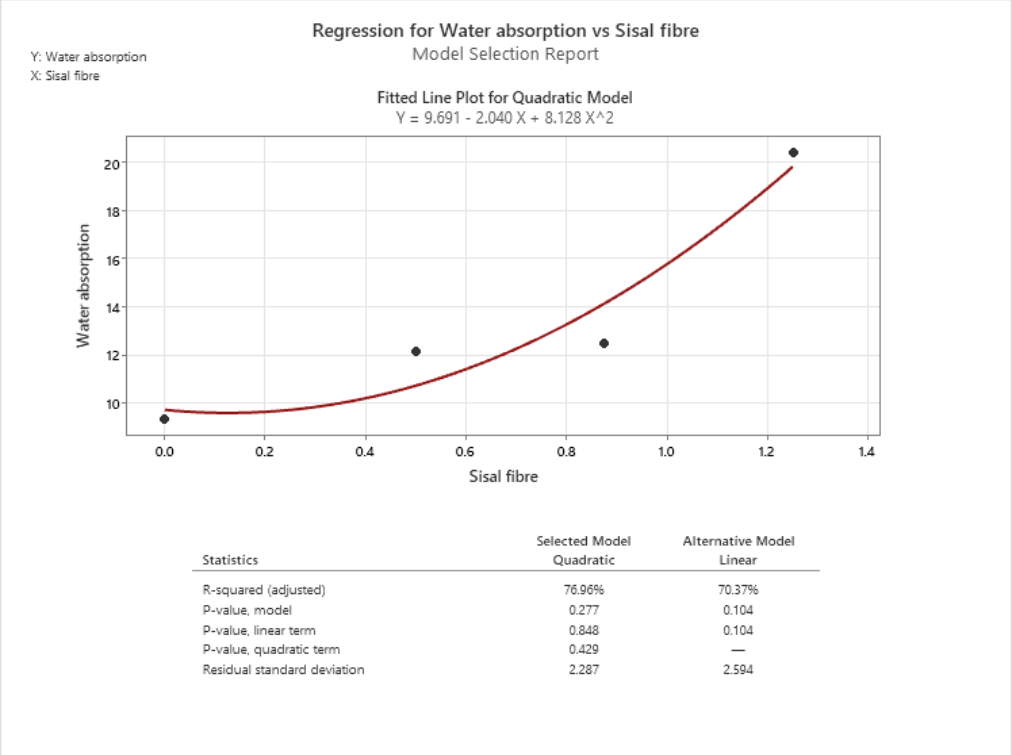

Figure 5.9: Correlation between the sisal fibre content and the water absorption

The water absorption and the sisal fibre seem to have a quadratic relationship with a correlation factor (R^2) of about 77%. The high cellulose content in the sisal fibres could further contribute to more water penetrating the interface through the voids induced by the swelling of fibres (Muñoz & García-Manrique, 2015; Salih et al., 2020; Ugwuishiwu et al., 2013).

2. Karsten tube test analysis

The Karsten tube showed that the modified geopolymer samples were reasonably stable and less porous. The rate of water absorption observed with the Karsten test tube is presented in Table 5.3.

Table 5.3: Karsten tube test water absorption versus time

Water absorption (ml)	Time (mins)			
	D100	DS0.5	DS0.875	DS1.25
0	0	0	0	0
1	21	16	15	13
2	58	45	41	35
3	94	73	67	57
4	131	101	93	80

The rate of water absorption continually increased as sisal fibre content increased. The specimens with the highest fibre incorporation took the least time to absorb 4 ml of water.

Through statistical analysis using the Minitab software, equations that related the amount of water absorbed with the time taken during the absorption were generated. These equations were used to determine whether the specimens fall within the allowable water absorption specification of less than 20 % within the first 20 minutes, as set forth by Hendrickx (2013). Table 5.4 was used to evaluate the viability of the geopolymer specimens in terms of the Karsten water absorption behaviour. Figure 5.10 presents the graphical analysis for the water absorption through the Karsten test tube.

Table 5.4: Karsten test analysis table

Specimen name	Equation generated	Water absorbed (y) when time (x) =20 minutes	Percentage of water absorption (tube length=5ml)
D100	Y = 0.2005 + 0.02960 X	0.79 ml	15.85 %
DS0.5	Y = 0.2009 + 0.03828 X	0.97 ml	19.33 %
DS0.875	Y = 0.2003 + 0.04166 X	1.03 ml	20.67 %
DS1.25	Y = 0.2020 + 0.04859 X	1.17 ml	23.48 %

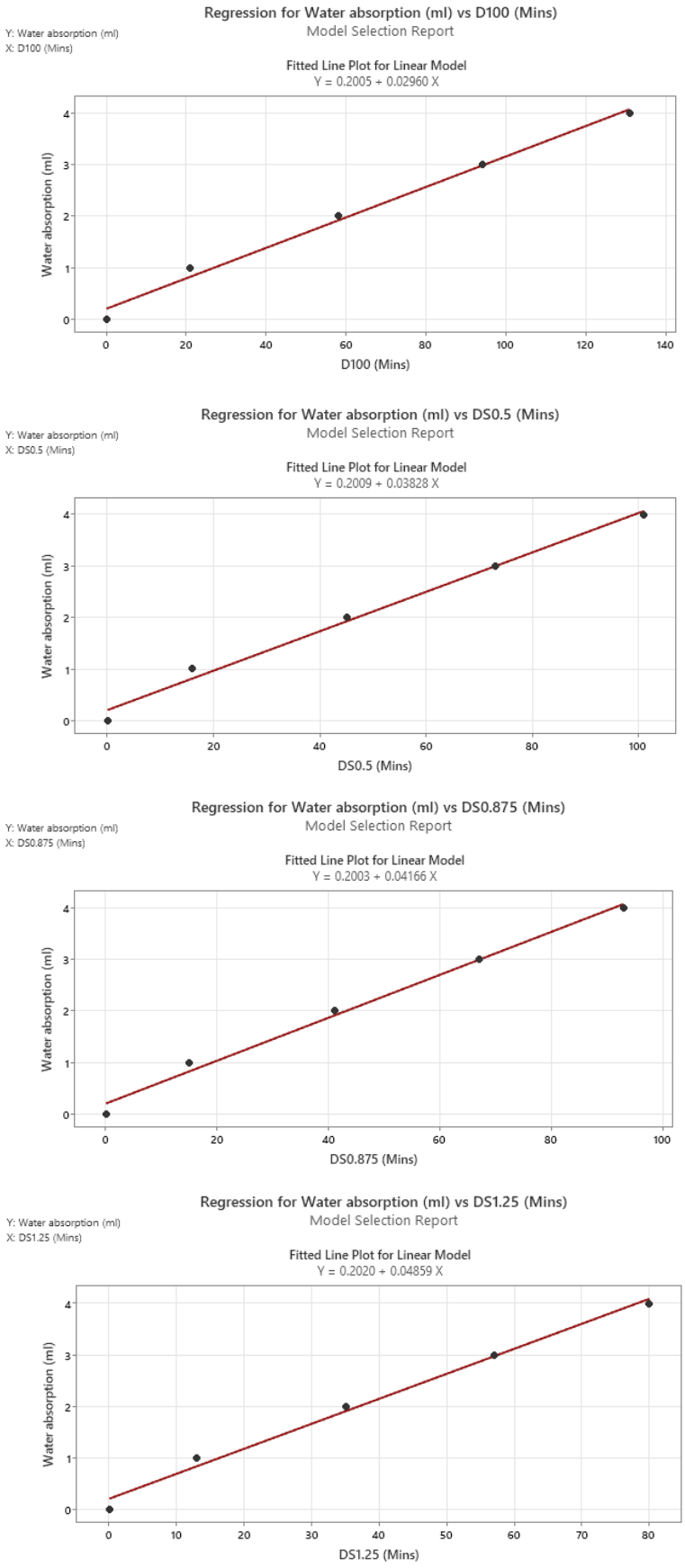

Figure 5.10: Karsten test water absorption versus time

The specimens under investigation, which contained up to 0.875 % sisal fibres, met Hendrickx (2013) criterion for appropriate water absorption behaviour. This is because, during the first 20 minutes of testing, the water level in the Karsten tube did not drop by more than 20% of its original height. However, the specimens that had 1.25 % of sisal fibres absorbed 23.48 % of water within the first 20 minutes of testing.

From the observed effects of sisal fibre inclusion on the characteristics of geopolymer concretes, it can be inferred that fibre inclusion needs to be critically assessed to strike a healthy balance.

5.2.5 Thermal conductivity analysis

The thermal conductivity values for the tested specimens tabulated in Table 5.1 ranged between 0.309 and 0.491 W/mK. Maximum thermal conductivity was found in the specimens devoid of sisal fibres, whilst minimum thermal conductivity was found in those with the highest sisal fibre incorporation.

The thermal conductivity as shown in Figure 5.11 indicates a declining trend with an increase in the number of sisal fibres incorporated. This explains the fact that the increase in porosity brought forth by fibre incorporation lowers the heat transfer tendency.

The attained thermal conductivity agreed with the recommendation by Asadi et al. (2018) and Zhang et al. (2020) that lightweight concrete thermal conductivity should be between the range of 0.2 to 1.9 W/mK. However, apart from the specimens that had no sisal fibres which indicated thermal conductivity of 0.491 W/mk, all the other specimen samples had their thermal conductivities falling within the acceptable range of 0.22 to 0.43 W/mK as stipulated in ASTM C332-17 (2009).

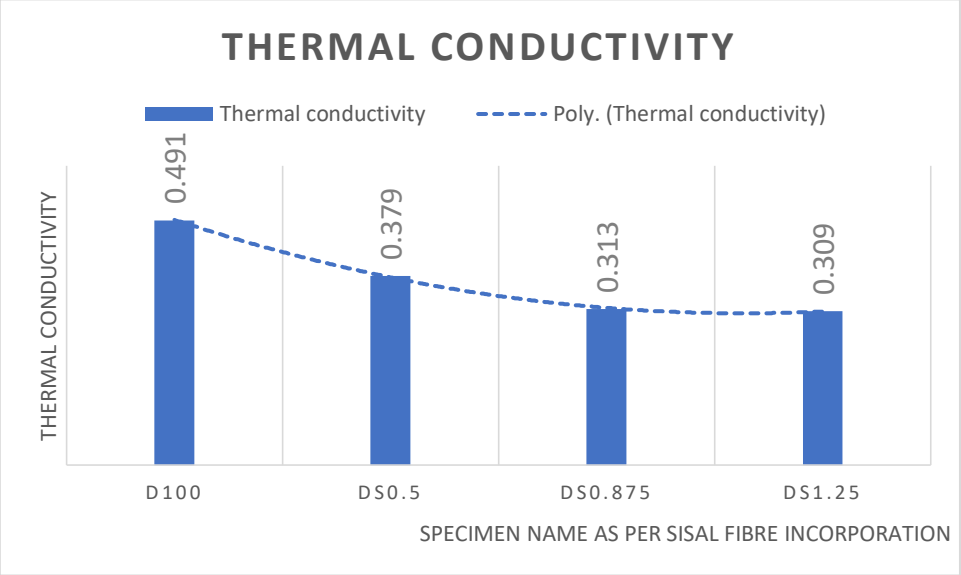

Figure 5.11: Thermal conductivity versus sisal fibre incorporation

Figure 5.12 shows that there is a strong correlation (correlation coefficient of R^2= 85.78%) between the thermal conductivity of concrete and the quantity of the sisal fibre incorporated. The observed relationship is an inverse proportionality, whereby an increase in sisal fibre content results in a decrease in the heat transmission of the concrete. The inverse proportionality is caused by the increase in porosity that occurs when fibres are added to concrete; demonstrating that the addition of fibre significantly improves the thermal insulation of the geopolymers. The high air content created by the geopolymer's substantial porosity as a result of the fibre inclusion decreases the rate of thermal conduction through the material.

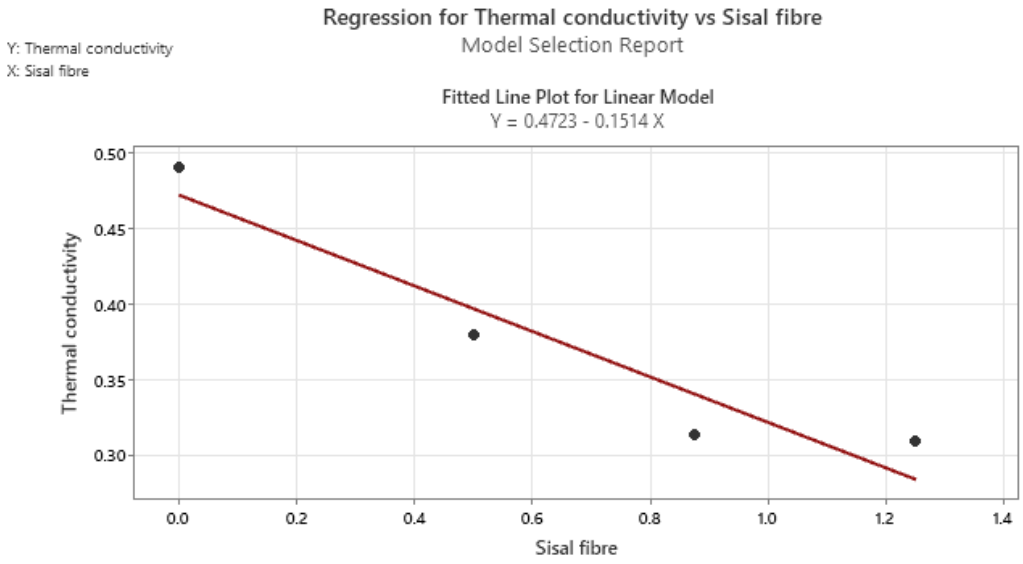

Statistics	Selected Model Linear	Alternative Model Quadratic
R-squared (adjusted)	85.78%	98.10%
P-value, model	0.049*	0.080
P-value, linear term	0.049*	0.089
P-value, quadratic term	—	0.166
Residual standard deviation	0.032	0.012

** Statistically significant ($p < 0.05$)*

Figure 5.12: Correlation between the sisal fibre content and the thermal conductivity.

5.3 Performance property optimization

Even though the performance properties for the NaOH/Na_2SiO_3 activated diatomaceous earth specimens containing sisal fibres discussed in section 5.2, were in line with the preset performance specifications, their optimization is necessary to identify the optimal mixture composition. The statistical analysis was carried out using the Minitab software to reach the performance optimization target. The characteristic features presented in Table 5.1 formed the basis of the optimization analysis. Table 5.5 displays the input parameters for the response optimization operation.

Table 5.5: Response optimization input parameters

Characteristic property	**Goal**	**Lower**	**Target**	**Upper**
Compressive strength (MPa)	Maximum	22.9750	34.0525	34.0525
Bulk density (g/cm^3)	Minimum	1.2878	1.2878	1.3809
Water absorption (%)	Minimum	9.3213	9.3213	20.4158
Thermal conductivity (W/mK)	Minimum	0.3090	0.3090	0.4910

The optimization solution for the $NaOH/Na_2SiO_3$ activated diatomaceous earth specimens containing sisal fibres is presented in Table 5.6 and illustrated in Figure 5.13.

Table 5.6: Response optimization solution for $NaOH/Na_2SiO_3$ activated diatomaceous earth specimens

Optimal Solution			**Predicted Responses**			
			Compression Strength (MPa)	Density (g/cm^3)	Water absorption (%)	Thermal conductivity (W/mK)
Diatomite % Weight	=	99.14	34.10	1.322	13.93	0.323
Sisal % Weight	=	0.86				

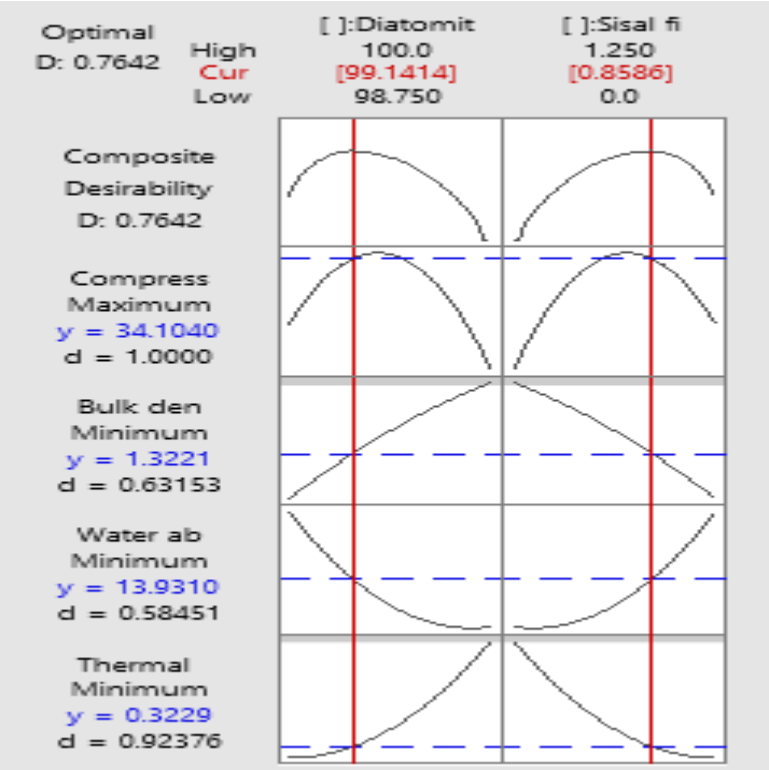

Figure 5.13: Performance optimization of $NaOH/Na_2SiO_3$ activated geopolymers

With $NaOH/Na_2SiO_3$ activation, the optimization of the performance responses showed that a geopolymer concrete with a compressive strength of 34.1 MPa, density of 1.322 g/cm^3, water absorption of 13.93 % and thermal conductivity of 0.323 could be achieved.

In general, the performance assessment of the $NaOH/Na_2SiO_3$ activated diatomaceous earth-based geopolymers demonstrates that sisal fibres and diatomaceous earth can be successfully combined to create sustainable geopolymer concrete.

5.4 Process and Performance Correlation Modelling

This section lays out the relationships between the different experimental results of the alkaline-activated diatomaceous earth-based geopolymer that is the subject of this investigation. The engineering characteristics of the diatomaceous earth-based geopolymer under investigation include its compressive strength, bulk density, water absorption capacity, as well as its thermal conductivity.

The developed sisal fibre-reinforced diatomaceous earth-based geopolymer's correlation matrix for process and response (performance) parameters is shown in Table 5.7. The correlation matrix demonstrates that most of the examined parameters have substantial correlations, making correlational modelling between the parameters possible.

Table 5.7: Correlation matrix for the process and response (performance) factors

Variables	Diatomite	Sisal fibre	Compressive strength	Bulk density	Water absorption	Thermal conductivity
Diatomite	**1**					
Sisal fibre	-1	**1**				
Compressive strength	-0.99	0.99	**1**			
Bulk density	-0.92	0.92	-0.82	**1**		
Water absorption	-0.76	0.76	0.97	-0.58	**1**	
Thermal conductivity	0.98	-0.98	-0.22	0.92	-0.29	**1**

The parameters that displayed a strong correlation were linked using statistical correlation modelling utilizing the Minitab analysis tool.

5.4.1 Correlation between the quantity of sisal fibre incorporated and the compressive strength attained

Figure 5.14 shows that there is a strong relationship between the quantity of sisal fibre incorporation and the geopolymer compressive strength gained. The amount of sisal fibre and compressive strength appear to have a non-linear relationship, and the quadratic model best describes their relationship.

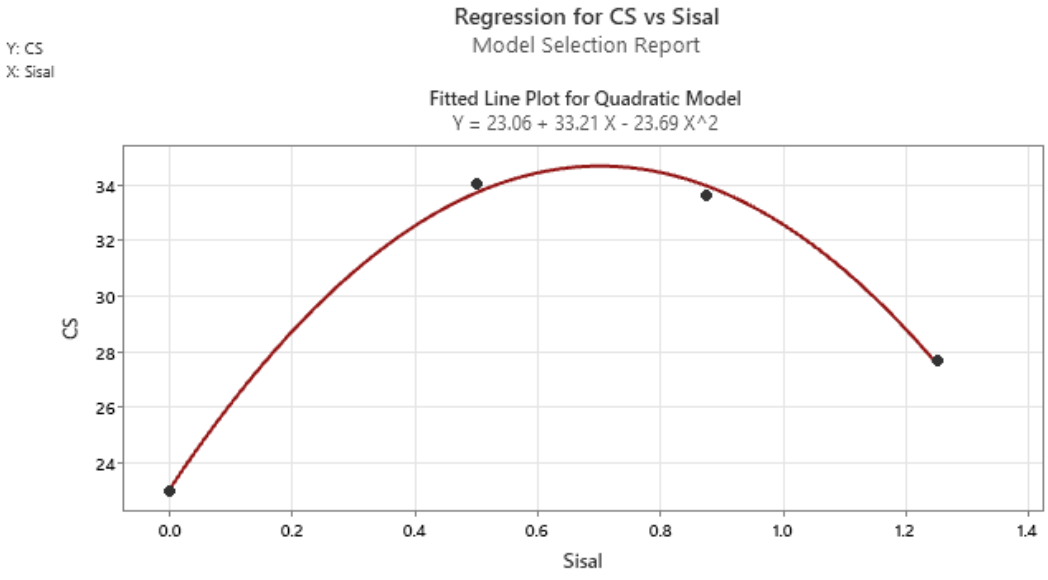

Statistics	Selected Model Quadratic	Alternative Model Linear
R-squared (adjusted)	99.10%	0.00%
P-value, model	0.055	0.599
P-value, linear term	0.035*	0.599
P-value, quadratic term	0.038*	—
Residual standard deviation	0.501	5.921

** Statistically significant ($p < 0.05$)*

Figure 5.14: Correlation between sisal fibre incorporation and the compressive strength

The quadratic model that links the sisal fibres and the compressive strength is given as;

$$Y = 23.06 + 33.21X - 23.69X^2$$

Where, Y = Compressive strength and X = Sisal fibre quantity

5.4.2 Correlation between the sisal fibre incorporation and the bulk density

Figure 5.15 indicates that there is a strong linear relationship between the quantity of sisal fibre incorporated and the bulk density of the developed geopolymer.

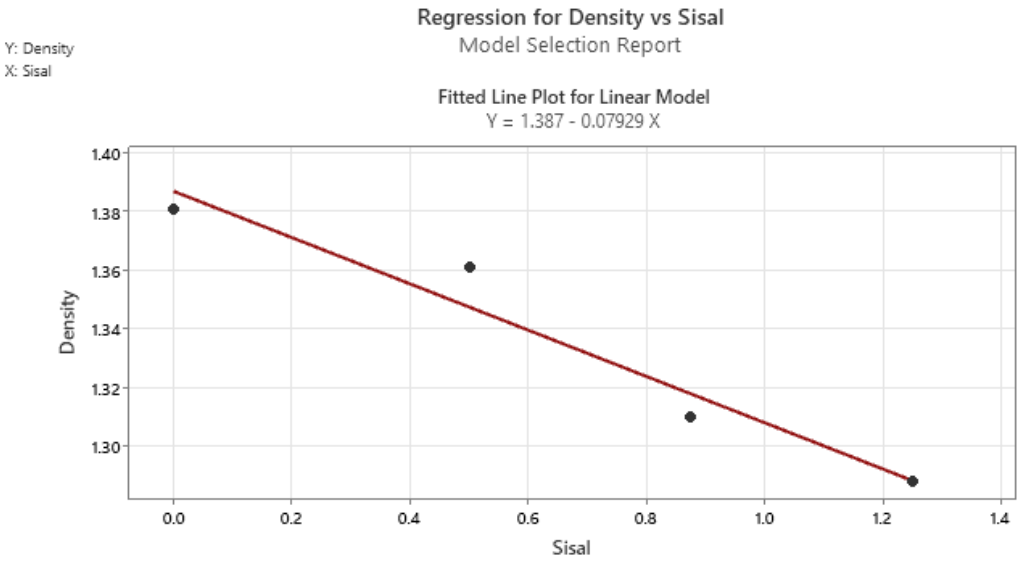

Statistics	Selected Model Linear	Alternative Model Quadratic
R-squared (adjusted)	92.28%	87.45%
P-value, model	0.026*	0.205
P-value, linear term	0.026*	0.517
P-value, quadratic term	—	0.715
Residual standard deviation	0.012	0.015

** Statistically significant ($p < 0.05$)*

Figure 5.15: Correlation between the sisal fibres and the bulk density

The linear equation that best relates the quantity of sisal fibre incorporated and the bulk density of the geopolymer is given as;

$$Y = 1.387 - 0.079X$$

Where, Y = Bulk density and X = Sisal fibre quantity

5.4.3 Correlation between the sisal fibre incorporation and the thermal conductivity

According to Figure 5.16, the amount of sisal fibre incorporated and the achieved thermal conductivity capacity have a statistically significant linear relationship.

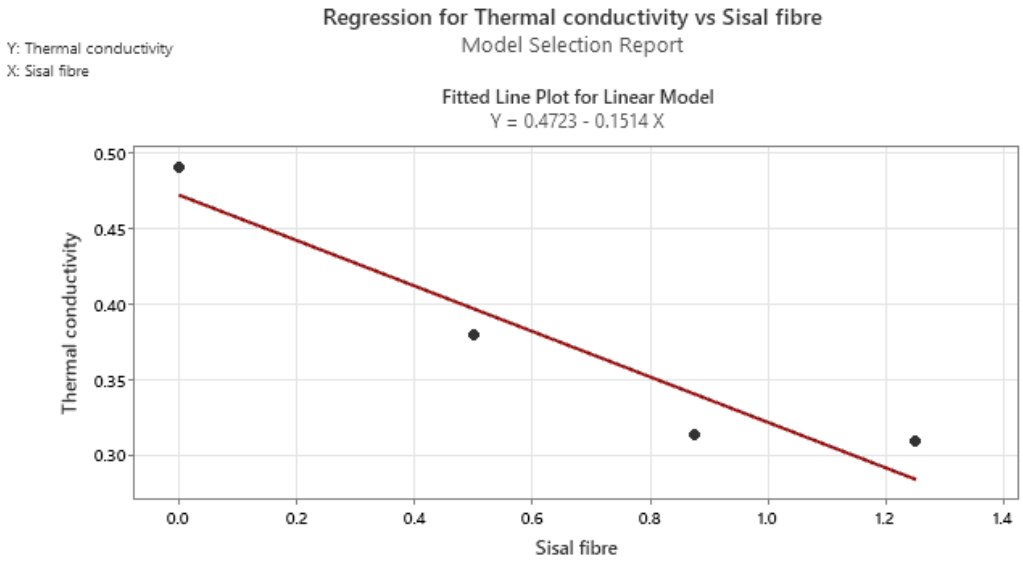

Statistics	Selected Model Linear	Alternative Model Quadratic
R-squared (adjusted)	85.78%	98.10%
P-value, model	0.049*	0.080
P-value, linear term	0.049*	0.089
P-value, quadratic term	—	0.166
Residual standard deviation	0.032	0.012

** Statistically significant ($p < 0.05$)*

Figure 5.16: Correlation between the sisal fibres and the thermal conductivity

The linear equation that best relates the quantity of sisal fibre incorporated and the thermal conductivity of the geopolymer is given as;

$$Y = 0.4723 - 0.1514X$$

Where, Y = Thermal conductivity and X = Sisal fibre quantity

5.4.4 Correlation between Compressive Strength and the bulk density

The geopolymer's compressive strength and bulk density have a significant nonlinear relationship, as seen in Figure 5.17, and the quadratic model best describes this relationship.

The quadratic model that links the compressive strength and the bulk density is given as;

$$Y = -9921 + 14960X - 5618X^2$$

Where, Y = Compressive strength and X = Bulk density

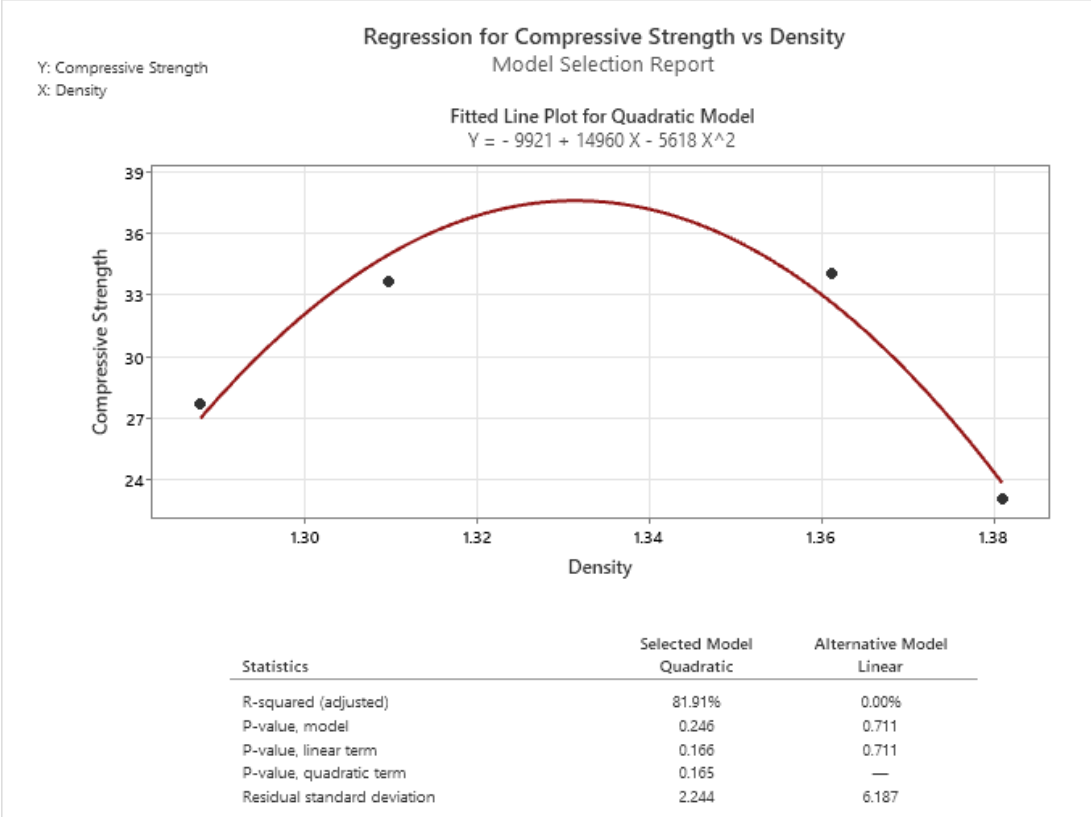

Statistics	Selected Model Quadratic	Alternative Model Linear
R-squared (adjusted)	81.91%	0.00%
P-value, model	0.246	0.711
P-value, linear term	0.166	0.711
P-value, quadratic term	0.165	—
Residual standard deviation	2.244	6.187

Figure 5.17: Correlation between the compressive strength and the bulk density

5.4.5 Correlation between Compressive Strength and the water absorption

According to Figure 5.18, the compressive strength and water absorption capacity of the geopolymer exhibit a strong nonlinear relationship, and the quadratic model best expresses the relationship.

The quadratic model that relates the compressive strength and the water absorption capacity is given as;

$$Y = -55.78 + 12.12X - 0.3936X^2$$

Where, Y = Compressive strength and X = Water absorption

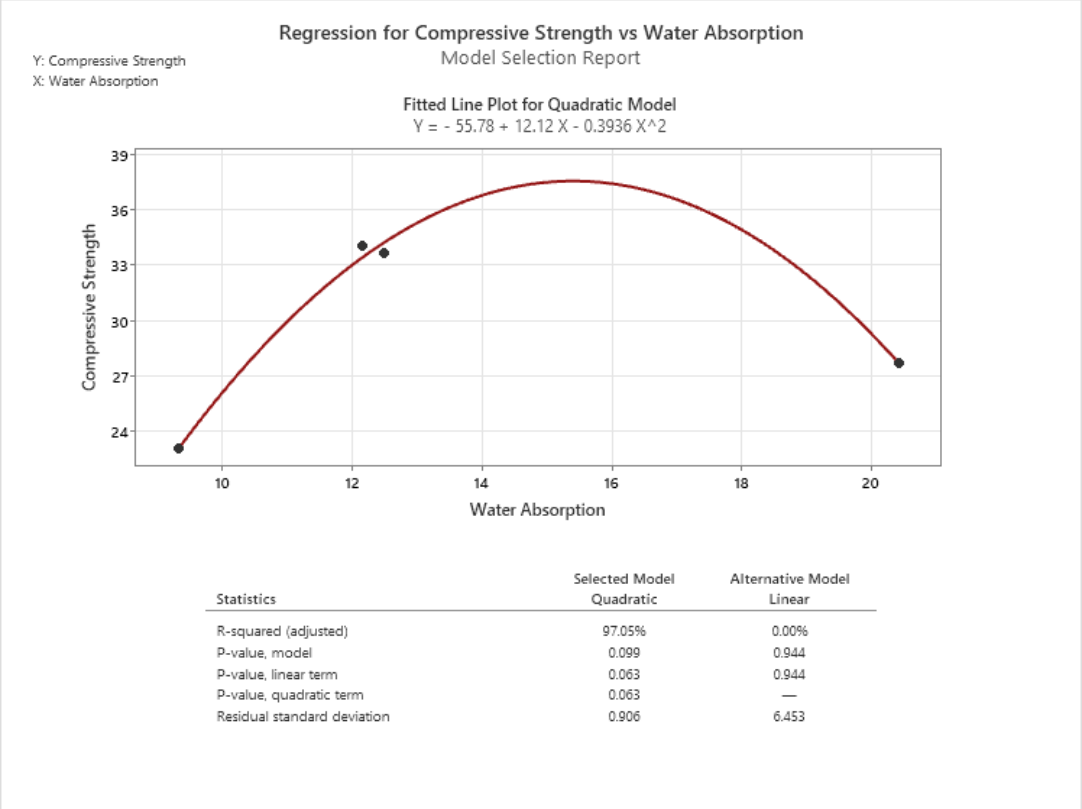

Statistics	Selected Model Quadratic	Alternative Model Linear
R-squared (adjusted)	97.05%	0.00%
P-value, model	0.099	0.944
P-value, linear term	0.063	0.944
P-value, quadratic term	0.063	—
Residual standard deviation	0.906	6.453

Figure 5.18: Correlation between the compressive strength and the water absorption

5.4.6 Correlation between bulk density and the thermal conductivity

The bulk density and thermal conductivity of the geopolymer exhibit a strong nonlinear relationship, and the quadratic model best describes this relationship (see Figure 5.19).

The thermal insulation capacity and bulk density are related by a quadratic model given as;

$$Y = 0.5054 + 3.874X - 4.26X^2$$

Where, Y = Bulk density and X = Thermal conductivity

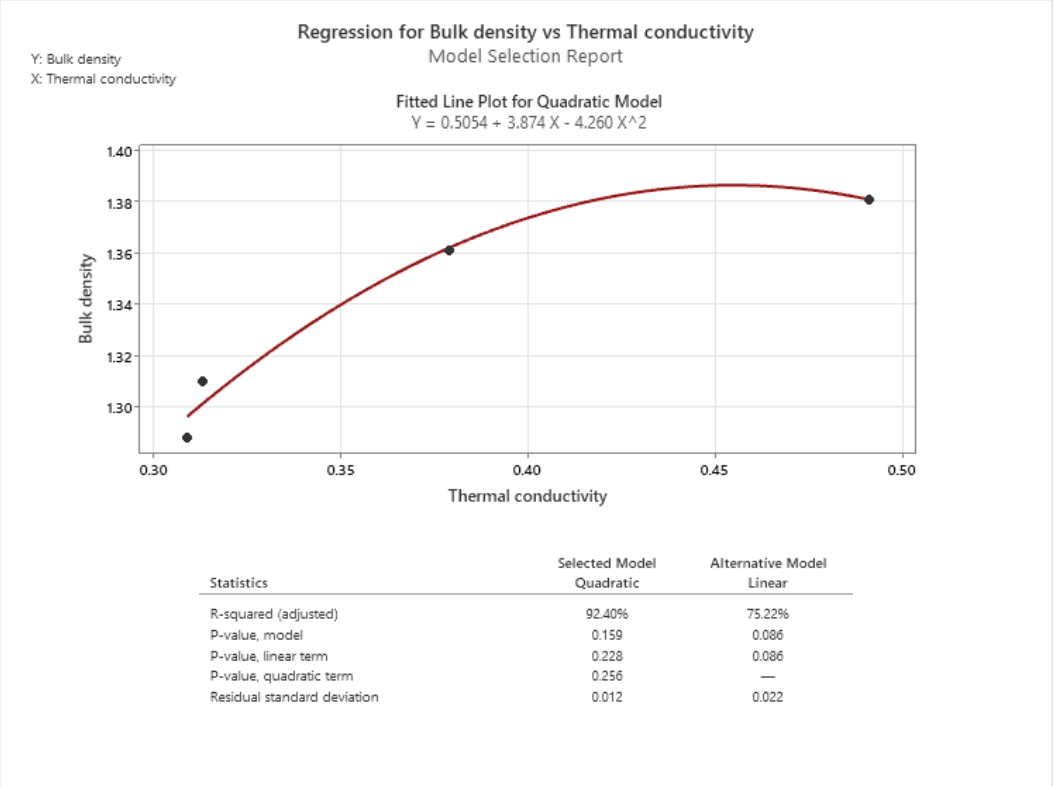

Figure 5.19: Correlation between the bulk density and the thermal conductivity

5.4.7 Correlation between the water absorption capacity and sisal fibre quantity

Water absorption capacity and the quantity of sisal fibre incorporated seem to have a positive correlation of about 70% as shown in Figure 5.20. Although the relationship between the amount of sisal fibres and the water absorbed has a correlation coefficient that is less than 80%, the relationship nevertheless shows that adding more sisal fibres to concrete increases its ability to absorb water.

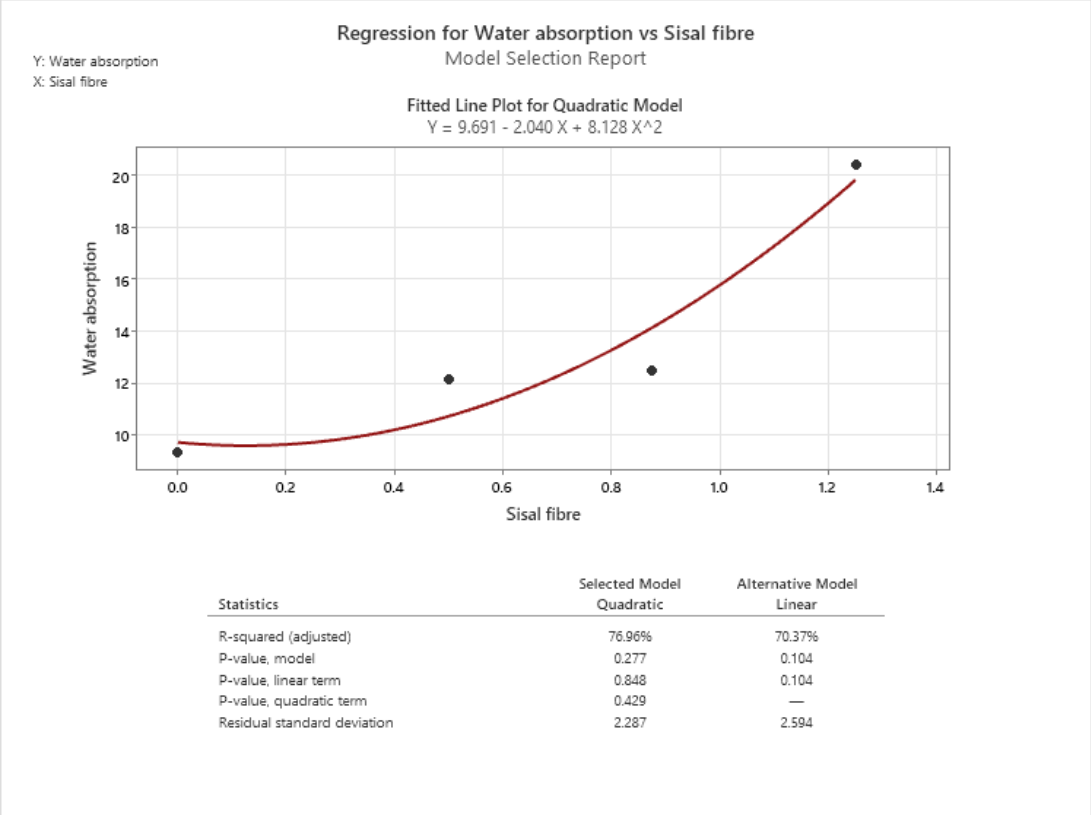

Figure 5.20: Correlation between the sisal fibres and the water absorption capacity

It is worth noting that the model relationships created in this study are empirical and occasionally subject to limitations because of the influence of various factors, including the mineral and chemical properties of the precursor material, mixing effectiveness, the ratio of water to binder, ageing, and curing, among others. However, the correlations help to provide a broad understanding of the interactions between some processes and performance parameters related to the geopolymer under study.

5.5 Comparison Between Lime-Activated and Sodium Hydroxide/Sodium Silicate-Activated Geopolymer

The performance of the alkaline-activated and NaOH/Na_2SiO_3-activated geopolymers is compared in Table 5.8.

Table 5.8: Comparison between the performance of the alkaline activated and the $NaOH/Na_2SiO_3$ activated geopolymers

Performance property	**Optimum attained for Lime-activated specimens**	**Optimum attained for sodium hydroxide/sodium silicate specimens**	**Percentage increase (%)**
Compressive strength (MPa)	2.715	34.10	1156
Bulk density (g/cm^3)	0.72	1.322	84
Water absorption (%)	-could not be measured	13.93	-
Thermal conductivity (W/mK)	0.109	0.323	196

The compressive strength of the geopolymer concrete was enhanced by more than 1000% by replacing the lime activator with a sodium-based alkaline activator and eliminating the HDPE component. This could imply that the strong polymerization reactivity of the sodium-based alkaline activators and diatomaceous earth allowed for the complete dissolution of the silicon and aluminium phases, leading to the creation of the final hardened materials with suitable cohesive properties.

The sodium-based alkaline activator increased the geopolymerization reaction that generated a strong bond between the diatomaceous earth particles, which in turn reduced the geopolymer's porosity and increased bulk density and thermal conductivity.

CHAPTER SIX: CONCLUSION AND RECOMMENDATION

6.1 Conclusions

This research sought to develop and evaluate the performance properties of Diatomaceous earth-based Geopolymer concrete that incorporated sisal fibres and high-density polyethylene (HDPE) wastes. The employed diatomaceous earth was subjected to characterization to ascertain whether it has the properties required to be used as a geopolymer precursor. The alkaline-activated diatomaceous earth-based geopolymer concrete incorporating sisal fibres and HDPE wastes was fabricated. The impact of the incorporation of the sisal fibres and shredded high-density polyethylene wastes on the performance properties of the diatomaceous earth-based geopolymer was evaluated. Correlation and predictive models for the performance properties of the developed geopolymer concrete were generated. Findings gathered during the experimental phases of this study lead to the following conclusions:

1. Diatomaceous earth characterization

- It was determined that the studied diatomaceous earth is an acidic rock falling within the opal CT category, according to the chemical composition, which revealed silica (SiO_2) to be its major component. Therefore, the siliceous nature of Kenyan diatomaceous earth is of a rather high grade, comparable to a silicate glass material or a typical Class F kind of pozzolan.
- The Kenyan diatomaceous earth may have originated as biogenic silica opal-A before dissolving or re-forming as opal-CT as a result of the thermal alteration of the rock caused by the high heat flow rates created in the rift zones by the penetration of dacite sills as a mechanism of the volcano-sedimentary succession.

- The Atterberg limit examination and particle size analysis revealed that diatomaceous earth is a fine, cohesive, and medium silt material.
- Diatomite is a material that is thermally stable and has a melting point greater than 950 °C, according to the TGA experiment. Moreover, significant diatomite loss on ignition (LOI), as determined by TGA, revealed that the material is porous, with low thermal conductivity and high thermal insulation capacity.

2. Diatomaceous earth-based geopolymer fabrication

- The most significant result of this research was the discovery that a diatomaceous earth-based geopolymer may be made by activating the natural pozzolan in a very alkaline environment, such as with sodium silicate and sodium hydroxide alkaline activators. This kind of concrete can aid in reducing energy usage and environmental effects, particularly in nations with greater access to the natural pozzolan (diatomite).

3. Diatomaceous earth-based geopolymer performance evaluation

- Lime, an alkaline activator, and diatomaceous earth, a geopolymer precursor, have poor geopolymerization reactivity; as a result, low compressive strength products are formed.
- Although recycling high-density polyethylene materials is highly beneficial to the environment, this study found that it was inadequate to incorporate HDPE in the diatomaceous earth-based geopolymer. Its chemical inertness hinders the reactivity between the geopolymer precursor material and the alkaline activator.
- Similar to other types of fibre that have been researched, the inclusion of sisal fibres improves the strength properties of concrete up to a certain point before starting to decline.

- When sisal fibre is added to the concrete mixture, the porosity increases but the density decreases.
- The use of diatomaceous earth as a precursor incorporated with 0.86 wt.% of sisal fibres and activated with 50 wt.% Na_2SiO_3 and 20 wt.% 12 M NaOH relative to the initial weight of the raw diatomite particles, geopolymer bricks with a compressive strength of 34.10 MPa, a density of 1.32 g/cm^3, water absorption of 13.93 % and thermal conductivity of 0.323 W/mK can be developed. The mechanical, physical and thermal performance of the developed geopolymer falls within the acceptable limits for concrete masonry units.

4. Performance correlation and predictive models

- There was a strong correlation between certain performance characteristics and the amount of sisal fibre incorporation. Additionally, strong correlations between performance properties were found.
- New correlation models would allow for the prediction of the concrete's performance properties such as compressive strength, bulk density, water absorption and thermal conductivity. Models that would indicate how much sisal fibre to incorporate for specific performance qualities were also created.

In summary, the diatomaceous earth-based geopolymer investigated here can contribute to sustainable development because it is cementless and can use industrial wastes like spent diatomaceous earth and agricultural waste products such as sisal fibres, resulting in a decrease in the amount of carbon dioxide in the air, energy consumption, as well as the cost of construction.

6.2 Recommendations

This study produced valuable findings and information about the diatomaceous earth-based geopolymer coupled with sisal fibres and HDPE. However, more research on sisal fibre reinforcement is needed to increase the durability of diatomaceous earth-based geopolymer composites. The reason for this is that there are uncertainties surrounding the rate of cellulosic fibre-reinforced geopolymer degradation and the amount of time allowed for deterioration after durations longer than 28 days. The findings of the HDPE incorporation in this study also warrant further investigation. Based on the findings of this investigation, the following suggestions are made for further study into the activation and reinforcing of natural diatomaceous earth pozzolan to produce geopolymer concrete for construction purposes:

- Different water-to-binder ratios, alkaline activator concentrations, curing times, and other variables not taken into account in this study should be further investigated to understand how these variables affect the properties of the diatomaceous earth-based geopolymer.
- The lack of geopolymer standards and specifications is now a significant obstacle to the mass marketing and usage of geopolymer products. As a result, standards and specifications for the manufacture of geopolymers and their performance characteristics should be developed.
- More research should be done to determine the viability and cost-effectiveness of using geopolymer concrete in the industry.
- Geopolymer technology has the potential to be used for more than just building concrete, so further research should be done to uncover specific applications of the technology. This would lead to research areas that are explicitly targeted towards specific applications.

- The durability of cellulosic fibre-reinforced diatomaceous earth-based concrete should be further researched, especially regarding acid attacks, shrinkages, and crack propagation. Lack of data on the geopolymer's durability is a serious issue that needs to be solved before it is widely adopted and used in engineering fields.
- Further research is required to develop universal geopolymer performance prediction models for mechanical, physical, and thermal properties based on diatomaceous earth.

REFERENCES

3600, A. S. A. (2009). Australian Standard AS 3600 Concrete structures. In *Concrete Structures* (Vol. 123, Issue January).

Abd Razak, R., Abdullah, M. M. A. B., Hussin, K., Subaer, Yahya, Z., Mohamed, R., & Abdullah, A. (2021). Performance of Sintered Pozzolanic Artificial Aggregates as Coarse Aggregate Replacement in Concrete. *Lecture Notes in Civil Engineering*, *129*(February), 191–210. https://doi.org/10.1007/978-981-33-4918-6_10

Abdullah, M. M. A., Ibrahim, W. M. W., & Tahir, M. F. M. (2015). The properties and durability of fly ash-based geopolymeric masonry bricks. *Eco-Efficient Masonry Bricks and Blocks: Design, Properties and Durability*, *December*, 273–287. https://doi.org/10.1016/B978-1-78242-305-8.00012-7

Abrão, P. C. R. A., Cardoso, F. A., & John, V. M. (2019). Evaluation of Portland pozzolan blended cements containing diatomaceous earth. *Ceramica*, *65*, 75–86. https://doi.org/10.1590/0366-6913201965S12596

ACI Committee 213. (2013). Guide for Structural Lightweight-Aggregate Concrete - (ACI 213R-03). *ACI Manual of Concrete Practice*.

ACI committee 318. (2011). Building Code Requirements for Structural Concrete and Commentary (ACI 318M-11). In *American Concrete Institute, Farmington Hills, MI*.

ACI Committee 363. (2005). High-Strength Concrete (ACI 363R). In *ACI Symposium Publication* (Vol. 228).

Adam, E., & Agib, A. (2001). Compressed Stabilised Earth Block Manufacture in Sudan. *Printed by Graphoprint for the United Nations Educational Scientific and Cultural Organization, France, Pa*, 101. http://unesdoc.unesco.org/images/0012/001282/128236e.pdf

Afrin, H., Huda, N., & Abbasi, R. (2021). An Overview of Eco-Friendly Alternatives as the Replacement of Cement in Concrete. *IOP Conference Series: Materials Science and Engineering*, *1200*(1). https://doi.org/10.1088/1757-899x/1200/1/012003

Aghdam, K. A., Rad, A. F., Shakeri, H., & Sardroud, J. M. (2018). Approaching green buildings using eco-efficient construction materials: a review of the state-of-the-art. *Journal of Construction Engineering and Project Management*, *8*(3), 1–23.

Ahmad, R., Hamid, R., & Osman, S. A. (2019). Physical and chemical modifications of plant fibres for reinforcement in cementitious composites. *Advances in Civil Engineering*, *2019*. https://doi.org/10.1155/2019/5185806

Ahmad, S., Iqbal, Y., & Muhammad, R. (2017). Effects of coal and wheat husk additives on the physical, thermal and mechanical properties of clay bricks. *Boletin de La Sociedad Espanola de Ceramica y Vidrio*, *56*(3), 131–138. https://doi.org/10.1016/j.bsecv.2017.02.001

Ahmadi, Z., Esmaeili, J., Kasaei, J., & Hajialioghli, R. (2018). Properties of sustainable cement mortars containing high volume of raw diatomite. *Sustainable Materials and Technologies*, *16*, 47–53. https://doi.org/10.1016/j.susmat.2018.05.001

Ahmed, H. U., Mohammed, A. S., Mohammed, A. A., & Faraj, R. H. (2021). Systematic multiscale models to predict the compressive strength of fly ash-based geopolymer concrete at various mixture proportions and curing regimes. *PLoS ONE*, *16*(6 June). https://doi.org/10.1371/journal.pone.0253006

Ahmed, M .M., and Raju, S. S. (2015). Use of Waste Plastic in the Production of Light Weight Concrete. *International Journal & Magazine of Engineering, Technology, Management and Research*, *2*(April), 365–369.

Ajmal, M. M., Qazi, A. U., Ahmed, A., Mughal, U. A., Abbas, S., Kazmi, S. M. S., & Munir, M. J. (2023). Structural Performance of Energy Efficient Geopolymer Concrete Confined Masonry: An Approach towards Decarbonization. *Energies*, *16*(8). https://doi.org/10.3390/en16083579

Akhtar, F., Rehman, Y., & Bergström, L. (2010). A study of the sintering of diatomaceous earth to produce porous ceramic monoliths with bimodal porosity and high strength. *Powder Technology*, *201*(3), 253–257. https://doi.org/10.1016/j.powtec.2010.04.004

Akinwumi, I. I., Domo-Spiff, A. H., & Salami, A. (2019). Marine plastic pollution and affordable housing challenge: Shredded waste plastic stabilized soil for producing compressed earth bricks. *Case Studies in Construction Materials*, *11*, e00241. https://doi.org/10.1016/j.cscm.2019.e00241

Al Bakri Abdullah, M. M., Jamaludin, L., Kamarudin, H., Binhussain, M., Ruzaidi Ghazali, C. M., & Ahmad, M. I. (2013). Study on fly ash based geopolymer for coating applications. *Advanced Materials Research*, *686*. https://doi.org/10.4028/www.scientific.net/AMR.686.227

Alani, A. H., Bunnori, N. M., Noaman, A. T., & Majid, T. A. (2019). Durability performance of a novel ultra-high-performance PET green concrete (UHPPGC). *Construction and Building Materials*, *209*. https://doi.org/10.1016/j.conbuildmat.2019.03.088

Al-Bakri Abdullah, M. M., Jamaludin, L., Hussin, K., Bnhussain, M., Ghazali, C. M. R., & Ahmad, M. I. (2012). Fly ash porous material using geopolymerization process for high temperature exposure. *International Journal of Molecular Sciences*, *13*(4). https://doi.org/10.3390/ijms13044388

Ali, N., Din, N., Khalid, F. S., Shahidan, S., Abdullah, S. R., Abdul Samad, A. A., & Mohamad, N. (2017). Compressive strength and initial water absorption rate for cement brick containing high-density polyethylene (HDPE) as a substitutional material for sand. *IOP Conference Series: Materials Science and Engineering*, *271*(1), 0–7. https://doi.org/10.1088/1757-899X/271/1/012083

Almutairi, A. L., Tayeh, B. A., Adesina, A., Isleem, H. F., & Zeyad, A. M. (2021). Potential applications of geopolymer concrete in construction: A review. *Case Studies in Construction Materials*, *15*. https://doi.org/10.1016/j.cscm.2021.e00733

Alomayri, T., & Low, I. M. (2013). Synthesis and characterization of mechanical properties in cotton fiber-reinforced geopolymer composites. *Journal of Asian Ceramic Societies*, *1*(1), 30–34. https://doi.org/10.1016/j.jascer.2013.01.002

Alrefaei, Y., Wang, Y. S., & Dai, J. G. (2019). The effectiveness of different superplasticizers in ambient cured one-part alkali activated pastes. *Cement and Concrete Composites*, *97*. https://doi.org/10.1016/j.cemconcomp.2018.12.027

Altarazi, S. A., & Allaf, R. M. (2017). Designing and analyzing a mixture experiment to optimize the mixing proportions of polyvinyl chloride composites. *Journal of Applied Statistics*, *44*(8). https://doi.org/10.1080/02664763.2016.1214243

Alvarado, C., Alvarado-Quintana, H., & Siche, R. (2023). Ceramic Thermal Insulator Based on Diatomite Obtained by Starch Consolidation Casting. *Materials*, *16*(11). https://doi.org/10.3390/ma16114028

Alzeer, M., & MacKenzie, K. (2013). Synthesis and mechanical properties of novel composites of inorganic polymers (geopolymers) with unidirectional natural flax fibres (phormium tenax). *Applied Clay Science*, *75–76*. https://doi.org/10.1016/j.clay.2013.03.010

American Society for Testing and Materials. (2008). ASTM C191-08 Standard Test Methods for Time of Setting of Hydraulic Cement by Vicat Needle. In *Annual Book of ASTM Standards 191-04: Vol. i*.

American Society for Testing and Materials. (2009). ASTM C305-14 - Standard Practice for Mechanical Mixing of Hydraulic Cement Pastes and Mortars of Plastic Consistency. *ASTM International*, *04*(01).

American Society for Testing and Materials. (2019). ASTM C31-19_Standard Practice for Making and Curing Concrete Test Specimens in the Field. *ASTM International*, *04*.

American Society For Testing And Materials (ASTM). (2002). Astm C78/C78M - 02: *Standard Test Method for Flexural Strength of Concrete (Using Simple Beam with Third-Point Loading) ASTM International*. *USA*, *04.02*.

Amran, Y. H. M., Alyousef, R., Alabduljabbar, H., & El-Zeadani, M. (2020). Clean production and properties of geopolymer concrete; A review. *Journal of Cleaner Production*, *251*, 119679. https://doi.org/10.1016/j.jclepro.2019.119679

Ansell, M. P., & Mwaikambo, L. Y. (2009). The structure of cotton and other plant fibres. In *Handbook of Textile Fibre Structure* (Vol. 2, Issue December 2009). Woodhead Publishing Limited. https://doi.org/10.1533/9781845697310.1.62

Anthony, S. (2009). *Use of diatomaceous earth as a siliceous material in the formation of alkali activated fine-aggregate limestone concrete*. *June*.

Ardanuy, M., Claramunt, J., & Toledo Filho, R. D. (2015). Cellulosic fiber reinforced cement-based composites: A review of recent research. *Construction and Building Materials*, *79*, 115–128. https://doi.org/10.1016/j.conbuildmat.2015.01.035

Asadi, I., Shafigh, P., Abu Hassan, Z. F. Bin, & Mahyuddin, N. B. (2018). Thermal conductivity of concrete – A review. In *Journal of Building Engineering* (Vol. 20). https://doi.org/10.1016/j.jobe.2018.07.002

ASTM. (1999). ASTM C373-14 Standard Test Method for Water Absorption, Bulk Density, Apparent Porosity, and Apparent Specific Gravity of Fired Whiteware Products. *Astm C373-88*, *88*(Reapproved).

ASTM. (2014). Astm C618. *Annual Book of ASTM Standards*, *C*.

ASTM. (2015). Standard Test Method for Water Penetration and Leakage Through Masonry. *Astm*, *90*(Reapproved).

ASTM B822-17. (2017). Standard test method for particle size distribution of metal powders and related compounds by light scattering. *ASTM International, West Conshohocken, PA*.

ASTM C20-00. (2015). Standard Test Methods for Apparent Porosity , Water Absorption , Apparent Specific Gravity , and Bulk Density of Burned Refractory Brick and Shapes by Boiling Water. *American Society for Testing and Materials*, *00*(Reapproved 2015). https://doi.org/10.1520/C0020-00R10.2

ASTM C109/C109M, A. (2007). Compressive Strength of Hydraulic Cement Mortars (Using 2-in . or [50-mm] Cube Specimens) 1. *American Society for Testing and Material*.

ASTM C129. (2017). Standard Specification for NonLoadbearing Concrete Masonry Units. *ASTM International*, *04*(C).

ASTM C136/C136M - 14, 2014. (2014). ASTM C136-14_Método de prueba estándar para la determinación granulométrica de agregados finos y gruesos. *Annual Book of ASTM Standards*.

ASTM C187. (2016). Standard Test Method for Amount of Water Required for Normal Consistency of Hydraulic Cement Paste. *ASTM International*.

ASTM C332-17. (2009). Standard Specification for Lightweight Aggregates for Insulating Concrete. *ASTM International*, *552*(18).

ASTM C597. (2016). Standard Test Method for Pulse Velocity Through Concrete ASTM C 597. *ASTM International*.

ASTM C1113. (1999). Standard Test Method for Thermal Conductivity of Refractories by Hot Wire (Platinum Resistance Thermometer Technique) 1. *Wire*, *15*(July).

ASTM C1365. (2006). Standard Test Method for Determination of the Proportion of Phases in Portland Cement and Portland-Cement Clinker Using X-Ray Powder Diffraction Analysis. *American Society for Testing and Materials*.

ASTM C1634. (2020). Standard specification for concrete facing brick and other concrete masonry facing Units 1. *ASTM International*.

ASTM D 7348-13. (2013). Standard Test Methods for Loss on Ignition (LOI) of Solid Combustion Residues. *ASTM International*, *i*.

ASTM D3039. (2010). ASTM D 3039 - Standard Test Method for Tensile Properties of Polymer Matrix Composite Materials. In *ASTM Book of Standards*.

ASTM D6913 / D6913M-17. (2017). Standard Test Methods for Particle-Size Distribution (Gradation) of Soils Using Sieve Analysis. *ASTM International*.

ASTM E1131. (2015). Standard Test Method for Compositional Analysis by Thermogravimetry. *ASTM International*, *08*(Reapproved 2014).

ASTM International. (2010). ASTM C114-10 - Standard Test Methods for Chemical Analysis of Hydraulic Cement. *Book of Standards Volume: 04.01*.

ASTM International. (2017). ASTM D4318-17. *Standard Test Methods for Liquid Limit, Plastic Limit, and Plasticity Index of Soils*.

ASTM Standard: C773-88. (2007). Standard Test Method for Compressive (Crushing) Strength of Fired Whiteware Materials. *Annual Book of ASTM Standards*, *i*(Reapproved 2006).

ASTM-C642. (2013). ASTM C642-13 Standard Test Method for Density, Absorption, and Voids in Hardened Concrete. *Annual Book of ASTM Standards*, *3*.

ASTM-D854. (2010). Standard Test for Specific Gravity of Soil Solids by Water Pycnometer. In *ASTM International* (Issue March).

Azimi, E. A., Al Bakri Abdullah, M. M., Ming, L. Y., Yong, H. C., Hussin, K., & Aziz, I. H. (2015). Review of geopolymer materials for thermal insulating applications. *Key Engineering Materials*, *660*. https://doi.org/10.4028/www.scientific.net/KEM.660.17

Aziz, I. H., Al Bakri Abdullah, M. M., Yong, H. C., Ming, L. Y., Hussin, K., Surleva, A., & Azimi, E. A. (2019). Manufacturing parameters influencing fire resistance of geopolymers: A review. *Proceedings of the Institution of Mechanical Engineers, Part L: Journal of Materials: Design and Applications*, *233*(4), 721–733. https://doi.org/10.1177/1464420716668203

Bagci, C., Kutyla, G. P., & Kriven, W. M. (2017). Fully reacted high strength geopolymer made with diatomite as a fumed silica alternative. *Ceramics International*, *43*(17). https://doi.org/10.1016/j.ceramint.2017.07.222

Baghabra Al-Amoudi, O. S., Al-Kutti, W. A., Ahmad, S., & Maslehuddin, M. (2009). Correlation between compressive strength and certain durability indices of plain and blended cement concretes. *Cement and Concrete Composites*, *31*(9). https://doi.org/10.1016/j.cemconcomp.2009.05.005

Balczár, I., Korim, T., Kovács, A., & Makó, E. (2016). Mechanochemical and thermal activation of kaolin for manufacturing geopolymer mortars – Comparative study. *Ceramics International*, *42*(14). https://doi.org/10.1016/j.ceramint.2016.06.182

Banerjee, P., Ray, D. P., Satya, P., Debnath, S., Mondal, D., Saha, S. C., & Biswas, P. K. (2015). Evaluation of Ramie Fibre Quality : A Review. *International Journal of Bioresource Science*, *2*(1).

Barnard, R. (2014). Mechanical properties of fly ash/slag based geopolymer concrete with the addition of macro fibres. *Masters. Stellenbosch University*.

Batista dos Santos, G. Z., Passos de Oliveira, D., de Almeida Melo Filho, J., & Marques da Silva, N. (2021). Sustainable geopolymer composite reinforced with sisal fiber: Durability to wetting and drying cycles. *Journal of Building Engineering*, *43*. https://doi.org/10.1016/j.jobe.2021.102568

Bediako, M., & Frimpong, A. O. (2013). Alternative Binders for Increased Sustainable Construction in Ghana—A Guide for Building Professionals. *Materials Sciences and Applications*, *04*(12), 20–28. https://doi.org/10.4236/msa.2013.412a004

Belmokaddem, M., Mahi, A., Senhadji, Y., & Pekmezci, B. Y. (2020). Mechanical and physical properties and morphology of concrete containing plastic waste as aggregate. *Construction and Building Materials*, *257*. https://doi.org/10.1016/j.conbuildmat.2020.119559

Benayache, S., Alleg, S., Mebrek, A., & Suñol, J. J. (2018). Thermal and microstructural properties of paraffin/diatomite composite. *Vacuum*, *157*(July), 136–144. https://doi.org/10.1016/j.vacuum.2018.08.044

Bhutta, A., Farooq, M., & Banthia, N. (2019). Performance characteristics of micro fiber-reinforced geopolymer mortars for repair. *Construction and Building Materials*, *215*. https://doi.org/10.1016/j.conbuildmat.2019.04.210

Bogoevski, S., & Boskovski, B. (2014). Characterization of Diatomaceous Earth From the Slavishko Locality in the Republic of Macedonia. *Geologica Macedonia*, *28*(May), 39–43.

Bondar, D. (2009). *Alkali activated of Iranian natural pozzolans to produce geopolymer cement and concrete*. *June*.

Borges, A. L., Soares, S. M., Freitas, T. O. G., Junior, A. O., Ferreira, E. B., & Ferreira, F. G. S. (2021). Evaluation of the pozzolanic activity of glass powder in three maximum grain sizes. *Materials Research*, *24*(4). https://doi.org/10.1590/1980-5373-MR-2020-0496

Broeren, M. L. M., Dellaert, S. N. C., Cok, B., Patel, M. K., Worrell, E., & Shen, L. (2017). Life cycle assessment of sisal fibre – Exploring how local practices can influence environmental performance. *Journal of Cleaner Production*, *149*. https://doi.org/10.1016/j.jclepro.2017.02.073

Brown Mathematics, L. J. (2014). *General Blending Models For Mixture Experiments: Design And Analysis*.

Bruno, A. W., Gallipoli, D., Perlot, C., & Mendes, J. (2016). Effect of very high compaction pressures on the physical and mechanical properties of earthen materials. *E3S Web of Conferences*, *9*. https://doi.org/10.1051/e3sconf/20160914004

Bs En 196. (2016). Publication Methods of Testing Cement Part 1: Determination of Strength. *Bs En 196*.

Busari, A., Akinmusuru, J., & Dahunsi, B. (2019). Strength and durability properties of concrete using metakaolin as a sustainable material: Review of literatures. In *International Journal of Civil Engineering and Technology* (Vol. 10, Issue 1).

C311/C311M, A. (2013). Standard Test Method for Sampling and Testing Fly Ash or Natural Pozzolans for use in Portland-Cement Concrete. *Annual Book of ASTM Standards*.

Castillo, H., Collado, H., Droguett, T., Vesely, M., Garrido, P., & Palma, S. (2022). State of the art of geopolymers: A review. In *E-Polymers* (Vol. 22, Issue 1). https://doi.org/10.1515/epoly-2022-0015

Chen, F., Miao, Y., Ma, L., Zhan, F., Wang, W., Chen, N., & Xie, Q. (2020). Optimization of pore structure of a clayey diatomite. In *Particulate Science and Technology* (Vol. 38, Issue 5). https://doi.org/10.1080/02726351.2019.1567635

Chihaoui, R., Siad, H., Senhadji, Y., Mouli, M., Nefoussi, A. M., & Lachemi, M. (2022). Efficiency of natural pozzolan and natural perlite in controlling the alkali-silica reaction of cementitious materials. *Case Studies in Construction Materials*, *17*. https://doi.org/10.1016/j.cscm.2022.e01246

Chindaprasirt, P., & Ridtirud, C. (2020). High calcium fly ash geopolymer containing natural rubber latex as additive. *International Journal of GEOMATE*, *18*(69), 124–129. https://doi.org/10.21660/2020.69.9321

Chithra, S., Kumar, S. R. R. S., Chinnaraju, K., & Alfin Ashmita, F. (2016). A comparative study on the compressive strength prediction models for High Performance Concrete containing nano silica and copper slag using regression analysis and Artificial Neural Networks. *Construction and Building Materials*, *114*. https://doi.org/10.1016/j.conbuildmat.2016.03.214

Ciancio, D., Beckett, C. T. S., & Carraro, J. A. H. (2014). Optimum lime content identification for lime-stabilised rammed earth. *Construction and Building Materials*, *53*, 59–65. https://doi.org/10.1016/j.conbuildmat.2013.11.077

Columbu, S. (2018). Petrographic and geochemical investigations on the volcanic rocks used in the Punic-Roman archaeological site of Nora (Sardinia, Italy). *Environmental Earth Sciences*, *77*(16). https://doi.org/10.1007/s12665-018-7744-4

Cong, P., & Cheng, Y. (2021). Advances in geopolymer materials: A comprehensive review. *Journal of Traffic and Transportation Engineering (English Edition)*, *8*(3), 283–314. https://doi.org/10.1016/j.jtte.2021.03.004

Conley, D. J., & Carey, J. C. (2015). Silica cycling over geologic time. *Nature Geoscience*, *8*(6). https://doi.org/10.1038/ngeo2454

Costa, J. A. C., Martinelli, A. E., do Nascimento, R. M., & Mendes, A. M. (2020). Microstructural design and thermal characterization of composite diatomite-vermiculite paraffin-based form-stable PCM for cementitious mortars. *Construction and Building Materials*, *232*. https://doi.org/10.1016/j.conbuildmat.2019.117167

Curtis, N. J., Gascooke, J. R., Johnston, M. R., & Pring, A. (2019). A Review of the Classification of Opal with Reference to Recent New Localities. *Minerals*, *9*(5), 299. https://doi.org/10.3390/min9050299

da Silva Alves, L. C., dos Reis Ferreira, R. A., Bellini Machado, L., & de Castro Motta, L. A. (2019). Optimization of metakaolin-based geopolymer reinforced with sisal fibers using response surface methology. *Industrial Crops and Products*, *139*. https://doi.org/10.1016/j.indcrop.2019.111551

Danso, H. (2016). Influence of Compacting Rate on the Properties of Compressed Earth Blocks. *Advances in Materials Science and Engineering*, *2016*. https://doi.org/10.1155/2016/8780368

Danso, H. (2019). *3 rd International Conference on Bio-Based Building Materials Micro-Analysis on the Internal Structure of Fibre-Soil Composite*. *37*(2), 460–466.

Danso H, & Adu S. (2019). Characterization of Compressed Earth Blocks Stabilized with Clay Pozzolana. *Journal of Civil & Environmental Engineering*, *9*(1), 1–6. https://doi.org/10.4172/2165-784X.1000331

Danso, H., Martinson, D. B., Ali, M., & Williams, J. B. (2015). Physical, mechanical and durability properties of soil building blocks reinforced with natural fibres. *Construction and Building Materials*, *101*, 797–809. https://doi.org/10.1016/j.conbuildmat.2015.10.069

Daryati, D., Widiasanti, I., Septiandini, E., Ramadhan, M. A., Sambowo, K. A., & Purnomo, A. (2019). Soil characteristics analysis based on the unified soil classification system. *Journal of Physics: Conference Series*, *1402*(2). https://doi.org/10.1088/1742-6596/1402/2/022028

Davidovits, J. (2005). Geopolymer, Green Chemistry and Sustainable Development Solutions: Proceedings of the World Congress Geopolymer 2005. *Sustainable Development*.

Davidovits, J. (2020). Geopolymer Chemistry and Applications. 5-th edition. In *J. Davidovits.–Saint-Quentin, France* (Issue April).

Day, K. W., Aldred, J., & Hudson, B. (2013). Concrete mix design, quality control and specification, fourth edition. In *Concrete Mix Design, Quality Control and Specification, Fourth Edition*. https://doi.org/10.1201/b15624

Deboucha, S., & Hashim, R. (2011). A review on bricks and stabilized compressed earth blocks. *Scientific Research and Essays*, *6*(3), 499–506. https://doi.org/10.5897/SRE09.356

Declercq, Y., Delbecque, N., De Grave, J., De Smedt, P., Finke, P., Mouazen, A. M., Nawar, S., Vandenberghe, D., Van Meirvenne, M., & Verdoodt, A. (2019). A comprehensive study of three different portable XRF scanners to assess the soil geochemistry of an extensive sample dataset. *Remote Sensing*, *11*(21). https://doi.org/10.3390/rs11212490

Degirmenci, N., & Yilmaz, A. (2009). Use of diatomite as partial replacement for Portland cement in cement mortars. *Construction and Building Materials*, *23*(1), 284–288. https://doi.org/10.1016/j.conbuildmat.2007.12.008

Dianingrum, A., & Rahmadaniyati, D. (2017). Evaluation of Sustainable Housing Concept on Kampung Sepoloh, An Informal Settlement in Surabaya, Indonesia. *Journal of Architecture & Environment*, *16*(1). https://doi.org/10.12962/j2355262x.v16i1.a3028

Dobrosielska, M., Dobrucka, R., Gloc, M., Brząkalski, D., Szymański, M., Kurzydłowski, K. J., & Przekop, R. E. (2021). A new method of diatomaceous earth fractionation—a bio-raw material source for epoxy-based composites. *Materials*, *14*(7). https://doi.org/10.3390/ma14071663

Dondi, M., Mazzanti, F., Principi, P., Raimondo, M., & Zanarini, G. (2004). Errata for "Thermal Conductivity of Clay Bricks." *Journal of Materials in Civil Engineering*, *16*(3), 287–287. https://doi.org/10.1061/(asce)0899-1561(2004)16:3(287)

Dong, M., Elchalakani, M., & Karrech, A. (2020). Development of high strength one-part geopolymer mortar using sodium metasilicate. *Construction and Building Materials*, *236*. https://doi.org/10.1016/j.conbuildmat.2019.117611

Dove, C. (2014). The development of unfired earth bricks using seaweed biopolymers. *WIT Transactions on the Built Environment*, *142*, 219–230. https://doi.org/10.2495/ARC140201

Duarte, R., Flores-colen, I., & Brito, J. De. (2011). In Situ Testing Techniques for Evaluation of Water Penetration in Rendered Facades - the Portable Moisture Me- ter and Karsten Tube. *International Conferencie on Durabilty of Building Materials and Components, Porto-Portugal, 12-15 April, XII DBMC*, 1–8.

Duarte, R., Flores-Colen, I., de Brito, J., & Hawreen, A. (2020). Variability of in-situ testing in wall coating systems - Karsten tube and moisture meter techniques. *Journal of Building Engineering*, *27*. https://doi.org/10.1016/j.jobe.2019.100998

Duxson, P., Provis, J. L., Lukey, G. C., & van Deventer, J. S. J. (2007). The role of inorganic polymer technology in the development of "green concrete." *Cement and Concrete Research*, *37*(12). https://doi.org/10.1016/j.cemconres.2007.08.018

Ejigu, A. A., Ketemu, D. G., Endalew, S. A., & Assen, W. Y. (2022). Characterization of Natural Precious Opal Using Modern Spectroscopic Techniques in Ethiopia: The Case from Delanta, South Wollo. *Journal of Spectroscopy*, *2022*. https://doi.org/10.1155/2022/3194151

Elahi, M. M. A., Hossain, M. M., Karim, M. R., Zain, M. F. M., & Shearer, C. (2020). A review on alkali-activated binders: Materials composition and fresh properties of concrete. *Construction and Building Materials*, *260*(November). https://doi.org/10.1016/j.conbuildmat.2020.119788

El-Dieb, A. S. (2016). Cementless concrete for sustainable construction. *MOJ Civil Engineering*, *1*(2). https://doi.org/10.15406/mojce.2016.01.00008

Elgarahy, A. M., Maged, A., Eloffy, M. G., Zahran, M., Kharbish, S., Elwakeel, K. Z., & Bhatnagar, A. (2023). Geopolymers as sustainable eco-friendly materials: Classification, synthesis routes, and applications in wastewater treatment. *Separation and Purification Technology*, *324*, 124631. https://doi.org/10.1016/j.seppur.2023.124631

Elmahdoubi, F., Mabroum, S., Hakkou, R., & Ibnoussina, M. (2021). Geopolymer materials based on natural pozzolans from the Moroccan middle atlas. *Minerals*, *11*(12). https://doi.org/10.3390/min11121344

Ergün, A. (2011). Effects of the usage of diatomite and waste marble powder as partial replacement of cement on the mechanical properties of concrete. *Construction and Building Materials*, *25*(2). https://doi.org/10.1016/j.conbuildmat.2010.07.002

Escalera, E., Garcia, G., Terán, R., Tegman, R., Antti, M. L., & Odén, M. (2015). The production of porous brick material from diatomaceous earth and Brazil nut shell ash. *Construction and Building Materials*, *98*, 257–264. https://doi.org/10.1016/j.conbuildmat.2015.08.003

Escobar, N., Espejo, J., & Rodríguez, L. (2014). Evaluation of the effect of diatomaceous earth as a sustainable alternative in commercial interest crops in Colombia. *WIT Transactions on Ecology and the Environment*, *181*. https://doi.org/10.2495/EID140351

Esparham, A. (2022). A review of the features of geopolymer cementitious composites for use in green construction and sustainable urban development. *Central Asian Journal of Environmental Science and Technology Innovation*, *3*(3), 64–74. https://doi.org/10.22034/CAJESTI.2022.03.01

Ev, K., Prsanya, S., & Devi, S. (2018). *Structural Behaviour of Reinforced Geopolymer Concrete Members and Effect of Fibres Inclusion-A Review* (Vol. 5). www.jetir.org

Fahrmeir, L., Kneib, T., Lang, S., & Marx, B. (2013). Regression: Models, methods and applications. In *Regression: Models, Methods and Applications* (Vol. 9783642343339). https://doi.org/10.1007/978-3-642-34333-9

Fan, F. (2015). Mechanical and Thermal Properties of Fly ash-based Geopolymer Cement. *MSc Thesis*, *May*.

Farías, R. D., García, C. M., Palomino, T. C., & Arellano, M. M. (2017). Effects of wastes from the brewing industry in lightweight aggregates manufactured with clay for green roofs. *Materials*, *10*(5). https://doi.org/10.3390/ma10050527

Farooq, F., Ahmed, W., Akbar, A., Aslam, F., & Alyousef, R. (2021). Predictive modeling for sustainable high-performance concrete from industrial wastes: A comparison and optimization of models using ensemble learners. *Journal of Cleaner Production*, *292*. https://doi.org/10.1016/j.jclepro.2021.126032

Favier, A., De Wolf, C., Scrivener, K., & Habert, G. (2018). A sustainable future for the European Cement and Concrete Industry Technology assessment for full decarbonisation of the industry by 2050. *BRISK Binary Robust Invariant Scalable Keypoints*.

Fernández-Jiménez, A. M., Palomo, A., & López-Hombrados, C. (2006). Engineering properties of alkali-activated fly ash concrete. *ACI Materials Journal*, *103*(2). https://doi.org/10.14359/15261

Ferraz, E., Coroado, J., Silva, J., Gomes, C., & Rocha, F. (2011). Manufacture of ceramic bricks using recycled brewing spent kieselguhr. *Materials and Manufacturing Processes*, *26*(10). https://doi.org/10.1080/10426914.2011.551908

Firdous, R., Stephan, D., & Djobo, J. N. Y. (2018). Natural pozzolan based geopolymers: A review on mechanical, microstructural and durability characteristics. In *Construction and Building Materials* (Vol. 190). https://doi.org/10.1016/j.conbuildmat.2018.09.191

Font, A., Soriano, L., Reig, L., Tashima, M. M., Borrachero, M. V., Monzó, J., & Payá, J. (2018). Use of residual diatomaceous earth as a silica source in geopolymer production. *Materials Letters*, *223*. https://doi.org/10.1016/j.matlet.2018.04.010

Fopossi, A. J., Mutuku, R. N., & Ngapgue, F. (2014). Effects of Stabilizers on Compressive Strength of Soil Blocks : a Case Study Using Mangu Soil. *International Journal of Structural and Civil Engineering Research*, *3*(4), 122–130.

Fragoulis, D., Stamatakis, M. G., Chaniotakis, E., & Columbus, G. (2004). Characterization of lightweight aggregates produced with clayey diatomite rocks originating from Greece. *Materials Characterization*, *53*(2–4), 307–316. https://doi.org/10.1016/j.matchar.2004.05.004

Galal Mors, H. E. (2010). Diatomite: Its Characterization, Modifications and Applications. *Asian Journal of Materials Science*, *2*(3), 121–136. https://doi.org/10.3923/ajmskr.2010.121.136

Galán-Arboledas, R. J., Cotes-Palomino, M. T., Bueno, S., & Martínez-García, C. (2017). Evaluation of spent diatomite incorporation in clay based materials for lightweight bricks processing. *Construction and Building Materials*, *144*, 327–337. https://doi.org/10.1016/j.conbuildmat.2017.03.202

Galvan, D., Effting, L., Cremasco, H., & Conte-Junior, C. A. (2021). Recent applications of mixture designs in beverages, foods, and pharmaceutical health: A systematic review and meta-analysis. In *Foods* (Vol. 10, Issue 8). MDPI AG. https://doi.org/10.3390/foods10081941

Ganesan, N., Ramesh Babu, C., & Meyyappan, P. L. (2019). Influence of Alkaline Activator Ratio on Compressive Strength of GGBS Based Geopolymer Concrete. *IOP Conference Series: Materials Science and Engineering*, *561*(1). https://doi.org/10.1088/1757-899X/561/1/012083

Gardete, D., & Luzia, R. (2020). Experimental Study on Soils Stabilized with Two Types of Plastic Waste. *KnE Engineering*, *2020*, 40–50. https://doi.org/10.18502/keg.v5i6.7020

Gencel, O., Del Coz Diaz, J. J., Sutcu, M., Koksal, F., Álvarez Rabanal, F. P., & Martínez-Barrera, G. (2016). A novel lightweight gypsum composite with diatomite and polypropylene fibers. *Construction and Building Materials*, *113*, 732–740. https://doi.org/10.1016/j.conbuildmat.2016.03.125

Gevera, P., & Mouri, H. (2018). Natural occurrence of potentially harmful fluoride contamination in groundwater: an example from Nakuru County, the Kenyan Rift Valley. *Environmental Earth Sciences*, *77*(10). https://doi.org/10.1007/s12665-018-7466-7

Ghafoor, M. T., Fujiyama, C., & Maekawa, K. (2021). Mix design processing for self compacting geopolymer mortar. *Journal of Advanced Concrete Technology*, *19*(11). https://doi.org/10.3151/jact.19.1133

Ghazy, M. F., Elaty, M. A. A., & Mostafa, S. M. (2022). Properties of One-Part Versus Two-Part Geopolymers Composites-A Review. *American Journal of Engineering Research*, *11*(06).

Ghisoli, C., Caucia, F., & Marinoni, L. (2010). XRPD patterns of opals: A brief review and new results from recent studies. *Powder Diffraction*, *25*(3), 274–282. https://doi.org/10.1154/1.3478554

Gong, X., Tian, W., Wang, L., Bai, J., Qiao, K., & Zhao, J. (2019). Biological regeneration of brewery spent diatomite and its reuse in basic dye and chromium (III) ions removal. *Process Safety and Environmental Protection*, *128*. https://doi.org/10.1016/j.psep.2019.05.024

González-Montijo, M. A., Soto-Toro, H., Rivera-Pérez, C., Esteves-Klomsingh, S., & Suárez, O. M. (2019). Design and characterization of concrete masonry parts and structural concrete using repurposed plastics as aggregate. *Journal of the Mechanical Behavior of Materials*, *28*(1). https://doi.org/10.1515/jmbm-2019-0010

Gupta, V., Chai, H. K., Lu, Y., & Chaudhary, S. (2020). A state of the art review to enhance the industrial scale waste utilization in sustainable unfired bricks. *Construction and Building Materials*, *254*, 119220. https://doi.org/10.1016/j.conbuildmat.2020.119220

Ha, J. H., Lee, J., Song, I. H., & Lee, S. H. (2015). The effects of diatomite addition on the pore characteristics of a pyrophyllite support layer. *Ceramics International*, *41*(8), 9542–9548. https://doi.org/10.1016/j.ceramint.2015.04.013

Hadi, M. N. S., Al-Azzawi, M., & Yu, T. (2018). Effects of fly ash characteristics and alkaline activator components on compressive strength of fly ash-based geopolymer mortar. *Construction and Building Materials*, *175*. https://doi.org/10.1016/j.conbuildmat.2018.04.092

Hall, M. R., Najim, K. B., & Keikhaei Dehdezi, P. (2012). Soil stabilisation and earth construction: Materials, properties and techniques. In *Modern Earth Buildings: Materials, Engineering, Constructions and Applications*. https://doi.org/10.1533/9780857096166.2.222

Halvaei, M., Jamshidi, M., & Latifi, M. (2016). Effect of fiber geometry and tenacity on the mechanical properties of fine aggregates concrete. *Journal of Industrial Textiles*, *45*(5). https://doi.org/10.1177/1528083714553687

Han, Y., Cui, X., Lv, X., & Wang, K. (2018). Preparation and characterization of geopolymers based on a phosphoric-acid-activated electrolytic manganese dioxide residue. *Journal of Cleaner Production*, *205*. https://doi.org/10.1016/j.jclepro.2018.09.141

Hanane, B., Jihad, R., Naima, B., Soukaina, T., Nadia, B., & Naima, B. T. (2022). Characterisation and Valorisation of the Moroccan Diatomite. *Journal of Geoscience and Environment Protection*, *10*(02). https://doi.org/10.4236/gep.2022.102008

Hao, L., Gao, W., Yan, S., Niu, M., Liu, G., & Hao, H. (2019). Preparation and characterization of porous ceramics with low-grade diatomite and oyster shell. *Materials Chemistry and Physics*, *235*(March), 121741. https://doi.org/10.1016/j.matchemphys.2019.121741

Hardjito, D., & Rangan, B. V. (2006). Development of Fly Ash-Based Geopolymer Concrete : Progress and Research Needs. *2nd. Asian Concrete Federation Conference*.

Harni, S., Melaka, Z. P., Ali, S., & Melaka, P. (2018). Effect of Fly Ash and HDPE on Concrete Strength. In *Politeknik & Kolej Komuniti Journal of Engineering and Technology* (Vol. 3).

Hasan, M., Saidi, T., & Afifuddin, M. (2021). Mechanical properties and absorption of lightweight concrete using lightweight aggregate from diatomaceous earth. *Construction and Building Materials*, *277*, 122324. https://doi.org/10.1016/j.conbuildmat.2021.122324

Hasan, M., Saidi, T., Muyasir, A., Alkhaly, Y. R., & Muslimsyah, M. (2020). Characteristic of calcined diatomaceous earth from Aceh Besar District - Indonesia as cementitious binder. *IOP Conference Series: Materials Science and Engineering*, *933*(1). https://doi.org/10.1088/1757-899X/933/1/012008

Hasanbeigi, A., Price, L., & Lin, E. (2012). Emerging energy-efficiency and CO 2 emission-reduction technologies for cement and concrete production: A technical review. In *Renewable and Sustainable Energy Reviews* (Vol. 16, Issue 8). https://doi.org/10.1016/j.rser.2012.07.019

Hasanzadeh, B., & Sun, Z. (2019). Impacts of Diatomaceous Earth on the Properties of Cement Pastes. *Journal of Building Materials and Structures*, *5*(2), 197–211. https://doi.org/10.34118/jbms.v5i2.58

Hassan, A., Arif, M., & Shariq, M. (2019). Use of geopolymer concrete for a cleaner and sustainable environment – A review of mechanical properties and microstructure. In *Journal of Cleaner Production* (Vol. 223). https://doi.org/10.1016/j.jclepro.2019.03.051

Hassan, H. J. A., Rasul, J., & Samin, M. (2021). Effects of Plastic Waste Materials on Geotechnical Properties of Clayey Soil. *Transportation Infrastructure Geotechnology*, *8*(3), 390–413. https://doi.org/10.1007/s40515-020-00145-4

Hassan, H. S., Abdel-Gawwad, H. A., Vásquez-García, S. R., Israde-Alcántara, I., Flores-Ramirez, N., Rico, J. L., & Mohammed, M. S. (2019). Cleaner production of one-part white geopolymer cement using pre-treated wood biomass ash and diatomite. *Journal of Cleaner Production*, *209*. https://doi.org/10.1016/j.jclepro.2018.11.137

He, R., Dai, N., & Wang, Z. (2020). Thermal and Mechanical Properties of Geopolymers Exposed to High Temperature: A Literature Review. *Advances in Civil Engineering*, *2020*. https://doi.org/10.1155/2020/7532703

Heah, C. Y., Kamarudin, H., Mustafa Al Bakri, A. M., Binhussain, M., Luqman, M., Khairul Nizar, I., Ruzaidi, C. M., & Liew, Y. M. (2011). Effect of curing profile on kaolin-based geopolymers. *Physics Procedia*, *22*. https://doi.org/10.1016/j.phpro.2011.11.048

Hendrickx, R. (2013). Using the Karsten tube to estimate water transport parameters of porous building materials: The possibilities of analytical and numerical solutions. *Materials and Structures/Materiaux et Constructions*, *46*(8). https://doi.org/10.1617/s11527-012-9975-2

Hermann, E., Kunze, C., Gatzweiler, R., Kießig, G., & Davidovits, J. (1999). Solidification of Various Radioactive Residues By Géopolymère® With Special Emphasis on Long-Term-Stability. *Géopolymère '99 Proceeding*.

Hoc Thang, N. (2020). Novel Porous Refractory Synthesized from Diatomaceous Earth and Rice Husk Ash. *Journal of Polymer & Composites*, *August*. https://doi.org/10.37591/jopc.v8i2.4295

Hoffman, G. K. (2006). Pozzolans and Supplementary Cemetitious Materials. In *Industrial minerals & rocks : commodities, markets, and uses.*

Huang, B., Gao, X., Xu, X., Song, J., Geng, Y., Sarkis, J., Fishman, T., Kua, H., & Nakatani, J. (2020). A Life Cycle Thinking Framework to Mitigate the Environmental Impact of Building Materials. In *One Earth* (Vol. 3, Issue 5). https://doi.org/10.1016/j.oneear.2020.10.010

Huang, G., Ji, Y., Li, J., Hou, Z., & Dong, Z. (2018). Improving strength of calcinated coal gangue geopolymer mortars via increasing calcium content. *Construction and Building Materials*, *166*. https://doi.org/10.1016/j.conbuildmat.2018.02.005

Hung Anh, L. D., & Pásztory, Z. (2021). An overview of factors influencing thermal conductivity of building insulation materials. *Journal of Building Engineering*, *44*. https://doi.org/10.1016/j.jobe.2021.102604

Ibrahim, S. S., & Selim, A. Q. (2012). Heat treatment of natural diatomite. *Physicochemical Problems of Mineral Processing*, *48*(2), 413–424. https://doi.org/10.5277/ppmp120208

Imran, H., Al-Abdaly, N. M., Shamsa, M. H., Shatnawi, A., Ibrahim, M., & Ostrowski, K. A. (2022). Development of Prediction Model to Predict the CompressiveStrength of Eco-Friendly Concrete Using MultivariatePolynomial Regression Combined with Stepwise Method. *Materials*, *15*(1). https://doi.org/10.3390/ma15010317

Ince, C., Derogar, S., Ball, R. J., Ekinci, A., & Yuzer, N. (2019). Long-term mechanical properties of cellulose fibre-reinforced cement mortar with diatomite. *Advances in Cement Research*, *31*(8). https://doi.org/10.1680/jadcr.17.00179

Indra, A., Edison, E., & Nofrianto, H. (2018). Optimization of compaction pressure on brick. *MATEC Web of Conferences*, *215*. https://doi.org/10.1051/matecconf/201821501025

Irfan Khan, M., Azizli, K., Sufian, S., Khan, A. S., Ullah, H., & Man, Z. (2014). *Geopolymers as a Sustainable Binder of 21st Century: A Review*. https://doi.org/10.3390/wsf-4-d010

IS 1725: 2013. (2013). Soil based blocks used in general building construction - specification. *Bureau of Indian Standard (BIS)*.

Ishii, E., Sanada, H., Iwatsuki, T., Sugita, Y., & Kurikami, H. (2011). Mechanical strength of the transition zone at the boundary between opal-A and opal-CT zones in siliceous rocks. *Engineering Geology*, *122*(3–4). https://doi.org/10.1016/j.enggeo.2011.05.007

Islam, M. S., Elahi, T. E., Shahriar, A. R., & Mumtaz, N. (2020). Effectiveness of fly ash and cement for compressed stabilized earth block construction. *Construction and Building Materials*, *255*, 119392. https://doi.org/10.1016/j.conbuildmat.2020.119392

Ivanov, S. É., & Belyakov, A. V. (2008). Diatomite and its applications. *Glass and Ceramics (English Translation of Steklo i Keramika)*, *65*(1–2), 48–51. https://doi.org/10.1007/s10717-008-9005-6

Jambhulkar, H. P., Shaikh, S. M. S., & Kumar, M. S. (2018). Fly ash toxicity, emerging issues and possible implications for its exploitation in agriculture; Indian scenario: A review. In *Chemosphere* (Vol. 213). https://doi.org/10.1016/j.chemosphere.2018.09.045

Jamshaid, H., Mishra, R. K., Raza, A., Hussain, U., Rahman, M. L., Nazari, S., Chandan, V., Muller, M., & Choteborsky, R. (2022). Natural Cellulosic Fiber Reinforced Concrete: Influence of Fiber Type and Loading Percentage on Mechanical and Water Absorption Performance. *Materials*, *15*(3). https://doi.org/10.3390/ma15030874

Janfeshan Araghi, H., Nikbin, I. M., Rahimi Reskati, S., Rahmani, E., & Allahyari, H. (2015). An experimental investigation on the erosion resistance of concrete containing various PET particles percentages against sulfuric acid attack. *Construction and Building Materials*, *77*. https://doi.org/10.1016/j.conbuildmat.2014.12.037

Jaskula, B. W. (2020). *U.S. Geological Survey, 2020, Mineral commodity summaries 2020*. USGS.

Jassim, A. K. (2017). Recycling of Polyethylene Waste to Produce Plastic Cement. *Procedia Manufacturing*, *8*(October 2016), 635–642. https://doi.org/10.1016/j.promfg.2017.02.081

Jeong, Y., Oh, J. E., Jun, Y., Park, J., Ha, J. H., & Sohn, S. G. (2016). Influence of four additional activators on hydrated-lime [Ca(OH)2] activated ground granulated blast-furnace slag. *Cement and Concrete Composites*, *65*. https://doi.org/10.1016/j.cemconcomp.2015.10.007

Jia, Y., & Wang, B. (2017). Mineralogy and thermal analysis of natural pozzolana opal shale with nano-pores. *Journal Wuhan University of Technology, Materials Science Edition*, *32*(3). https://doi.org/10.1007/s11595-017-1629-3

Joshua, O., Matawal, D. S., Akinwumi, T. D., Olusola, K. O., Ogunro, A. S., & Lawal, R. B. (2018). Development of a fully pozzolanic binder for sustainable construction: Whole cement replacement in concrete applications. *International Journal of Civil Engineering and Technology*, *9*(2), 1–2.

Journal, I., & Sambhaji, P. P. (2016). Use of Waste Plastic in Concrete Mixture as Aggregate Replacement. *International Journal of Advanced Engineering Research and Science*, *3*(12), 115–118. https://doi.org/10.22161/ijaers/3.12.23

Jules, F. A., Raphael, N. M., & Francois, N. (2018). *Effects of stabilizers on the physical and mechanical properties of clays blocks: A case study using Mangu soil (Kenya)*. 1–158.

Kang, S. H., Kwon, Y. H., Hong, S. G., Chun, S., & Moon, J. (2019). Hydrated lime activation on byproducts for eco-friendly production of structural mortars. *Journal of Cleaner Production*, *231*. https://doi.org/10.1016/j.jclepro.2019.05.313

Ke, X., Bernal, S. A., Ye, N., Provis, J. L., & Yang, J. (2015). One-part geopolymers based on thermally treated red Mud/NaOH blends. *Journal of the American Ceramic Society*, *98*(1). https://doi.org/10.1111/jace.13231

Kett, I. (1999). Engineered concrete mix design and test methods. In *Engineered Concrete Mix Design and Test Methods*. https://doi.org/10.1201/9781420049831

Khashab, R. H. (2018). *Optimal Design of Experiments with Mixtures*.

Kipsanai, J. J., Wambua, P. M., Namango, S. S., & Amziane, S. (2022). *A Review on the Incorporation of Diatomaceous Earth as a Geopolymer-Based Concrete Building Resource*.

Klopp, J. M., & Petretta, D. L. (2017). The urban sustainable development goal: Indicators, complexity and the politics of measuring cities. *Cities*, *63*. https://doi.org/10.1016/j.cities.2016.12.019

Korkmaz, A. V. (2022). Mechanical activation of diabase and its effect on the properties and microstructure of Portland cement. *Case Studies in Construction Materials*, *16*. https://doi.org/10.1016/j.cscm.2021.e00868

Korniejenko, K., Frączek, E., Pytlak, E., & Adamski, M. (2016). Mechanical Properties of Geopolymer Composites Reinforced with Natural Fibers. *Procedia Engineering*, *151*. https://doi.org/10.1016/j.proeng.2016.07.395

Koteng, D. O. (2013). Concrete use for sustainable development Concrete use for sustainable development. *The 20th Engineers' International Institution of Engineers Conference*, 1–19.

Kumari, N., & Mohan, C. (2021). Basics of Clay Minerals and Their Characteristic Properties. In *Clay and Clay Minerals*. https://doi.org/10.5772/intechopen.97672

Kurda, R., Silvestre, J. D., & de Brito, J. (2018). Toxicity and environmental and economic performance of fly ash and recycled concrete aggregates use in concrete: A review. In *Heliyon* (Vol. 4, Issue 4). https://doi.org/10.1016/j.heliyon.2018.e00611

Kurpińska, M., Pawelska-mazur, M., Gu, Y., & Kurpiński, F. (2022). The impact of natural fibers ' characteristics on mechanical properties of the cement composites. *Scientific Reports*, 1–14. https://doi.org/10.1038/s41598-022-25085-6

Lamberti, F., Mazzariol, C., Spolaore, F., Ceccato, R., Salmaso, L., & Gross, S. (2022). Design of Experiment: A Rational and Still Unexplored Approach to Inorganic Materials' Synthesis. *Sustainable Chemistry*, *3*(1), 114–130. https://doi.org/10.3390/suschem3010009

Lavanya, B., Kuriya, P. D., Suganesh, S., Indrajith, R., & Chokkalingam, R. B. (2020). Properties of geopolymer bricks made with flyash and GGBS. *IOP Conference Series: Materials Science and Engineering*, *872*(1). https://doi.org/10.1088/1757-899X/872/1/012141

Lazorenko, G., Kasprzhitskii, A., Kruglikov, A., Mischinenko, V., & Yavna, V. (2020). Sustainable geopolymer composites reinforced with flax tows. *Ceramics International*, *46*(8). https://doi.org/10.1016/j.ceramint.2020.01.184

Lee, J. (2014). *Evaluation of Diatomaceous Earth Content in Natural Soils*. https://minds.wisconsin.edu/handle/1793/69737

Li, J., Zhang, W., Li, C., & Monteiro, P. J. M. (2019). Green concrete containing diatomaceous earth and limestone: Workability, mechanical properties, and life-cycle assessment. *Journal of Cleaner Production*, *223*, 662–679. https://doi.org/10.1016/j.jclepro.2019.03.077

Li, N., Guo, Q., Wang, Q., & Liao, L. (2022). Water characterization and structural attribution of different colored opals. *RSC Advances*, *12*(47), 30416–30425. https://doi.org/10.1039/d2ra04197a

Li, W., Shumuye, E. D., Shiying, T., Wang, Z., & Zerfu, K. (2022). Eco-friendly fibre reinforced geopolymer concrete: A critical review on the microstructure and long-term durability properties. *Case Studies in Construction Materials*, *16*. https://doi.org/10.1016/j.cscm.2022.e00894

Limami, H., Manssouri, I., Cherkaoui, K., & Khaldoun, A. (2020). Study of the suitability of unfired clay bricks with polymeric HDPE & PET wastes additives as a construction material. *Journal of Building Engineering*, *27*. https://doi.org/10.1016/j.jobe.2019.100956

Lingyu, T., Dongpo, H., Jianing, Z., & Hongguang, W. (2021). Durability of geopolymers and geopolymer concretes: A review. In *Reviews on Advanced Materials Science* (Vol. 60, Issue 1). https://doi.org/10.1515/rams-2021-0002

Liu, S., Wang, R., Yu, J., Peng, X., Cai, Y., & Tu, B. (2020). Effectiveness of the anti-erosion of an MICP coating on the surfaces of ancient clay roof tiles. *Construction and Building Materials*, *243*. https://doi.org/10.1016/j.conbuildmat.2020.118202

Lloyd, N., & Rangan, V. (2009). Geopolymer concrete - Sustainable cementless concrete. *American Concrete Institute, ACI Special Publication*, *261 SP*. https://doi.org/10.14359/51663200

Loganina, V. I., Simonov, E. E., Jezierski, W., & Małaszkiewicz, D. (2014). Application of activated diatomite for dry lime mixes. *Construction and Building Materials*, *65*(19), 29–37. https://doi.org/10.1016/j.conbuildmat.2014.04.098

Luan, X., Li, J., Liu, L., & Yang, Z. (2019). Preparation and characteristics of porous magnesium phosphate cement modified by diatomite. *Materials Chemistry and Physics*, *235*(April), 121742. https://doi.org/10.1016/j.matchemphys.2019.121742

Lutyński, M., Sakiewicz, P., & Lutyńska, S. (2019). Characterization of diatomaceous earth and halloysite resources of Poland. *Minerals*, *9*(11). https://doi.org/10.3390/min9110670

Luukkonen, T., Abdollahnejad, Z., Yliniemi, J., Kinnunen, P., & Illikainen, M. (2018). One-part alkali-activated materials: A review. In *Cement and Concrete Research* (Vol. 103). https://doi.org/10.1016/j.cemconres.2017.10.001

Ma, C. K., Awang, A. Z., & Omar, W. (2018). Structural and material performance of geopolymer concrete: A review. *Construction and Building Materials*, *186*, 90–102. https://doi.org/10.1016/j.conbuildmat.2018.07.111

MacEdo, A. R. S., Silva, A. S., Da Luz, D. S., Ferreira, R. L. S., Lourenço, C. S., & Gomes, U. U. (2020). Study of the effect of diatomite on physico-mechanical properties of concrete. *Ceramica*, *66*(377), 50–55. https://doi.org/10.1590/0366-69132020663772561

Mackenzie, K. J. D., & Welter, M. (2014). Geopolymer (aluminosilicate) composites: Synthesis, properties and applications. *Advances in Ceramic Matrix Composites*, *February*, 445–470. https://doi.org/10.1533/9780857098825.3.445

Mahesh, M., Venkat, B., Rao, N., & Satya Sri, C. H. (2016). Re-Use of Polyethylene Plastic Waste In Concrete. *2016 Ijedr |*, *4*(July), 2321–9939. www.ijedr.org

Mahmood, A., Noman, M. T., Pechočiaková, M., Amor, N., Petrů, M., Abdelkader, M., Militký, J., Sozcu, S., & Ul Hassan, S. Z. (2021). Geopolymers and fiber-reinforced concrete composites in civil engineering. In *Polymers* (Vol. 13, Issue 13). https://doi.org/10.3390/polym13132099

Mahmood, R. A., & Kockal, N. U. (2020). Cementitious materials incorporating waste plastics: a review. *SN Applied Sciences*, *2*(12), 1–13. https://doi.org/10.1007/s42452-020-03905-6

Majhi, R. K., & Nayak, A. N. (2020). Production of sustainable concrete utilising high-volume blast furnace slag and recycled aggregate with lime activator. *Journal of Cleaner Production*, *255*. https://doi.org/10.1016/j.jclepro.2020.120188

Makusa, G. P. (2012). Soil Stabilization Methods and Materials in Engineering Practice. *Journal*, *1*, 1–35.

Man, J., Gao, W., Yan, S., Liu, G., & Hao, H. (2017). Preparation of porous brick from diatomite and sugar filter mud at lower temperature. *Construction and Building Materials*, *156*, 1035–1042. https://doi.org/10.1016/j.conbuildmat.2017.09.021

Mandal, A. K. (2021). Synthesis of a two-part geopolymer from red mud and silica fume. *Journal of Metals, Materials and Minerals*, *31*(2). https://doi.org/10.14456/jmmm.2021.14

Mansour, M. Ben, Jelidi, A., Cherif, A. S., & Jabrallah, S. Ben. (2016). Optimizing thermal and mechanical performance of compressed earth blocks (CEB). *Construction and Building Materials*, *104*, 44–51. https://doi.org/10.1016/j.conbuildmat.2015.12.024

Manzano, H., Enyashin, A. N., Dolado, J. S., Ayuela, A., Frenzel, J., & Seifert, G. (2012). Do cement nanotubes exist? *Advanced Materials*, *24*(24). https://doi.org/10.1002/adma.201103704

Maraveas, C. (2020). Production of sustainable construction materials using agro-wastes. *Materials*, *13*(2). https://doi.org/10.3390/ma13020262

Martínez-García, C., Andreola, F., Lancellotti, I., Farías, R. D., Cotes-Palomino, M. T., & Barbieri, L. (2021). Cleaner design and production of lightweight aggregates (LWAs) to use in agronomic application. *Applied Sciences (Switzerland)*, *11*(2), 1–18. https://doi.org/10.3390/app11020800

Matalkah, F., Xu, L., Wu, W., & Soroushian, P. (2017). Mechanochemical synthesis of one-part alkali aluminosilicate hydraulic cement. *Materials and Structures/Materiaux et Constructions*, *50*(1). https://doi.org/10.1617/s11527-016-0968-4

Mateo, S., Cuevas, M., La Rubia, M. D., & Eliche-Quesada, D. (2017). Preliminary study of the use of spent diatomaceous earth from the brewing industry in clay matrix bricks. *Advances in Applied Ceramics*, *116*(2), 77–84. https://doi.org/10.1080/17436753.2016.1221019

Matsunaga, C., Fukushima, M., Hyuga, H., & Yoshizawa, Y. ichi. (2017). Fabrication of porous silica ceramics by gelation-freezing of diatomite slurry. *Journal of the European Ceramic Society*, *37*(16). https://doi.org/10.1016/j.jeurceramsoc.2017.05.001

Mehmedi Vehbi GÖKÇE. (2012). Use of diatomite in the production of lightweight building elements with cement as binder. *Scientific Research and Essays*, *7*(7), 774–781. https://doi.org/10.5897/sre11.236

Mejia, E. E. (2015). Characterization and Preparation of Lightweight Silica Based Ceramics for Building Applications. In *Doctoral Thesis*.

Mesbah, A., Morel, J. C., Walker, P., & Ghavami, Kh. (2004). Development of a Direct Tensile Test for Compacted Earth Blocks Reinforced with Natural Fibers. *Journal of Materials in Civil Engineering*, *16*(1), 95–98. https://doi.org/10.1061/(asce)0899-1561(2004)16:1(95)

Milad, A., Ali, A. S. B., Babalghaith, A. M., Memon, Z. A., Mashaan, N. S., Arafa, S., & Nur, N. I. (2021). Utilisation of waste-based geopolymer in asphalt pavement modification and construction; a review. In *Sustainability (Switzerland)* (Vol. 13, Issue 6). https://doi.org/10.3390/su13063330

Miller, S. A., Sakulich, A. R., Barsoum, M. W., & Jud Sierra, E. (2010). Diatomaceous earth as a pozzolan in the fabrication of an alkali-activated fine-aggregate limestone concrete. *Journal of the American Ceramic Society*, *93*(9), 2828–2836. https://doi.org/10.1111/j.1551-2916.2010.03788.x

Mohajerani, A., Suter, D., Jeffrey-Bailey, T., Song, T., Arulrajah, A., Horpibulsuk, S., & Law, D. (2019). Recycling waste materials in geopolymer concrete. In *Clean Technologies and Environmental Policy* (Vol. 21, Issue 3). https://doi.org/10.1007/s10098-018-01660-2

Mohammed, A. A., Ahmed, H. U., & Mosavi, A. (2021). Survey of mechanical properties of geopolymer concrete: A comprehensive review and data analysis. In *Materials* (Vol. 14, Issue 16). https://doi.org/10.3390/ma14164690

Mohammed, M. K., Al-Hadithi, A. I., & Mohammed, M. H. (2019). Production and optimization of eco-efficient self compacting concrete SCC with limestone and PET. *Construction and Building Materials*, *197*. https://doi.org/10.1016/j.conbuildmat.2018.11.189

Mohanty, A. K., Misra, M., & Drzal, L. T. (2005). Natural fibers, biopolymers, and biocomposites. In *Natural Fibers, Biopolymers, and Biocomposites*. https://doi.org/10.1201/9780203508206.ch1

Mohd Shukry, N. A., Hassan, N. A., Abdullah, M. E., Hainin, M. R., Md Yusoff, N. I., Jaya, R. P., & Mohamed, A. (2018). Effect of various filler types on the properties of porous asphalt mixture. *IOP Conference Series: Materials Science and Engineering*, *342*(1). https://doi.org/10.1088/1757-899X/342/1/012036

Mondal, M. K., Bose, B. P., & Bansal, P. (2019). Recycling waste thermoplastic for energy efficient construction materials: An experimental investigation. *Journal of Environmental Management*, *240*(March), 119–125. https://doi.org/10.1016/j.jenvman.2019.03.016

Mooi, E., & Sarstedt, M. (2011). A Concise Guide to Market Research. In *A Concise Guide to Market Research*. https://doi.org/10.1007/978-3-642-12541-6

Mostafa, M., & Uddin, N. (2016). Experimental analysis of Compressed Earth Block (CEB) with banana fibers resisting flexural and compression forces. *Case Studies in Construction Materials*, *5*, 53–63. https://doi.org/10.1016/j.cscm.2016.07.001

Mucsi, G., & Ambrus, M. (2018). *Raw Materials for Geopolymerisation*. https://doi.org/10.26649/musci.2017.008

Muliauwan, H. N., Prayogo, D., Gaby, G., & Harsono, K. (2020). Prediction of Concrete Compressive Strength Using Artificial Intelligence Methods. *Journal of Physics: Conference Series*, *1625*(1). https://doi.org/10.1088/1742-6596/1625/1/012018

Mumbi, A. W., & Watanabe, T. (2022). Cost Estimations of Water Pollution for the Adoption of Suitable Water Treatment Technology. *Sustainability (Switzerland)*, *14*(2). https://doi.org/10.3390/su14020649

Muñoz, E., & García-Manrique, J. A. (2015). Water absorption behaviour and its effect on the mechanical properties of flax fibre reinforced bioepoxy composites. *International Journal of Polymer Science*, *2015*. https://doi.org/10.1155/2015/390275

Muntohar, A. S., Widianti, A., Hartono, E., & Diana, W. (2013). Engineering Properties of Silty Soil Stabilized with Lime and Rice Husk Ash and Reinforced with Waste Plastic Fiber. *Journal of Materials in Civil Engineering*, *25*(9), 1260–1270. https://doi.org/10.1061/(asce)mt.1943-5533.0000659

Mustoe, G. E. (2005). Diatomaceous origin of siliceous shale in Eocene lake beds of central British Columbia. *Canadian Journal of Earth Sciences*, *42*(2), 231–241. https://doi.org/10.1139/e04-099

Nahar, K. (2018). *Strength Characteristics of Compressed Stabilized Earth Block Made With Selected Regional Soil*.

Nakashima, Y., Fukushima, M., & Hyuga, H. (2021). Preparation of porous diatomite ceramics by an alkali treatment near room temperature. *Journal of the European Ceramic Society*, *41*(1). https://doi.org/10.1016/j.jeurceramsoc.2020.08.056

Namango, S. S. (2006). Development of Cost-Effective Earthen Building Material for Housing Wall Construction: Investigations into the Properties of Compressed Earth Blocks Stabilized with Sisal Vegetable Fibres, Cassava Powder and Cement Compositions. *These*, *6*, 189.

Namango, S. S., Madara, D. S., Makokha, A. B., & Ataro, E. (2015). Model for Testing Compressive and Flexural Strength of Sisal Fibre Reinforced Compressed Earth Blocks in the Absence of Laboratory Facilities. *International Journal for Innovation Education and Research*, *3*(3), 132–145. https://doi.org/10.31686/ijier.vol3.iss3.333

Naqi, A., & Jang, J. G. (2019). Recent progress in green cement technology utilizing low-carbon emission fuels and raw materials: A review. In *Sustainability (Switzerland)* (Vol. 11, Issue 2). https://doi.org/10.3390/su11020537

Nath, S. K., & Kumar, S. (2019). Role of alkali concentration on reaction kinetics of fly ash geopolymerization. *Journal of Non-Crystalline Solids*, *505*. https://doi.org/10.1016/j.jnoncrysol.2018.11.007

Nawaz, M., Heitor, A., & Sivakumar, M. (2020). Geopolymers in construction - recent developments. In *Construction and Building Materials* (Vol. 260). https://doi.org/10.1016/j.conbuildmat.2020.120472

Nematollahi, B., Sanjayan, J., Qiu, J., & Yang, E. H. (2017). High ductile behavior of a polyethylene fiber-reinforced one-part geopolymer composite: A micromechanics-based investigation. *Archives of Civil and Mechanical Engineering*, *17*(3). https://doi.org/10.1016/j.acme.2016.12.005

Ngui Joan Monthe, B. (2021). *Leverage and Firm Value of Cement Manufacturing Firms in Kenya*. 1–40.

Nithurshan, M., & Elakneswaran, Y. (2023). A systematic review and assessment of concrete strength prediction models. *Case Studies in Construction Materials*, *18*. https://doi.org/10.1016/j.cscm.2023.e01830

Nodehi, M., & Taghvaee, V. M. (2022). Alkali-Activated Materials and Geopolymer: a Review of Common Precursors and Activators Addressing Circular Economy. *Circular Economy and Sustainability*, *2*(1). https://doi.org/10.1007/s43615-021-00029-w

Nurruddin, et al. (2018). Methods of curing geopolymer concrete: A review. *International Journal of Advanced and Applied Sciences*, *5*(1), 31–36. https://doi.org/10.21833/ijaas.2018.01.005

Nyale, S. M., Eze, C. P., Akinyeye, R. O., Gitari, W. M., Akinyemi, S. A., Fatoba, O. O., & Petrik, L. F. (2014). The leaching behaviour and geochemical fractionation of trace elements in hydraulically disposed weathered coal fly ash. *Journal of Environmental Science and Health - Part A Toxic/Hazardous Substances and Environmental Engineering*, *49*(2). https://doi.org/10.1080/10934529.2013.838929

Ojha, A., & Aggarwal, P. (2022). Fly Ash Based Geopolymer Concrete: a Comprehensive Review. In *Silicon* (Vol. 14, Issue 6). https://doi.org/10.1007/s12633-021-01044-0

Okeyinka, O. M., Oloke, D. A., Adebisi, W. A., & Ayininuola, G. M. (2019). Investigation into the applicability of brewery sludge residue-ash as a base material for geopolymer concrete. *Construction and Building Materials*, *223*. https://doi.org/10.1016/j.conbuildmat.2019.06.214

Olga, B., & Antonios, R. (2019). Housing Construction as a Leading Economic Indicator. *Studies in Business and Economics*, *14*(3). https://doi.org/10.2478/sbe-2019-0041

Olofinnade, O. M., Ede, A. N., & Booth, C. A. (2019). Sustainability of Waste Glass Powder and Clay Brick Powder as Cement Substitute in Green Concrete. In *Handbook of Environmental Materials Management*. https://doi.org/10.1007/978-3-319-73645-7_112

Osborne, D. (2013). The Coal Handbook: Towards Cleaner Production. In *The Coal Handbook: Towards Cleaner Production* (Vol. 2). https://doi.org/10.1533/9781782421177

Oti, J. E., Kinuthia, J. M., & Bai, J. (2009). Engineering properties of unfired clay masonry bricks. *Engineering Geology*, *107*(3–4), 130–139. https://doi.org/10.1016/j.enggeo.2009.05.002

Panwar, R. S., Sonthwal, V. K., & Kaswan, S. (2018). Enhancing the engineering properties of soil by using sisal fibre and fly ash. *International Journal of Technical Innovation in Modern Engineering & Science*, *4*(7).

PAVÍA, S., & WALKER, R. (2010). Behaviour and Properties of Lime-Pozzolan Pastes. *8th International Masonry Conference Dresden*.

Pavlíková, M., Rovnaníková, P., Záleská, M., & Pavlík, Z. (2022). Diatomaceous Earth—Lightweight Pozzolanic Admixtures for Repair Mortars—Complex Chemical and Physical Assessment. *Materials*, *15*(19). https://doi.org/10.3390/ma15196881

Payá, J., Agrela, F., Rosales, J., Morales, M. M., & Borrachero, M. V. (2018). Application of alkali-activated industrial waste. In *New Trends in Eco-efficient and Recycled Concrete*. https://doi.org/10.1016/B978-0-08-102480-5.00013-0

Pereira, E. L., de Oliveira Junior, A. L., & Fineza, A. G. (2017). Optimization of mechanical properties in concrete reinforced with fibers from solid urban wastes (PET bottles) for the production of ecological concrete. *Construction and Building Materials*, *149*. https://doi.org/10.1016/j.conbuildmat.2017.05.148

Phoo-Ngernkham, T., Chindaprasirt, P., Sata, V., & Sinsiri, T. (2013). High calcium fly ash geopolymer containing diatomite as additive. *Indian Journal of Engineering and Materials Sciences*, *20*(4).

Pimraksa, K., & Chindaprasirt, P. (2009). Lightweight bricks made of diatomaceous earth, lime and gypsum. *Ceramics International*, *35*(1), 471–478. https://doi.org/10.1016/j.ceramint.2008.01.013

Pokorný, J., Pavlíková, M., Medveď, I., Pavlík, Z., Zahálková, J., Rovnaníková, P., & Cerný, R. (2016). Influence of various amount of diatomaceous earth used as cement substitute on mechanical properties of cement paste. *AIP Conference Proceedings*, *1738*(June 2016). https://doi.org/10.1063/1.4952067

Poonyakan, A., Rachakornkij, M., Wecharatana, M., & Smittakorn, W. (2018). Potential use of plastic wastes for low thermal conductivity concrete. *Materials*, *11*(10). https://doi.org/10.3390/ma11101938

Posi, P., Lertnimoolchai, S., Sata, V., & Chindaprasirt, P. (2013). Pressed lightweight concrete containing calcined diatomite aggregate. *Construction and Building Materials*, *47*, 896–901. https://doi.org/10.1016/j.conbuildmat.2013.05.094

Prachasaree, W., Limkatanyu, S., Hawa, A., Sukontasukkul, P., & Chindaprasirt, P. (2020). Manuscript title: Development of strength prediction models for fly ash based geopolymer concrete. *Journal of Building Engineering*, *32*. https://doi.org/10.1016/j.jobe.2020.101704

Pradena, M., & César, A. (2022). Different Approaches to Develop More Sustainable Concrete Alternatives. In *Sustainability of Concrete With Synthetic and Recycled Aggregates*. https://doi.org/10.5772/intechopen.100194

Pramanik, P. K. D., Mukherjee, B., Pal, S., Pal, T., & Singh, S. P. (2021). Green smart building: Requisites, architecture, challenges, and use cases. In *Research Anthology on Environmental and Societal Well-Being Considerations in Buildings and Architecture* (Issue January). https://doi.org/10.4018/978-1-7998-9032-4.ch002

Prof. Krishna Reddy, U. (2016). Engineering Properties of Soils Based on Laboratory Testing. *Test*, *3*.

Provis, J. L. (2014). Geopolymers and other alkali activated materials: Why, how, and what? *Materials and Structures/Materiaux et Constructions*, *47*(1–2). https://doi.org/10.1617/s11527-013-0211-5

Qaidi, S., Najm, H. M., Abed, S. M., Ahmed, H. U., Al Dughaishi, H., Al Lawati, J., Sabri, M. M., Alkhatib, F., & Milad, A. (2022). Fly Ash-Based Geopolymer Composites: A Review of the Compressive Strength and Microstructure Analysis. *Materials*, *15*(20). https://doi.org/10.3390/ma15207098

Ramsden, K. (2020). Cement and Concrete: The Environmental Impact. In *Princeton Student Climate Initiative*.

Rangan, B., & Hardjito, D. (2005). Studies on fly ash-based geopolymer concrete. *Proc. 4th World …*, *November*.

Reka, A. A., Pavlovski, B., Boev, B., Boev, I., & Makreski, P. (2000). *Chemical, Mineralogical and Structural Characterization of Diatomite From Republic of Macedonia*. 3–5.

Reka, A. A., Pavlovski, B., Fazlija, E., Berisha, A., & Pacarizi, M. (2021). *Diatomaceous Earth : Characterization, thermal modi fi cation, and application*. 451–461.

Reka, A. A., Pavlovski, B., & Makreski, P. (2017). New optimized method for low-temperature hydrothermal production of porous ceramics using diatomaceous earth. *Ceramics International*, *43*(15), 12572–12578. https://doi.org/10.1016/j.ceramint.2017.06.132

Ren, X., Wang, Q., Chen, X., Zhang, Y., Sun, Y., Li, R., Li, J., & Zhang, Z. (2021). Elucidating the optimum added dosage of Diatomite during co-composting of pig manure and sawdust: Carbon dynamics and microbial community. *Science of the Total Environment*, *777*. https://doi.org/10.1016/j.scitotenv.2021.146058

Riza, F. V., Rahman, I. A., & Zaidi, A. M. A. (2011). Possibility of Lime as a Stabilizer in Compressed Earth Brick (CEB). *International Journal on Advanced Science, Engineering and Information Technology*, *1*(6), 582. https://doi.org/10.18517/ijaseit.1.6.117

Rockwell, B. W., & Hofstra, A. H. (2008). Identification of quartz and carbonate minerals across northern Nevada using aster thermal infrared emissivity data-implications for geologic mapping and mineral resource investigations in well-studied and frontier areas. *Geosphere*, *4*(1). https://doi.org/10.1130/GES00126.1

Rostami, R., Khoshnava, S. M., Rostami, R., & Lamit, H. (2015). Green and sustainability policy, practice and management in construction sector, a case study of Malaysia. *Research Journal of Applied Sciences, Engineering and Technology*, *9*(3). https://doi.org/10.19026/rjaset.9.1393

Roy, S., & Kumar Bhalla, S. (2017). Role of Geotechnical Properties of Soil on Civil Engineering Structures. *Resources and Environment*, *7*(4).

S. Abo Dhaheer, M., H.K, A., & M.T, A. (2018). Improving the Properties of Clay Brick Using Polyvinyl Alcohol (PVA). *International Journal of Engineering & Technology*, *7*(4.20), 568. https://doi.org/10.14419/ijet.v7i4.20.26420

S, P., & P, R. (2022). Waste recycled plastic granules substitute for aggregate in concrete – Review. *Materials Today: Proceedings*, *xxxx*. https://doi.org/10.1016/j.matpr.2022.04.405

Sá Ribeiro, R. A., Sá Ribeiro, M. G., Sankar, K., & Kriven, W. M. (2016). Geopolymer-bamboo composite – A novel sustainable construction material. *Construction and Building Materials*, *123*. https://doi.org/10.1016/j.conbuildmat.2016.07.037

Sadrmomtazi, A., Dolati-Milehsara, S., Lotfi-Omran, O., & Sadeghi-Nik, A. (2016). The combined effects of waste Polyethylene Terephthalate (PET) particles and pozzolanic materials on the properties of selfcompacting concrete. *Journal of Cleaner Production*, *112*. https://doi.org/10.1016/j.jclepro.2015.09.107

Saeed, I. A., Mohammed, T. J., & Jihad, S. A. A. (2020). Production of Earth Units Compressed and Stabilized by Using Cement and Pozzolana. *IOP Conference Series: Materials Science and Engineering*, *745*(1), 0–12. https://doi.org/10.1088/1757-899X/745/1/012126

Salih, M. M., Osofero, A. I., & Imbabi, M. S. (2020). Critical review of recent development in fiber reinforced adobe bricks for sustainable construction. *Frontiers of Structural and Civil Engineering*, *14*(4), 839–854. https://doi.org/10.1007/s11709-020-0630-7

Saman, N. S. M., Deraman, R., & Hamzah, M. H. (2017). Development of low thermal conductivity brick using rice husk, corn cob and waste tea in clay brick manufacturing. *AIP Conference Proceedings*, *1901*. https://doi.org/10.1063/1.5010567

Samuel, D. M., Inumerable, N., Stumpf, A., & Kriven, W. M. (2023). Thermal conductivity of several geopolymer composites and discussion of their formulation. *International Journal of Applied Ceramic Technology*, *20*(1). https://doi.org/10.1111/ijac.14200

Santos, J. O. S., & Hartmann, L. A. (2021). Chemical classification of common volcanic rocks based on degree of silica saturation and CaO/K2O ratio. *Anais Da Academia Brasileira de Ciencias*, *93*(3). https://doi.org/10.1590/0001-3765202120201202

Šaponjić, A., Stanković, M., Majstorović, J., Matović, B., Ilić, S., Egelja, A., & Kokunešoski, M. (2015). Porous ceramic monoliths based on diatomite. *Ceramics International*, *41*(8), 9745–9752. https://doi.org/10.1016/j.ceramint.2015.04.046

Sarıdemir, M., Çelikten, S., & Yıldırım, A. (2020). Mechanical and microstructural properties of calcined diatomite powder modified high strength mortars at ambient and high temperatures. *Advanced Powder Technology*, *31*(7), 3004–3017. https://doi.org/10.1016/j.apt.2020.05.024

Schincaglia, V. T. (2022). *Concrete Blocks With Incorporation Of*. *July*.

Scrivener, K. L., John, V. M., & Gartner, E. M. (2018). Eco-efficient cements: Potential economically viable solutions for a low-CO2 cement-based materials industry. *Cement and Concrete Research*, *114*. https://doi.org/10.1016/j.cemconres.2018.03.015

Sharma, N., Sharma, P., & Verma, S. kr. (2021). Influence of Diatomite on the properties of mortar and concrete: A Review. *IOP Conference Series: Materials Science and Engineering*, *1116*(1), 012174. https://doi.org/10.1088/1757-899x/1116/1/012174

Silva, G., Kim, S., Aguilar, R., & Nakamatsu, J. (2020). Natural fibers as reinforcement additives for geopolymers – A review of potential eco-friendly applications to the construction industry. *Sustainable Materials and Technologies*, *23*, e00132. https://doi.org/10.1016/j.susmat.2019.e00132

Silva, G., Kim, S., Bertolotti, B., Nakamatsu, J., & Aguilar, R. (2020). Optimization of a reinforced geopolymer composite using natural fibers and construction wastes. *Construction and Building Materials*, *258*. https://doi.org/10.1016/j.conbuildmat.2020.119697

Singh, B., Ishwarya, G., Gupta, M., & Bhattacharyya, S. K. (2015). Geopolymer concrete: A review of some recent developments. In *Construction and Building Materials* (Vol. 85). https://doi.org/10.1016/j.conbuildmat.2015.03.036

Smallwood, A. G., Thomas, P. S., & Ray, A. S. (2008). Comparative analysis of sedimentary and volcanic precious opals from Australia. *Journal of the Australian Ceramic Society*, *44*(2), 17–22.

Snellings, R., Mertens, G., & Elsen, J. (2012). Supplementary cementitious materials. *Reviews in Mineralogy and Geochemistry*, *74*(Blezard 2001), 211–278. https://doi.org/10.2138/rmg.2012.74.6

Sofi, I. R., Manzoor, J., Bhat, R. A., & Munvar, R. (2019). *Plastic Pollution and the Ecological Impact on the Aquatic Ecosystem*. https://doi.org/10.4018/978-1-5225-9452-9.ch005

Song, X.J., Marosszeky, M., Brungs, M. and Munn, R., Song, X. J., Marosszeky, M., Brungs, M., Munn, R., Song, X.J., Marosszeky, M., Brungs, M. and Munn, R., Song, X. J., Marosszeky, M., Brungs, M., & Munn, R. (2005). Durability of fly ash based Geopolymer concrete against sulphuric acid attack. *10DBMC International Conference On Durability of Building Materials and Components*, *April*.

Sotelo-Piña, C., Aguilera-González, E. N., & Martínez-Luévanos, A. (2019). Geopolymers: Past, present, and future of low carbon footprint eco-materials. In *Handbook of Ecomaterials* (Vol. 4). https://doi.org/10.1007/978-3-319-68255-6_54

Sousa, S. M. T., Carvalho, C. M. De, Torres, S. M., Barbosa, N. P., Gomes, K. C., & Ghavami, K. (2012). Mechanical properties and durability of geopolymer stabilized earth blocks. *11° International Conference on the Study and Conservation of Earthen Heritage*, *March 2016*.

Stamatakis, M. G., Fragoulis, D., Antonopoulou, S., & Stamatakis, G. (2010). The opaline silica-rich sedimentary rocks of Milos Island, Greece and their behaviour as pozzolanas in the manufacture of cement. *Advances in Cement Research*, *22*(3), 171–183. https://doi.org/10.1680/adcr.2010.22.3.171

Stefanou, E., Kantiranis, N., Chatzicharalambous, K., Mytiglaki, C., Stamatakis, M., & Georgiadis, G. (2022). Diatomaceous Silica in Environmental Applications: A Case Study from the Lacustrine Deposit of Limnos Island, Aegean Sea, Greece. *Minerals*, *12*(5). https://doi.org/10.3390/min12050523

Stevulova, N., Schwarzova, I., Hospodarova, V., & Junak, J. (2016). Implementation of waste cellulosic fibres into building materials. *Chemical Engineering Transactions*, *50*, 367–372. https://doi.org/10.3303/CET1650062

Sturm, P., Greiser, S., Gluth, G. J. G., Jäger, C., & Brouwers, H. J. H. (2015). Degree of reaction and phase content of silica-based one-part geopolymers investigated using chemical and NMR spectroscopic methods. *Journal of Materials Science*, *50*(20). https://doi.org/10.1007/s10853-015-9232-5

Taallah, B., Guettala, A., Guettala, S., & Kriker, A. (2014). Mechanical properties and hygroscopicity behavior of compressed earth block filled by date palm fibers. *Construction and Building Materials*, *59*. https://doi.org/10.1016/j.conbuildmat.2014.02.058

Taoukil, D., El meski, Y., Lahlaouti, M. lhassane, Djedjig, R., & El bouardi, A. (2021). Effect of the use of diatomite as partial replacement of sand on thermal and mechanical properties of mortars. *Journal of Building Engineering*, *42*(May), 103038. https://doi.org/10.1016/j.jobe.2021.103038

Tavares, A., Costa, A., Rocha, F., & Velosa, A. (2016). Absorbent materials in waterproofing barriers, analysis of the role of diatomaceous earth. *Construction and Building Materials*, *102*, 125–132. https://doi.org/10.1016/j.conbuildmat.2015.10.169

Teixeira, E. R., Machado, G., De Adilson, P., Guarnier, C., Fernandes, J., Silva, S. M., & Mateus, R. (2020). Mechanical and thermal performance characterisation of compressed earth blocks. *Energies*, *13*(11). https://doi.org/10.3390/en13112978

Thiago, R. dos S. M., Pedro, P. M. de M., & Eliana, F. C. S. (2014). Solid wastes in brewing process: A review. *Journal of Brewing and Distilling*, *5*(1). https://doi.org/10.5897/jbd2014.0043

Thong, C. C., Teo, D. C. L., & Ng, C. K. (2016). Application of polyvinyl alcohol (PVA) in cement-based composite materials: A review of its engineering properties and microstructure behavior. *Construction and Building Materials*, *107*, 172–180. https://doi.org/10.1016/j.conbuildmat.2015.12.188

Tokyay, M. (2016). Cement and concrete mineral admixtures. In *Cement and Concrete Mineral Admixtures*. https://doi.org/10.1201/b20093

Tramontin, V., Loggia, C., & Trois, C. (2012). Strategies for stustainable building design and retrofit in developing countries. New goals for green buildings in South Africa. In *Journal of Construction* (Vol. 5, Issue 1).

TS EN 206. (2016). EN 206:2013 Concrete Concrete - Specification, performance, production and conformity ©. In *National Standards Authority of Ireland* (Issue May).

Ugwuishiwu, B. O., Echiegu, E. A., Okoye, N. M., & Chukwuma, G. O. (2013). Natural Fibre Induced Properties on Stabilized Earth Bricks. *Indian Journal of Research*, *October*, 1–4.

Ünal, O., Uygunoğlu, T., & Yildiz, A. (2007). Investigation of properties of low-strength lightweight concrete for thermal insulation. *Building and Environment*, *42*(2), 584–590. https://doi.org/10.1016/j.buildenv.2005.09.024

U.S.G.S. (2023). Mineral commodity summaries 2023: U.S. Geological Survey, 210 p. In *U.S. Geological Survey*.

Vanitha, S., Natarajan, V., & Praba, M. (2015). Utilisation of waste plastics as a partial replacement of coarse aggregate in concrete blocks. *Indian Journal of Science and Technology*, *8*(12). https://doi.org/10.17485/ijst/2015/v8i12/54462

Vejmelková, E., Keppert, M., Rovnaníková, P., Ondráček, M., Keršner, Z., & Černý, R. (2012). Properties of high performance concrete containing fine-ground ceramics as supplementary cementitious material. *Cement and Concrete Composites*, *34*(1). https://doi.org/10.1016/j.cemconcomp.2011.09.018

Verma, M., & Dev, N. (2022). Effect of Liquid to Binder Ratio and Curing Temperature on the Engineering Properties of the Geopolymer Concrete. *Silicon*, *14*(4). https://doi.org/10.1007/s12633-021-00985-w

Vijai, K., Kumutha, R., & Vishnuram, B. G. (2010). Effect of types of curing on strength of geopolymer concrete. *International Journal of Physical Sciences*, *5*(9).

Vora, P. R., & Dave, U. V. (2013). Parametric studies on compressive strength of geopolymer concrete. *Procedia Engineering*, *51*. https://doi.org/10.1016/j.proeng.2013.01.030

Vu, D. H., Wang, K. S., Bac, B. H., & Nam, B. X. (2013). Humidity control materials prepared from diatomite and volcanic ash. *Construction and Building Materials*, *38*(300), 1066–1072. https://doi.org/10.1016/j.conbuildmat.2012.09.040

Wan Ibrahim, W. M., Hussin, K., Al Bakri Abdullah, M. M., Abdul Kadir, A., & Binhussain, M. (2015). A Review of Fly Ash-Based Geopolymer Lightweight Bricks. *Applied Mechanics and Materials*, *754–755*, 452–456. https://doi.org/10.4028/www.scientific.net/amm.754-755.452

Wang, J., Lyu, X. J., Wang, L., Cao, X., Liu, Q., & Zang, H. (2018). Influence of the combination of calcium oxide and sodium carbonate on the hydration reactivity of alkali-activated slag binders. *Journal of Cleaner Production*, *171*. https://doi.org/10.1016/j.jclepro.2017.10.077

Washbourn-Kamau, C. K. (1971). Late Quaternary Lakes in the Nakuru-Elmenteita Basin, Kenya. *The Geographical Journal*, *137*(4). https://doi.org/10.2307/1797148

Wattanachai, P., & Suwan, T. (2017). Strength of Geopolymer Cement Curing at Ambient Temperature by Non-Oven Curing Approaches: An Overview. *IOP Conference Series: Materials Science and Engineering*, *212*(1). https://doi.org/10.1088/1757-899X/212/1/012014

Wardhono, A. (2018). Comparison Study of Class F and Class C Fly Ashes as Cement Replacement Material on Strength Development of Non-Cement Mortar. *IOP Conference Series: Materials Science and Engineering*, *288*(1). https://doi.org/10.1088/1757-899X/288/1/012019

Wei, J., Chen, T., Liu, G., & Yang, J. (2016). Higher-order Multivariable Polynomial Regression to Estimate Human Affective States. *Scientific Reports*, *6*. https://doi.org/10.1038/srep23384

Westover, K. S., Stone, J. R., Yost, C. L., Scott, J. J., Cohen, A. S., Rabideaux, N. M., Stockhecke, M., & Kingston, J. D. (2021). Diatom paleolimnology of late Pliocene Baringo Basin (Kenya) paleolakes. *Palaeogeography, Palaeoclimatology, Palaeoecology*, *570*. https://doi.org/10.1016/j.palaeo.2019.109382

Wongsa, A., Kunthawatwong, R., Naenudon, S., Sata, V., & Chindaprasirt, P. (2020). Natural fiber reinforced high calcium fly ash geopolymer mortar. *Construction and Building Materials*, *241*. https://doi.org/10.1016/j.conbuildmat.2020.118143

Wu, C., Li, Z., Li, Y., Wu, J., Zhao, Y., & Liao, Y. (2023). Effect of starch on pore structure and thermal conductivity of diatomite-based porous ceramics. *Ceramics International*, *49*(1). https://doi.org/10.1016/j.ceramint.2022.08.352

Xiao, L. G., & Liu, X. X. (2019). Effect of Diatomite on Thermal Insulation Properties of Straw Fiber Cement-based Composites. *IOP Conference Series: Earth and Environmental Science*, *295*(3). https://doi.org/10.1088/1755-1315/295/3/032047

Xie, T., Visintin, P., Zhao, X., & Gravina, R. (2020). Mix design and mechanical properties of geopolymer and alkali activated concrete: Review of the state-of-the-art and the development of a new unified approach. *Construction and Building Materials*, *256*. https://doi.org/10.1016/j.conbuildmat.2020.119380

Xu, B., & Li, Z. (2014). Performance of novel thermal energy storage engineered cementitious composites incorporating a paraffin/diatomite composite phase change material. *Applied Energy*, *121*. https://doi.org/10.1016/j.apenergy.2014.02.007

Xu, S., Wang, J., Jiang, Q., & Zhang, S. (2016). Study of natural hydraulic lime-based mortars prepared with masonry waste powder as aggregate and diatomite/fly ash as mineral admixtures. *Journal of Cleaner Production*, *119*, 118–127. https://doi.org/10.1016/j.jclepro.2016.01.069

Yadav, M., & Agarwal, M. (2021). Biobased building materials for sustainable future: An overview. *Materials Today: Proceedings*, *43*, 2895–2902. https://doi.org/10.1016/j.matpr.2021.01.165

Yalley, P. P.-K., & Manu, D. (2021). Effect of Cow Dung on Compressive Strength, Density, Abrasion Resistance and Permeability Properties of Earth Brick. In *New Visions in Science and Technology Vol. 7*. https://doi.org/10.9734/bpi/nvst/v7/5148f

Yan, L., Kasal, B., & Huang, L. (2016). A review of recent research on the use of cellulosic fibres, their fibre fabric reinforced cementitious, geo-polymer and polymer composites in civil engineering. *Composites Part B: Engineering*, *92*, 94–132. https://doi.org/10.1016/j.compositesb.2016.02.002

Yang, K. H., Cho, A. R., Song, J. K., & Nam, S. H. (2012). Hydration products and strength development of calcium hydroxide-based alkali-activated slag mortars. *Construction and Building Materials*, *29*. https://doi.org/10.1016/j.conbuildmat.2011.10.063

Yang, K.-H., Mun, J.-H., Lee, K.-S., & Song, J.-K. (2011). Tests on Cementless Alkali-Activated Slag Concrete Using Lightweight Aggregates. *International Journal of Concrete Structures and Materials*, *5*(2). https://doi.org/10.4334/ijcsm.2011.5.2.125

Yewale, V. V, Shirsath, M. N., & Hake, S. L. (2016). Evaluation of Efficient Type of Curing for Geopolymer Concrete. *International Journal of New Technologies in Science and Engineering*, *3*(8).

Yilmaz, B., & Ediz, N. (2008). The use of raw and calcined diatomite in cement production. *Cement and Concrete Composites*, *30*(3). https://doi.org/10.1016/j.cemconcomp.2007.08.003

Yu, M., Mao, H., Huang, R., Ge, Z., Tian, P., Sun, L., Wu, Q., & Sun, K. (2018). Mechanical and Thermal Properties of R-High Density Polyethylene Composites Reinforced with Wheat Straw Particleboard Dust and Basalt Fiber. *International Journal of Polymer Science*, *2018*. https://doi.org/10.1155/2018/5101937

Yuan, P., Liu, D., Zhou, J., Tian, Q., Song, Y., Wei, H., Wang, S., Zhou, J., Deng, L., & Du, P. (2019). Identification of the occurrence of minor elements in the structure of diatomaceous opal using FIB and TEM-EDS. *American Mineralogist*, *104*(9), 1323–1335. https://doi.org/10.2138/am-2019-6917

Yun, K. K., & Choi, P. (2014). Causes and controls of cracking at bridge deck overlay with very-early strength latex-modified concrete. *Construction and Building Materials*, *56*. https://doi.org/10.1016/j.conbuildmat.2014.01.055

Zahajská, P., Opfergelt, S., Fritz, S. C., Stadmark, J., & Conley, D. J. (2020). What is diatomite? In *Quaternary Research (United States)* (Vol. 96, pp. 48–52). Cambridge University Press. https://doi.org/10.1017/qua.2020.14

Záleská, M., Pavlíková, M., Pokorný, J., Jankovský, O., Pavlík, Z., & Černý, R. (2018). Structural, mechanical and hygrothermal properties of lightweight concrete based on the application of waste plastics. *Construction and Building Materials*, *180*. https://doi.org/10.1016/j.conbuildmat.2018.05.250

Zhang, H. (2011). Building Materials in Civil Engineering. In *Building Materials in Civil Engineering*. https://doi.org/10.1533/9781845699567

Zhang, P., Gao, Z., Wang, J., Guo, J., Hu, S., & Ling, Y. (2020). Properties of fresh and hardened fly ash/slag based geopolymer concrete: A review. In *Journal of Cleaner Production* (Vol. 270). https://doi.org/10.1016/j.jclepro.2020.122389

Zhang, P., Wang, K., Li, Q., Wang, J., & Ling, Y. (2020). Fabrication and engineering properties of concretes based on geopolymers/alkali-activated binders - A review. *Journal of Cleaner Production*, *258*. https://doi.org/10.1016/j.jclepro.2020.120896

Zhou, B., Wang, L., Ma, G., Zhao, X., & Zhao, X. (2020). Preparation and properties of bio-geopolymer composites with waste cotton stalk materials. *Journal of Cleaner Production*, *245*. https://doi.org/10.1016/j.jclepro.2019.118842

Zuluaga, D. A., Sabogal, D., Buenaventura, C. A., & Slebi, C. J. (2021). Physical and mechanical behavior of fine soil according to the content of multispecies diatoms. *Journal of Physics: Conference Series*, *2118*(1). https://doi.org/10.1088/1742-6596/2118/1/012011

APPENDICES

Appendix 1: An extract of Diatomaceous earth XRD data

2θ (°)	Int (a.u)	2θ (°)	Int (a.u)	2θ (°)	Int (a.u)	2θ (°)	Int (a.u)	2θ (°)	Int (a.u)
18.98095	4848	20.35128	5762	21.7216	9772	23.0585	5810	24.3954	4913
19.01437	4863	20.3847	5853	21.75502	10447	23.09192	5743	24.42883	4977
19.0478	4879	20.41812	5728	21.78844	10796	23.12535	5747	24.46225	5022
19.08122	4894	20.45154	5836	21.82187	10807	23.15877	5857	24.49567	4979
19.11464	4910	20.48497	5775	21.85529	10608	23.19219	5564	24.52909	4902
19.14806	4925	20.51839	5934	21.88871	9932	23.22561	5623	24.56252	5012
19.18149	4941	20.55181	6021	21.92213	8982	23.25904	5431	24.59594	5083
19.21491	4956	20.58523	5956	21.95556	8388	23.29246	5667	24.62936	4861
19.24833	4972	20.61866	5974	21.98898	7635	23.32588	5346	24.66278	5037
19.28175	4987	20.65208	6071	22.0224	7139	23.3593	5516	24.69621	4961
19.31518	5003	20.6855	5975	22.05582	6761	23.39273	5522	24.72963	4942
19.3486	5018	20.71892	6003	22.08925	6628	23.42615	5481	24.76305	5070
19.38202	5034	20.75235	6114	22.12267	6440	23.45957	5385	24.79647	4948
19.41544	5049	20.78577	6070	22.15609	6306	23.49299	5571	24.8299	5064
19.44887	5065	20.81919	6023	22.18952	6227	23.52642	5580	24.86332	4984
19.48229	5080	20.85261	6158	22.22294	6109	23.55984	5538	24.89674	4952
19.51571	5096	20.88604	6303	22.25636	6061	23.59326	5666	24.93016	5052
19.54913	5111	20.91946	5931	22.28978	6224	23.62668	5636	24.96359	5148
19.58256	5127	20.95288	6134	22.32321	6019	23.66011	5746	24.99701	4824
19.61598	5142	20.9863	6106	22.35663	6230	23.69353	5566	25.03043	4868
19.6494	5158	21.01973	6224	22.39005	6003	23.72695	5736	25.06385	4842
19.68282	5173	21.05315	6250	22.42347	6060	23.76037	5621	25.09728	4758
19.71625	5189	21.08657	6178	22.4569	6035	23.7938	5493	25.1307	4844
19.74967	5204	21.11999	6032	22.49032	5958	23.82722	5323	25.16412	4727
19.78309	5220	21.15342	6188	22.52374	5887	23.86064	5288	25.19754	4844
19.81651	5235	21.18684	6320	22.55716	5823	23.89406	5440	25.23097	4833
19.84994	5251	21.22026	6297	22.59059	5714	23.92749	5225	25.26439	4796
19.88336	5266	21.25368	6396	22.62401	5722	23.96091	5216	25.29781	4913
19.91678	5282	21.28711	6228	22.65743	5827	23.99433	5338	25.33123	4858
19.95021	5297	21.32053	6394	22.69085	5744	24.02775	5462	25.36466	4704
19.98363	5313	21.35395	6464	22.72428	5820	24.06118	5239	25.39808	4697
20.01705	5328	21.38737	6485	22.7577	5769	24.0946	5254	25.4315	4663
20.05047	5344	21.4208	6582	22.79112	5808	24.12802	5143	25.46492	4662
20.0839	5359	21.45422	6794	22.82454	5848	24.16144	5340	25.49835	4668
20.11732	5375	21.48764	6876	22.85797	5886	24.19487	5186	25.53177	4674
20.15074	5390	21.52106	7211	22.89139	5791	24.22829	5171	25.56519	4840
20.18416	5406	21.55449	7653	22.92481	5627	24.26171	5122	25.59861	4674
20.21759	5421	21.58791	7702	22.95823	5750	24.29513	5170	25.63204	4635
20.25101	5437	21.62133	8248	22.99166	5645	24.32856	5105	25.66546	4500
20.28443	5888	21.65475	9031	23.02508	5816	24.36198	5263	25.69888	4616

Appendix 2: Particle analysis data for raw diatomite

Particle size (µm)	% Volume	Dv (10) =7.58 µm Dv (50) =23.3 µm Dv (90) =50.4 µm
0.767	0.07	
0.872	0.1	
0.991	0.14	
1.13	0.18	
1.28	0.23	
1.45	0.29	
1.65	0.36	
1.88	0.42	
2.13	0.49	
2.42	0.55	
2.75	0.6	
3.12	0.64	
3.55	0.68	
4.03	0.74	
4.58	0.83	
5.21	0.98	
5.92	1.22	
6.72	1.56	
7.64	2.03	
8.68	2.61	
9.86	3.27	
11.2	3.99	
12.7	4.73	
14.5	5.44	
16.4	6.09	
18.7	6.65	
21.2	7.09	
24.1	7.36	
27.4	7.41	
31.1	7.17	
35.3	6.62	
40.1	5.78	
45.6	4.71	
51.8	3.55	
58.9	2.43	
66.9	1.48	
76	0.7	
86.4	0.34	
98.1	0.19	
111	0.1	
127	0.09	
144	0.06	
163	0.04	

Appendix 3: Particle analysis data for calcined diatomite

Particle size (µm)	% Volume	Dv (10) =21.0 µm Dv (50) =168 µm Dv (90) =728 µm
0.767	0.04	
0.872	0.08	
0.991	0.09	
1.13	0.11	
1.28	0.12	
1.45	0.14	
1.65	0.15	
1.88	0.16	
2.13	0.16	
2.42	0.16	
2.75	0.16	
3.12	0.17	
3.55	0.17	
4.03	0.19	
4.58	0.21	
5.21	0.24	
5.92	0.29	
6.72	0.36	
7.64	0.44	
8.68	0.53	
9.86	0.65	
11.2	0.78	
12.7	0.93	
14.5	1.09	
16.4	1.26	
18.7	1.44	
21.2	1.63	
24.1	1.81	
27.4	1.99	
31.1	2.16	
35.3	2.31	
40.1	2.44	
45.6	2.55	
51.8	2.65	
58.9	2.72	
66.9	2.78	
76	2.82	
86.4	2.83	
98.1	2.8	
111	2.73	
127	2.62	
144	2.5	

163	2.39	
Particle size (µm)	**% Volume**	
186	2.32	
211	2.33	
240	2.44	
272	2.68	
310	3.04	
352	3.5	
400	4.03	
454	4.54	
516	4.91	
586	5.02	
666	4.75	
756	4.07	
859	2.97	
976	1.52	

Appendix 4: Publications

The following three articles were created as a result of this thesis:

1. **Janet J. Kipsanai1; Paul M. Wambua; Saul S. Namango; Sofiane Amziane.** A Review on the Incorporation of Diatomaceous Earth as a Geopolymer-Based Concrete Building Resource. Materials 2022, 15, 7130. https://doi.org/10.3390/ma15207130

2. **Janet J. Kipsanai1; Sofiane Amziane.; Paul M. Wambua; Saul S. Namango.** An Evaluation of The Mechanical and Physical Properties of Sisal Fibre-Reinforced Alkaline Activated Diatomaceous Earth-Based Geopolymer Concrete. http://ijeais.org/wp-content/uploads/2023/4/IJAER230404.pdf

3. **Janet J. Kipsanai; Sofiane Amziane; Paul M. Wambua; Saul S. Namango.** Characterization of diatomaceous earth to evaluate its potential as a resource for geopolymer concrete development. https://www.researchgate.net/publication/373255819

Appendix 5: Antiplagiarism Report

SR252

ISO 9001:2019 Certified Institution

EDU 999 THESIS WRITING COURSE

PLAGIARISM AWARENESS CERTIFICATE

This certificate is awarded to

KIPSANAI JEPCHUMBA JANET

ENG/DPHIL/IE/01/18

In recognition for passing the University's plagiarism

Awareness test for thesis: **DEVELOPMENT AND PERFORMANCE EVALUATION OF DIATOMACEOUS EARTH-BASED GEOPOLYMER CONCRETE INCORPORATED WITH SISAL FIBRES AND HIGH-DENSITY POLYETHYLENE (HDPE) WASTES** with a similarity index of 11% and striving to maintain academic integrity.

Awarded by:

Prof. Anne Syomwene Kisilu
CERM-ESA Project Leader Date: 21/08/2023

SIMILARITY INDEX

By KIPSANAI, JEPCHUMBA JANET

WORD COUNT	54393	TIME SUBMITTED	21-AUG-2023 12:21PM
		PAPER ID	102135764

SIMILARITY INDEX

ORIGINALITY REPORT

11%
SIMILARITY INDEX

PRIMARY SOURCES

1	www.mdpi.com Internet	3329 words — 6%
2	ijeais.org Internet	2039 words — 4%
3	researchonline.ljmu.ac.uk Internet	525 words — 1%

EXCLUDE QUOTES	ON	EXCLUDE SOURCES	< 1%
EXCLUDE BIBLIOGRAPHY	ON	EXCLUDE MATCHES	OFF